Activities of the

Oil Implementation Task Force

Reporting Period December 1990–February 1991

63

Contracts for field projects
and supporting research on . . .

Enhanced Oil Recovery

Reporting Period April–June 1990

DOE/BC-90/3
(DE91002206)
PROGRESS REVIEW
Quarter Ending June 30, 1990

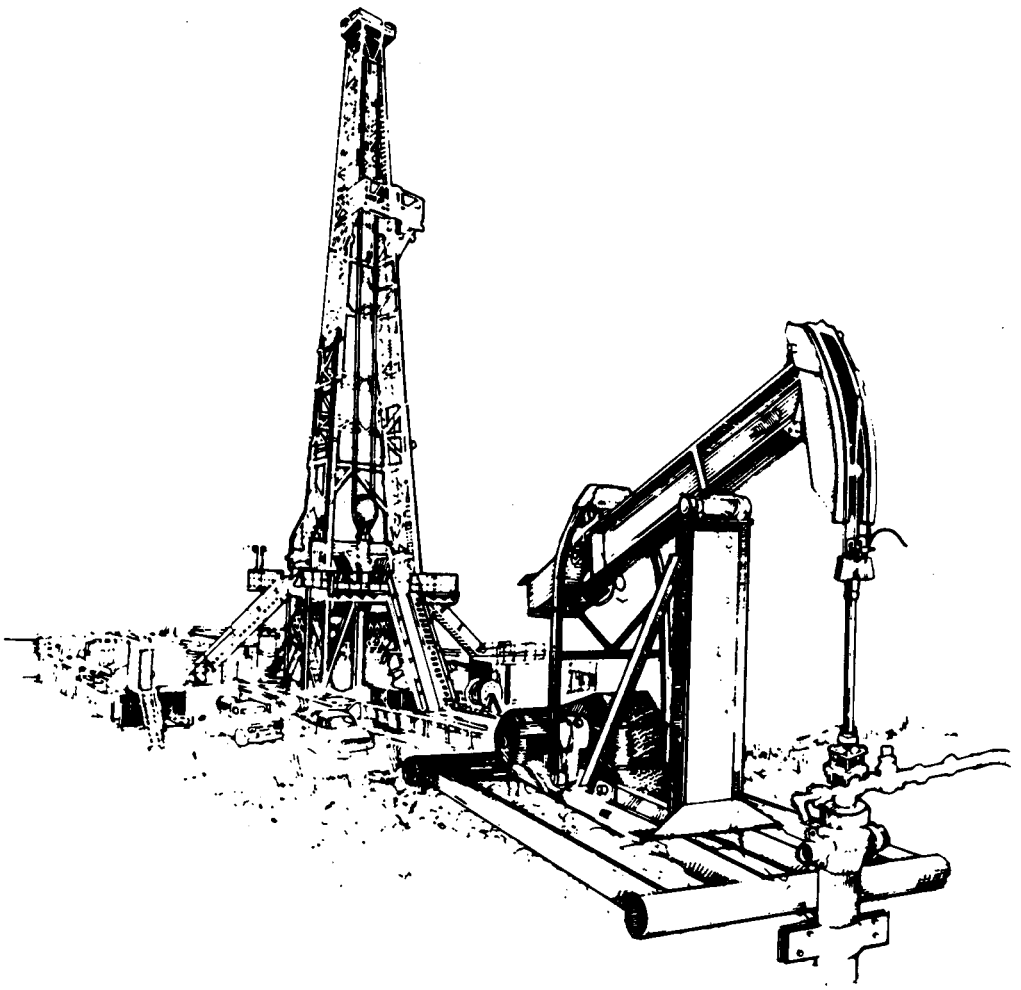

United States Department of Energy
Office of Oil, Gas, and Shale Technology
and Bartlesville Project Office

DISCLAIMER

Available to DOE and DOE contractors from the Office of Scientific and Technical Information, P.O. Box 62, Oak Ridge, Tennessee 37831; prices available from (615)576-8401, FTS 626-8401.

Available to the public from the National Technical Information Service, U.S. Department of Commerce, 5285 Port Royal Rd., Springfield, Virginia 22161.

Printed in the United States of America, Office of Scientific and Technical Information, Oak Ridge, Tennessee

SECTION INDEX

SECTION I

Activities of the Oil Implementation Task Force

U.S. Department of Energy
Washington, D.C. 20545

ROBERT H. GENTILE
Assistant Secretary
for Fossil Energy
Room 4G-084 Forrestal Building
Telephone Number (202) 586-4695

MARVIN SINGER
Deputy Assistant Secretary for Oil,
Gas, Shale, and Special
Technologies

ROBERT L. FOLSTEIN
Director, Oil Implementation
Task Force

Bartlesville Project Office
P.O. Box 1398
Bartlesville, Oklahoma 74005
Telephone No. 918/337-4401

THOMAS C. WESSON
Director

EDITOR:
HERBERT A. TIEDEMANN
Project Manager for
Technology Transfer

DOE/BC-90/3
(DE91002206)
Distribution Category UC-122

PROGRESS REVIEW NO. 63

ACTIVITIES OF THE OIL IMPLEMENTATION TASK FORCE

December, 1990-February, 1991

Date Published - March 1991

UNITED STATES DEPARTMENT OF ENERGY

INDEX

DOE Members of the
Oil Implementation Task Force

DIRECTORY

Name	Phone number	Task Force function
	U.S. Department of Energy **Oil, Gas, Shale and Special Technologies** **Mail Stop D-123, Washington, D.C. 20545**	
Ralph Avellanet	301-353-2737 – FTS 745-2737	Heavy Oil
Marvin Brooks	301-353-4462 – FTS 233-4462	AEPT
Edward Ferrero	301-353-2790 – FTS 233-2790	AEPT Alternate
Robert Folstein	301-353-2709 – FTS 233-2709	Chairman
Arthur Hartstein	301-353-2760 – FTS 233-2760	Environment
Carolyn Klym	301-353-2430 – FTS 233-2430	Administrative
Ronald Parent	301-353-3484 – FTS 233-3484	Planning & Schedule
Linda Simons	301-353-2703 – FTS 233-2703	Secretary
George Stosur	301-353-2749 – FTS 233-2749	Budget Coordinator
	U.S. Department of Energy **Headquarters, Forrestal Building** **Washington, D.C. 20585**	
William Hochheiser	202-586-5614 – FTS 896-5614	Geoscience
Nancy Johnson	202-586-6458 – FTS 896-6458	Environmental Policy
Elena S. Melchert	202-586-5095 – FTS 896-5095	Naval Petrol. Reserve
	Bartlesville Project Office **P.O. Box 1398** **Bartlesville, Oklahoma 74005**	
Edith Allison	918-337-4390 – FTS 745-4390	Manager, Reservoir Class I
Jerry Casteel	918-337-4412 – FTS 745-4412	Supporting Research
R. Michael Ray	918-337-4403 – FTS 745-4403	Data & Analysis
Thomas Reid	918-337-4233 – FTS 745-4233	Heavy Oil
H. A. Tiedemann	918-337-4293 – FTS 745-4293	Technology Transfer
	Morgantown Energy Technology Center **P.O. Box 880** **Morgantown, West Virginia 26505**	
James Ammer	304-291-4383 – FTS 923-4383	Tar Sands
John Guide	304-291-4930 – FTS 923-4930	Assistant Chairman
	Pittsburgh Energy Technology Center **P.O. Box 10940** **Pittsburgh, Pennsylvania 15326-0940**	
James J. Lacey	412-892-6144 – FTS 723-6144	Reservoir Field Tests
Dale Siciliano	412-892-6208 – FTS 723-6208	Procurement
	Metairie Site Office **900 Commerce East** **New Orleans, Louisiana 70123**	
E. B. Nuckols	504-734-4806 – FTS 686-4806	Manager, Reservoir Class II

INTRODUCTION TO THE OIL IMPLEMENTATION TASK FORCE

In August, 1990, Robert H. Gentile, The Department of Energy's Assistant Secretary for Fossil Energy, appointed a Task Force, comprising technical and management expertise, to put into place the Department's new Oil Research Program Implementation Plan. This new plan grew out of DOE's continuing effort to formulate a National Energy Strategy.

The previous program emphasis on long-term, high-risk research has been redirected to address the needs of current conditions in the petroleum industry. The 1986 price collapse, falling domestic production, and increased well abandonments that threaten future access to reservoirs containing a vast potential of recoverable oil were the major factors that led to this new direction.

In 1987 the Department initiated a study that highlighted the risk to national energy security posed by rising imports and pointed to the need for greater efforts in research. This recommendation was reinforced in an independent study by the Energy Research Advisory Board, which emphasized greater integration and coordination of geoscience and extraction research.

DOE sent a team of technical and management experts across the country to canvass the entire petroleum industry — majors, independents, consultants, service companies, universities — to obtain input on what they thought was needed to increase domestic production. Information gained from this effort led to a DOE Enhanced Oil Recovery (EOR) Initiative that recommended expansion of the research program to include near- and mid-term measures to improve domestic production, inclusion of mobile as well as immobile oil, and emphasis on technology transfer, particularly in relation to the independent producer.

In 1988, Congress directed DOE's Office of Fossil Energy to create, as part of a Hydrocarbon Geoscience Research Strategy, a plan to refocus oil research programs with a specific goal of increasing domestic oil production. In late 1989 and early 1990 the Department held a series of public hearings throughout the U.S., heard hundreds of witnesses and gathered thousands of pages of testimony from a cross-section of the nation. These meetings provided the background material for the formulation of a National Energy Strategy that seeks to strike a balance between competing resources and national priorities in arriving at a sensible, cohesive approach to a national energy policy.

Other concurrent studies emphasized additional facets of the energy security situation. Analysis by DOE's Tertiary Oil Recovery Information System (TORIS), an extensive compilation of petroleum-related information, disclosed the urgency posed by the increasing rate of well abandonment. The Hydrocarbon Geoscience Research Coordinating Committee, in cooperation with the Geoscience Institute for Oil and Gas Recovery Research, published a strategy document that urged a balance of near-, mid- and long-term research, and stressed the need to increase our understanding of reservoir complexities.

In response to these studies, on January 31, 1990, DOE announced its new Oil Research Program Implementation Plan. It recommended a program of field-based research on prioritized classes of reservoirs to rapidly demonstrate cost-effective advances in recovery technology. Under this new plan a balance of near-, mid- and long-term research will pursue the goals of better reservoir knowledge and improved recovery technologies. Research results will need to be evaluated at reservoir scale to be of value.

Building upon its predecessor, the plan establishes a program of highly targeted research, development and demonstration in collaboration with the states, industry and the academic community. It focuses on the reduction of technical and economic constraints on producibility to realize the enormous potential of the resource remaining in known domestic reservoirs. The program sets three time-specific goals:

- In the near term (within five years), preserve access to reservoirs with high recovery potential that are rapidly approaching their economic limits and are in danger of being abandoned.
- In the mid term (within ten years), develop, test and transfer the best, currently defined, advanced technologies to operators of the reservoirs with the greatest potential for incremental recovery.
- In the long term, develop sufficient fundamental understanding to define new recovery techniques for the oil left after application of the most advanced, currently defined mid-term processes, and for major classes of reservoirs for which no advanced technologies are anticipated to be available.

The primary goal of the new Oil Research Program is to increase domestic producibility and preserve access to those reservoirs containing the largest volumes of oil that are at the greatest risk of being abandoned.

A vast resource remains in existing reservoirs after conventional recovery. Of the more than 500 billion barrels of original oil in place in the U.S., less than ⅓ has been produced, and a mere 5% — less than 30 billion barrels — remains as proven reserves. With well-designed research and effective technology transfer, reserve additions of 76 billion barrels are possible within the next ten years — 15 billion barrels in the near-term (within five years), at present economic conditions with currently available and proven technologies. For the mid-term research component (five to ten years) reserve additions of 61 billion barrels are possible with the application of currently identified, yet-to-be-proven technologies.

The top priority for the Task Force is to preserve access to those reservoirs that have the largest potential for oil recovery. TORIS analysis shows that the present abandonment rate of 17-18,000 wells a year threatens future access to a significant portion of our oil resource. Calculations based on the principal reservoirs in nine states, representing over 75% of the remaining resource in the Lower-48, indicate that by 1987 access to 40% of the remaining oil in place had been abandoned. Even at $34 per barrel nearly 60% of the resource could be abandoned by the year 2000, and more than three quarters would be lost by the early 21st century if lower prices persist and technology advances are delayed (see References).

The first step in preserving reservoir access is identifying those reservoirs with significant remaining oil in place that are at the greatest risk of being abandoned. Information relating to the 3700 reservoirs contained in TORIS's reservoir database is being expanded and refined. Using TORIS in an ongoing Multi-State Study, BPO and the Interstate Oil Compact Commission have classified nearly 2000 of the nation's 2500 largest reservoirs, covering 25 of the 29 oil-producing states and 65% of the original oil in place. The reservoirs have been tentatively grouped into 25 classes, 16 sandstone and 9 carbonate, based on common geologic characteristics, and their associated production potential is being estimated.

The Task Force will prioritize the reservoir classes, based on volume of remaining oil in place, risk of abandonment, and the expectation that DOE-sponsored research can contribute to improved recovery. A preliminary selection for the first reservoir class has been made from the clastic reservoirs. Other selections will be made in the succeeding months.

Industry and other public comment on the reservoir selection process and the research needs of each class will be used along with other data to make the final selections and to design research keyed to the needs of the particular reservoir class. Field demonstrations of both currently existing and promising new recovery techniques will be implemented in reservoirs where they are deemed applicable. Successful results will be made available through DOE's Technology Transfer Program, and will be directed particularly to operators in the reservoirs where the results are applicable.

The Task Force is proceeding with these multiple approaches. Data is being collected, refined and analyzed to provide criteria for ranking and selection of reservoir classes, and plans are being made for the first of a series of meetings on the selection process. Reports on the activities of the various Task Force Teams are contained in this volume, and will continue in subsequent volumes.

References

1. U.S. Department of Energy, Bartlesville Project Office, "Abandonment Rates of the Known Domestic Oil Resource," DOE/BC-89/6/SP, November 1989.
2. U.S. Department of Energy, "Oil Research Program Implementation Plan," DOE/FE-0188P, April 1990.

TORIS DATA AND ANALYSIS

Data and Analysis Manager:
R. Michael Ray
Bartlesville Project Office

Report Period: December 1990-February 1991

Objectives

The role of TORIS data and analysis in the work of the Task Force is to:

- Provide baseline data for the classification of reservoirs, the determination of urgency relative to abandonment, the geographic distribution of reservoirs, and the identification of applicable recovery processes.
- Provide baseline data to prioritize reservoir classes.
- Estimate the impact of research and development successes and failures on increasing the economic producibility of the known remaining oil resources in each reservoir class.

Summary of Progress

Status of Reservoir Classification

A panel of experts involved in the Interstate Oil Compact Commission (IOCC) Multi-State met in Dallas on January 16-17, 1991, to review the status of the reservoir classification effort. Present were the Task Force TORIS Data and Analysis Manager and Reservoir Class I and II Managers, the Multi-State Study regional coordinators, and support staff.

The panel's tasks were to examine the validity and repeatability of the classification system, and to place the resulting reservoir categories into meaningful groups that are manageable in the analysis process.

Discussion and Analysis – After reviewing the nearly 2,200 individual reservoir descriptions and 172 combinations based on depositional system, diagenetic overprint and structural overprint, the panel affirmed that association of reservoirs by like processes and attendant similarities was meaningful, and that a smaller, more manageable number of classes would assist research and modeling.

Dividing the reservoirs into clastic and carbonate supergroups, the panel used 42 TORIS depositional systems as a framework to establish 16 clastic and 6 carbonate classes, based on extensive discussions of lithology, depositional system, diagenesis and structure. These classes are expected to manifest distinct types of heterogeneities as a result of their similar lithologies and despositional patterns.

Clastic Reservoirs – The 16 clastic classes (Figure 1) were derived from 27 reported depositional systems. Diagenetic overprint is unknown or insignificant throughout the class, and was therefore eliminated as a classifier. Structural overprint, however, is meaningful, and each class is implicitly understood to have a structured and unstructured subclass.

Overriding similarities in internal reservoir characteristics led to combination of depositional systems into single classes for a number of reservoir types, including Eolian, Alluvial Fan, Lacustrine, Shelf, Basin and Slope/Basin reservoirs.

Deltas were classed as wave-, fluvial- and tide-dominated, plus an undifferentiated class, which includes complex combinations of the 3 major classes. Strandplain reservoirs were divided on the basis of quality and abundance into a higher-quality Strandplain/Barrier Core/Barrier Shoreface class, a poorer-quality Strandplain/Backbarrier class,

and a sparsely populated Strandplain/Undifferentiated class that includes the tidal processes of tidal channels, deltas and washover fans. Fluvial classes separate Fluvial/Braided and Fluvial/Meandering reservoirs from Fluvial/Undifferentiated on the basis of their significant differences in reservoir character.

Carbonate Reservoirs – Diagenetic overprint is a prominent and variable contributor to carbonate reservoir heterogeneity. The panel combined the diagenetic descriptors into the subspecies of "Dolomitization," "Massive Dissolution," and "Other," to differentiate three carbonate subclasses, except in the case of the Slope/Basin class, in which all reservoirs are described by the diagenetic process of silicification, and was therefore given this subclass (Figure 2).

Structure does not define carbonate subclasses effectively, 88% of the reservoirs being described as unstructured. In those that are structured, natural fracturing can have a strong effect on heterogeneity.

The Peritidal class comprises the peritidal, supratidal and intertidal depositional systems, reflecting both the similarities in environments of deposition and of subsequent alteration which affect reservoir heterogeneity. The peritidal/subtidal group, however, was combined with shallow shelf/restricted to form the Shallow Shelf/Restricted Class.

This latter class and the Shallow Shelf/Open Class received various undifferentiated shallow shelf reservoirs on the basis of close spatial relationship, analogous rock types and commonly similar diagenetic environments.

The last two carbonate classes, Shelf Margin and Reef, were retained essentially unchanged, in spite of having internal architecture similar to other classes.

Conclusions – The reservoir heterogeneity classification system is considered a reliable and repeatable classification tool. It was used during this review to successfully group TORIS reservoirs into meaningful, manageable geologic classes, combining similar reservoir characteristics within a geologic framework for focused research into reservoir heterogeneity.

Natural fracturing and authigenic clays were recommended for further investigation as crosscutting research that could have a widespread impact on the understanding of reservoir heterogeneity and the flow of fluids within the reservoirs.

Classification of Clastic Reservoirs

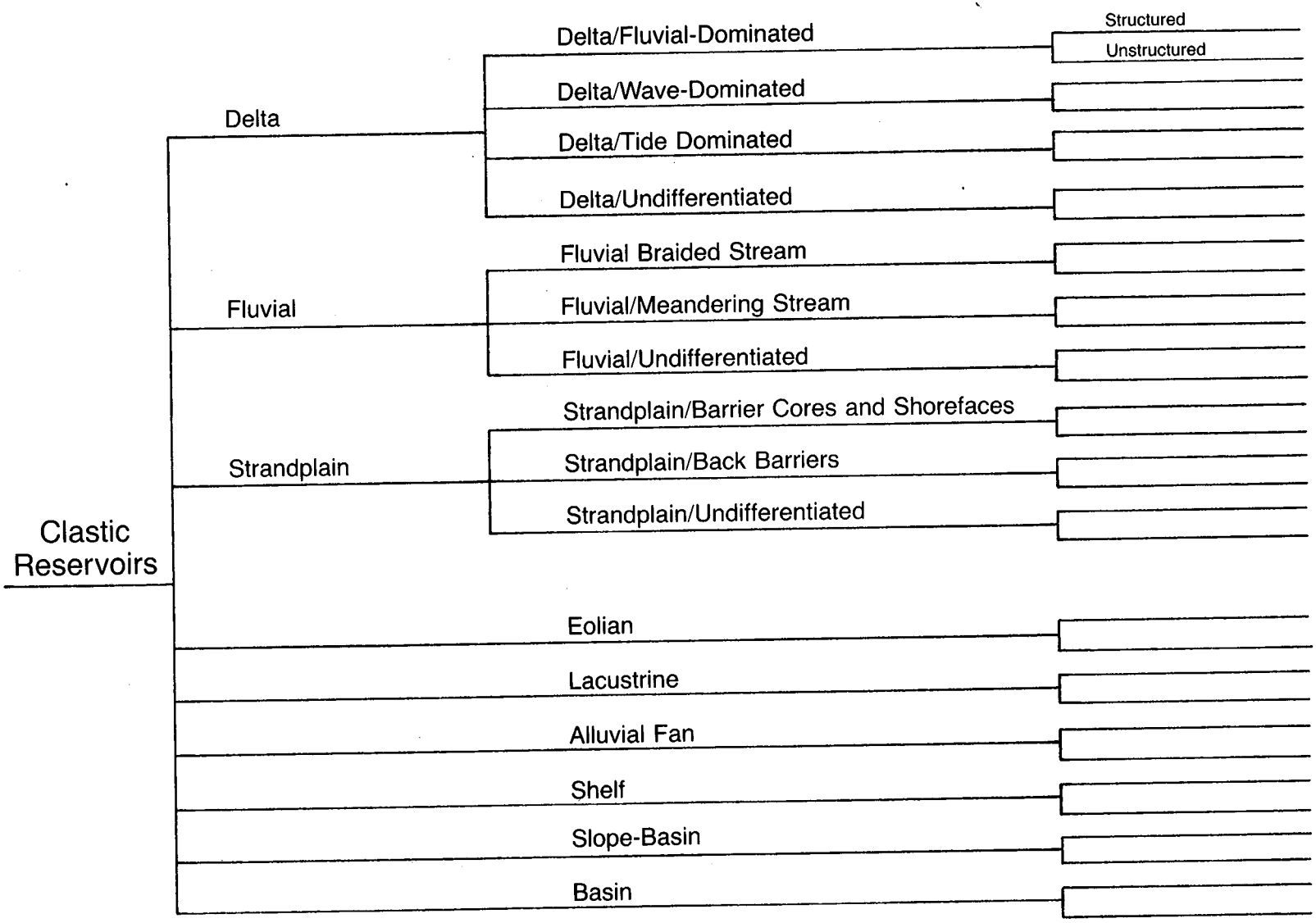

Figure 1

Classification of Carbonate Reservoirs

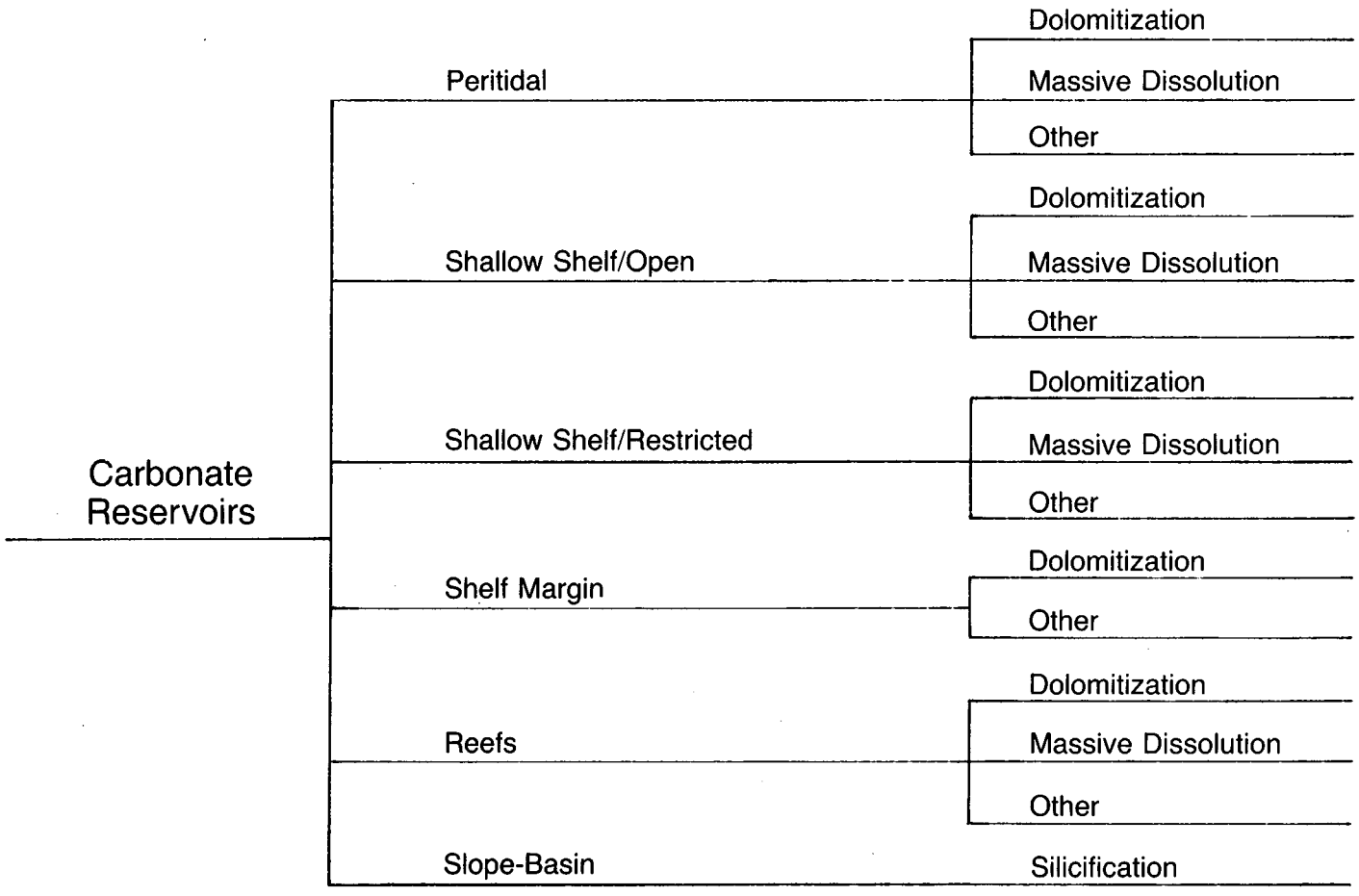

Figure 2

FIELD RESEARCH, DEVELOPMENT AND DEMONSTRATION

Reservoir Class I Manager:
Edith Allison
Bartlesville Project Office

Reservoir Class II Manager:
E. B. Nuckols
Metairie Site Office

Reporting Period: December 1990-February 1991

Objectives

The Field Research, Development and Demonstration (RD&D) effort will contribute to the Oil Implementation Plan objectives by: 1) selecting for study several classes of reservoirs, each of which has a common geologic history; 2) soliciting industry and other public input regarding technical constraints to improved production and mechanisms for overcoming those constraints for each class of reservoirs; 3) implementing near-term demonstrations of conventional technology that will assist operators in maintaining production and preventing abandonment of oil resources; 4) conducting research to better characterize the reservoirs in the class, and 5) implementing field demonstrations of advanced technology to overcome the reservoir constraints identified in the characterization research.

Summary of Progress

The Department of Energy Oil Implementation Task Force sponsored a Technical Symposium on "Opportunities to Improve Oil Productivity in Unstructured Deltaic Reservoirs" in Dallas, Texas, January 29-30, 1991, in partial fulfillment of the second objective listed above.

General Background

Organized and chaired by Edith Allison, Reservoir Class I Manager, the symposium was the first in a series of meetings designed to provide an overview of constraints and near-term and mid-term technological advances affecting the producibility of a large portion of the U.S. domestic oil resource. At these meetings operators and other technical personnel will be encouraged to share information about their problems and technical experiences in selected classes of oil reservoirs.

Unstructured deltaic reservoirs were chosen as the focus for this first symposium, on the basis of having a large potential for recoverable oil and high risk of abandonment. Reservoirs of this class, widespread in the U.S., are characterized by lack of continuity of productive flow units, which results in low recovery efficiency, leaving a large volume of mobile oil (the target for geologically targeted infill drilling and waterflooding) as well as immobile oil (a chemical flooding target).

Attendance

The symposium, held in the Hyatt Regency/DFW Hotel, East Tower, at the Dallas/Fort Worth International Airport, was well attended, with more than 250 participants, in-

cluding 79 small independent oil operators, 25 major oil company staff, 22 from service companies, and 39 consultants. In addition, there were 13 from state and Federal geological agencies, 33 university researchers, and several representatives from the French Petroleum Institute.

Speakers and Technical Sessions

Robert H. Gentile, DOE Assistant Secretary for Fossil Energy, opened the symposium with keynote remarks, emphasizing the importance of the new initiatives set forth in DOE's revised Oil Research Program Implementation Plan. He also stressed that the objective of the symposium was to provide a forum for industry operators to share ideas that would be helpful in implementing technology to increase productivity.

Following Mr. Gentile's address, the background for the symposium was outlined by Ms. Allison. R. Michael Ray, BPO Deputy Director, reviewed the reservoir classification system and selection methodology, and E. B. Nuckols, Reservoir Class II Manager, discussed the geologic and engineering characteristics of deltaic reservoirs.

Thirteen presentations, given during the remaining three half-day technical sessions, addressed critical technologies necessary to improve the description, analysis, and prediction of reservoir properties affecting oil productivity in deltaic reservoirs. Speakers represented large and small oil companies, service companies and consultants, state geological agencies and university research departments.

Discussion and Comment

The technical presentations were well received, and generated many questions and comments during the discussion periods. Additional comments on specific needs or problems hindering greater productivity were received from many operators during informal discussions throughout the two days of the meeting.

Following are some of the more important contributions distilled from comments by operators and researchers:

- Much additional oil could be recovered by better, more widespread use of conventional technology. Underutilization of conventional technology is due mostly to lack of knowledge of technology benefits and where to obtain technology.
- Large and small operators, service companies and research facilities were interested in participating in cost-shared project with DOE. Independents are confident that technology in a familiar format can improve their productivity.
  - Different segments of the industry have varying technology needs and levels of technical sophistication.
  - Some majors believe they can conduct successful chemical floods because of recent design improvements.
  - Small companies need relief, or at least consistency from regulatory agencies, and would welcome DOE help.
- Some problems mentioned:
  - In reservoir analysis, sweep efficiency is not simple; some heterogeneous reservoirs may be better swept and have less unrecovered mobile oil than analyses suggest.
  - Not all reservoirs are worth the manpower and cost required to enhance productivity; industry does only the minimum analysis necessary, using available reservoir data; the more advanced the implemented technology, the more sophisticated the data base and assessment required.
  - Reservoir characterization was recognized as essential, but it was noted that it requires close cooperation between reservoir engineers, geologists, geophysicists, et al.

Distribution of Publications

Numerous copies of DOE publications were distributed to interested attendees during the meeting, including general information, abstracts, a list of deltaic reservoir operators, "Doing Business with DOE's Fossil Energy Office," the Hydrocarbon Geoscience Research Strategy booklet, the Well Abandonment Study, Bartlesville Project Office publication lists, and the Quarterly Progress Review #62 containing the initial report on Oil Implementation Task Force activities.

Meeting Report

A comprehensive report of meeting activities and results will be published in the near future. It will contain a general introduction and background to DOE's revised Oil Research Program Implementation Plan and activities of the Oil Implementation Task Force, a detailed synopsis of the meeting, including comments and suggestions, a section of technical information on deltaic reservoirs, and a review of reservoir classification systems. The report will be available to interested scientists, research, technical and administrative personnel.

SUPPORTING RESEARCH

Supporting Research Manager:
Jerry Casteel
Bartlesville Project Office

Reporting Period: December 1990-February 1991

Objectives

The objective of Supporting Research is to conduct near- and mid-term research targeted toward improving oil recovery from reservoirs within the selected classes, and to conduct mid- and long-term discipline-oriented research directed toward developing advanced oil recovery methods.

These objectives will be achieved by incorporating the disciplines of reservoir description, extraction technology, and environmental technology into an integrated, interactive plan which meets the objectives and goal of the Oil Research Program Implementation Plan.

Summary of Progress

Enhanced Oil Recovery (EOR) Project Database

A database of supporting research has been created that contains 327 current and past EOR-related projects dating back to the early 1970s. Some of the past projects may have originated under the Advanced Extraction and Process Technology sub-program.

Table 1 shows Department of Energy (and ERDA) vs. contractor funding for various contractor and project types, field tests, supporting research and general and other categories. For example, Industry contractors conducted 70 projects, which account for 34.90% of the DOE (ERDA) funds and 52.58% of the total funds, and field tests account for 40.75% of the DOE funds and 57.95% of the total funds.

Most of the projects were managed through the Bartlesville Project Office (BPO) and its predecessor, the Bartlesville Energy Technology Center.

Funding for FY 1990 and FY 1991

Table 2 summarizes the funding for Supporting Research that is in place for FY 1990 and FY 1991. The research is categorized into specific types under the three broad classes of Reservoir Description, Extraction Technology and Environmental Technology.

Suggested Supporting Research Categories

Task Force members and supporting contract personnel met at the DOE Germantown office on January 18, 1991, to discuss methods of categorizing the various disciplines and areas of Supporting Research. A preliminary classification of Supporting Research was suggested as shown below:

University Oil Research Program – A university program for supporting oil research modeled after the University Coal Research Program.

Cooperative Research Program – A program comprising cooperative projects between DOE and industry, in which industry would fund at least 50%. The Los Alamos/Sandia National Labs-Industry cooperative Oil Recovery Technology Partnership would be included.

TABLE 1

Summary of Projects in Database
(December 27, 1990)

	TOTAL	DOE/ERDA ($)	CONTRACTOR ($)	OTHER ($)	TOTAL ($)	DOE (%)	TOTAL (%)
General							
Total Database	327	299,512,257	181,022,596	9,165,500	489,700,353	100.00	100.00
AEPT Funding (EOR Type Projects)	38	23,281,069	341,000	1,224,000	24,846,069	7.77	5.07
EOR Funding	285	265,212,188	180,681,596	7,941,500	453,835,284	88.55	92.68
Other Funding	4	11,019,000	0	0	11,019,000	3.68	2.25
Type of Contractor							
Government: City	2	8,133,829	10,450,743	0	18,584,572	2.72	3.80
Government: State	13	6,343,866	7,130,000	0	13,473,866	2.12	2.75
GURC Funding	2	1,094,384	0	0	1,094,384	0.37	0.22
Industry	70	104,533,573	151,639,749	1,329,500	257,502,822	34.90	52.58
METC	3	3,605,000	0	0	3,605,000	1.20	0.74
National Laboratories	25	45,552,500	0	591,000	46,143,500	15.21	9.42
NIPER	58	51,428,500	998,000	1,629,000	54,055,500	17.17	11.04
Universities	134	56,259,605	10,804,104	5,616,000	72,679,709	18.78	14.84
TBD	15	20,926,000	0	0	20,926,000	6.99	4.27
WRI	1	1,542,000	0	0	1,542,000	0.51	0.31
Not Classed	4	93,000	0	0	93,000	0.03	0.02
Type of Project							
Analytical Oil	2	2,005,000	0	0	2,005,000	0.67	0.41
Chemical Flooding	62	79,851,295	103,732,152	399,000	183,982,447	26.66	37.57
Environmental	13	3,013,000	0	0	3,013,000	1.01	0.62
Gas Flooding	49	37,483,657	17,072,021	4,154,500	58,710,178	12.51	11.99
Geoscience	94	70,995,553	14,575,503	2,366,000	87,937,056	23.70	17.96
Microbial Flooding	22	8,077,700	1,776,000	1,420,000	11,273,700	2.70	2.30
Novel	9	9,244,500	7,734,000	5,000	16,983,500	3.09	3.47
Support: Technology Transfer	4	1,394,384	0	0	1,394,384	0.47	0.28
Support: Not Classed	16	15,151,000	0	0	15,151,000	5.06	3.09
Thermodynamics	5	4,198,000	0	310,000	4,508,000	1.40	0.92
Thermal Recovery	46	67,915,668	35,792,920	391,000	104,099,588	22.68	21.26
Well Projects	5	182,500	340,000	120,000	642,500	0.06	0.13
Field Tests							
Cost-Shared Field Tests	29	82,956,113	150,733,619	0	233,689,732	27.70	47.72
Other Field Tests	13	39,093,000	8,592,000	2,397,000	50,082,000	13.05	10.23
Total Field Tests	42	122,049,113	159,325,619	2,397,000	283,771,732	40.75	57.95
Supporting Research							
All Projects	265	165,976,144	21,048,977	6,768,500	193,793,621	55.42	39.57
Other Areas							
All Projects	20	11,487,000	648,000	0	12,135,000	3.84	2.48

National Institute for Petroleum and Energy Research (NIPER) – A program under which NIPER would continue to support the DOE mission through its Energy Production Research Base Program.

Extraction Research – This area would include the various types of extraction technology such as chemical, gas and microbial flooding and sweep improvement.

Geoscience – Areas of research would include instrumentation, interpretation, geological modeling and reservoir characterization.

This classification of research categories will be reviewed by the Task Force and adapted to the future needs of the Oil Research Program Implementation Plan.

TABLE 2

Funding by Level for FY90 and FY91 Projects

LEVEL	SECOND LEVEL	THIRD LEVEL	FOURTH LEVEL	FIFTH LEVEL	FY90 ($) (No. Projects)	FY91 ($) (No. Projects)
12111	Disciplinary Research	Reservoir Description	Advanced Instrumentation	Hi Resolution Seismic	274,305 (1)	292,711 (1)
12112	Disciplinary Research	Reservoir Description	Advanced Instrumentation	Log Through Casing	283,000 (2)	217,000 (1)
12113	Disciplinary Research	Reservoir Description	Advanced Instrumentation	Measurement While Drilling	197,000 (3)	350,000 (2)
12114	Disciplinary Research	Reservoir Description	Advanced Instrumentation	Novel Techniques	701,000 (2)	885,000 (2)
12115	Disciplinary Research	Reservoir Description	Advanced Instrumentation	Other Advanced Instrumentation	—	—
12121	Disciplinary Research	Reservoir Description	Advanced Interpretation	Geostatistics	239,500 (2)	150,000 (1)
12122	Disciplinary Research	Reservoir Description	Advanced Interpretation	Well Testing	—	—
12123	Disciplinary Research	Reservoir Description	Advanced Interpretation	Geological Scaling & Modeling	2,319,901 (6)	2,168,732 (6)
12124	Disciplinary Research	Reservoir Description	Advanced Interpretation	Integrated Interpretation Protocols	548,000 (2)	480,000 (2)
12125	Disciplinary Research	Reservoir Description	Advanced Interpretation	Other Advanced Interpretation	105,652 (1)	61,733 (1)
12131	Disciplinary Research	Reservoir Description	Fundamental Geoscience	Reservoir Chemistry/Physics	247,728 (2)	376 (1)
12132	Disciplinary Research	Reservoir Description	Fundamental Geoscience	Rock-Fluid Systems	1,167,004 (8)	992,747 (9)
12133	Disciplinary Research	Reservoir Description	Fundamental Geoscience	Other Fundamental Geoscience	1,587,000 (1)	700,000 (1)
12141	Disciplinary Research	Reservoir Description	General Res Description	Non Plan	1,327,892 (12)	778,294 (9)
12142	Disciplinary Research	Reservoir Description	General Res Description	Not Classed	2,123,000 (3)	2,455,000 (4)
12211	Disciplinary Research	Extraction Technology	Reservoir Simulation	Model Development	126,000 (1)	—
12212	Disciplinary Research	Extraction Technology	Reservoir Simulation	Tracer Models	—	—
12213	Disciplinary Research	Extraction Technology	Reservoir Simulation	Water Flood Models	—	—
12214	Disciplinary Research	Extraction Technology	Reservoir Simulation	Enhanced Oil Recovery Models	—	350,000 (2)
12215	Disciplinary Research	Extraction Technology	Reservoir Simulation	Other Reservoir Simulation	50,000 (1)	—
12221	Disciplinary Research	Extraction Technology	Adv Pri/Sec Oil Recovery	Disciplinary Infill Drilling	—	—
12222	Disciplinary Research	Extraction Technology	Adv Pri/Sec Oil Recovery	Completion/Simulation	97,000 (4)	105,500 (1)
12223	Disciplinary Research	Extraction Technology	Adv Pri/Sec Oil Recovery	Permeability Modification	369,564 (3)	385,245 (3)
12224	Disciplinary Research	Extraction Technology	Adv Pri/Sec Oil Recovery	Drilling/Horizontal Wells	153,000 (1)	—
12225	Disciplinary Research	Extraction Technology	Adv Pri/Sec Oil Recovery	Other Advanced Primary/Sec	—	—
12231	Disciplinary Research	Extraction Technology	Advanced TOR	Gas Flooding	1,792,000 (11)	1,836,500 (8)
12232	Disciplinary Research	Extraction Technology	Advanced TOR	Chemical Flooding	2,263,000 (5)	1,367,000 (3)
12233	Disciplinary Research	Extraction Technology	Advanced TOR	Thermal Flooding	3,161,878 (9)	2,426,278 (10)
12234	Disciplinary Research	Extraction Technology	Advanced TOR	Microbial Flooding	1,530,655 (12)	386,623 (10)
12235	Disciplinary Research	Extraction Technology	Advanced TOR	Novel	—	—
12236	Disciplinary Research	Extraction Technology	Advanced TOR	Other Advanced Tertiary Oil Recovery	—	—
12241	Disciplinary Research	Extraction Technology	Gen Extraction Tech	Non Plan	260,792 (3)	118,639 (2)
12242	Disciplinary Research	Extraction Technology	Gen Extraction Tech	Not Classed	197,000 (1)	—

TABLE 2 (Continued)

Funding by Level for FY90 and FY91 Projects

LEVEL	SECOND LEVEL	THIRD LEVEL	FOURTH LEVEL	FIFTH LEVEL	FY90 ($) (No. Projects)	FY91 ($) (No. Projects)
12311	Disciplinary Research	Environmental Tech	Impacts Rec Processes	Impacts of Advanced Technologies	—	100,000 (1)
12312	Disciplinary Research	Environmental Tech	Impacts Rec Processes	Health and Safety	—	340,000 (1)
12313	Disciplinary Research	Environmental Tech	Impacts Rec Processes	Technical Support	50,000 (1)	50,000 (1)
12314	Disciplinary Research	Environmental Tech	Impacts Rec Processes	Other Impacts of Recovery Processes	—	—
12321	Disciplinary Research	Environmental Tech	Oil Field Waste	Drilling and Production Waste	—	50,000 (1)
12322	Disciplinary Research	Environmental Tech	Oil Field Waste	Underground Injection Control	—	—
12323	Disciplinary Research	Environmental Tech	Oil Field Waste	Air Emissions	—	—
12324	Disciplinary Research	Environmental Tech	Oil Field Waste	Wetlands Mitigation	—	300,000 (1)
12325	Disciplinary Research	Environmental Tech	Oil Field Waste	Endangered Species	—	—
12326	Disciplinary Research	Environmental Tech	Oil Field Waste	Other Oil Field Waste	—	—
12331	Disciplinary Research	Environmental Tech	Well Integrity	Idle and Temporarily Abandoned Wells	300,000 (2)	500,000 (3)
12332	Disciplinary Research	Environmental Tech	Well Integrity	Reversible Well Plugging	—	—
12333	Disciplinary Research	Environmental Tech	Well Integrity	Other Well Integrity	—	—
12341	Disciplinary Research	Environmental Tech	Gen Env Technology	Non Plan	99,500 (2)	—
12342	Disciplinary Research	Environmental Tech	Gen Env Technology	Not Classed	—	—

U.S. Department of Energy
Washington, D.C. 20545

ROBERT H. GENTILE
Assistant Secretary
for Fossil Energy
Room 4G-084 Forrestal Building
Telephone Number (202) 586-4695

MARVIN SINGER
Deputy Assistant Secretary for Oil,
Gas, Shale, and Special
Technologies

JAMES D. BATCHELOR
Director for Oil, Gas,
and Shale Technology

ARTHUR HARTSTEIN
Deputy Director of Oil, Gas,
and Shale Technology

J. J. STOSUR
Enhanced Oil Recovery Program Manager
Mail Stop D-116, Germantown
Telephone Number (301) 353-2749

Bartlesville Project Office
P.O. Box 1398
Bartlesville, Oklahoma 74005

Telephone No. 918/337-4401

THOMAS C. WESSON
Director

R. M. RAY
Deputy Director

FRED W. BURTCH
Program Coordinator,
Enhanced Oil Recovery

HERBERT A. TIEDEMANN
Project Manager for
Technology Transfer

DOE/BC-90/3
(DE91002206)
Distribution Category UC-122

PROGRESS REVIEW NO. 63

CONTRACTS FOR FIELD PROJECTS AND SUPPORTING RESEARCH ON ENHANCED OIL RECOVERY

Date Published - March 1991

UNITED STATES DEPARTMENT OF ENERGY

PUBLICATIONS LIST

AVAILABILITY OF PUBLICATIONS

The Department of Energy makes the results of all DOE-funded research and development efforts available to DOE and DOE contractors from the **Office of Scientific and Technical Information, P.O. Box 62, Oak Ridge, TN 37831; prices available from (615) 576-8401, FTS 626-8401.**

Available to the public from the **National Technical Information Service, U.S. Department of Commerce, 5285 Port Royal Road, Springfield, VA 22161; prices available from (703) 487-4650.**

Give the full title of the report and the report number.

Sometimes there are slight delays between the time reports are shipped to NTIS and the time it takes for NTIS to process the reports and make them available. Accordingly, we will provide one copy of any individual report as long as our limited supply lasts. Please help us in our effort to eliminate wasteful spending on government publications by requesting only those publications needed. Order by the report number listed at the beginning of each citation and enclose a self-addressed mailing label. Available from **DOE Bartlesville Project Office, ATTN: Herbert A. Tiedemann, P.O. Box 1398, Bartlesville, OK 74005; (918) 337-4293.**

Quarterly Reports

DOE/BC–89/4 Contracts for Field Projects and Supporting Research on Enhanced Oil Recovery. Progress Review No. 60. Quarter ending September 30, 1990. July 1990. Order No. DE90000219. Status reports are given for various enhanced oil recovery and gas recovery projects sponsored by the Department of Energy. The field tests and supporting research on enhanced oil recovery include chemical flooding, gas displacement, thermal/heavy oil, resource assessment, geoscience technology, microbial technology, novel technology, and environmental technology.

Chemical Flooding

DOE/BC/10847–20 Enhanced Oil Recovery Through In-Situ Generated Surfactants Augmented by Chemical Injection. Final Report for 1988-1989. Illinois Institute of Technology. August 1990. 152 pp. Order No. DE90000253. Both experimental and theoretical studies are conducted to advance understanding and predictability in the successful application of the combined surfactant-enhanced alkaline flooding for tertiary oil recovery. During the past year, an experimental investigation of the buffered surfactant-enhanced alkaline flooding system chemistry was undertaken to determine the influence of the various species present on interfacial tension and phase behavior. It was found that the minimum in interfacial tension and the region of spontaneous emulsification correspond to a particular pH range, so that by buffering the aqueous pH against changes in alkali concentration, low interfacial tension can be maintained when the amount of alkali decreases due to the influence of external factors, such as divalent ions, acids, rock consumption, and dispersion. Reflected light micro-interferometry study was conducted to observe stratification (i.e., the kinetics of layered drainage) in thin liquid films (associated with emulsion and foam systems) formed from micellar solutions of nonionic surfactants, such as ethoxylated alcohols. For the first time, the formation of colloid crystal-like structures were revealed inside the film with thicknesses of the order of 100nm containing nonionic surfactants. In the case of micellar solutions of nonionic surfactants the stratification which results in the enhanced stability of films (and therefore the colloidal dispersion) is very sensitive to temperature. A new microwave interference dielectrometer was developed for characterizing oil-in-water and water-in-oil macroemulsions. The apparatus is readily applicable to either on-line or laboratory measurements. In addition, the complex dielectric properties of macroemulsions in the microwave frequence region were analyzed using interaction potential models and effective medium theories.

DOE/BC/14449–2 A Study of Surfactant-Assisted Waterflooding. Final Report. University of Oklahoma. September 1990. 60 pp. Order No. DE90000261. In surfactant-assisted waterflooding, a surfactant slug is injected into a reservoir, followed by a brine spacer, followed by a second slug. The charge on the surfactant in the first slug has opposite sign to that in the second slug. When the two slugs mix in the reservoir, a precipitate or coacervate is formed which plugs the permeable region of the reservoir. Subsequently injected water or brine is forced through the low permeability region of the reservoir, increasing sweep efficiency of the waterflood, compared to a waterflood not using surfactants. Past work has demonstrated the feasibility of this new process for permeability modification in cores and sandpacks without oil present. Background work on surfactant precipitation phase boundaries and adsorption isotherms of surfactants have supported the work. A two-dimensional reservoir simulation model has outlined the promise and limitations of the method. In this part of the work, two major tasks were performed. First, corefloods were performed with oil present to demonstrate the improvement in incremental oil production, as well as permeability modification. Second, a reservoir simulation model will be proposed to further delineate the optimum strategy for implementation of the surfactant-assisted waterflooding, as well as indicate the reservoir types for which it would be most effective.

Carbon Dioxide Flooding

DOE/MC/21136–24 Improvement of CO_2 Flood Performance. Fifth Annual Report for the Period October 1, 1988-September 30, 1989. New Mexico Institute of Mining and Technology. August 1990. 388 pp. Order No. DE90000254. The report describes results obtained from the fifth year of a six-year research program designed to improve oil recovery through carbon dioxide flooding. Two tasks were addressed during the year that covered research on displacements of pure and impure CO_2 and CO_2 mobility control and flow heterogeneities. In the first task, work continued on assembling a comprehensive viscosity, density, and composition database on CO_2 crude oil, CO_2 synthetic oil, and lean gas crude oil systems. A new procedure for estimating CO_2 crude oil viscosities applicable to both single-phase and equilibrium vapor- and liquid-phase mixtures from a single, internally consistent equation was developed using the database. A series of coreflood displacements concerning the effect of solution gas and free gas on the development of miscibility, using the new foam coreflood apparatus to investigate flow through fractured rock systems are presented. Results were matched with the newly developed foam conducted to compare the performances of SAG and WAG displacements as well as pregenerated vs. in-situ generated foams. A mechanistic foam generator has been developed and will be distributed to project participants. The second task consisted of research concerned with the reduced efficiency of floods caused by nonuniformity of flow in reservoirs. Research involving the extent of the effect caused by reservoir heterogeneity and its assessment in the field includes three separate areas: (1) the mathematical description of rock heterogeneity, using the relatively new field of geostatistics with special emphasis on the correlation of geostatistical parameters with calculated sweep efficiency; (2) the history of tracer production from a well, as calculated from simulated displacements in synthetic random fields; and (3) the measurement of small-scale heterogeneities in laboratory samples of reservoir rock, with an evaluation of their effect on flood results and scaling to the field. A principal result of the experiments this year has been the quantitative definition of the variation of relative mobility on CO_2-foam with the permeability of the rock through which it flows. New apparatus has been developed for the generation and study of CO_2-foam at reservoir conditions, providing a further screening test of surfactant effectiveness.

DOE/BC/14126–16 A Study of Newton Related Nonlinear Methods in Well Test Analysis, Production Schedule Optimization and Reservoir Simulation. SUPRI TR 70. Stanford University. August 1990. 120 pp. Order No. DE90000249. The research described in this report covers the study of the use of alternative nonlinear methods in automated well test analysis, production, and injection schedule optimization and in reservoir simulation. In automated well test analysis the advantages and disadvantages of second-order partial derivatives were investigated. Newton's method is shown to be prone to difficulties, however, by adjusting the eigenvalues of the Hessian matrix the performance can be improved. In optimizing the cyclic steam injection process, Newton's method is compared with the Quasi-Newton method using a simplified model to simulate the process. The Quasi-Newton method does significantly better than Newton's method in saving function evaluations. Specific operating strategies for the process were identified: (1) the need to eliminate soak; (2) the need for greatly increased steam volumes and temperatures; and (3) the need to optimize a combination of economic objectives. The two methods were compared in reservoir simulation. Tests show that depending upon the linear scheme used, and the difficulty of the problem, the Quasi-Newton method may prove to be less expensive than Newton's method in certain cases. The study also addresses the issue of building scalable parallel reservoir simulators. Residual constraints are used to improve the robustness of the parallel matrix solution scheme. The solution of the constraint matrix is shown to be a critical point in achieving good performance on a parallel machine.

DOE/BC/14126–20 The Accurate Measurements of Heat Flux Using Thin Film Heat Flux Sensors with Application to Petroleum Engineering. SUPRI TR 74. Stanford University. July 1990. 68 pp. Order No. DE90000236. This report details how commercially-available thin film heat flux sensors may be used within the petroleum engineering laboratory to accurately measure heat flux. As with many other devices, the presence of a heat flux sensor often changes the magnitude of the quantity to be measured. The application of a sensor to a surface will disturb the flow of heat through the surface. Heat flow will be disturbed because the sensor possesses a non-zero thermal resistance, the contact between the sensor and the surface is imperfect, and the emissivity of the sensor may differ significantly from that of the surface upon which it is placed. It is possible to correct the measured heat flux for these three potentially-significant factors to obtain the true undisturbed heat flux. In this report the data reduction equations required to perform the corrections are derived for two different experimental systems. To illustrate the proper application of the sensor and the correct interpretation of the experimental results, a laboratory investigation is described. Five thin film heat flux sensors were used to study heat transfer processes occurring within a one-dimensional sandpack which was first steamflooded, then injected with a surfactant solution and a non-condensible gas to spontaneously generate steam foam. The sensors were attached to the outside of the sandpack beneath a layer of insulation. Their use allowed parameters such as the steam front velocity and inclination, and the quality of produced steam to be determined. Variations in the rates of heat transfer from the sandpack to the surroundings proved to be significant with both time and position along the one-dimensional model. The sensors proved to be valuable tools in understanding the heat transfer mechanisms occurring within the system and correctly interpreting the experimental results.

DOE/BC/14126–22 SUPRI Heavy Oil Research Program. Thirteenth Annual Report. SUPRI TR 76. Stanford University. August 1990. 144 pp. Order No. DE90000250. A theoretical solution to flow into a well via perforations is synthesized using Green's functions. The solution is three-dimensional and applies to steady-state single phase homogeneous flow. The complete solution for a cylindrical perforation involves double infinite summation and triple integration and is difficult to compute. A useful approximation is made by treating the perforation as a line-sink; this reduces the solution to a double infinite summation and a single integration. The solution contains expressions of Bessel functions and their derivatives. The infinite summation is over the order and the argument of these functions. An array of eigenvalues are first computed from an implicit equation. These eigenvalues are then used for computation of a solution. The solution involves five physical parameters: wellbore diameter, perforation diameter, perforation length, perforation density (vertical spacing) and phasing (angular spacing). These parameters influence the cost as well as the efficiency of a well completion. A sensitivity analysis can be done for an optimization of the completion design using this analytical solution. Perforation length is the most important parameter and performance improves with increasing length. Initially, even a small increase in length gives a significant improvement. Perforation density is an important parameter, but beyond an optimum number of shots per foot there is little gain in productivity ratio. This result will lead to a saving cost, since a higher shot density is generally used by industry. The phasing of perforations influences the performance. A phasing of 90° in the same horizontal plane or along a spiral gives a significant advantage over 0° phasing, and this improvement increases with an increase in perforation length.

DOE/BC/14126–26 Effect of Metallic Additives on In Situ Combustion of Huntington Beach Crude Experiments. SUPRI TR 78. 84 pp. Stanford University. August 1990. Order No. DE90000259. In this study, combustion tube runs were performed using the metallic additives: ferrous chloride ($FECl_2.4H_2O$) zinc chloride ($ZnCl_2$) and stannic chloride ($SnCl_2.5H_2O$). Soluble salts of these metals were selected from the results observed in the studies by De Los Rios. Unconsolidated cores were prepared by mixing predetermined amounts of an aqueous solution of the metal salt, Huntington Beach crude oil, Ottawa sand and clay in order to achieve the desired fluid saturations. The mixture was then tamped into the combustion tube. Dry air combustion tube runs were performed keeping the conditions of saturation, air flux, and injection pressure approximately the same during each run. The nature of the fuel formed and its impact on the combustion parameters were determined and compared with a control run, an experiment performed with no metallic additive.

DOE/BC/14126–27 Characterization of Surfactants as Steamflood Additives—SUPRI TR 79. Stanford University. September 1990. 72 pp. Order No. DE90000263. Steamflood efficiency can be increased by adding surface active agents to steam such that foam can be generated, can preferentially reduce permeability to steam in previously swept zones, and can divert the steam to undepleted regions of the reservoir. Even though the detrimental effect of oil on foam formation has been observed since the mid 1960s, most of the laboratory testing of surfactants as steamflood additives was performed with no oil present. In this study, a linear model was used to compare and characterize eight surfactants as steamflood additives under typical California conditions of moderate temperature and pressure. The evaluation of foamability was based on pressure gradient changes and steam mobility reduction along the model. Two sets of experiments were made. In the first, no oil was present in the sandpack. In the second, West Newport crude oil was used at residual saturation after steamflooding. All runs were performed under the same operating conditions. Results from the first set of runs indicated that alpha olefin sulfonates generated the strongest foam. Flow resistance due to foam increased as the alkyl chain length increased. Enrichment in disulfonate content enhanced the propagation speed of an alpha olefin sulfonate but reduced its foam strength. Significant steam mobility reduction was achieved for all surfactants tested. Relative permeability to steam was reduced to between 0.005 and 0.02 when no oil was present. Analysis of temperature and pressure profiles indicated the formation of a nitrogen foam ahead of a steam foam. This proves that nitrogen can help stabilize and maintain foam as steam condenses away from the injection port. In the presence of oil, no increase in pressure gradient was observed for any of the surfactants tested.

DOE/SF/00098–T16 A Dual-Gas Tracer Technique for Determining Trapped Gas Saturation During Steady Foam Flow in Porous Media—Topical Report. University of California. September 1990. 36 pp. Order No. DE90000260. Currently, only qualitative information is available on the actual amounts of trapped gas. To obtain quantitative measurements of trapped gas saturations, a unique experimental apparatus employing dual gas tracers has been developed. During steady foam flow in a porous medium, dilute sulfur hexafluoride (SF_6) and methane (CH_4) tracers in a nitrogen carrier are injected, and the effluent concentration is monitored by gas chromatography. The measured tracer histories are fit to a simple mass transfer model which describes any partitioning between the mobile and trapped foam phases. Tracer effluent concentrations predicted by the model are strongly influenced by the solubility of each tracer in the liquid phase. This behavior is observed in the experimental histories as well. Hence, multiple gas tracers provide a discriminating assessment of trapped gas saturation during foam flow through porous media.

Fundamental Petroleum Chemistry

NIPER–422 **Determination of Ideal-Gas Enthalpies of Formation for Key Compounds—The 1988 Project Results. Topical Report (DIPPR Project 871). National Institute for Petroleum and Energy Research. July 1990. 52 pp. Order No. DE90000247.** The results of a study aimed at improvement of group contribution methodology for estimation of thermodynamic properties of organic substances are reported. Specific weaknesses where particular group-contribution terms were unknown, or estimated because of lack of experimental data, are addressed by experimental studies of enthalpies of combustion in the condensation phase and vapor-pressure measurements. Ideal-gas enthalpies of formation are reported for 3-methylbuta-1,2-diene; 2,5-dimethylhexa-2,4-diene; acetaldoxime; N,N-diethylhydroxylamine; 1-methylpyrroliden-2-one; and phenanthrene. Solid and liquid-phase enthalpies of formation at 298.15 K are determined for benzamide. Ring corrections, group terms, and next-nearest neighbor interaction terms useful in the application of group contribution correlations are derived.

Resource Assessment Technology

DOE/BC/14000–3 **Production Potential of Unrecovered Mobile Oil Through Infield Development: Integrated Geologic and Engineering Studies—Overview. ICF Resources Incorporated and The Bureau of Economic Geology, The University of Texas. August 1990. 120 pp. Order No. DE90000255.** This report is part of a coordinated series of research efforts designed to prepare preliminary evaluations of important components of the domestic unrecovered oil resource. The specific resource of interest is the oil that is displaceable by water and remains in the Nation's reservoirs after conventional production. Integrated geologic, engineering, and economic evaluations in this series estimate future reserve additions from this unrecovered mobile oil (UMO) resource under various circumstances. The individual studies (Volumes 2 through 5) consider the effects of changes in oil prices and advances in production technology on the economic recovery potential of the UMO resource. This report (Volume 1) discusses and compares the approaches and results of the individual studies. Several recovery technologies are evaluated, including the use of waterflooding in conjunction with infill drilling to displace and produce UMO at decreased well spacings.

DOE/BC/14000–4 **An Assessment of the Reserve Growth Potential of the San Andres/Grayburg Carbonate (South Central Basin Platform) Play in Texas. ICF Resources Incorporated and The Bureau of Economic Geology. The University of Texas. August 1990. 174 pp. Order No. DE90000256.** The purpose of this study is to begin to develop an alternative approach to estimating reserve growth. This approach uses detailed geologic and engineering-based analyses to estimate the volume of economically recoverable hydrocarbons from infill drilling. This report represents the results of the first several phases of this study — the estimate of economically recoverable hydrocarbons from the San Andres/Grayburg Carbonate (South Central Basin Platform) Play, a collection of 19 fields in the Permian Basin of West Texas. This study describes the methodology that was used to determine the increase in contacted reservoir volume that results from more closely spaced infill wells, discusses the approach used to calculate recoverable oil and associated natural gas, and concludes with an economic analysis of the reserve growth potential for the play.

DOE/BC/14000–5 **An Assessment of the Reserve Growth Potential of the Clear Fork Platform Carbonate Play in Texas. ICF Resources Incorporated and The Bureau of Economic Geology, The University of Texas. August 1990. 92 pp. Order No. DE90000257.** This report presents the results of an analysis of the potential recovery of the unswept mobile oil resource in the Clear Fork Platform Carbonate Play in West Texas. This study, part of a larger analysis of several major oil plays in Texas, was performed with the objective of improving the geologic knowledge base of Texas oil plays, increasing the understanding of reservoir heterogeneity as it relates to the geologic system of a play, and refining the conceptual and analytical tools necessary for characterizing and assessing the recovery potential of the unswept mobile oil resource in these plays. The results of this work can help better define the economic potential of the U.S. unswept mobile oil resource and assist operators in improving recovery in mature Texas oil fields. The objective of this study is to determine the economic viability of infill drilling to recover unswept oil remaining in the Clear Fork Platform Carbonate Play. The geologic, engineering, and economic models used for assessing the potential recovery of the unswept mobile oil resource were adapted to conform with data availability and analysis time frames. The analysis was performed using "off the shelf" studies, available in the literature, and data obtained from public sources. This information was examined and utilized under a specified conceptual and analytical framework, but without independent, detailed geologic characterization and quantification of reservoir heterogeneity.

DOE/BC/14000–6 **An Assessment of the Reserve Growth Potential of the Frio Barrier-Strandplain Play in Texas. ICF Resources Incorporated and The Bureau of Economic Geology, The University of Texas. August 1990. 142 pp. Order No. DE90000258.** This report represents the second in a series of studies designed to quantify the potential of unrecovered mobile oil (UMO) production from infill development in several major Texas oil plays. This analysis focuses on the Frio Barrier-Strandplain Play, a major clastic oil play in the Texas Gulf Coast. The two fundamental objectives in this analysis are (1) to increase the understanding of geologic heterogeneity in the Frio Barrier-Strandplain Play as it related to hydrocarbon production, and (2) to integrate this understanding with engineering and economic analyses to quantify the economic potential of recovering hydrocarbons from the play through infill drilling. This study analyzes the potential hydrocarbon recovery from the play under two separate approaches to infield development: blanket (uniform) infill drilling and strategic (geologically targeted) infill drilling. The results from each case show that a considerable volume of oil and associated gas could be economically recovered from intensive infill development. At oil prices below $30 per barrel, however, a geologically targeted infill drilling program would contribute greater reserve additions than would result from a blanket infill development program.

BNL 43811R **A Perfluorocarbon Tracer Transport and Dispersion Experiment in the North Sea Ekofisk Oil Field. Brookhaven National Laboratory. July 1990. 80 pp. Order No. DE90000248.** A perfluorocarbon tracer (PFT) transport and dispersion experiment has been performed in the Ekofisk section of the North Sea oil fields. Fifty grams each of three PFTs were injected into a well, and 28 surrounding wells were sampled for the presence of PFT. Sampling was accomplished by initially collecting bottles of reservoir hydrocarbon gas and subsequently transferring 5 liter (gas phase) aliquots onto Capillary Adsorbent Tracer (CAT) samplers. The resulting CAT samplers were analyzed for PFT in a specially configured laboratory gas chromatograph with electron capture detection. The limit of detection for PFT as determined by standard addition experiments was circa 1 to 10 femtoliters (10-15L) per liter of sampled reservoir gas. Sampling was performed up to two years past the injection time; approximately two hundred samples were analyzed. PFT was observed only in four sampling wells at four different times, though the PFT analysis of earlier samples lack sufficient sensitivity to PFT detection due to a hydrocarbon interferent problem which was resolved during this experiment. The PFT concentrations observed in these four wells appeared to follow an exponential dilution law with a dilution half-life approximately 70 days in the reservoir.

INDEX

COMPANIES AND INSTITUTIONS

CONTENTS BY EOR PROCESS

DOE Technical Project Officers for Enhanced Oil Recovery

DIRECTORY

Name	Phone number	Name of contractor
U. S. Department of Energy Oil, Gas, and Shale Technology Mail Stop, D-116 GTN, Washington, D.C. 20545		
J. J. Stosur	301/353-2749	
Bartlesville Project Office P. O. Box 1398 Bartlesville, Oklahoma 74005		
Edith C. Allison	918/337-4390 - FTS 745-4390	Brookhaven National Laboratory Fairleigh Dickinson Laboratory Idaho National Engineering Laboratory National Institute for Petroleum and Energy Research Texas A&M University University of Oklahoma University of Texas at Austin
Jerry F. Casteel	918/337-4412 - FTS 745-4412	Columbia University Johns Hopkins University National Institute for Petroleum and Energy Research University of Texas at Austin
Alex B. Crawley	918/337-4406 - FTS 745-4406	National Institute for Petroleum and Energy Research
Robert E. Lemmon	918/337-4405 - FTS 745-4405	Colorado School of Mines National Institute for Petroleum and Energy Research Pennsylvania State University Sandia National Laboratories Southwest Research Institute University of California University of Michigan University of Texas at Austin
Chandra Nautiyal	918/337-4409 - FTS 745-4409	Geological Survey of Alabama Kansas Geological Survey National Institute for Petroleum and Energy Research University of Texas at Austin
R. Michael Ray	918/337-4403 - FTS 745-4403	Oklahoma Geological Survey
Thomas B. Reid	918/337-4233 - FTS 745-4233	Lawrence Berkeley Laboratory Lawrence Livermore National Laboratory National Institute for Petroleum and Energy Research Petrolphysics, Inc. Stanford University Union Carbide Corporation University of Southern California
Metairie Project Office 900 Commerce Road, East New Orleans, Louisiana 70123		
Jerry Ham	504/734-4906 - FTS 686-4906	Louisiana State University

Morgantown Energy Technology Center
P. O. Box 880
Morgantown, W. Va. 26505

Royal J. Watts	304/291-4218 - FTS 923-4218	Morgantown Energy Technology Center New Mexico Institute of Mining and Technology Stanford University

CHEMICAL FLOODING—SUPPORTING RESEARCH

INTERACTIONS OF STRUCTURALLY MODIFIED SURFACTANTS WITH RESERVOIR MINERALS: CALORIMETRIC, SPECTROSCOPIC, AND ELECTROKINETIC STUDY

Contract No. DE-FG22-89BC14432

Columbia University
New York, N.Y.

Contract Date: July 1, 1989
Anticipated Completion: Aug. 30, 1990
Government Award: $99,935

Principal Investigator:
P. Somasundaran

Project Manager:
Jerry F. Casteel
Bartlesville Project Office

Reporting Period: Apr. 1–June 30, 1990

Objectives

The objectives of this project are to elucidate mechanisms of adsorption of structurally modified surfactants on reservoir minerals and to develop a full understanding of the effect of the surfactant structure on the nature of the adsorbed layers at the molecular level. An additional aim is to study the adsorption of surfactant mixtures on simple well-characterized minerals and on complex minerals representing real conditions. The practical goal of these studies is the identification of the optimum surfactant structures and their combinations for micellar flooding.

Summary of Technical Progress

Adsorption of surfactants on reservoir minerals represents an economic loss in enhanced oil recovery by micellar flooding. An understanding of the mechanisms of adsorption and the effect of different parameters on adsorption is important to minimize this loss. Manipulation of surfactant structure offers the best means to control surfactant adsorption since adsorption is very sensitive to changes in structure.[1–4] In addition, surfactants used in chemical flooding processes are invariably mixtures of surfactants of different structures. Studies with well-defined surfactant mixtures of pure surfactants are needed to reliably model the behavior in actual systems. The adsorption behavior of each component from mixtures (especially in anionic–nonionic systems) needs to be explored because chromatographical adsorption of the components will not only cause loss of surfactants but will also change the compositional balance for maximum oil recovery.

Previously, the effect of position of sulfonate and methyl groups on the adsorption and micellization of two alkyl xylene sulfonates (structures are shown in experimental section) and calorimetric studies on the surfactants were reported. The studies indicated that entropy was the main driving force for micellization of the two surfactants. In the case of adsorption, enthalpy was the driving force at low adsorption densities, whereas adsorption at higher concentrations was entropy driven.

During this quarter, the surface and bulk properties of alkyl xylene sulfonate with a different position of the methyl and sulfonate groups as compared with the previous two was examined. Calorimetry was used to measure the enthalpy of micellization of the surfactant. Measurements on the enthalpy of adsorption of the surfactant are in progress and shall be reported subsequently. Also, the adsorption of different mixtures of dodecyl sulfate and ethoxylated alcohol on kaolinite is reported.

Experimental

Materials

The surfactants used in these experiments were 4C11 124 *m*-xylene sulfonate (124MXS), 4C11 135 *m*-xylene sulfonate (135MXS), and 4C11 125 *p*-xylene sulfonate (125PXS). The surfactants (obtained from ARCO Exploration and Technology Company) were specified to be at least 97% isomerically pure. Their structures are given as follows:

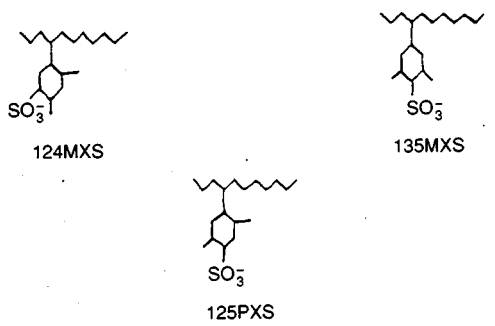

Dodecyl sulfate (purchased from Fluka Chemicals) was specified to be 99% pure and was used as received. Octaethylene glycol *n*-dodecyl ether ($C_{12}EO_8$) (purchased from Nikko Chemicals) was specified to be 98% pure and was used as received.

High-purity Linde A alumina (purchased from Union Carbide) was used. The specific surface area was determined by nitrogen adsorption to be 15 m^2/g.

A well-crystallized sample of Georgia Kaolinite (purchased from the clay repository at the University of Missouri) was subjected to an ion-exchange treatment[5] to yield homoionic kaolinite. The surface area determined by nitrogen adsorption was 8.2 m^2/g.

Experimental Conditions

All the experiments with *m*-xylene sulfonates were carried out at 43.3°C and at a constant ionic strength of 3×10^{-2} kmol/m^3 sodium chloride (NaCl). The adsorption of the anionic–nonionic surfactant mixtures was carried out at 25°C and at an ionic strength of 3×10^{-2} kmol/m^3 NaCl.

Methods

The anionic surfactants were analyzed by a two-phase titration technique.[6] The nonionic surfactant was analyzed by high-pressure liquid chromatography (HPLC) with refractive index detection. The stationary phase was a C_{18}-bonded silica column, and the mobile phase was a 90:10 mixture of acetonitrile and water.

Calorimetric experiments were performed with an LKB 2107 differential microcalorimetry system. The instrument and its working principles were described in a previous quarterly report.[7]

The electrokinetic potential of the mineral was measured with a Zeta Meter Model D system.

Results

Adsorption, Zeta Potential, and Surface Tension of 125PXS

The adsorption isotherm obtained for 125 *p*-xylene sulfonate on alumina was studied, and the isotherm is shown in Fig. 1. Also, for comparison, the isotherms of the *m*-xylene sulfonate are shown in the same plot. As shown in the figure, the adsorption of 125PXS is the same as that of 135MXS, and both are higher than that of 124MXS. The difference between 125PXS and 135MXS is the position of the methyl groups. The sulfonate position is the same for both surfactants. However, the sulfonate for 124MXS is closer to the alkyl chain. The position of sulfonate is more important than that of methyl groups with respect to the surfactant adsorption. The charge characteristics of 125PXS

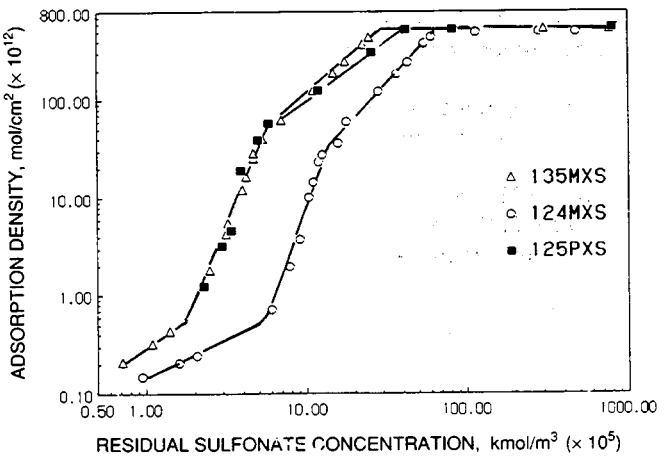

Fig. 1 Adsorption of 125PXS, 124MXS, and 135MXS on alumina.

were investigated by measuring the zeta potential of alumina after the surfactant adsorption and are shown in Fig. 2 along with the results obtained for 124MXS and 135MXS. The zeta potential is the same for all three surfactants, which indicates that the structural variation has no measurable effect on the charge of the surfactants.

For the study of the solution behavior of 125PXS, surface tension of the surfactant solution was measured as a function of concentration; the results are given in Fig. 3. The critical micelle concentration (CMC) of 125PXS is $5.3 \times 10^{-4} M$ as compared with 3.3×10^{-4} for 135MXS and 6.3×10^{-4} for 124MXS. The solution behavior is more sensitive to the changes in structure as compared with the adsorption characteristics. Microcalorimetry was used to measure the enthalpy of micellization of 125PXS, and the results are discussed.

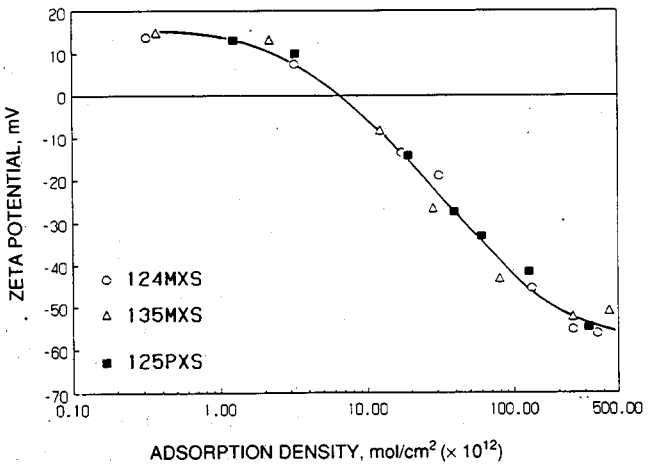

Fig. 2 Zeta potential of alumina after adsorption of 125PXS, 124MXS, and 135MXS.

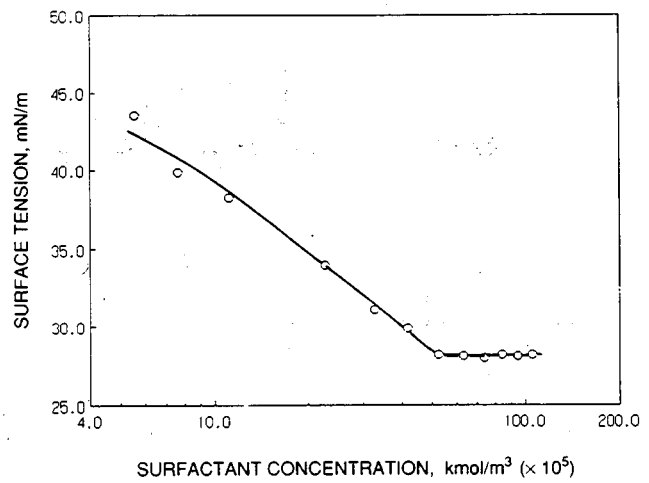

Fig. 3 Surface tension of 125PXS.

Enthalpy of Micellization of 125PXS

Heat of dilution data for premicellar and micellar 125PXS solutions are given in Tables 1 and 2, respectively.

TABLE 1

Heat of Dilution of Premicellar Solutions at 43.3°C and 3×10^{-2} kmol/m³ NaCl

C_{init}, kmol/m³	C_{fin}, kmol/m³	H_{dil}, cal/mol
2.86×10^{-4}	1.43×10^{-4}	−363
2.86×10^{-4}	1.42×10^{-4}	−348
3.98×10^{-4}	1.98×10^{-4}	−365
3.98×10^{-4}	2.00×10^{-4}	−344
		−354

TABLE 2

Heat of Dilution of Micellar Solutions at 43.3°C and 3×10^{-2} kmol/m³ NaCl

C_{init}, kmol/m³	C_{fin}, kmol/m³	Q_{dil}, cal	H_m, cal/mol
1.06×10^{-3}	5.2×10^{-4}	5.3×10^{-4}	−1652
1.06×10^{-3}	5.1×10^{-4}	5.0×10^{-4}	−1677
8.52×10^{-4}	4.3×10^{-4}	4.96×10^{-4}	−1685
			−1671

The dilution of premicellar solutions results in an exothermic change of −354 cal/mol and is due to dilution of sulfonate monomers. For the dilution of micellar solutions, demicellization accounts for the bulk of the heat change, which, for 125PXS, is endothermic. In addition to demicellization, dilution of micellar solutions will result in dilution of micelles if the final concentration is above the CMC or dilution of monomers if it is below CMC.

For the calculation of the enthalpy of micellization, experiments were designed so that correction for dilution of micelles was not required (i.e., micellar solutions were diluted to below the corresponding CMC). The values obtained in this manner (column 3 of Table 2) were then corrected for monomer dilution using the value of −354 cal/mol from Table 1 and assuming pseudo-phase separation at a CMC of 5.3×10^{-4} kmol/m³. Mathematically, this can be expressed as

$$H_m = -\frac{Q_t - H_s C_i V_i}{(C_i - CMC)\, V_i}$$

where H_m = enthalpy of micellization
H_s = enthalpy of monomer dilution
Q_t = total heat change measured
C_i = surfactant concentration before dilution
V_i = volume of surfactant solution before dilution

The H_m values are given in column 4 of Table 2 and show excellent consistency with a mean value of −1671 cal/mol. Since the standard state of micelles is defined to be the state of infinite dilution (i.e., CMC) and the dilution measurements are carried out in the region of the CMC, the value of −1671 cal/mol is approximately H_m^o.

Surfactant	Enthalpy of micellization, cal/mol
124MXS	−774
135MXS	−1091
125PXS	−1671

The enthalpy of micellization of 125PXS is more exothermic than that of the other two surfactants. Note that the enthalpy of 125PXS is more than that of 135MXS even though the CMC of 135MXS is lower. This indicates that the entropy of micellization of 125PXS is lower than that of 135MXS and hence results in its higher CMC.

Adsorption from Surfactant Mixtures

The effect of mixing the anionic and nonionic surfactants on the adsorption behavior of individual components is shown in Figs. 4 and 5. The isotherms in these figures have been divided into two regions, one on each side of mixed CMCs in the solution to facilitate the explanation of the results.

Adsorption isotherms—Region I. The isotherms for the adsorption of sodium dodecyl sulfate (SDS) from mixtures of different composition are shown in Fig. 4, whereas those of $C_{12}EO_8OH$ are plotted in Fig. 5. As shown in Fig. 4, the affinity of SDS to the surface is enhanced by the presence of ethoxylated alcohol ($C_{12}EO_8$), as indicated

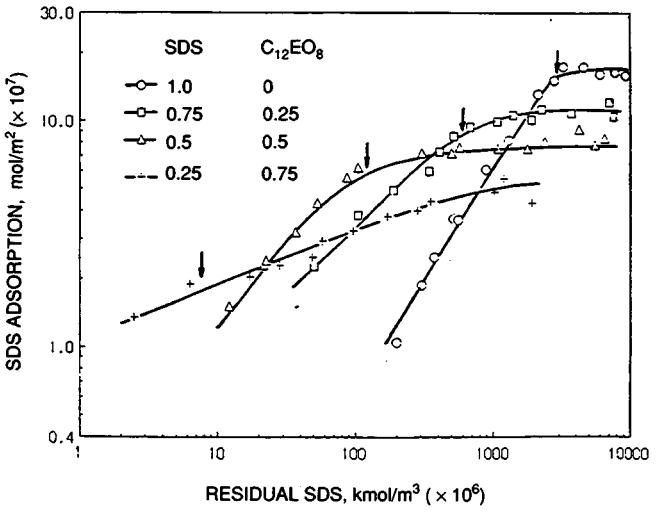

Fig. 4 Isotherms for the adsorption of sodium dodecyl sulfate (SDS) from SDS–$C_{12}EO_8$ mixtures on kaolinite. (Ionic strength, 0.03*M* NaCl; pH, 5; T, 25°C.)

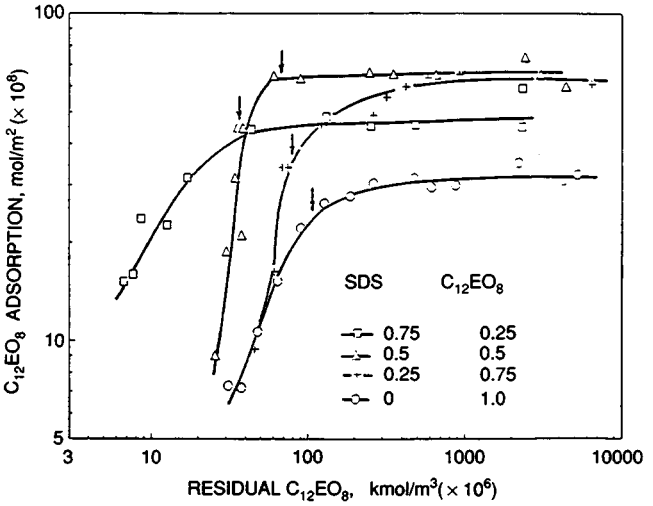

Fig. 5 Isotherms for the adsorption of $C_{12}EO_8$ from SDS–$C_{12}EO_8$ mixtures on kaolinite. (Ionic strength, 0.03*M* NaCl; pH, 5; T, 25°C.)

by the continuous shift of SDS isotherms toward the left with an increase in the molar ratio of $C_{12}EO_8$. This can be explained in terms of the coadsorption of SDS and $C_{12}EO_8$, as shown schematically in part a of Fig. 6, where SDS adsorption is assisted, in addition to its electrostatic interaction with the positive sites on kaolinite, by the chain–chain interaction with the adjacently adsorbed $C_{12}EO_8$. Because of the free energy gain from such a chain–chain interaction, the residual concentration, or the chemical potential, of SDS required to achieve a certain level of adsorption is reduced; this results in a shift of the isotherms toward the left.

Another feature to be noted on the SDS adsorption isotherm is that the slope of the isotherm decreases as the molar ratio of $C_{12}EO_8$ is increased. For pure SDS adsorption on kaolinite, a slope of 1 is obtained on a logarithmic

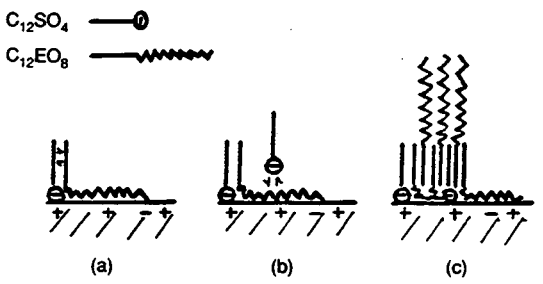

Fig. 6 Schematic representation of the mechanism of surfactant mixture adsorption on kaolinite. (a) Chain–chain interaction between adjacently adsorbed sodium dodecyl sulfate (SDS) and ethoxylated alcohol ($C_{12}EO_8$) molecules results in enhanced adsorption in the lower concentration range (pre-critical micelle concentration region) for both surfactants. (b) Electrostatic hindrance for further SDS adsorption results from the masking of the positive sites on kaolinite by ethylene oxide chain adsorption. (c) Formation of mixed surfactant clusters and abstraction of $C_{12}EO_8$ hydrocarbon chains into the clusters.

plot, which indicates the absence of lateral chain–chain interaction.[8] A fractional value of slope, as shown in Fig. 4, suggests that SDS experiences electrostatic hindrance resulting possibly from the masking of the positive sites by ethylene oxide chains adsorbed at the interface (part b of Fig. 6).

The adsorption of $C_{12}EO_8$, similar to that of SDS, is enhanced by the presence of SDS as seen from a continuous shift in the isotherm to the left with increase in the molar ratio of SDS. This result can again be attributed to the chain–chain interaction. It is conceivable that, because of chain–chain interaction between adsorbed SDS and $C_{12}EO_8$, mixed surfactant clusters will be formed at the interface. These mixed surfactant clusters, serving as hydrophobic pools, enhance the adsorption of $C_{12}EO_8$ by abstracting the hydrocarbon chains of the highly surface-active nonionic surfactant leaving the ethylene oxide segments protruding into the bulk solution, as is schematically shown in part c of Fig. 6.

Adsorption isotherms—Region II. As shown in Fig. 3, in Region II (above CMC) the adsorption of SDS alone reaches a plateau, whereas in the presence of $C_{12}EO_8$, adsorption density of SDS continues to increase even above CMC. This is because in mixed surfactant systems, unlike in single surfactant solutions, the monomer concentration of anionic surfactant increases above CMC, whereas that of the nonionic surfactant decreases.[9,10] A consistent decrease of SDS adsorption in Region II is observed as the molar ratio of $C_{12}EO_8$ in the mixture increases. This can be attributed to: (a) reduced SDS monomer concentration as the result of mixed micellization with $C_{12}EO_8$ as indicated by the decrease in CMC with increase in the molar ratio of $C_{12}EO_8$ and (b) masking of the positive sites that are responsible for SDS adsorption by the ethylene oxide chains of the adsorbed $C_{12}EO_8$.

In the case of nonionic surfactant, since the monomer concentration decreases with increase in the total surfactant concentration,[9,10] the isotherms of $C_{12}EO_8$ will be expected to pass through a maximum at mixed CMC. However, as shown in Fig. 5, $C_{12}EO_8$ adsorption isotherms in Region II are either flat or have a positive slope. This can be attributed to the increased affinity of $C_{12}EO_8$ toward the surface modified by the adsorption of SDS. As shown in Fig. 4, the adsorption of SDS increases even above mixed CMC. Such continued modification of the interface apparently outweighs the effect of decrease in $C_{12}EO_8$ monomer concentration. Figure 5 also shows that the plateau adsorption density value of $C_{12}EO_8$ is, in all cases, enhanced by the presence of SDS. Such an enhancement can be accounted for, as explained earlier, by the abstraction of additional $C_{12}EO_8$ chains into the mixed surfactant clusters at the interface (see part c of Fig. 6). Such hydrocarbon chain abstraction is apparently highly dependent on the organization of the mixed surfactant clusters at the interface, and therefore maximum adsorption increase occurs at a certain molar ratio between the two surfactants. As shown in Fig. 5, the maximum $C_{12}EO_8$ adsorption in Region II occurs at about 1:1 molar ratio between SDS and $C_{12}EO_8$. The dependence of $C_{12}EO_8$ hydrocarbon chain abstraction on the organization of mixed surfactant clusters is also revealed by the change in the slope of $C_{12}EO_8$ isotherms in Region I. As shown in Fig. 5, the slope of the adsorption isotherms increases in the presence of SDS with the maximum slope occurring around 1:1 molar ratio, which indicates the most compact arrangement of the adsorbed surfactants in the cluster, which eventually leads to maximum $C_{12}EO_8$ abstraction as shown by the highest plateau adsorption density value at this ratio.

The theory of abstraction of the hydrocarbon chain of $C_{12}EO_8$ into the hydrophobic pool formed by the clusters of mixed surfactant is also supported by the (skin) flotation results. The floatability of kaolinite was found to decrease as the adsorption density of $C_{12}EO_8$ increased in the presence of SDS adsorption (Fig. 7), which suggests orientation of ethylene oxide chains toward the bulk.

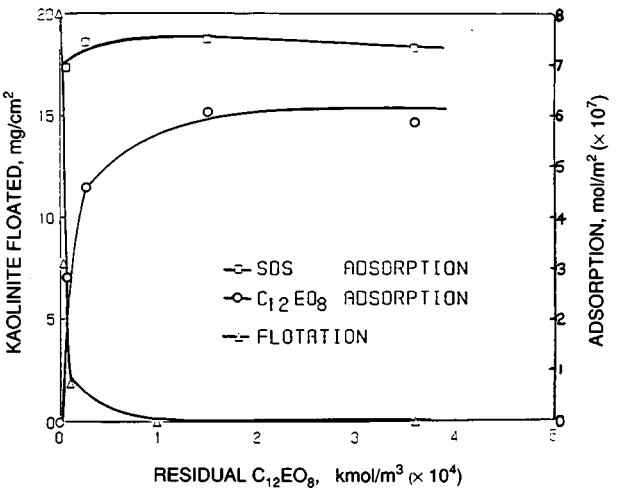

Fig. 7 Skin flotation of kaolinite after mixed surfactant adsorption. Sodium dodecyl sulfate (SDS) concentration fixed at 1.0 m*M*. (Ionic strength 0.03*M* NaCl; pH, 5; T, 25°C.)

References

1. P. Somasundaran, R. Middleton, and K. V. Viswanathan, in *Structure/Performance Relationship in Surfactants*, M. J. Rosen (Ed.), pp. 270-290, ACS Symposium Series, No. 253 (1984).
2. N. M. van Os, G. J. Danne, and T. A. B. M. Bolsman, *J. Coll. Interface Sci.*, 115: 402 (1987).
3. N. M. van Os, G. J. Danne, and T. A. B. M. Bolsman, *J. Coll. Interface Sci.*, 123: 267 (1988).
4. M. J. Rosen, Z. H. Zhu, B. Gu, and D. S. Murphy, *Langmuir*, 4: 1273 (1988).
5. P. A. Siracusa and P. Somasundaran, *J. Coll. Interface Sci.*, 114: 184 (1986).
6. Z. Li and M. J. Rosen, *Anal. Chem.*, 53: 516 (1981).
7. P. Somasundaran, *Interactions of Structurally Modified Surfactants with Reservoir Minerals: Calorimetric, Spectroscopic and Electrokinetic Study*, October 15, 1989–January 15, 1990, quarterly report submitted to the Department of Energy.

8. P. Somasundaran and D. W. Fuerstenau, *J. Phys. Chem.*, 70: 90 (1966).
9. Edward Fu, Ph.D. Thesis, Columbia University, New York, 1987.
10. D. N. Rubing, in *Solution Chemistry of Surfactants*, K. L Mittal (Ed.), Vol. 1, p. 337, Plenum Press, New York, 1978.

DEVELOPMENT OF IMPROVED MOBILITY-CONTROL METHODS

Cooperative Agreement DE-FC22-83FE60149, Project BE4C

National Institute for Petroleum and Energy Research
Bartlesville, Okla.

Contract Date: Oct. 1, 1983
Anticipated Completion: Sept. 30, 1990
Funding for FY 1990: $200,000

Principal Investigators:
Troy R. French
Hong W. Gao

Project Manager:
Jerry F. Casteel
Bartlesville Project Office

Reporting Period: Apr. 1–June 30, 1990

Objectives

The objectives of this research are to determine the applicability of low-molecular-weight polymer gels for mobility-control applications and to determine the effects of permeability and depth of gel penetration on oil recovery efficiency.

Summary of Technical Progress

Screening tests showed that polymer–Al(III) gel systems prepared with a low-molecular-weight (400,000 daltons) polyacrylamide polymer, which was 20% hydrolyzed, gelled at the fastest rate and retained the strongest gel strength among the polymer–Al(III) gel systems prepared with four low-molecular-weight (400,000 daltons) polyacrylamide polymers, which were 10, 20, 30, and 40% hydrolyzed, respectively.

Different extents of deep gel penetration in the high-permeability layer were obtained from simulation runs on a two-layer, cross-section reservoir model ($k_v/k_h = 0.1$) with different gelation rate constants, different slug sizes, different injection rates, and different chemical concentrations of the gel system. Because of the high cross flow of the gel system from the high-permeability layer to the low-permeability layer, the permeability in the low-permeability layer was also reduced to some degree. Attempts to correlate the incremental oil recovery with the depth of gel penetration were unsuccessful because of different extents of permeability reduction that occurred at different locations in the low-permeability layer.

Application to EOR

Mechanical degradation of high-molecular-weight polyacrylamides is a problem in field applications. A mobility-control system based on cross-linking a low-molecular-weight polyacrylamide may be much less susceptible to mechanical degradation. A permeability modification simulator is very useful to facilitate the design of treatments and assess potential fields for permeability modification treatments using gelled polymers.

Screening Tests

The effect of the degree of hydrolysis on gelation kinetics and gel strength was studied with four low-molecular-weight (400,000 daltons) polyacrylamide polymers, which were 10% (HPAM1-10), 20% (HPAM1-20), 30% (HPAM1-30), and 40% (HPAM1-40) hydrolyzed, and an aluminum citrate cross-linker in 53 meq/L NaCl (pH = 7) at room temperature (22.4°C). Polymer concentrations used ranged from 6,000 to 17,000 ppm, and Al(III) concentrations used ranged from 25 to 2,800 ppm. All the samples were agitated and aged under a nitrogen atmosphere in a bottle. Viscosity measurements were used to monitor the progress of gelation.

Typical results of the effect of the degree of hydrolysis on gelation kinetics and gel strength are shown in Fig. 1 for

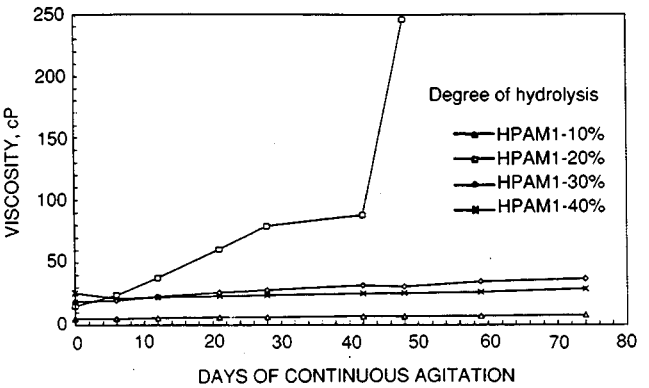

Fig. 1 Effect of the degree of hydrolysis on gelation rate and gel strength of polymer–Al(III) gel systems at 22.4°C [12,000-ppm polymer–350-ppm Al(III) in 53 meq/L NaCl at pH = 7.0; shear rate, 5.96 s^{-1}].

four gel systems, each of which contained 12,000 ppm of polymer and 350 ppm of Al(III). Among the four gel systems, the one prepared with HPAM1-20 gelled at the fastest rate and retained the highest gel strength. Similar results were observed for all other gel systems prepared at polymer concentrations from 12,000 to 17,000 ppm with HPAM1-10, HPAM1-20, HPAM1-30, and HPAM1-40 and Al(III) concentrations from 350 to 1,400 ppm. Among the samples prepared at a polymer concentration of 6,000 ppm and Al(III) concentrations from 50 to 2,800 ppm, only samples prepared with HPAM1-20 formed gels after 53 d of continuous agitation under a nitrogen atmosphere. These results indicated that the optimal degree of hydrolysis for making weak gels was about 20%. Of these systems, those which contained 15,000 to 17,000 ppm of HPAM1-10 and 350 to 700 ppm of Al(III), 12,000 to 15,000 ppm of HPAM1-30 and 350 ppm of Al(III), 12,000 to 17,000 ppm of HPAM1-40 and 350 ppm of Al(III), and 12,000 ppm of HPAM1-40 and 700 ppm of Al(III) formed weak gels (viscosity lying between 10 and 100 cP at 5.96 s^{-1}) after 74 d of continuous agitation under a nitrogen atmosphere. Gel systems prepared with 12,000 ppm of HPAM1-10 and 350 to 1,400 ppm of Al(III) formed very weak gels (viscosity lower than 10 cP at 5.96 s^{-1}). These gel systems had the potential for use as mobility-control agents.

Increasing the polymer (Fig. 2) or cross-linker concentration (not shown) increased the gelation rate and gel strength. After 53 d of continuous agitation under a nitrogen atmosphere, those gel systems which contained 350 ppm of Al(III) and 12,000 to 17,000 ppm of HPAM1-20 (Fig. 2) and 8,000 ppm of HPAM1-20 and 1,400 ppm of Al(III) formed visible gels (viscosity higher than 100 cP at 5.96 s^{-1}). These systems were too viscous to be used as mobility-control agents.

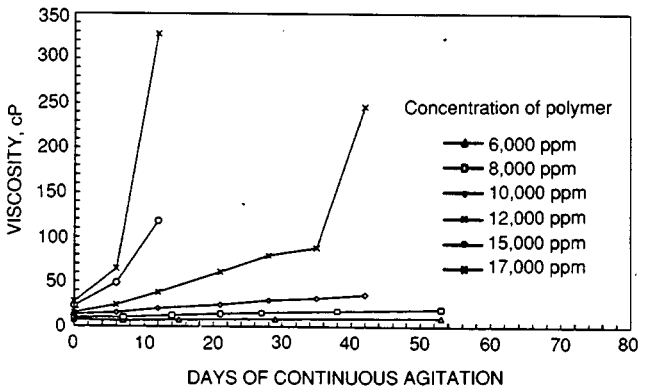

Fig. 2 Effect of polymer concentration on gelation rate and gel strength of HPAM1-20–350-ppm Al(III) gel systems at 22.4°C [HPAM1-20–350-ppm Al(III) in 53 meq/L NaCl at pH = 7.0; shear rate, 5.96 s^{-1}].

Effect of Shear on Gelation

For the development of a mixing procedure that will produce constant rheological properties, the effect of shear on gelation kinetics and gel strength of two HPAM1-20–aluminum citrate gel systems in 53 meq/L NaCl at pH = 7.0 was investigated in a glass bead pack and in a 1200-cm, 0.125-in.-OD tubing. The glass bead pack was used for tests at high shear conditions (apparent shear rates higher than 800 s^{-1} or flow rates higher than 1640 ft/d), and the 1200-cm tubing was used for tests at low shear conditions (apparent shear rates ranging from 50 to 195 s^{-1}). The glass bead pack, which was 7.5 cm in length and 0.4 cm in diameter, had a brine permeability of 4200 mD and a porosity of 35%. Beads used to pack the glass bead pack had a particle size distribution ranging from 170 to 200 mesh. A 390-mesh screen was placed at each end of the glass bead pack to retain the bead particles.

A gelation test for a gel system that contained 12,000 ppm of HPAM1-20 and 200 ppm of Al(III) in 53 meq/L NaCl at pH = 7.0 was conducted in the glass bead pack. Before injection through the porous medium, the gel system was agitated in a bottle for 3 d and was filtered through a 325-mesh screen. Viscosity measurements using a Contraves viscometer were made to monitor the progress of gelation. After one, two, and more than fifteen times (3 d) of passing through the porous medium, no viscosity enhancement was observed, which indicated that no gelation occurred in the porous medium at high shear conditions. However, for the same gel system agitated in a bottle for 3 d, the viscosity measured at a shear rate of 5.96 s^{-1} increased from 16.2 to 18.5 cP, an increase of 14%. A separate gelation test using the same gel system in a Brookfield viscometer also showed that the viscosity increased by 20% after 3 d of continuous shearing at a shear rate of 46 s^{-1}. These results indicated that a high shear had an adverse effect on the gelation of the gel system tested.

Gelation tests for another gel system that contained 10,000 ppm of HPAM1-20 and 200 ppm of Al(III) in 53 meq/L NaCl at pH = 7.0 were conducted in a bottle under continuous agitation and in a flow system that contained about 1200 cm of 0.125-in.-OD tubing at apparent shear rates between 50 and 195 s^{-1}. Results are shown in Fig. 3. The average apparent shear rate used

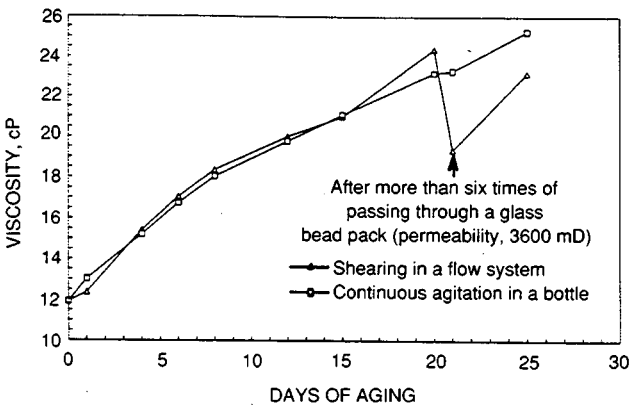

Fig. 3 Effect of shearing and agitation on the gelation rate of a 10,000-ppm HPAM1-20–200-ppm Al(III) gel system (53 meq/L NaCl at pH = 7.0) at 22°C shear rate, 5.96 s^{-1}.

during the first to sixth day and fifteenth to twentieth day was about 55 s^{-1}. During the sixth to fifteenth day, the apparent shear rate used was about 195 s^{-1}. As shown in Fig. 3, the rate of gelation reaction for the gel system under shearing condition in the flow system was about the same as that in a bottle under continuous agitation. These results indicated that, for a gel system that had a slow gelation rate, the rate of gelation reaction in a bottle under continuous agitation would be close to that in a flow system under low shear condition. The progress of gelation reaction under continuous agitation in the bottle is being monitored until a constant rheological property is obtained.

For a test to determine whether the gel system was degradable and injectable through a porous medium, the preceding gel system was injected through a glass bead pack (7.51 cm in length and 0.4 cm in diameter; brine permeability, 3600 mD) at apparent shear rates higher than 1000 s^{-1} (highest apparent shear rate used was about 2200 s^{-1}) after 20 d of continuous circulation in the flow system. After more than six passes, the viscosity of the gel system measured at a shear rate of 5.96 s^{-1} decreased from 24.4 to 19.4 cP (as shown in Fig. 3), which indicates that some of the cross-linking bonds were broken under a high shear condition. This test also demonstrated that the gel system (more than 1460 PV) was injectable through a porous medium. After the high shear condition was removed, gelation reaction resumed, and the viscosity increased from 19.4 to 23.42 cP (Fig. 3) after 4 d of shearing in the flow system at low shear condition.

Permeability Modification

So that the effect of the depth of gel penetration on oil recovery could be investigated, simulation runs using different gelation rate constants, different slug sizes, different injection rates, and different chemical concentrations of the gel system were conducted on a two-dimensional, two-layer, cross-section reservoir model (k_1, 100 mD; k_2, 1000 mD; k_v/k_h, 0.1) that was 500 ft in the x direction and 30 ft in the z direction. The grid block used was 10 ft in the x direction and 15 ft in the z direction. For a deep placement of gel, no polymer adsorption was assumed in all simulation runs. Parameters (other than those mentioned here) used in all simulation runs have been reported.[1] Typical results of the distributions of permeability reduction factors in both layers and oil recoveries are shown in Figs. 4 and 5, respectively, for two cases. Concentrations of dichromate, thiourea, and polymer used in both cases (runs 6 and 7b) were 500, 700, and 1500 ppm, respectively. Gelation rate constants used in runs 6 and 7b were 1×10^{-4} and 1×10^{-6} ppm^{-3} d^{-1}, respectively. As shown in Fig. 4, permeability in both high-permeability and low-permeability layers was reduced by polymer gel. This was caused by the cross flow of the gel system from the high-permeability layer to the low-permeability layer. These phenomena were seen in all 14 simulation runs. In all three

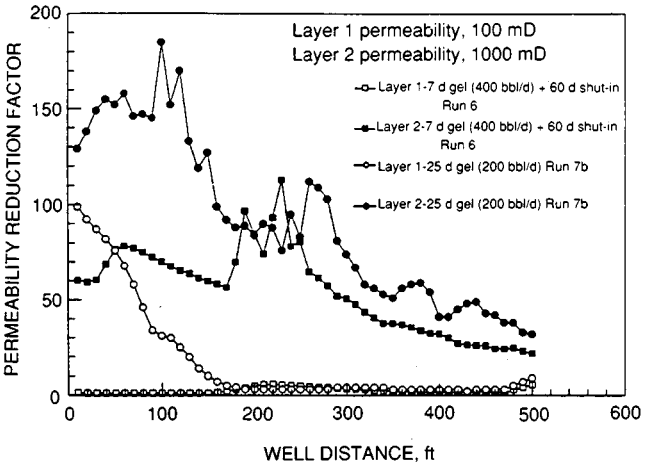

Fig. 4 Distributions of permeability reduction factors in both layers (gel treatments were initiated at 200 d).

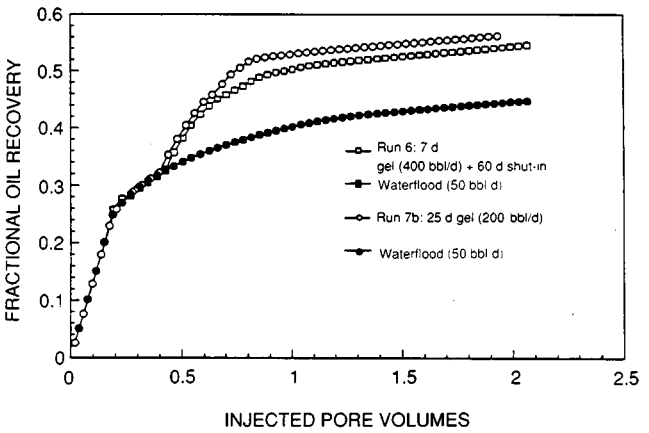

Fig. 5 Fractional oil recovery as a function of injected pore volumes (1 PV, 53,428 bbl; gel treatments were initiated at 200 d).

cases, the permeability reduction factor in the injection well grid block of the low-permeability layer was 90 or more. The higher incremental oil recovery from run 7b, as compared with that from run 6 (Fig. 5), was believed to be caused by a higher ratio of permeability-reduction factors in both layers that occurred in a higher oil saturation zone (between 190 and 310 ft from the injection wellbore). Because of differences in the extent of permeability reduction that occurred at different locations in the low-permeability layer, attempts to correlate the incremental oil recovery with the depth of gel penetration were made on the basis of different ratios (10 to 50) of the permeability-reduction factors in both layers. Unfortunately, good correlation could not be obtained. Further simulation runs will be conducted with an assumed permeability reduction in the high-permeability layer only.

Reference

1. H. W. Gao and M. M. Chang, *A Three-Dimensional, Three-Phase Simulator for Permeability Modification Treatments Using Gelled Polymers*, DOE Report NIPER-388, 1990 (NTIS order No. DE90000227).

DEVELOPMENT OF IMPROVED ALKALINE FLOODING METHODS

Cooperative Agreement DE-FC22-83FE60149, Project BE4B

National Institute for Petroleum and Energy Research
Bartlesville, Okla.

Contract Date: Oct. 1, 1983
Anticipated Completion: Sept. 30, 1990
Funding for FY 1990: $140,000

Principal Investigator:
Troy R. French

Project Manager:
Thomas B. Reid
Bartlesville Project Office

Reporting Period: Apr. 1–June 30, 1990

Objective

The objective of this research is to develop cost-effective and efficient chemical flooding formulations with surfactant-enhanced, low-pH alkaline systems. Specific tasks toward achieving this objective for FY90 are: (1) to investigate the applicability of alkaline–surfactant flooding for use in reservoirs with crude oils having very low acid numbers, (2) to test commercially-available enhanced oil recovery (EOR) chemicals that could be used in a pilot alkaline flood, and (3) to compare the effect of divalent ions on surfactant loss and the transient interfacial tension (IFT) behavior of carbonate–surfactant systems with the effects previously observed for carbonate–phosphate–surfactant mixtures.

Summary of Technical Progress

Oil recovery tests and IFT experiments indicated that surfactant-enhanced alkaline flooding is applicable to low-gravity, low-acid-number crude oils. These results were obtained with two Kansas crude oils. The total acid numbers of the two oils were 0.01 and 0.27 mg potassium hydroxide (KOH)/g oil.

Monohydrogen phosphate (HPO_4^{2-}) ions improved the IFT behavior of surfactant-enhanced alkaline formulations very little, if any. The effect of HPO_4^{2-} ions on surfactant adsorption was significant. In experiments conducted at equal ionic strengths, adsorption was reduced 30% with HPO_4^{2-} ions.

Application to Enhanced Oil Recovery

Prior work has shown that the acidic content of a crude oil, which is usually expressed as acid number, is not necessarily a reliable indicator of how amenable an oil is to alkaline flooding.[1] If surfactant-enhanced alkaline flooding methods can be applied to recover crude oils with low acid content, then the target resource for this technology would be greater than was previously thought.

Interfacial Tension Measurements with a Nonacidic Crude Oil

Dynamic IFT experiments were performed with crude oil from the Bartlesville sand in Allen County, Kans. This oil has a total acid number (TAN) that is near zero (0.01 mg KOH/g oil). The purpose of the experiments was to separate the effects of weak alkali and surfactant in IFT reduction with a very low TAN crude oil. The experiments were performed with an anionic surfactant (Petrostep B-100) that is sparingly soluble at the upper range of ionic strength values of the mixtures tested. The pH of the test solutions was either unadjusted (about pH 6.3) or pH 9.5. The pH was adjusted with an appropriate carbonate mixture. Total calculated ionic strength of the mixtures ranged from 0 to 0.748. The actual ionic strength values for the carbonate mixtures may vary from the calculated values as the result of equilibrium reactions between the carbonate ion species.

The effect of the carbonate mixture on IFT was tested over a broad range of ionic strengths, 0.238 to 0.648. All the IFT values obtained with the oil and carbonate mixtures were above 10 mN/m. These results were not unexpected since the very low TAN of the oil should result in very low reactivity to weak alkali.

The IFT measurements were also conducted with a low concentration (0.1%) of surfactant and ionic strengths from 0.051 (0.3% NaCl) to 0.510*M* (3.0% NaCl). Because of solubility limitations, the IFT of this surfactant was not measurable in the 3% NaCl solution. The results are shown in Fig. 1. The best results with the pH 6.3 (pH unadjusted) surfactant mixture were obtained at ionic strengths of 0.205 (1.2% NaCl) and 0.410 (2.4% NaCl). In 2.4% NaCl, the transient IFT was very slowly reduced over a period of 169 min from an initial IFT of 773 μN/m to an equilibrium value of 306 μN/m.

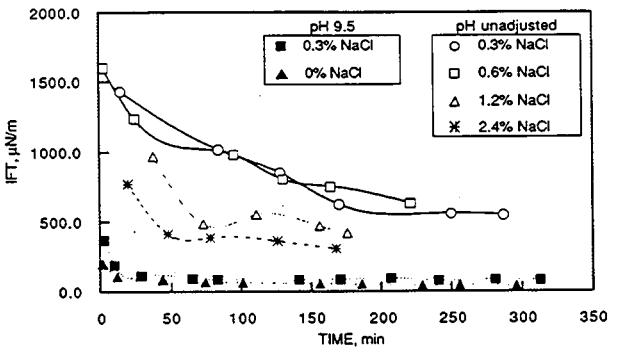

Fig. 1 Dynamic interfacial tension of a crude oil with total acid number of 0.01 mg KOH/g oil and 0.1% Petrostep B-100 surfactant, 30°C.

Figure 1 also shows the transient IFT behavior of the surfactant mixture at pH 9.5. The ionic strengths of the pH 9.5 carbonate mixtures were 0.238 (no added salt) and 0.289 in 0.3% NaCl. As shown in Fig. 1, the IFT values of the surfactant in weak alkali were much lower than those for similar ionic strength surfactant mixtures that did not contain alkali. At pH 9.5 and ionic strength 0.238 (no added salt), the initial IFT value was 202 μN/m, and this decreased to an equilibrium value of 86 μN/m after 44 min. An increase in the ionic strength to 0.289 with added salt caused slightly higher IFT values. All these experiments were performed at 30°C, which is near reservoir temperature.

The IFT experiments were also performed at 52°C with the same crude oil and weak alkali at similar ionic strengths. Those results are shown in Fig. 2. At the higher temperature, lower IFT values were obtained from 0.289 (alkali in 0.3% NaCl) to 0.409 (alkali in 1.0% NaCl) values of ionic strength. This effect of increasing temperature yielding lower initial IFT values and lower equilibrium IFT values has been observed with other slightly acidic crude oils and alkali–surfactant mixtures.

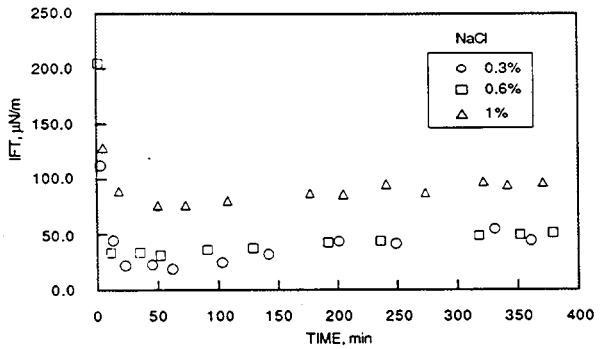

Fig. 2 Dynamic interfacial tension of a crude oil with total acid number of 0.01 mg KOH/g oil and 0.1% Petrostep B-100 surfactant, pH 9.5, 52°C.

A conclusion based on these results is that low, but not necessarily ultralow, IFT values can be obtained with slightly acidic crude oils and mixtures that contain dilute concentrations of surfactant under weakly alkaline conditions. Furthermore, the IFT obtained under alkaline conditions is lower than that obtained with surfactant alone or alkali alone. The conditions studied covered a broad range of ionic strengths.

Oil Recovery Tests

Recent results,[2] which indicate that surfactant-enhanced alkaline flooding is applicable to low-gravity, low-acid-number crude oils, were confirmed by the results of an oil recovery test performed with crude oil from the Densmore (Kansas) oil field. The Densmore crude has an acid number of 0.27 mg KOH/g oil, which is low, and a gravity of 19.8° API. The oil recovery test was designed from previous results that indicated IFT values favorable to the mobilization of residual oil.[3] The coreflood was conducted with a surfactant-enhanced weakly alkaline system (pH 9.5). The salinity was 0.6% NaCl, which is the optimal salinity for low IFT. The initial IFT between this chemical system and the Densmore crude was 6.9 μN/m, which decreased to about 1 μN/m within a few minutes.

A Berea sandstone core was first saturated with crude oil (S_o = 83.9%) and then waterflooded to residual oil saturation (S_{owf} = 43.8%). Chemical flooding followed the waterflood and reduced the oil saturation to 29.5%. Figure 3 shows the changes in oil cut and oil saturation that occurred during the chemical flood. The oil recovery efficiency of the chemical flood was 32.5% of the oil that remained after waterflood.

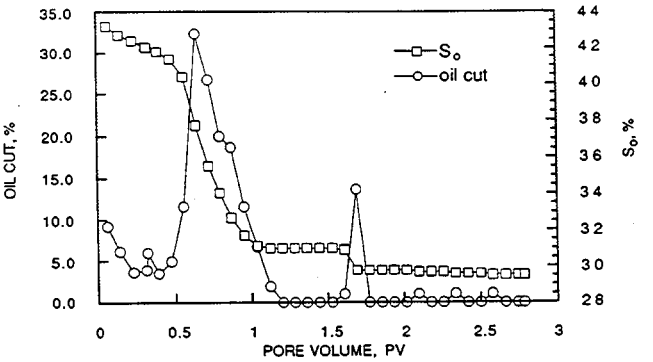

Fig. 3 Oil recovery of a crude oil with total acid number of 0.27 mg KOH/g oil, 52°C.

Effects of Monohydrogen Phosphate Ion Species on Interfacial Tension and Adsorption

Carbonate mixtures are effective for the removal of calcium ions, and to a lesser extent magnesium ions, from reservoir brines by precipitation reactions.[4] However, low concentrations of divalent ions still remain in a reservoir after an alkaline preflush. Divalent ions that remain in solution may have deleterious effects that might include degradation of IFT behavior and surfactant losses by precipitation and adsorption.

Between pH 8.5 and 10.5, a large fraction of phosphate ions exists in the form of HPO_4^{2-} which readily complexes cations.[5] The resultant complexing of calcium and magnesium ions by HPO_4^{2-} may help protect the low concentration of synthetic surfactant used in surfactant-enhanced alkaline floods from the deleterious effects of the divalent ions.

The effect of divalent ions on IFT behavior was compared for carbonate and carbonate–phosphate systems. The experiments were conducted at pH 10.5, where most of the phosphate ions exist as the HPO_4^{2-} species. The formulation that included orthophosphate ions contained 0.0104*M* $NaHCO_3$, 0.0546*M* Na_2CO_3, 0.065*M* Na_2HPO_4, and 0.051*M* NaCl (ionic strength, 0.410). The formulation without orthophosphate ions contained 0.0232*M* $NaHCO_3$,

0.0418*M* Na_2CO_3, and 0.05*1M* NaCl (ionic strength, 0.200). The surfactant was 0.1% Petrostep B-100.

The results of the IFT experiments are shown in Table 1.

TABLE 1

Effect of Monohydrogen Phosphate on the Interfacial Tension (IFT) of Wilmington Crude Oil and Weakly Alkaline Surfactant Mixtures, 0.1% Petrostep B-100 Surfactant, pH 10.5

Divalent ion	Divalent ion concentration, mg/L	Carbonate mixture	Phosphate–carbonate mixture
	Initial IFT, μN/m		
Ca^{2+}	0	8.2	3.4
	10	7.5	5.8
	100*	9.5	3.4
Mg^{2+}	0	1.6	0.1
	10	0.1	0.3
	100*	6.7	4.0
	Minimum IFT, μN/m		
Ca^{2+}	0	2.8	2.4
	10	7.5	3.4
	100*	9.5	2.3
Mg^{2+}	0	1.6	0.1
	10	0.1	0.1
	100*	0.1	0.3

*Concentration exceeds the solubility limit.

All the IFT values measured with the orthophosphate-containing solution were lower than those measured with carbonate only. All the values were ultralow (<10 μN/m), and even the values without divalent ions present were lower for the orthophosphate-containing formulation. This indicates that the reduction in IFT with the solutions that contained orthophosphate ions was not the result of the presence of orthophosphate ions but instead reflects an ionic strength that was nearer to optimal.

It was concluded, therefore, that orthophosphate ions do not reduce the deleterious effects of divalent ions on IFT behavior in carbonate solutions where the deleterious effect of divalent ions is already so low that it is nearly absent. It also indicates that the precipitation reactions of carbonate mixtures provide adequate mitigation of the divalent ion effects in weakly alkaline surfactant solutions.

The effect of orthophosphate on surfactant loss was measured in bottle tests conducted with 250- to 425-μm crushed Berea sandstone. These experiments were conducted at pH 9.5 and with constant ionic strength. The alkaline solutions were 0.095*M* $NaHCO_3$ + 0.0475*M* Na_2CO_3 (ionic strength, 0.238) and 0.053*M* Na_2HPO_4 + 0.0127*M* Na_2CO_3 + 0.0402*M* $NaHCO_3$ (ionic strength, 0.237). The surfactant was 0.1% Petrostep B-100.

The results are shown in Table 2. Magnesium concentration varied from 0 to 100 ppm, the level at which magnesium solubility at these conditions is exceeded. The results show no correlation between the amount of reduction in surfactant loss in the presence of HPO_4^{2-} ions and the magnesium ion level. However, overall surfactant adsorption was reduced about 30% by the presence of orthophosphate. This leads to the possibility that simple phosphate ion species, as well as polyphosphates, can significantly reduce surfactant losses.

TABLE 2

Effect of Monohydrogen Phosphate on the Adsorption of Petrostep B-100 Surfactant in Weakly Alkaline Mixtures, pH 9.5

Mg^{2+} concentration, mg/L	Adsorption, meq/kg		Reduction, %
	Carbonate mixture	Phosphate–carbonate mixture	
0	0.878	0.566	35.5
10	0.900	0.570	36.7
100	1.134	0.834	26.5

Conclusions

Surfactant-enhanced alkaline flooding should be effective for the recovery of low-acid crude oils. The presence of HPO_4^{2-} ions serves as an additional source of alkalinity and reduces surfactant adsorption.

References

1. T. R. French, *Design and Optimization of Phosphate-Containing Alkaline Flooding Formulations*, DOE Report NIPER-446, (NTIS Order No. DE90000217) 1989.
2. T. R. French and T. E. Burchfield, *Design and Optimization of Alkaline Flooding Formulations*, paper SPE/DOE 20238 presented at the Seventh SPE/DOE Symposium on Enhanced Oil Recovery, Tulsa, Okla., April 23–25, 1990.
3. National Institute for Petroleum and Energy Research, *Quarterly Technical Report for January 1–March 31, 1990*, DOE Report NIPER-470, Vol. 2, pp. 28-31, May 1990.
4. J. Labrid and B. Bazin, Alkaline Preflush in a Low-Permeability Clayey Sandstone, *J. Pet. Sci. Eng.*, 3: 111-120 (1989).
5. W. Stumm and J. J. Morgan, *Aquatic Chemistry*, Wiley–Interscience, Inc., New York, 1970.

DEVELOPMENT OF IMPROVED SURFACTANT FLOODING METHODS

Cooperative Agreement DE-FC22-83FE60149, Project BE4A

National Institute for Petroleum and Energy Research
Bartlesville, Okla.

Contract Date: Oct. 1, 1983
Anticipated Completion: Sept. 30, 1990
Funding for FY 1990: $605,000

Principal Investigator:
Leo A. Noll

Project Manager:
Jerry F. Casteel
Bartlesville Project Office

Reporting Period: Apr. 1–June 30, 1990

Objectives

The objective of this work is to develop more effective surfactant flooding systems that have broader tolerance to variations in salinity. Specific objectives are to determine whether surfactant systems of similar hydrophilic–lipophilic balance (HLB) and solubility parameter values can be combined so that salinity tolerance and resistance to chromatographic separation are improved and to study the solution properties of such mixtures; to study the use of alkaline additives to surfactant systems for light oils; and to use this information to develop improved surfactant–property relationships.

Summary of Technical Progress

Mixed Surfactant Systems

Interfacial tension (IFT) measurements were previously reported for a binary mixture of an alkyl-aryl sulfonate (AAS), LXS-1314, and a carboxymethylated ethoxylated surfactant (CME), RS-16, with *n*-decane. These measurements were conducted as a function of salinity and weight percent CME in the surfactant formulation.[1] Results from these measurements showed that the combination of the two surfactants yielded relatively low IFT values ($<10^{-2}$ mN/m) even at high salinities. In conjunction with these IFT measurements, a salinity scan of the surfactant binary system was conducted to map the extent of the Winsor type III behavior.[2] For this purpose, phase tubes containing the surfactants and the hydrocarbon at different salinities were equilibrated at 50°C with the water/oil ratio (WOR) fixed at 1:1. The results of the phase tube volume measurements can be used to determine solubilization parameters and to construct a salinity requirement diagram to determine the extent of the midpoint salinity with respect to total surfactant concentration.[3]

Figure 1 shows a representation of three types of phase diagrams for a system containing surfactant, brine, and oil and their relationship with observed phase tube volume fractions.[4] The middle-phase region composition can be

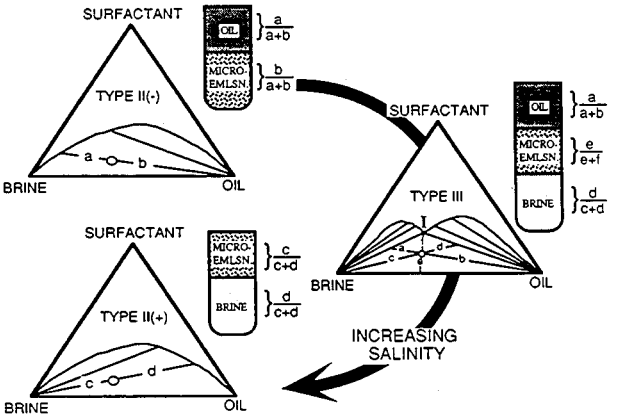

Fig. 1 Ternary phase diagrams for Winsor type phase behavior.

calculated with these phase–volume relationships. The surfactant–hydrocarbon system will yield type II(−) behavior at lower salinity ranges, whereas the system will exhibit a type II(+) behavior at higher salinity ranges. Ideally, the closer the invariant composition is to the brine–oil baseline of the ternary diagram, the more favorable are the IFTs. Under such conditions, the middle phase is more swollen with brine and oil and thus yields lower IFTs between the microemulsion–brine and microemulsion–oil.[3] The surfactant system, the combination of 1.6% LXS-1314 + 0.4% RS-16, yielded a middle-phase microemulsion from 3.0 to 5.0 wt % NaCl, whereas the solutions containing 1.4% LXS-1314 + 0.6% RS-16 yielded a middle-phase microemulsion from 6.0 to 10 wt % NaCl. The estimated midpoint salinities for the two surfactant combinations are 3.6 and 7.5 wt %.

Similar phase behavior measurements have been conducted with a combination of two other CME surfactants as secondary surfactants, MA-18 and CES 6.5. Relatively low IFT values have been measured ($<10^{-2}$ mN/m) at salinities as high as 14 wt % NaCl (Ref. 5). The proportion of the different surfactants in the system was fixed, whereas the total surfactant concentration varied from 0.5 to 4%. The results indicate that the total amount of surfactant did not seem to alter the composition of the middle phase. The increase in total concentration appears to favor the decrease in surfactant concentration in the middle phase. The midpoint salinity of the system is estimated to be about 6.5 to 7.0 wt % NaCl on the basis of equal concentration of brine and oil in the middle phase. The solubilization

parameters calculated for this system reflect a similar range of midpoint salinities.

Two coreflood experiments were performed this quarter to evaluate oil recovery using mixed surfactant systems. The surfactant mixture (1.5% LXS-1314, 0.75% MA-18, and 0.75% CES 6.5) in 6.65% NaCl, 1.53% $CaCl_2$, and 0.24% $MgCl_2$ brine was used to produce decane and North Burbank Unit (NBU) oil from unfired Berea sandstone cores. Oil production results were disappointing. Total oil production was 5 and 15% of residual oil in place for decane and NBU oil, respectively. Tests for the presence of surfactants in the effluent solutions are in progress.

Adsorption of Mixed Surfactant Systems

Experiments were conducted to determine the static and dynamic adsorption of the surfactant mixture (LXS-1314, MA-18, and CES 6.5) on crushed Berea sandstone. In addition, dynamic adsorption experiments were conducted with a mixture of LXS-1314 and an ethoxylated sulfate surfactant, CO-436. The results from static adsorption experiments for this surfactant mixture were reported in the previous quarterly report. The objectives of these experiments were to determine total surfactant loss at ambient conditions and if chromatographic separation of the components occurred.

Measurements of surfactant loss for the LXS–MA–CES mixture under static and dynamic conditions are summarized in Table 1. The surfactant mixtures containing a higher percentage of CME surfactants showed slightly lower surfactant loss. Good agreement was seen between the static and dynamic test results. For these surfactant loss experiments, brine composition of the solutions was 6.65% NaCl, 1.53% $CaCl_2$, and 0.24% $MgCl_2$. At this salinity, the LXS surfactant phase separated and showed 100% surfactant loss without the presence of CME surfactants in solution.

Total surfactant loss was reduced slightly when the ratio of CME surfactants to LXS-1314 was increased from 40 to 50%. A 10-fold increase in total surfactant concentration from 0.2 to 2.0% showed little effect on total surfactant loss. Agreement was good between surfactant loss values measured in static and dynamic tests.

TABLE 1

Total Surfactant Loss for a Mixed Surfactant System

LXS-1314, wt %	MA-18, wt %	CES 6.5, wt %	Surfactant loss, mg/g
	Static Tests		
1.0	0.5	0.5	3.8 ± 0.2
0.1	0.05	0.05	3.5 ± 0.2
0.6	0.2	0.2	4.6 ± 0.5
	Dynamic Test		
0.6	0.2	0.2	5.3 ± 0.9

A high-pressure liquid chromatography (HPLC) analysis of surfactant concentration for the mixed system indicated two main components of the mixture that eluted separately from the reverse-phase HPLC column. All three surfactants were present in peak 1, which was approximately five times as great in area as peak 2. In peak 2 only components of the CME surfactants that had previously been identified as the nonionic (noncarboxylated) components of these commercial surfactants appeared to be present. The presence of LXS-1314, an ionic surfactant, did not appear to change the peak area of peak 2. In the dynamic test, components of peaks 1 and 2 appeared to travel through the sandpack together. Of the injected slug, 92% of the components in peak 2 were retained in the column. A slightly smaller amount of the components in peak 1 (87%) was retained in the column. The surfactant loss values for the dynamic test were calculated with these relative retention values.

Surfactant loss for the surfactant mixture LXS-1314 and CO-436 in 3% NaCl brine for the dynamic test with a crushed Berea sandstone column was 2.2 mg/g. This value falls within the range of values determined in the static surfactant loss tests of 1.0 to 2.3 mg/g as reported last quarter. Surfactant loss may be lower for this surfactant mixture than for the LXS–MA–CES mixture because of lower solution brine concentration.

Dilution Calorimetry of Mixed Surfactant Systems

Dilution calorimetric experiments of an AAS, LXS-1314, in water and in 0.5% brine, as well as a mixture of Sandopan RS-16 with LXS at 25, 50, and 90°C, have been completed. All heats of dilution are quite small. The dilution data have been fitted with a least-squares spline fit to obtain relative molar enthalpies.

Figure 2 shows the results of the dilution calorimetry for the mixture of LXS-1314 with RS-16 in brine at 25, 50, and

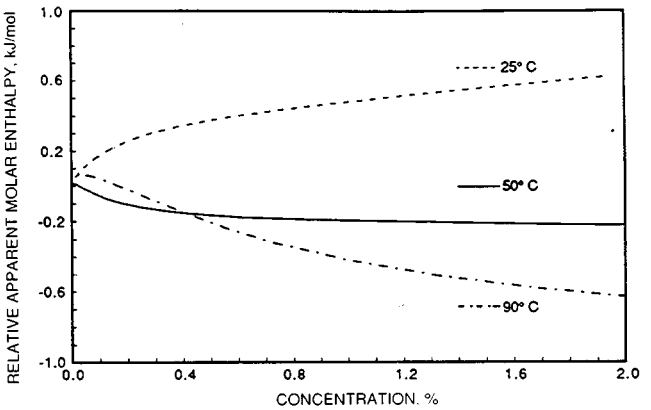

Fig. 2 Dilution calorimetry of LXS-1314–RS-16 mixture in 0.05% brine.

90°C. The dilution curve has no maximum at 25°C but is uniformly positive. At 50°C there is a maximum in the curve at 0.22%, whereas at 90°C there is a maximum at 0.04% total surfactant concentration. These maxima are generally associated with the critical micelle concentration (CMC), which occurs at a low concentration even at 90°C.

Additives for Surfactant Formulations

Many midcontinent crude oils have low acid contents. Total acid numbers (TAN) are usually below 0.5 mg KOH/g oil. Previous research has shown that lower IFT values can be achieved if an alkaline additive is included in a dilute surfactant formulation. This research is focused on the use of dilute surfactant concentrations because of the resultant improvement in economics. Only weak alkalis, such as carbonate mixtures, are practical because of the overwhelming consumption reactions that occur with stronger alkaline additives. Other beneficial effects of the alkaline additives are reduced surfactant adsorption and reduced divalent ion effects.[6]

This research is complicated because surfactant formulations containing dilute surfactant concentrations fail to exhibit the types of phase behavior that can be used to easily identify optimal formulations. Therefore primary reliance must be placed on IFT measurements. The results of IFT measurements with two low-TAN crude oils and surfactant–alkali formulations are given in Table 2, which includes the initial values of IFT and the equilibrium values that are obtained after about 20 to 60 min of equilibration time.

Table 2 gives the IFT values obtained at 30°C during salinity scans conducted with Delaware–Childers crude oil and three surfactant formulations that contain weak alkaline additives. The results show that equilibrium IFT values below 10 μN/m were achieved with the Delaware–Childers oil at some conditions but that very low initial values were not achieved. This contrasts with IFT values previously measured at 52°C; the difference is very low values for initial IFT measured at the higher temperature.[7] Although the initial IFT values shown in Table 2 were not ultralow, a series of coreflood tests was designed to test the potential for producing incremental Delaware–Childers oil at 30°C, which is near reservoir temperature.

Table 2 also gives the IFT results obtained with Teapot Dome oil at 52°C, which is the approximate temperature of the deep zones in that oil field. With the Teapot Dome oil, some salinities that gave both ultralow initial IFT and very low equilibrium IFT values were identified. Ultralow IFT values were obtained with Petrostep B-100 surfactant at 0.3 and 0.6% NaCl concentrations. These results were used to design oil recovery tests with Teapot Dome oil.

The results of the oil recovery (coreflood) tests are summarized in Table 3. One of the tests was conducted in Berea sandstone cores with Teapot Dome oil, three tests were conducted in native-state cores with Delaware–Childers oil, and one test was conducted in Berea sandstone with Delaware–Childers oil. The coreflood conducted with Teapot Dome oil was performed at 0.3% NaCl concentration; the initial IFT was measured to be 0.6 μN/m and the equilibrium IFT was 9.6 μN/m (Table 2). Injection of the surfactant formulation resulted in recovery of 60.8% of the oil that remained in the core after a previous waterflood. The oil saturation was lowered from 39.5 (S_{ow}) to 15.5% (S_{oc}) during chemical flood. This extremely good incremental oil recovery demonstrates the high efficiency potential of properly designed dilute surfactant solutions that contain weak alkaline additives.

The effluent analysis for the flood conducted with Teapot Dome oil is shown in Fig. 3. Surfactant adsorption was 0.129 meq/kg, which is low. There was, however, an interesting separation of the surfactant and polymer in the effluent. The magnitude of this separation, over 0.5 PV, could be significant in a field situation and should be designed out of the system by appropriate surfactant and salinity selection.

TABLE 2

Dynamic Interfacial Tensions of Surfactant Formulations That Contain Alkaline Additives with Two Different Oils

pH	Temp., °C	NaCl, %	Initial IFT, μN/m	Equilibrium IFT, μN/m
Teapot Dome, 0.1% Petrostep B-100, Carbonate Mixture				
9.5	52	0	5.4	21.1
		0.3	0.6	9.6
		0.6	0.9	5.4
		1.0	10.0	8.7
Teapot Dome, 0.1% Neodol 25-9, Carbonate Mixture				
9.5	52	0	311.5	86.3
		1	564.6	228.6
		3	361.5	104.1
		5	525.3	154.2
		9	595.5	82.1
Delaware–Childers, 0.2% Petrostep B-100, Sodium Bicarbonate				
8.3	30	0	34.5	9.0
		0.3	61.3	23.6
		0.6	57.6	6.3
		1.0	121.9	13.8
Delaware–Childers, 0.2% Petrostep B-100, Carbonate Mixture				
9.5	30	0	67.1	7.4
		0.3	70.8	11.3
		0.6	67.1	13.8
		1.0	108.3	20.6
Delaware–Childers, 0.2% Neodol 25-9, Carbonate Mixture				
9.5	30	0	209.3	195.5
		1	261.7	326.6
		3	198.9	301.4
		5	188.4	253.5

TABLE 3

Summary of Corefloods Conducted with Surfactant Formulations That Contain Alkaline Additives

				Asp solutions*							
Coreflood	Core type	K_{abs}, mD	ϕ, %	Surfactant	Surfactant, %	pH	PV	S_{oi}, %	S_{ow}, %	S_{oc}, %	$Reff_o$, %
TP-1	Berea	811	22.9	Petrostep B-100	0.1	9.5	1.01	73.6	39.6	15.5	60.8
DCNS-1	Native-state	214	22.9	Petrostep B-100	0.2	8.3	0.73	22.0	22.0	22.0	0
DCNS-2	Native-state	143	20.7	Petrostep B-100	0.2	8.3	0.82	64.6	38.7	32.3	16.4
DCNS-3	Native-state	†	†	Neodol 25-9	0.2	9.5	(1.0)	†	†	†	0
DC-1	Berea	1151	21.7	Petrostep B-100	0.2	8.3	0.78	78.2	43.6	35.4	18.8

*Asp solutions contain weak alkali, low concentration surfactant, and Flocon 4800 CX biopolymer.
†Measurement not completed.

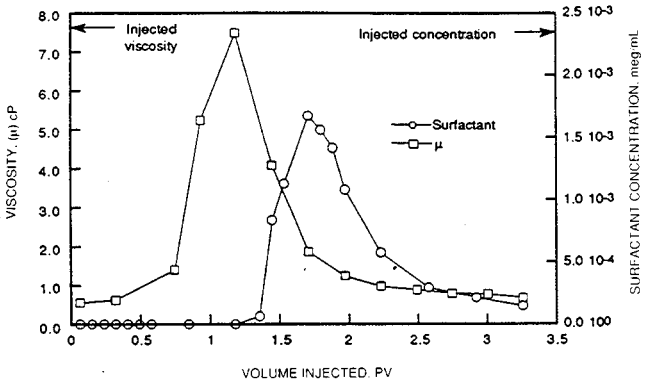

Fig. 3 Effluent analysis for chemical flood TP-1.

The other four corefloods shown in Table 3 were performed at 30°C with Delaware–Childers oil. As previously discussed, several of these systems gave very low equilibrium IFT values but did not give ultralow initial IFT values. Two of these corefloods (DCNS-1 and DCNS-3) were conducted with native-state cores that had very low initial oil saturations. No oil was recovered from these cores during the chemical floods.

Coreflood DCNS-2 was conducted in a native-state core that was restored to initial oil saturation, and coreflood DC-1 was conducted with a Berea sandstone core. In both cases, the chemical flood was conducted after waterflooding the cores to residual oil saturation. The oil recovery results from the two core tests are remarkably close. Recovery from the restored native-state core was 16.4%, and recovery from the Berea sandstone core was 18.8%.

The oil recoveries with Delaware–Childers oil were much lower than those achieved with Teapot Dome Oil and indicated that the surfactant formulations used did not have low enough IFT values to mobilize significant residual oil. Work to find a surfactant formulation that will be more effective at reservoir temperature is continuing. Apparently, low initial IFT may be more important for mobilization of oil than equilibrium values. An encouraging result is that the consumption of alkaline additive by the Delaware–Childers native-state core was relatively low. Analysis of the effluent revealed that 85.9% of the injected alkali passed through the native-state core.

Some of the conclusions reached about the use of alkaline additives in surfactant floods are that properly designed floods can be extremely efficient for mobilization of residual oil (the Teapot Dome result is an example), the consumption of weak alkalis by some native-state cores is low (the Delaware–Childers result is an example), and initial IFT may be more important than equilibrium IFT when designing surfactant floods that contain dilute surfactant with an alkaline additive.

References

1. National Institute for Petroleum and Energy Research, *Quarterly Technical Report for October 1–December 31, 1989*, Vol. II, DOE Report NIPER-463, pp. 28-33, 1990.
2. P. A. Winsor, *Solvent Properties of Amphiphillic Compounds*, Butterworth's Scientific Publication, London, 1954.
3. R. C. Nelson and G. A. Pope, Phase Relationships in Chemical Flooding, *Soc. Pet. Eng. J.*, 325-338 (October 1978).
4. R. N. Healy, R. L. Reed, and D. G. Stenmark, Multiphase Microemulsion Systems, *Soc. Pet. Eng. J.*, 147-160 (June 1976).
5. National Institute for Petroleum and Energy Research, *Quarterly Technical Report for January 1–March 31, 1990*, Vol. II, DOE Report NIPER-470, pp. 21-27, May 1990.
6. P. B. Lorenz, *Combination Alkaline–Surfactant Flooding: A State-of-the-Art Review*, DOE Report NIPER-349, 1988.
7. T. R. French and T. E. Burchfield, Design and Optimization of Alkaline Flooding Formulations, SPE/DOE paper 20238, presented at the Seventh SPE/DOE Symposium on EOR, Tulsa, Okla., April 1990.

GAS DISPLACEMENT—SUPPORTING RESEARCH

STATISTICALLY DESIGNED STUDY OF PARAMETERS OF A CARBON DIOXIDE EQUATION OF STATE

Contract No. DE-AC22-89BC14200

Johns Hopkins University
Baltimore, Md.

Principal Investigators:
Marc D. Donohue
Daniel Q. Naiman
Gang Jin
Joseph R. Loehe

Project Manager:
Jerry F. Casteel
Bartlesville Project Office

Contract Date: Sept. 29, 1989
Anticipated Completion: Sept. 28, 1990
Government Award: $205,350

Reporting Period: Apr. 1–June 30, 1990

Objective

The objective of this project is to select equations of state (EOS) to calculate the thermodynamic properties of carbon dioxide (CO_2) and its mixtures relevant to enhanced oil recovery (EOR). These EOS are then studied using a statistically designed factorial or fractional factorial computer analysis. The purpose of this study is to determine the importance and sensitivity of thermodynamic variables and of the parameters in the equations. An important aspect of this is to determine how the accuracy or precision (or both) of these parameters affects the agreement with experimental data.

Summary of Technical Progress

Tasks completed during the report period were intended to satisfy the intermediate objectives:

1. Finalize the ranges of parameter values for the Adachi–Lu–Sugie (ALS)[1] and Suresh–Elliott–Donohue (SED)[2] EOS for the computational program.
2. Identify appropriate test mixtures for which liquid-phase densities and critical locus data are available in the literature.

3. Begin assimilation of the EOS and factorial design concepts into a computer program to be used for the computational test program.

The remainder of this report describes in slightly greater detail the completion of these tasks and indicates the directions planned for the final quarter of the project.

Parameter Ranges

The Topical Report issued in February discussed the choice of the SED and ALS EOS as objects for study and recommended a range of 10% around the best-fit or accepted values of the independent parameters to be tested in the equations. After some discussion concerning stability of the algorithms for critical locus determination, the group decided to accept this range as a reasonable starting point. This range will be the first one attempted. If stability problems arise, it will be reduced and the test computations repeated.

Appropriate Test Mixtures

Several sets of mixture critical point data for CO_2–alkane systems were located, but mixture liquid density data, difficult to predict but an important property for EOR models, were not as readily available. Experimental data were located for two systems, i.e., CO_2–butane and CO_2–decane. This information has been entered into computer files and will be used in the test program.

Program Assimilation

The development of a computer program to construct and execute the computational test pattern requires writing the test pattern generating program and converting stand-alone programs for calculating the desired responses into subroutines for incorporation into the main program. At least two main programs, one for each physical property, will be constructed using this technique. The test-pattern generator and the stand-alone programs have been written and successfully tested. They now are being assimilated into a single code.

Future Objectives

The computational effort will continue and intensify to meet the scheduled project completion deadline of Sept. 29, 1990. The completed programs should be tested and ready for executing the plan computations by the middle of August. The remaining six weeks will be devoted to the detailed study of the results and follow-on computations that may be required. Delays or departures from the project schedule are not anticipated.

References

1. Y. Adachi, B. C.-Y. Lu, and H. Sugie, *Fluid Phase Equilibria*, 11: 29-48 (1983).
2. S. J. Suresh, J. R. Elliott, Jr., and M. D. Donohue, accepted by *Ind. Eng. Chem. Res.*, (1989).

FIELD VERIFICATION OF CO_2–FOAM

Contract No. DE-FG21-89MC26031

New Mexico Institute of Mining and Technology
Petroleum Research Center
Socorro, N. Mex.

Contract Date: September 1989
Anticipated Completion: September 1993

Total Project Cost:

DOE	$2,000,000
Contractor	$2,000,000
Total	$4,000,000

Principal Investigators:
F. David Martin
John P. Heller
William W. Weiss

Project Manager:
Royal J. Watts
Morgantown Energy Technology Center

Reporting Period: Apr. 1–June 30, 1990

Objectives

The objectives of this project are to (1) evaluate the use of foaming agents to improve the efficiency of CO_2 flooding in a New Mexico reservoir and (2) prove the concept of CO_2–foam in the field by selecting a suitable reservoir where CO_2 flooding is ongoing, characterizing the reservoir, modeling the process, and verifying the effectiveness and economics.

Summary of Technical Progress

As discussed in the first quarterly report, a suitable field site in New Mexico, the East Vacuum Grayburg/San Andres Unit, has been identified as appropriate for the proposed work. The initial site-specific plan was developed and submitted for unit working interest owner approval in May 1990. These details were discussed with the unit working interest owners at a meeting in Odessa, Tex., on May 21, 1990. The operator of the unit, Phillips Petroleum Company, submitted ballots for project approval. A sufficient number of unit working interest owners voted in favor of the project, and the project was approved on June 25, 1990.

Therefore, task 1 (site evaluation and selection) and most of task 2 (development of initial site-specific plan) of the project have been completed. The laboratory tests will

begin as soon as representative reservoir cores are received from Phillips Petroleum Company. A technical meeting to discuss additional details of the project will be held within the next two months. Reservoir simulation studies will begin after the technical meeting of the joint project task force.

ENHANCED OIL RECOVERY SYSTEMS ANALYSIS

Morgantown Energy Technology Center
Morgantown, W. Va.

FY90 Total Project Cost: $150,000

Principal Investigator:
James R. Ammer

Project Manager:
Royal J. Watts
Morgantown Energy Technology Center

Reporting Period: Apr. 1–June 30, 1990

Objective

The overall goal of the Systems Analysis Project is to incorporate results of laboratory investigations, model enhancements, and field experimental work into a systems approach to predict oil recovery and to estimate the increase in reserves for improved technology.

Specific Tasks for FY90

1. *Advanced Technology Assessment Study in the Delaware Basin*—Screening criteria will be used to select reservoirs amenable to CO_2 miscible EOR. These reservoirs will be categorized, and the CO_2PM will be used to identify the increase in reserves that results from applying advanced technologies.

- Screen reservoirs to determine the applicability of CO_2 miscible EOR.
- Collect and input reservoir data for use in the CO_2PM.
- Categorize reservoirs on the basis of physical and geological characteristics.
- Select a representative reservoir from each category for simulation studies.
- Review CO_2PM and recommend changes for modeling advanced technologies. Specific technologies being investigated are horizontal wells and CO_2–foam.

2. *University of Wyoming Horizontal Well Study*—Validate laboratory results through history matching and conduct optimization studies for field-scale floods.

- Investigate if viscous fingering affected laboratory results.
- History match laboratory results.

3. *Simulation Studies*—Two field simulation studies are being conducted to obtain a better understanding of the CO_2 displacement process. Once a history match has been obtained on these fields, the application of advanced technologies can be investigated through simulation studies that benefit from having a more accurately defined reservoir.

- Industry Cooperative Simulation Study
  — Match the primary production history.
  — Match the waterflood history.
- Griffithsville Simulation Study
  — Match the waterflood history.
  — Match the CO_2 tertiary flood history.

Summary of Technical Progress

Advanced Technology Assessment Study in the Delaware Basin

1. Three hundred twenty oil reservoirs have been identified in the Delaware Basin (232 in Texas and 88 in New Mexico). Oil gravity and reservoir depth/minimum miscibility pressure are currently being used as initial screening criteria to determine reservoirs amenable to CO_2 miscible flooding. Minimum original-oil-in place (OOIP) limits are being used to eliminate small reservoirs (OOIP < 5 million barrels). Reservoir data required to run the CO_2 predictive model (CO_2PM) were ordered from Dwight's Energydata.

2. Evaluation of the CO_2PM code and various foam flowing modeling techniques was continued. An empirical foam flow model is currently being investigated for incorporation into CO_2PM. Modifications to the solution algorithm to solve for the additional component (surfactant) and other necessary changes to the existing code are being identified.

University of Wyoming Horizontal Well Study

1. Simulation runs were completed for both injection scenarios (vertical and horizontal wells) with computer modeling group's (CMG) black oil miscible simulator for values of omega (mixing parameter) of 0.75, 0.50, and 0.25. Results showed that, for the same value of omega, a larger reduction in cumulative oil recovery from the base case (omega = 1) occurred for the vertical injector scenario.

Similar results were seen for the fingering parameter, beta, in CMG's compositional/incomplete mixing simulator. These results and the values of beta required to achieve a match of the laboratory results indicate that viscous fingering was probably more prevalent for the vertical injector scenario than for the horizontal injector scenario.

2. The abstract titled "Modeling the Performance of Horizontal Injection Wells in Carbon Dioxide Miscible Displacement Processes" was accepted for presentation at the 1991 Reservoir Simulation Symposium. The results show that horizontal wells can provide good mobility control for CO_2 enhanced oil recovery (EOR).

3. A contract titled "Investigation of Field-Scale Carbon Dioxide Flooding Using Horizontal Wells" was awarded to the University of Pittsburgh. Data sets of the following two actual reservoirs will be used to conduct the simulation studies: Griffithsville, a fairly homogeneous, nonlayered reservoir; and a layered, heterogeneous Permian Basin Reservoir.

Industry Cooperative Simulation Study

Calculations using Stone's modified equation for determining oil relative permeability were performed. Fluid saturations from the latest history match simulation were used to determine oil–water and oil–gas relative permeability data. On the basis of field-measured water-cut data, the oil relative permeability required to match a given water cut was used to back calculate the oil relative permeability to gas used in Stone's equation. New oil–gas relative permeability curves were constructed on the basis of these calculations. Better matches of water-cut data have resulted from the use of these new oil–gas relative permeability curves.

Griffithsville Simulation Study

The technical note on the Griffithsville simulation study was completed. The report is currently being processed for release.

IMPROVEMENT OF CO_2 FLOOD PERFORMANCE

Contract No. DE-FC21-84MC21136

New Mexico Institute of Mining and Technology
Petroleum Recovery Research Center
Socorro, N. Mex.

Contract Date: April 1984

Anticipated Completion: September 1990

Total Project Cost:

DOE	**$1,615,000**
State of New Mexico	**981,000**
Industry	**1,366,000**
Total	**$3,962,000**

Principal Investigators:
John P. Heller
F. David Martin

Project Manager:
Royal J. Watts
Morgantown Energy Technology Center

Reporting Period: Apr. 1–June 30, 1990

Objective

The objective of this project is to produce quantitative measurements of the influence of CO_2 flood performance of the following:

1. Displacement with pure and impure CO_2.
2. Evaluation and improvement of flow uniformity.

The experimental investigations and accompanying analysis and interpretation are designed to build understanding of fundamental physical mechanisms as a basis for improved performance prediction and for optimization of process performance.

Summary of Technical Progress

Task I: Phase Behavior and Fluid Properties

In this subarea, work continued on the viscosity–density–composition database. Continuous phase equilibrium (CPE) experiments are scheduled with a recombined Wasson San Andres crude oil. Run conditions range from 1500 to 2000 psia at 105°F with approximately 10 mol % contamination of the CO_2 stream. These experiments will investigate the effects of small amounts of impurities in the CO_2 stream on phase behavior and fluid properties of CO_2–crude oil systems. Two baseline CPE experiments were performed with the recombined Wasson oil. These two experiments were run with pure CO_2 injection at 1500 and 2000 psia, both at 105°F. A paper entitled "An Improved Viscosity Correlation for CO_2/Reservoir Oil Systems," by R. M. Lansangan, M. Taylor, J. L. Smith, and F. S. Kovarik, was presented by R. M. Lansangan in April at the SPE/DOE Seventh Symposium on Enhanced Oil Recovery in Tulsa, Okla.

The Effect of Free and Solution Gas on Miscibility

In the investigation of the effect of free and solution gas on the development of miscibility, the data obtained from

the experimental displacements for the two oil systems, Wasson + 35% C_1 and Wasson + 25% C_1, have been partially processed. The Peng–Robinson equation of state (EOS) model for the Wasson crude oil, as described in the last quarterly report, was used for the estimation of the liquid–vapor densities for these two oil systems as required for the sweep efficiency calculation.

Micromodel Studies

In the area of micromodel studies, flow visualization experiments were conducted to study the effect of gas/liquid volumetric ratio on sweep efficiency during the simultaneous injection of CO_2 and surfactant solution into the modified layered (MLAY) micromodel. The micromodel was first saturated with Maljamar separator oil with connate water. Four different gas/liquid ratios have been studied: 3:1, 4:1, 5:1, and 6:1. For a more consistent regulation of the flow of injection fluid into the micromodel, several changes have been made in our micromodel operating procedure.

High-Pressure Corefloods

Because of personnel changes in this area of work and coreflood apparatus modifications, our efforts this quarter have been devoted to testing the coreflood apparatus. Validation runs have been conducted. Preliminary CO_2–surfactant solution and CO_2–brine runs are under way with a homogeneous Berea sandstone core.

Foam Flood Simulation

In the area of foam flood simulation studies, some effort has been devoted to the development of a limited compositional foam flood simulator. This new simulator is being developed by refining the four-component reservoir simulator, which is supplied by the Department of Energy, with the mechanistic foam flood simulator. The mechanistic foam flood simulator was used to investigate the effect of relative permeability on the performance of a CO_2–foam flood. The gas relative-permeability end point affects the pressure drop across the system more significantly than does the water relative-permeability end point. However, the water relative-permeability curvature affects the pressure drop across the system more significantly than does the gas relative-permeability curvature. The effect of relative permeability on the liquid production history is not significant.

A paper entitled "The Effect of Microscopic Heterogeneity on CO_2–Foam Mobility: Part 2—Mechanistic Foam Simulation," by Shih-Hsien Chang, L. A. Owusu, S. B. French, and F. S. Kovarik, was presented by Shih-Hsien Chang in April at the SPE/DOE Seventh Symposium on Enhanced Oil Recovery in Tulsa, Okla. This paper focuses on three areas: (1) the visualization study of foam flow behavior in glass micromodels, (2) the foam coreflood displacements, and (3) the development of a mechanistic foam flood simulator.

Task II

Three topics dealing with the uniformity of flow and displacement in the reservoir are being investigated in Task II of this project. Although increased recovery efficiency of CO_2 floods is the primary target of this research, certain features of the results are relevant to other oil and gas production processes. In the first of the three topics, various aspects of the heterogeneity of reservoir rock were considered, especially regarding its effect on displacement. Research results in this area can be of use in securing more realistic diagnoses of reservoir problems and assessments of their economic effects. The second and third topics involve the development of methods of mobility control, especially for CO_2 floods, and thus have the potential for more immediate application to improved reservoir practices. Each of these subareas has seen significant progress during this quarter.

Rock Heterogeneity

This work aims at elucidating the effects of heterogeneity on reservoir operations. During this quarter, considerable time was spent perfecting and doing final debugging of the FORTRAN code. A new aspect of work concerns the question of how to use permeabilities derived from well tests in a conditioned simulation of the reservoir. This involves several considerations: (1) the proper weighting of local permeability values in the effective value for the larger area measured in a well test; (2) the relationship between the covariance data, which can be obtained from laboratory core measurements, and the appropriate extension of this to the larger scale covariance; and (3) the possible interactions of the particular location of the well in the heterogeneous field with the first and second factors. The development of a general mathematical procedure by which random fields can be conditioned to well test data will be a major contribution.

In the work on the assessment of reservoir heterogeneity from the results of well-to-well tracer tests, some mathematical and numerical matters remain. These concern recoding to take advantage of the special capabilities of the CM-2 "massively parallel" supercomputer and clarification of the means of integrating tracer output from the different streamlines. This calculation takes into account dispersive mixing as well as the effects of rock heterogeneity. The program, therefore, must follow a number of the isoconcentration lines that describe the front during the flow of the tracer slug through the reservoir.

Another concern is the smaller scale inhomogeneities, their effect on displacement efficiency, and their relationship with larger scale variability. This work also has implications for laboratory corefloods and other such

experiments. Analytical methods for small-scale permeability measurements are also being perfected.

Mobility Control—Direct Thickeners

The research aimed at the synthesis of CO_2-soluble polymers as viscosifiers has proceeded further along the lines previously reported and has concentrated on particular types of "Method II" polymers. These are ionomers made with "telechelic" polymers as starting compounds. Telechelic polymers are so named to indicate that their molecules bear functional groups at the ends of the polymer chains. For these purposes, the functional group is converted into an ion-carrying one. In solution in a nonpolar solvent, these ionomers are more able to form long pseudo-polymeric chains by association among the molecules than are ionomers containing their ionic groups at random positions.

During this quarter, the method of preparing "living polymers," which are characterized by an extremely narrow molecular-weight distribution, was further developed. In particular, this method has been applied with aliphatic and alicyclic alcohols to the preparation of new telechelic polyisobutylenes.

A variety of new, asymmetric and symmetric, living telechelic polyisobutylenes were prepared this quarter. These can be derivatized into nearly monodisperse, sulfonated ionomers by sulfonation and neutralization procedures. The chemical makeup of the ionomers is verified by infrared (FTIR) and nuclear magnetic resonance (NMR) spectroscopy; their molecular weights and distributions are characterized by gel permeation chromatography (GPC) and vapor pressure osmometry (VPO). Some of the solution properties of prepolymers (in both hexane and dense CO_2) and of the ionomers were also determined.

In solution in hexane, the association of these ionomers is verified by the large increase in solution viscosity with increasing concentration. Although the ionomer solubility in dense CO_2 has not yet been measured extensively, measurements thus far are quite encouraging. As a matter of principle, the influence of ionomer molecular weight on its solubility is expected to be somewhat different from that of similar hydrocarbon polymers that contain no ionic groups, but the details of the relationship remain to be seen.

Mobility Control—CO_2–Foams

During this quarter, work has progressed in three directions: (1) the measurement of CO_2–foam mobility, (2) the measurement of interfacial properties and "durability" of aqueous surfactant films against dense CO_2 at reservoir temperature and pressure, and (3) the further development of an apparatus for dynamic measurement of surfactant adsorption on reservoir rock.

Because of personnel and equipment changes, some of the mobility measurement efforts have been devoted to repeat runs on known systems to enable checks on procedures and to extend measurements of CO_2–foam mobility at low surfactant concentrations. In addition, both corrosion of the ISCO pump and contamination of surfactant–brine from the dead volume inherent in the design of the new model have been eliminated by the construction of a Teflon-lined transfer vessel to isolate the pump barrel from the aqueous liquid.

The measurements of CO_2–foam mobility in the past quarter have verified that higher mobility is attainable with lower surfactant concentrations. It has become more apparent that the stability of individual measurements is less—that is, there is more experimental scatter in the points and more time must be spent on data acquisition—when the surfactant concentration is low. The measurements on which this conclusion is based were made with Rock Creek Sandstone and Witcolate 1276 surfactant at 0.01 wt %, 0.50 wt %, and 0.1 wt % concentration. The surfactant was dissolved in 0.5% NaCl and 0.5% $CaCl_2$ brine, and the flowing foam quality was 80%.

The foam durability apparatus was used to investigate several surfactants to a further extent than previously. Two of these surfactants, manufactured by Chevron Chemical Company for use in CO_2 floods, are commercially available. Their test results, run at 40°C and 2500 psi, were reported previously, and work this quarter included measurements at the same CO_2 density, at 25°C and 1500 psi. The first of these two surfactants, Chevron Chaser CD1040, is a brine-tolerant sulfonate designed for use in sandstone reservoirs at temperatures up to 93°C (199.4°F). The second surfactant, Chevron Chaser CD1050, is also specified as brine tolerant, but it has been designed specifically for use in CO_2 floods in carbonate reservoirs.

Measurements of the interfacial tension (IFT), at 25°C and 1500 psi, were conducted between dense CO_2 and several surfactant solutions prepared in a 1% mixed brine solution. The critical micelle concentration (CMC) of the surfactants, at these conditions, was determined graphically in the usual manner, by observing the concentration at which the slope of the IFT curve changes.

An interesting point is that the CMC of Chevron Chaser CD1040 under this milder temperature was determined to be between 0.15 to 0.16 wt %, which agrees with the value of 0.15 wt % obtained previously at the higher temperature and pressure. By contrast, Chevron Chaser CD1050 has a much lower CMC at the lower temperature, and its CMC is much more dependent on temperature, at a constant density of CO_2. At 25°C the CMC is only 0.018 wt %, whereas at 40°C the CMC is 0.05 wt %.

These surfactants differ also in the length of time over which the undisturbed foam will persist. As noted in previous reports, this interval depends strongly on the concentration of the surfactant, assuming a maximum value that was often close to the CMC. The CO_2–foam produced by the CD1050 surfactant lasted much longer, at all the concentrations measured, than that produced by the

CD1040 surfactant. This was also the case when the surfactants were screened at the higher temperature and pressure. Although the foam durability is deemed to be adequate at both temperatures, both of these surfactants generally produced longer-lasting CO_2–foam at 25°C and 1500 psi than at the higher temperature and pressure.

SCALEUP OF MISCIBLE FLOOD PROCESSES

Contract No. DE-FG21-89MC26253

Stanford University
Stanford, Calif.

Contract Date: July 1989
Anticipated Completion: July 1992

Total Project Cost:

DOE	$756,000
Contractor	0
Total	$756,000

Principal Investigator:
F. M. Orr, Jr.

Project Manager:
Royal J. Watts
Morgantown Energy Technology Center

Reporting Period: Apr. 1–June 30, 1990

Objective

The objective of this research effort is to develop improved procedures for scaling predictions of miscible flood performance from laboratory scale, where the process is experimentally accessible, to field scale, where more accurate performance predictions are needed.

Phase Behavior, Fluid Properties, and Flow

The following steps will be performed:

- Determine how extraction of hydrocarbons depends on solvent density for CO_2, N_2, and CH_4 systems.
- Measure fluid properties for the same mixtures to determine how phase densities and viscosities vary with composition.
- Test theoretical and empirical predictions of fluid properties.
- Develop the use of supercritical fluid chromatography (SFC) for characterization of crude oils for miscible flooding.
- Determine how extraction of naphthenes, aromatics, normal alkanes, and branched alkanes varies with molecular weight of the molecule.
- Use the results to develop a recommended analytical technique for the evaluation of crude oils for miscible flooding.

Patterns and Scales of Nonuniform Flow

The following steps will be performed:

- Calculate combined efforts of gravity, heterogeneity, and viscous fingering.
- Include effects of ternary phase behavior and mobile water.
- Perform unstable displacement experiments in heterogeneous porous media and simulate the experimental displacements to determine whether the simulator captures the combined effects of heterogeneity, viscous instability, and viscous cross flow.
- Perform unstable displacement experiments with analog oil–water–alcohol systems to investigate the combined effects of phase behavior, capillary and viscous cross flow, and heterogeneity.
- Use the experimental results to test the validity of simulations of the combined mechanisms.
- Evaluate the feasibility of the use of acoustic measurements to determine finger dimensions in three-dimensional flows at laboratory scale.

Interaction of Nonuniform Flow, Cross Flow, and Phase Behavior in Large-Scale Flows

Two-dimensional compositional simulations will be performed to determine the range of values of capillary number and viscosity/gravity ratio.

Summary of Technical Progress

Phase Behavior, Fluid Properties, and Flow

The first in a set of pressure volume temperature (PVT) experiments, in which samples are obtained for compositional analysis, was completed. A mixture containing 85 mol % CO_2 with crude oil from the Means field was equilibrated at 105°F and 2000 psia. Samples of the resulting CO_2-rich and oil-rich phases were then taken. The samples will be subjected to a detailed analysis by several analytical techniques. A combination of standard gas chromatography for vapor and simulated distillation for liquid hydrocarbons will be used to determine the distribution of hydrocarbons present in each phase. Liquid hydrocarbons will be analyzed by SFC. A combination of gas

chromatography and mass spectrometry (GC–MS) will be used to identify specific compounds present in both the CO_2-rich and oil-rich phases. The resulting phase-composition data set will be the most comprehensive ever obtained for a CO_2–crude oil system. It will allow the examination of the differences in partitioning behavior between normal and branched alkanes, naphthenes, and aromatics, and it will be used to examine how components should be lumped for equation-of-state (EOS) calculations of phase behavior. They indicate that the three-phase (L_1–L_2–V) region for Means crude oil, which is relatively heavy compared with other Permian basin oils, occurs at pressures very similar to those for Maljamar, a lighter crude oil. That result is consistent with the idea that the formation of the three-phase region depends primarily on the properties of CO_2 as long as enough extractable hydrocarbons are present to allow formation of a CO_2-rich liquid at temperatures above the critical temperature of CO_2 (88°F).

Additional experiments were performed to develop the use of SFC to characterize hydrocarbons for EOS calculations. Elution times were measured for a variety of hydrocarbons in an attempt to determine how partial molar volumes of the hydrocarbons vary with molecular size and type. Independent measurement of the partial molar volume is needed if accurate values of binary interaction parameters are to be obtained.

Interaction of Nonuniform Flow, Cross Flow, and Phase Behavior

Experiments to investigate the effect of low interfacial tension (IFT) on recovery of oil by a combination of gravity segregation and capillary imbibition have also continued. The recovery of oil in imbibition experiments in vertically oriented Berea sandstone cores was investigated further. The recent experiments confirm the results reported previously, i.e., that the recovery of oil by imbibition and gravity segregation is surprisingly effective when IFT is low.

The phase behavior of the ternary fluid system of isooctane–isopropyl alcohol (IPA)–brine (2 wt % $CaCl_2$) mixtures used is shown in Fig. 1. In a typical experiment, a Berea sandstone core (length, 22.5 in.; diameter, 2.5 in.; porosity, 21.3%; permeability, 500 mD) is filled initially with oil phase. The core is then placed in a core holder with an annulus surrounding the core, and the annulus is filled with brine phase. Oil driven from the core by gravity segregation and capillary imbibition collects at the top of the annulus and is removed once each day.

Figure 2 summarizes results of experiments performed with the 500 mD Berea core. Table 1 reports fluid compositions and properties for the six runs shown in Fig. 2.

Runs 1 and 2 indicate the recovery obtained in repeat runs in which pure brine displaced pure isooctane. In those experiments, about 50% of the oil was recovered by some combination of imbibition and gravity segregation. Thus,

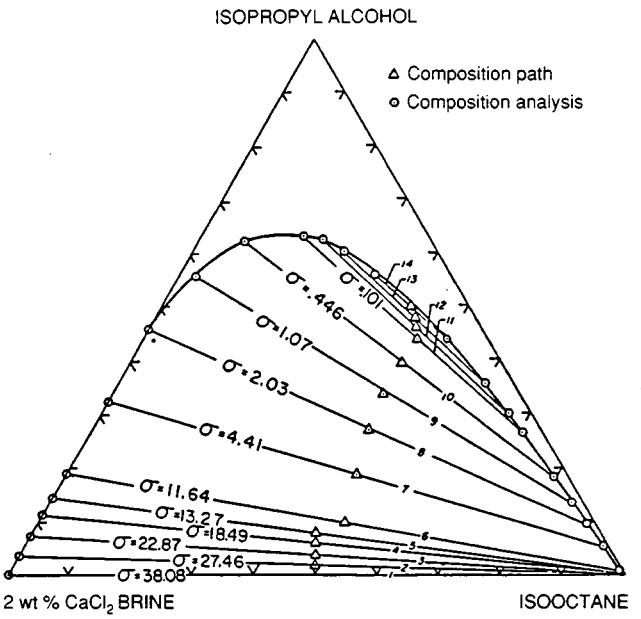

Fig. 1 Ternary diagram of 2 wt % brine–isopropyl alcohol–isooctane system.

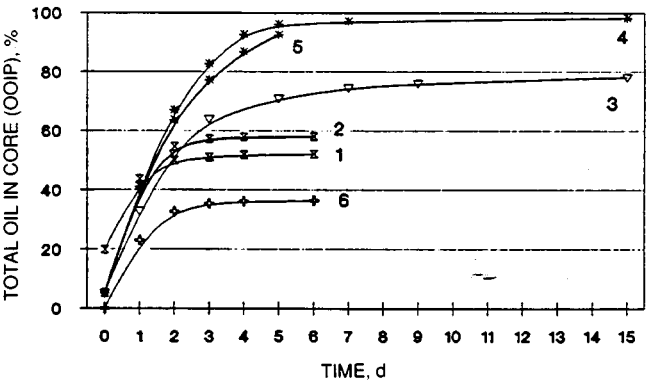

Fig. 2 Recovery of oil by imbibition; K = 500 mD. Numbers on curves indicate experiment numbers.

when the IFT was relatively high (38.1 dynes/cm), a large oil saturation remained in the core when the experiments were terminated.

Run 3 illustrates what happens when the IFT between phases was much lower. In that run, the oil phase present initially was equilibrated with the imbibing brine phase, and, as Table 1 indicates, the IFT was 0.1 dyne/cm. In that displacement, the recovery of the oil phase was nearly 80%. That result is surprising because the IFT is lower, which might be expected to lower the driving force for imbibition, and because the density difference is also lower, which would reduce the driving force for gravity segregation. Apparently the resistance to flow decreased more with the reduction in IFT than did the driving forces. Reasons for the reduction in flow resistance are under investigation.

TABLE 1

Compositions and Properties of Fluids Used in Imbibition Experiments*

Experiment No.	Initial oil phase composition, vol %			Imbibing brine phase composition, vol %			Equilibrated values		
	IPA	IC_8	Brine	IPA	IC_8	Brine	Density difference, g/cm	μ_w/μ_o	IFT, dynes/cm
1	0	100	0	0	0	100	0.33	2.0	38.1
2	0	100	0	0	0	100	0.33	2.0	38.1
3	26.5	70.5	3	63	17	20	0.11	3.7	0.1
4	0	100	0	63	17	20			
5	0	100	0	63	17	20			
6	55	45	0	0	0	100			

*IPA, isopropyl alcohol; IFT, interfacial tension.

In runs 4 and 5, the oil present initially contained no IPA, but the brine phase was equilibrated on the tie line, which showed an IFT of 0.1 dyne/cm. Those runs showed about the same level of repeatability as runs 1 and 2, which is reasonable though not perfect. Just as in run 3, the recovery was high. The recovery reported in Fig. 2 for runs 4 and 5 is the volume of oil phase recovered. It includes some IPA stripped from the oil. The amount of alcohol present in the recovered oil was not measured, but the isooctane fraction in the oil phase must have exceeded the equilibrium value of 70.5% for the brine phase that was imbibing. Thus the recovery in runs 4 and 5 was also substantially higher than that in runs 1 and 2.

Recovery in runs 4 and 5 was enhanced by IFT gradients and by swelling of the oil by IPA as it partitioned from the brine into the oil. As the brine phase, which contained significant amounts of IPA, imbibes into the core containing pure oil, some portion of the IPA partitions into the oil and thus swells and displaces it. The resulting tie line will show some IFT higher than 0.1 dyne/cm. As that equilibrated brine imbibes deeper into the core, more IPA will be stripped into the oil, and, as a result, the IFT will rise. Hence IFTs will be higher toward the interior of the core than at the edge, where the IPA concentration is replenished by brine from the annulus. Possibly the IFT gradient aids recovery because it induces additional flow into the core.

Results of run 6 are consistent with that interpretation. In that experiment, pure brine imbibed into oil containing 55% IPA. In that case, imbibing brine must have extracted IPA from the oil as the brine moved toward the interior of the core. If so, IFTs would decrease toward the interior, and the IFT gradient would impede flow. As Fig. 2 indicates, recovery in run 6 was the lowest of any of the displacements.

The results presented here suggest that enhanced cross flow may be observed in miscible floods. If injected CO_2, or other miscible injection fluid, removed nearly all the oil from a high-permeability layer, then uncontacted oil could move by capillary and gravity-driven cross flow in the zone of relatively low IFTs in the transition zone behind the CO_2 front. The results also suggest that oil recovery processes could be designed on the basis of low IFTs for use in fractured reservoirs.

DEVELOPMENT OF IMPROVED IMMISCIBLE GAS DISPLACEMENT METHODOLOGY

Cooperative Agreement DE-FC22-83FE60149, Project BE5B

National Institute for Petroleum and Energy Research
Bartlesville, Okla.

Contract Date: Oct. 1, 1983
Anticipated Completion: Sept. 30, 1990
Funding for FY 1990: $260,000

Principal Investigator:
Arden Strycker

Project Manager:
Jerry F. Casteel
Bartlesville Project Office

Reporting Period: Apr. 1–June 30, 1990

Objective

The objective of this research is to develop methods for improving sweep efficiency and mobility control for gas flooding.

Summary of Technical Progress

Foam Flow in Porous Media

Radial flow experiments in a cylindrical Berea sandstone core were used to study the effects of foam on gas injectivity. Foam flow in the high-pressure-drop, near-wellbore region surrounding an injection well was simulated. One goal of this research is to increase injectivity during foam flooding without decreasing mobility-control effects. Injection sequences and slug sizes of different fluids were varied to determine their effects on gas injectivity and foam generation and propagation. Experiments were conducted in the constant-pressure mode, with the inlet pressure fixed at 5 psig and the outlet fixed at atmospheric pressure; this allowed the rates to vary as the effective permeabilities changed.

All experiments used the same cylindrical core, which was 6 in. in outside diameter, 0.125 in. in inside (wellbore) diameter, and 1.91 in. thick. The fluids used were a 0.5 wt % NaCl brine, a foamer consisting of 0.5 wt % active Alipal CD-128 surfactant in that same brine, and pure nitrogen gas. Foam generation and propagation were tracked through the core by means of four intermediate pressure taps and monitoring five differential pressures across the core. The baseline experiment for injectivity (test No. 4) began with the core fully saturated with brine. After displacement of this brine to a residual water saturation by injection of nitrogen gas, a 0.1-pore volume (PV) slug of foamer was injected and followed by continuous nitrogen injection until differential pressures and flow rates stabilized. This procedure represented a common method of foam injection in which foam is generated in situ beginning at or near the wellbore face. Test No. 5 began with the core fully saturated with surfactant solution followed by continuous injection of nitrogen. Test No. 6, otherwise identical to test No. 4, attempted to move the point of foam formation away from the high-pressure-drop, near-wellbore region by injecting a 0.02-PV slug of brine after the foamer and before the gas injection. Similarly, test No. 7 used a smaller 0.012-PV slug of brine between the foamer and gas. For laterally homogeneous permeability, a disproportionate share of the pressure drop (36% for liquid and 40% for gas) across the core occurred in the first 0.73 in., which is where the first pressure tap was located. This represents only 24% of the distance to the outer producing radius and only 6% of the pore volume. In oil and gas fields, the near-wellbore pressure drop is even more disproportionate since the ratio of the wellbore radius to the drainage radius is even smaller than that of the core model being used in these experiments.

After many pore volumes (several thousand) of gas injection, the foam evenly distributed throughout the core in all cases tested. This conclusion was based on the resulting pressure distribution curves, which were very close to the idealized curve for steady-state gas flow through a core of homogeneous permeability. A comparison between test No. 4 (Fig. 1) and test No. 6 (Fig. 2) showed no significant differences between them. Also, results of test No. 7 were similar to those of No. 6.

The water slugs between the foamer and gas did not appear to increase injectivity. The average permeabilities measured across the entire core for the experiments conducted are compared in Table 1. The relative permeabilities to nitrogen were actually lower in tests 6 and 7 than in

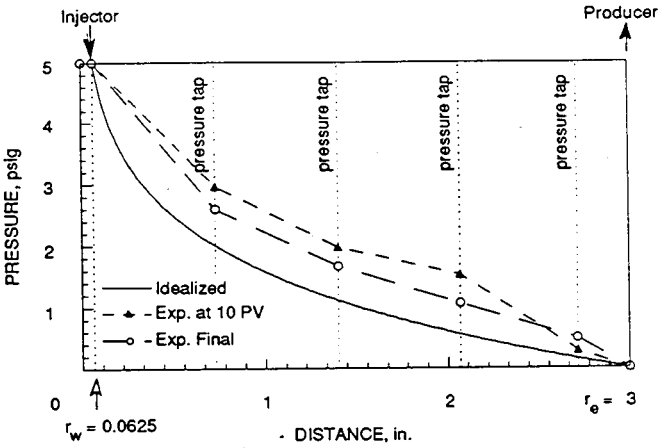

Fig. 1 Pressure distribution for foam test No. 4 during gas injection.

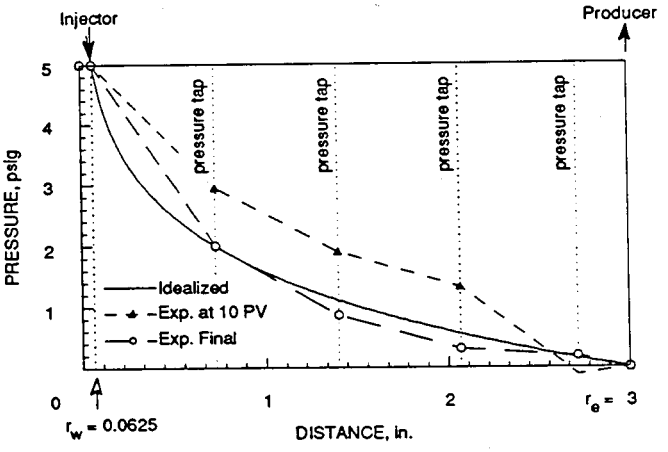

Fig. 2 Pressure distribution for foam test No. 6 during gas injection.

TABLE 1

Core Effective Permeabilities to N_2 After Foam Formation

Test No.	Permeability to nitrogen, mD	
	At 10 PV N_2 injection	Final
4	5.8	10.3
5	1.0	2.2
6	2.8	4.2
7	2.8	3.9

test 4. Since the brine slugs were too small to dilute the surfactant slug below its critical micelle concentration, the brine slug appeared to have a slightly beneficial effect of helping foam propagate, as was shown in previous long-distance slim-tube tests.[1]

Entrainers

The objective of this activity, evaluating carbon dioxide entrainers, is to continue to study some of the more promising entrainer candidates and to improve the efficiency of laboratory procedures used in making these evaluations. A carbon dioxide entrainer is a cosolvent that enhances the solution properties of carbon dioxide in some way. For enhanced oil recovery (EOR) applications, the entrainer should enhance the solubility of the crude oil and, if possible, improve the mobility properties of the injected gas. Ideally, the addition of an entrainer to carbon dioxide would increase the viscosity by one to two orders of magnitude and the crude oil solubility by a factor of 2 or more, but at the same time the entrainer would not adsorb onto reservoir rock or absorb into connate water. Some researchers have found that the addition of minor amounts of certain materials to carbon dioxide selectively increases the solubility of another desired material. Work completed over the past 2 yr in this laboratory has shown that some entrainer materials increase the percentage of heavy ends contained in the extracted crude oil. The objective of this task is to find a material as an entrainer that approaches these ideal properties for EOR applications.

For the effective development of entrainers in EOR applications, a predictive model to estimate solubilities of high-molecular-weight compounds (solid or liquid) in a gas at high pressure is essential to efficiently screen the many possible candidates. An accurate predictive model would be used to quickly screen candidate entrainers and to save time in conducting detailed experimental work. Discussions in the previous quarterly report outlined the best method, the Kirkwood–Buff solution theory as applied to supercritical carbon dioxide mixtures, for estimating entrainer solubilities in supercritical carbon dioxide.

Further, an assumption was made that the enhanced solubilities of crude oil by the addition of entrainers result from a beneficial modification of the carbon dioxide phase behavior. Solubility and phase behavior have been studied for a variety of compounds in supercritical carbon dioxide, nitrogen, and other gases. Various equations of state have been developed to relate phase behavior to composition, temperature, and pressure. However, as discussed previously,[2] most equations of state do not adequately predict behavior of mixtures near the critical region of the system, and it is near or above this temperature and pressure region that the greatest enhancement of solubilities is seen. An alternative approach was taken by relying on the well-established relationship between phase behavior and the development of miscibility. The method of Orr and Silva[3] for estimating minimum miscibility pressure (MMP) was used. This method is represented by the following equations:

$$\rho_{MMP} = -0.524F + 1.189 \qquad (1a)$$

where $F < 1.467$

and

$$\rho_{MMP} = 0.42 \qquad (1b)$$

where $F > 1.467$

$$F = \sum_{2}^{37} K_i w_{iC_{2+}} \qquad (2)$$

$$w_{iC_{2+}} = \frac{w_i}{\sum_{i=2}^{37} w_i} \qquad (3)$$

$$\log K_i = aC_i + b \qquad (4)$$

where the variable ρ_{MMP} = estimated MMP
F = weighted-composition factor
K_i = normalized partition coefficient for carbon number i
$w_{iC_{2+}}$ = normalized weight fraction of carbon number i in the C_{2+} fraction
w_i = weight fraction of carbon number i in the oil
C_i = carbon number
$a = -0.04175$
$b = 0.7611$

For purposes of prescreening, the estimated MMP values for a variety of compounds at various concentrations were compared to determine if certain groups of compounds appear more beneficial than other groups. Although the error of estimation based on these equations could be large, such errors were not considered critical since general information on groups of compounds was of more interest than accurate information on individual compounds.

A total of 83 compounds were screened on the basis of their critical properties (critical temperature, critical pressure, critical volume, vapor pressure, and density). The MMP was estimated for an arbitrarily selected crude oil (Wilmington field, Ford zone) at 50°C. Because of lack of information, some of the critical parameters were estimated for a few of these compounds with Somayajulu's procedures.[4] The critical volume was estimated for 28 compounds; the critical pressure was estimated for 8 compounds; and the critical temperature was estimated for 2 compounds. Values of MMP were estimated for three concentrations of entrainer: 5.0 mol %, 8.0 wt %, and maximum solubility in carbon dioxide for the given

conditions. The MMP corresponding to the lowest amount of entrainer from these three choices was selected for screening. The MMP factor shown in Figs. 3 to 5 is simply the ratio of estimated MMP for the respective compound over the MMP of carbon dioxide alone. A value of 0 would indicate that, under the stated conditions, the entrainer reduced the MMP to ambient pressures and would substantially enhance the ability of the carbon dioxide to recover oil under a variety of conditions. An additional simplification was made by not allowing the carbon dioxide entrainer to dissolve into the crude oil (condensing gas drive). To the extent that this occurs for selected compounds, equations 1 to 4 may not apply. Also, viscosity enhancements were not considered; therefore sweep efficiencies were not considered. This effect needs to be considered separately.

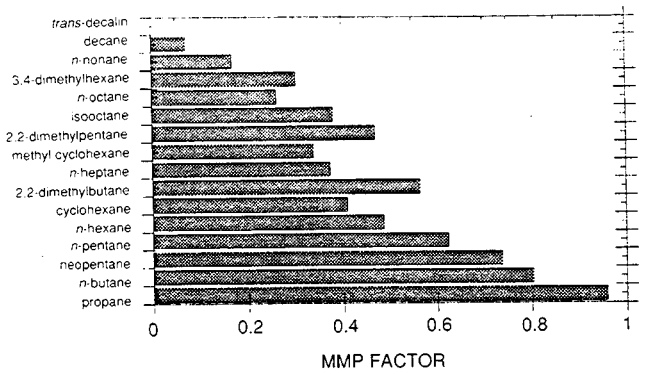

Fig. 3 Estimation of minimum miscibility pressure (MMP) factor for a variety of hydrocarbons.

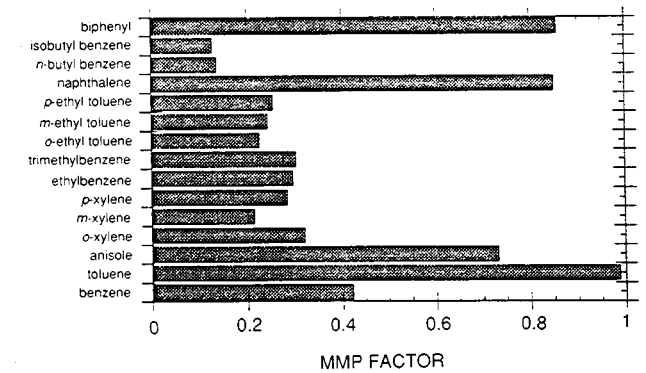

Fig. 4 Estimation of minimum miscibility pressure (MMP) factor for a variety of aromatic compounds.

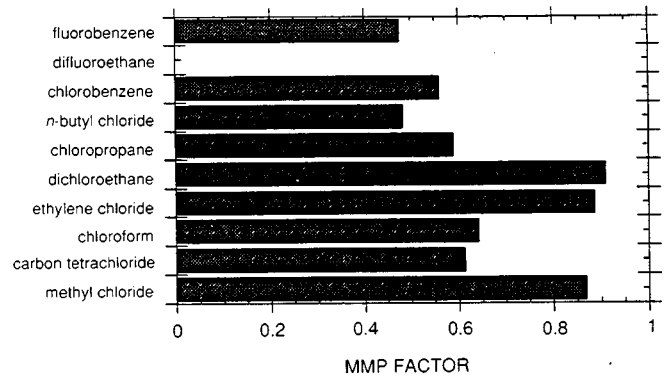

Fig. 5 Estimation of minimum miscibility pressure (MMP) factor for a variety of halogenated compounds.

A variety of hydrocarbon compounds was considered, and some are represented in Fig. 3. On the basis of the results in Fig. 3, longer-chain hydrocarbons provide the greatest benefit to carbon dioxide phase behavior. Branched hydrocarbons are beneficial for the larger molecules but not for the smaller molecules. The best candidates (Fig. 3) are *trans*-decalin, decane, *n*-nonane, and *n*-octane. Isooctane was previously studied in the laboratory and is estimated to be somewhat mid-range in MMP factor for the compounds studied.

Aromatic compounds were considered, and some are represented in Fig. 4. Essentially, any aromatic compound with some alkyl substituents substantially reduces MMP. Examples include xylenes, trimethyl benzene, ethyl toluene, and butyl benzene. Benzene, toluene, and di-aromatics do not appear to improve phase behavior very effectively.

Halogenated compounds were considered, and some are represented in Fig. 5. Although most of these compounds appear to provide some benefit, the only excellent choice was difluoroethane. Other compounds were also considered, including branched alcohols, phenols, carboxylic acids, nitriles, and nitrobenzene. Although some benefit was seen with some of the alcohols, none of them were as effective as alkyl substituted monoaromatics and long-chain hydrocarbons.

References

1. D. A. Hudgins and T-H. Chung, *Long-Distance Propagation of Foams*, SPE/DOE paper 20196, presented at the Seventh SPE/DOE Symposium on EOR, Tulsa, Okla., Apr. 22–25, 1990.
2. National Institute for Petroleum and Energy Research, *Quarterly Technical Report for January 1–March 3, 1990*, DOE Report NIPER-470, pp. 50-57, 1990.
3. F. M. Orr, Jr., and M. K. Silva, Effect of Oil Composition on Minimum Miscibility Pressure—Part 2: Correlation, *SPE Reservoir Eng.*, 479-491 (November 1987).
4. G. Raam Somayajulu, Estimation Procedures for Critical Constants, *J. Chem. Eng. Data*, 34(1): 106-120 (1989).

GAS-MISCIBLE DISPLACEMENT

Cooperative Agreement DE-FC22-83FE60149, Project BE5A

National Institute for Petroleum and Energy Research
Bartlesville, Okla.

Contract Date: Oct. 1, 1983
Anticipated Completion: Sept. 30, 1990
Funding for FY 1990: $380,000

Principal Investigator:
Ting-Horng Chung

Project Manager:
Jerry F. Casteel
Bartlesville Project Office

Reporting Period: Apr. 1–June 30, 1990

Objectives

The research of this project is designed to study the gas foaming technology for gas mobility control and the organic deposition problem in gas-miscible flooding. The objectives of this work are to develop a mathematical model that describes the adsorption and transport of foaming agents in reservoir rock and to develop a model that describes the deposition of organic materials under miscible conditions.

Summary of Technical Progress

Adsorption of Foaming Agents on Reservoir Rock

Adsorption studies for the two anionic surfactants, Alipal CD-128 (nonadecyldiethoxy ammonium sulfate) and sodium dodecyl sulfate (SDS), on different types of crushed rocks were continued this quarter. Both static (equilibrium) and dynamic (flow) experiments were conducted to investigate the effects of pH, temperature, salinity, alcohol, and sodium bicarbonate on the adsorption of the two surfactants on various rocks. The adsorbents used in this study included kaolinite, limestone, Berea Sandstone, and reservoir sand. Their properties are listed in Table 1.

The losses of Alipal CD-128 on limestone, kaolinite, and Berea Sandstone were compared on a surface-area basis (Fig. 1). The surfactant loss data were measured by static tests and chemical analysis with the hyamine titration method. The loss of the surfactant on limestone was much higher than that on Berea Sandstone and kaolinite. Adsorption appears to be only one of several mechanisms that contribute to high surfactant loss. Limestone is particularly noted for its high calcite content. Calcite, when dissolved in water, may produce the following main chemical species: Ca^{2+}, CO_3^{2-}, HCO_3^-, H_2CO_3, H^+, OH^-, $CaOH^+$, and $Ca(OH)_2$ (Ref. 1). Interaction of these ions with the anionic surfactants can produce precipitation.[2] Figure 2 shows the adsorption isotherm for the two anionic surfactants on limestone at 75°F. Alipal CD-128 has greater adsorption on limestone than SDS.

TABLE 1

Particle Size and Surface Area of Crushed Rock

Rock type	Particle size, μm	Surface area, m^2/g
Berea Sandstone	150 to 180 (80 to 100 mesh)	0.477
Liao He reservoir sand	250 to 425 (40 to 60 mesh)	1.88
Dolomitic limestone	250 to 425 (40 to 60 mesh)	0.17
Kaolinite	5 to 90 (170 to 500 mesh)	15.17

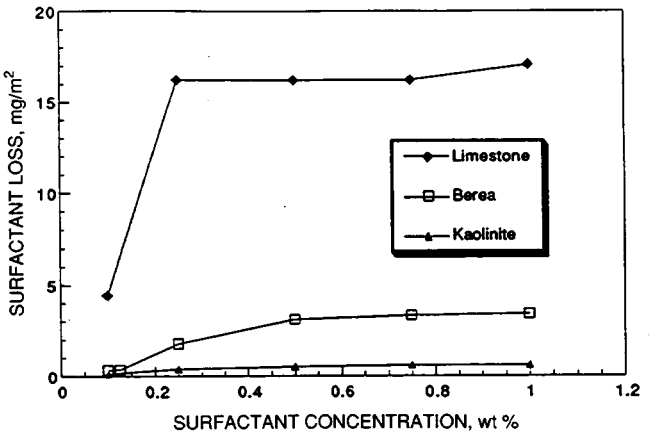

Fig. 1 Alipal CD-128 loss on various media. Alipal CD-128 in deionized water at 75°F.

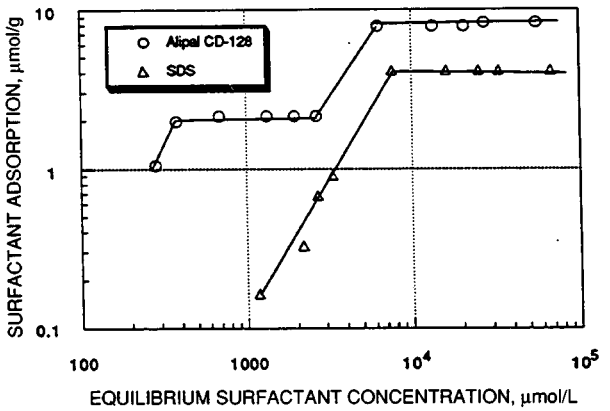

Fig. 2 Adsorption isotherms for anionic surfactants on 40- to 60-mesh limestone at 75°F.

The effects of pH, alkaline, salinity, alcohol, and temperature on surfactant adsorption were tested for Alipal CD-128 on kaolinite. The adsorption of Alipal CD-128 is higher at low pH values than at high pH values. With low-pH alkaline agents, such as sodium bicarbonate ($NaHCO_3$), surfactant adsorption is reduced significantly, as shown in Fig. 3, and may be one of the beneficial aspects of surfactant alkaline flooding.[3] Because of the reduction of surfactant adsorption in the presence of alkaline agents, the surfactant–alkaline injection method facilitates the use of low concentrations of surfactants. The addition of alcohol cosolvents, e.g., isopropanol (IPA), can also reduce surfactant adsorption, as shown in Fig. 4. Figures 3 and 4 also show that surfactant adsorption increases with NaCl concentration until it reaches a maximum at NaCl concentration below 0.5*M* and then slightly decreases. The temperature effect on surfactant adsorption is not significant.

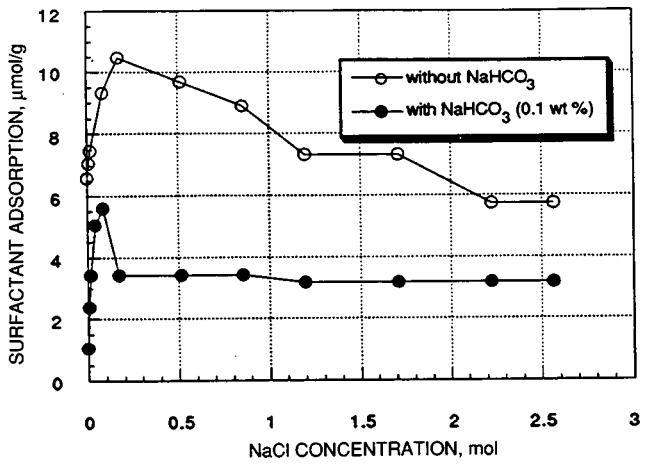

Fig. 3 Alkaline effect of 0.25% Alipal CD-128 adsorption on kaolinite at 75°F.

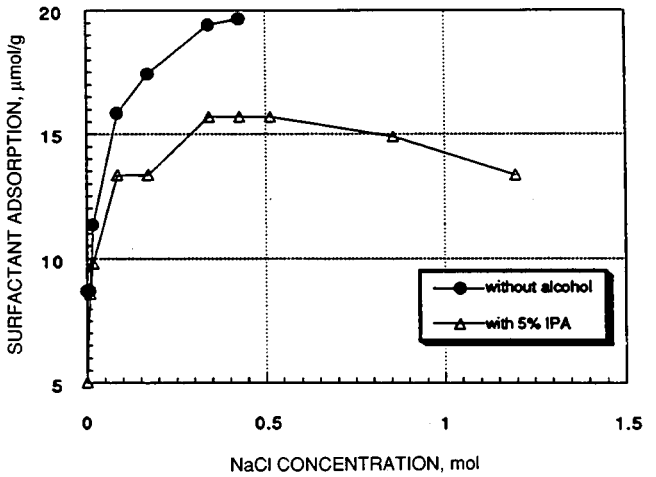

Fig. 4 Alcohol effect of 0.25% Alipal CD-128 adsorption on kaolinite at 75°F.

Modeling Chemical Adsorption–Desorption and Transport in Porous Media

The general one-dimensional (1-D) model for dynamic adsorption of chemical in porous media with stagnant volume (reported last quarter) was modified for radial flow patterns. An experimental project to study foam generation and propagation in a radial core is being performed. This model could be applied to the radial core experiment or near wellbore case to predict the propagation of surfactant. The physical model is shown in Fig. 5. Under the assumptions of homogeneous porous medium and constant injection rate, the macroscopic balance equation for surfactant solution can be written as

$$D\left[\frac{1\partial}{r\partial r}\left(r\frac{\partial C}{\partial r}\right)\right]-v(r)\frac{\partial C}{\partial r}=f\left[\frac{\partial C}{\partial t}+\frac{A_s}{\phi}\frac{\partial C_s}{\partial t}\right]+(1-f)\left[\frac{\partial C^*}{\partial t}+\frac{A_s}{\phi}\frac{\partial C_s^*}{\partial t}\right] \quad (1)$$

and the microscopic balance equations are

$$k(C-C^*)=\left(\frac{\partial C^*}{\partial t}+\frac{A_s}{\phi}\frac{\partial C_s^*}{\partial t}\right) \quad (2)$$

$$\frac{\partial C_s}{\partial t}=k_a(Q_s-C_s)C-k_dC_s \quad (3)$$

$$\frac{\partial C_s^*}{\partial t}=k_a(Q_s-C_s^*)C^*-k_dC_s^* \quad (4)$$

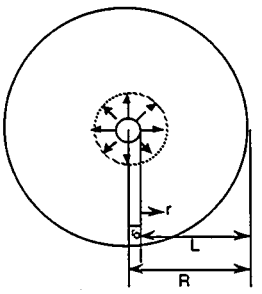

Fig. 5 Physical model of radial core.

Boundary conditions:

At $r = r_o$, $t > 0$,

$$VC - V_oC_o = D\frac{\partial C}{\partial r} \quad (5)$$

At r = R, t > 0,

$$\frac{\partial C}{\partial r} = 0 \qquad (6)$$

where C = surfactant concentration in flow fluid
C^* = surfactant concentration in stagnant volume
C_s = surfactant adsorption on the solid surface
C_o = injected surfactant concentration
D = dispersion coefficient
ϕ = porosity
f = fraction of pore space occupied by mobile fluid
A_s = solid interstitial area per unit volume
k = mass transfer coefficient
k_a = adsorption rate constant
k_d = desorption rate constant
Q_s = total adsorbent capacity
V_o = flow velocity at the inlet of well bore
v = interstitial velocity

V_o is constant and the balance equation is written in cylindrical coordination (r, Θ, Z). Since the porous media are homogeneous in porosity and permeability, there is no variation in flow in the Θ-direction and z-direction (ignoring gravity segregation). Since only r-direction flow is considered, this model is a 1-D radial flow model. These coupled partial differential equations were solved numerically by finite differences of the Crank–Nicolson scheme as the linear model. Computer coding has been completed.

Asphaltene Precipitation Study

Experiments to study the reversibility of asphaltene precipitation and dissolution in oil and the effects of aromatics on the reversible process have been conducted for New London (Arkansas) crude oil. First, experiments were designed to compare asphaltene precipitation by pentane titration for two samples of the same oil. Toluene (22%) was intentionally added to one sample before pentane titration. The amount of asphaltene precipitated by pentane for these two sample oils was the same (4.5 wt %). The morphology of the precipitated asphaltene is a fine granular structure and was similar for both samples. This shows that aromatic content does not affect asphaltene precipitation. Second, experiments were designed to study the reversibility of the asphaltene precipitation–dissolution process and the effect of aromatics. In the first test, precipitated asphaltene was redissolved in the original oil (asphaltene-free). The added pentane was vaporized, and thus the oil was recovered to its original composition (except asphaltene) before being mixed with the asphaltene. Results showed that approximately 23% of the asphaltene redissolved in the oil. The undissolved asphaltene was a hard asphaltic mass. In the second test, the asphaltene was dissolved in toluene (4:1 by weight) and then mixed with the oil. A solid asphaltic film was left on the filter. Approximately 56 wt % of the asphaltene was dissolved in the oil. These experiments show that the asphaltene dissolution–precipitation process is not totally reversible and that oil composition has some effect on this process.

References

1. P. Somasundaran and G. E. Agar, The Zero Point of Charge of Calcite, *J. Colloid Interface Sci.*, 24: 433 (1967).
2. H. S. Al-Hashim, M. S. Celik, M. M. Oskay, and H. Y. Al-Yousee, Adsorption and Precipitation Behaviour of Petroleum Sulfonates from Saudi Arabian Limestone, *J. Pet. Sci. Eng.*, 1: 335 (1988).
3. T. R. French and T. E. Burchfield, *Design and Optimization of Alkaline Flooding Formulations*, paper SPE/DOE 20238, presented at the Seventh SPE/DOE Symposium on EOR, Tulsa, Okla., Apr. 22–25, 1990.

QUANTIFICATION OF MOBILITY CONTROL IN ENHANCED RECOVERY OF LIGHT OIL BY CARBON DIOXIDE

Morgantown Energy Technology Center
Morgantown, W. Va.

FY90 Total Project Cost: $550,000

Principal Investigator:
Duane H. Smith

Project Manager:
Royal J. Watts
Morgantown Energy Technology Center

Reporting Period: Apr. 1–June 30, 1990

Objective

The current objective of the Morgantown Energy Technology Center (METC) enhanced oil recovery research is to conduct experimental and theoretical studies to improve the recovery efficiency of the carbon dioxide (CO_2) miscible flooding process. Since reducing the mobility ratio seems to provide efficient flood performance, the research is being directed to the study and use of viscous CO_2. The technique involves the use of surfactants to generate a CO_2 dispersion that would retard the growth of viscous fingers and also act as an in situ diverting agent. The merits of CO_2 dispersion will be determined by performing linear core-flow studies on large-scale systems. This effort will be supplemented by theoretical and experimental studies of CO_2 dispersions, studies of the effects of altered wettability of rock surfaces, and determination of in situ saturation profiles as probed by X-ray computerized tomography and nuclear magnetic

resonance imaging. The laboratory data will also be used to test the METC compositional model, and the model will be used to plan critical experiments.

Summary of Technical Progress

Background

The foams (or emulsions) created by capillary snap-off in CO_2 mobility control commonly produce pressure gradients in excess of 500 psi/ft in steady-state relative permeability measurements.[1] Pressure gradients of this magnitude are far too large for use in the field to modify CO_2 mobilities and could even hinder the use of CO_2 foams as blocking agents by making it difficult to inject the foaming agent.

Hence, as part of the search for ways to void excessive near-well pressure gradients from CO_2 dispersions, the effects of leave-behind lamellae on the flow properties of CO_2 (at typical miscible-flood pressures) have been studied to better characterize their utility for field processes. Leave-behind lamellae are created in a single-cycle surfactant alternating gas (SAG) process in which surfactant solution is first injected and then followed by CO_2.

Effect of Leave-Behind Lamellae on Relative Permeabilities for CO_2–Aqueous Surfactant Systems at Reservoir Pressure

Reliable relative permeability data are a prerequisite for the design of a recovery process through reservoir simulation and for modeling injection and production problems. The relative permeability concept is based on the assumption that the flowing phase is continuous and Darcy's law is valid. When CO_2 displaces an aqueous phase that contains a surfactant, lamellae can be formed, and both gas and water relative permeability can be substantially reduced.[2] The dominant lamella-generation mechanism at velocities below the critical velocity in relatively homogeneous porous media is the so-called "leave-behind" mechanism. The leave-behind lamellae form no separate gas bubbles, so the gas remains a continuous phase. Therefore the relative permeabilities can be computed with the dynamic displacement method of Johnson, Bossler, and Neumann.[3]

Figure 1 shows typical relative permeability curves for systems with 2% NaCl brine and with 0.0, 0.05, 0.1%, and 0.2 active wt % Alipal CD-128. Table 1 summarizes the results.

A relative permeability reduction factor was calculated at residual water saturation by dividing the pressure drop for the flow with surfactant by the pressure drop without surfactant at the same CO_2 saturation. It shows that the gas mobility can be reduced by more than an order of magnitude with low surfactant concentrations.

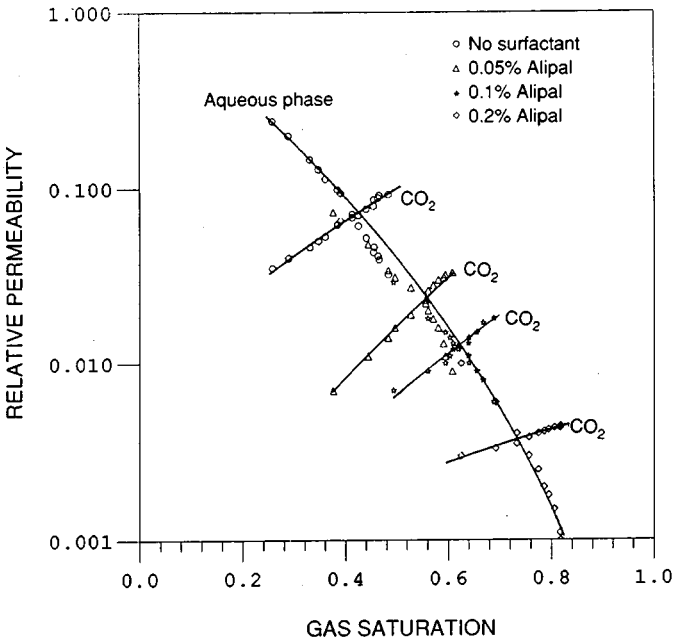

Fig. 1 Effect of leave-behind lamellae formed by Alipal CD-128 on relative permeabilities of the aqueous and the CO_2-rich phase.

TABLE 1

Summary of Relative Permeability Experiments with the Unsteady-State Method

Run	Surfactant concentration	Water saturation at CO_2 breakthrough	End-point CO_2 relative permeability	Relative permeability reduction factor*
1	0.0	0.64	0.026	1
2	0.05	0.52	0.01	2.6
3	0.01	0.41	0.006	4.33
4	0.2	0.31	0.001	26

*Relative permeability reduction factor equals CO_2 relative permeability without surfactant–CO_2 relative permeability with surfactant.

From the results of this work, the following observations can be made:

1. Aqueous-phase saturation at breakthrough decreased with increasing surfactant concentration, which indicates a more piston-like displacement of aqueous phase in the presence of surfactant (Table 1, column 3).

2. CO_2 relative permeabilities were always lower when surfactant was added to the brine. However, at higher surfactant concentrations, the gas relative permeability seemed to be less dependent on saturation.

3. The aqueous-phase relative permeability appeared to be a unique function of saturation, which is in concordance with the steady-state relative permeability measurements of Bernard, Holm, and Jacobs[4] and the displacement experiments of Friedman, Chen, and Gauglitz.[5] Also, lower

final water saturations were observed when surfactant was present. [However, the latter fact does not imply that the residual water saturation should be different when surfactant is present because the experiments were terminated for technical reasons at about 5 pore volumes (PV) of CO_2 injected.]

Experimental

Constant-rate CO_2 injection experiments were run by injecting supercritical CO_2 at 4.4 ft/d (superficial velocity) into Berea rock saturated with surfactant solution. The foaming surfactant, Alipal CD-128 (GAF Corporation), was dissolved in 2% NaCl brine. The Berea sandstone was 3.81 cm in diameter and 76.2 cm in length with a permeability to water of 0.5 μm (500 mD). The rock was coated with a viscous epoxy, mounted in shrinkable rubber sleeves, and placed inside the core holder. Pressure drops across the core and absolute upstream and downstream pressures were measured with Setra pressure transducers. The downstream back-pressure regulator was set at 1525 psi. The CO_2 was injected from a Temco pressure cell through a back-pressure regulator set at 1715 psi.

Effluent "water" volumes were measured in graded test tubes; the produced CO_2 was measured with a digitized wet test meter. Pressure data, times, and produced CO_2 were stored simultaneously on a hard disk. All these data were needed for individual relative permeability calculations with the unsteady-state method.[3]

Mobility Control by Means of Low-Molecular-Weight Surfactants

The use of low-molecular-weight surfactants at concentrations below their critical micelle concentrations may prove to be the most effective way to improve CO_2 mobility control. These materials may make it possible to use foams and/or other types of true fluid dispersions without creation of excessive pressure gradients. Studies of low-molecular-weight anionic surfactants have been reported in the literature;[6] low-molecular-weight nonionic surfactants have been investigated for this project.

The design of an injection scheme requires phase information for mixtures of the foamant with water. The phase diagram of the $C_6H_{13}(OC_2H_4)_2OH$–water system from 0 to 70°C has been measured. Like many of its homologues, this foamant has a miscibility gap with water; Fig. 2 shows the phase behavior. As obtained from a fit of critical scaling theory to the data, the lower consolute point is at 10.9°C and 12.9 wt % amphiphile. Thus the use of this foamant may appear to be limited to concentrations less than about 1 wt %. However, because the amphiphile should be used at low concentrations far below its critical micelle concentration, its limited solubility in water does not appear to present any significant practical problems.

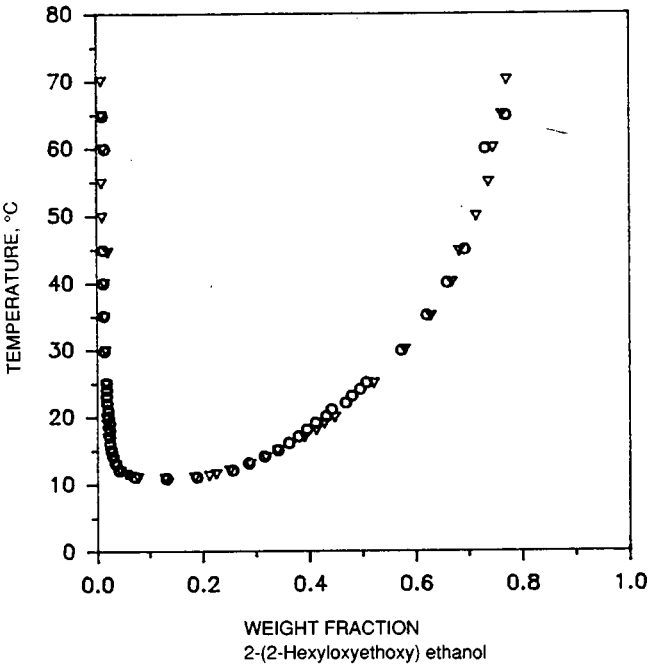

Fig. 2 Miscibility gap of $C_6H_{13}(OC_2H_4)_2OH$ with water and with 10 m*M* NaCl brine.

References

1. H. O. Lee and J. Heller, *Laboratory Measurements of CO_2–Foam Mobility*, paper SPE/DOE 17363 presented at the SPE/DOE Enhanced Oil Recovery Symposium, Tulsa, Okla., Apr. 17–20, 1989.
2. C. J. Radke and T. C. Ransohoff, *Mechanism of Foam Generation in Glass Bead Packs*, paper SPE 15441 presented at the 61st Annual Meeting of SPE, New Orleans, La., Oct. 5–8, 1986.
3. E. F. Johnson, D. P. Bossler, and V. O. Neumann, Calculation of Relative Permeability from Displacement Experiments, *Trans. AIME*, 370-372 (1959).
4. G. G. Bernard, L. W. Holm, and W. L. Jacobs, Effect of Foam on Trapped Gas Saturation and on Permeability of Porous Media to Water, *Soc. Pet. Eng. J.*, 295-300 (December 1965).
5. F. Friedmann, W. H. Chen, and P. A. Gauglitz, *Experimental and Simulation Study of High-Temperature Foam Displacement in Porous Media*, paper SPE/DOE 17357 presented at the SPE/DOE Enhanced Oil Recovery Symposium, Tulsa, Okla., Apr. 17–20, 1988.
6. M. Kuhlman et al., *Carbon Dioxide Foam with Surfactants Used Below Their Critical Micelle Concentrations*, paper SPE/DOE 20192 presented at the SPE/DOE Enhanced Oil Recovery Symposium, Tulsa, Okla., Apr. 22–25, 1990.

ENHANCED OIL RECOVERY MODEL DEVELOPMENT AND VALIDATION

Morgantown Energy Technology Center
Morgantown, W. Va.

FY90 Total Project Cost: $200,000

Principal Investigator:
Rodney A. Geisbrecht

Project Manager:
Royal J. Watts
Morgantown Energy Technology Center

Reporting Period: Apr. 1–June 30, 1990

Objectives

Plans for FY 1990 are organized into corefloods, microvisual models, pore-level mechanistic modeling, and reservoir simulation techniques. Corefloods will primarily focus on the relative merits of ex situ and in situ foam generation, with the possibility of measuring carbon dioxide (CO_2) flowing fraction under reservoir conditions. Pore-level network simulators will be used to explore basic mechanisms in foam flow, such as division, trapping, and mobilization. Microvisual models will be used in conjunction with network simulators and will also be used to screen surfactants on the basis of fluid–fluid interactions at reservoir conditions. Reservoir simulation techniques accounting for the fluid-flow instabilities associated with foaming flow (trapping) will be pursued.

One objective during the reporting period was to verify that measured relative permeability reductions for the first cycle of surfactant-alternating-gas (SAG) injection schemes are solely accountable by disjoining ("leave-behind") lamellae mechanisms.

Another objective during the reporting period was to assess whether leave-behind mechanisms are adequately represented in reservoir-scale simulators, and, if not, how their representation can be improved. Reservoir-scale simulators with mobility control features are typified by population balance models that include an empirical relative permeability curve for representing all the effects of leave-behind lamellae.[1]

These objectives support the Morgantown Energy Technology Center (METC) FY 1990–1991 goal of assessing outstanding technical issues concerning the use of leave-behind lamellae in particular, and SAG injection schemes in general, for mobility control and fluid diversion,[2] e.g., how mobility control depends upon rock permeability and surfactant formulation and how mass transfer between dendritic (dead end) channels and flowing channels affects optimal process design.

Summary of Technical Progress

During the current reporting period, pore-level "leave-behind" mechanisms were simulated in various numerical models, with emphasis on a modified version of a standard stochastic model known as gradient-governed growth.[3,4]

Modifications included flow rules that emulate the formation leave-behind lamellae and procedures that account for the effects of interfacial tension between immiscible fluids. The immiscible network models that resulted are distinct from miscible models used primarily for supporting studies.[5]

Immiscible vs. Miscible Network Modeling

The essential differences between immiscible and miscible modeling concern the handling of three factors that are strongly affected by interfacial tension: (1) ganglia trapping, (2) cross-flow checking, and (3) interface correlation. Ganglia trapping and cross-flow checking are well-known effects of interfacial tension at the pore scale. An efficient algorithm to detect and trap ganglia was developed along with a formal procedure to enforce cross-flow checking. Interface correlation is a hypothetical Haines jump phenomenon that can be easily implemented in simulations to generate more plausible immiscible fingering morphologies. It is described in a previous quarterly report.[6]

Leave-Behind Lamellae in Gradient-Governed Growth

The flow rules and interpretive schemes for investigating leave-behind lamellae in diffusion-limited aggregation and invasion percolation are described in the previous quarterly report.[7] Gradient-governed growth allows a test of the effects of leave-behind lamellae on the flow field of real (i.e., viscid) fluids.

The effect of leave-behind lamellae on the displacement pattern for the moderately unfavorable viscosity ratio of 100 is shown in Fig. 1. For much higher viscosity ratios, relative permeability reduction factors of about 10 do not significantly affect the pattern, as might be expected. Up to this point, reduction factors much above 10 have not been predictable regardless of ganglia trapping, cross-flow checking, or interface correlation. Experimental measurements up to the order of 100 have been measured.[8,9] Since simulations were confined to simple two-dimensional quadratic networks, the dimensionality, connectivity, and topology of the pore space may be important factors.

Mass Transfer in Networks of Leave-Behind Lamellae

Patterns generated by invasion percolation and gradient-governed growth, forced to full sweep efficiency without ganglia trapping or cross-flow checking, are compared in Fig. 2. An essential difference is the chaotic structure of dendrites by invasion percolation (inviscid fluids).

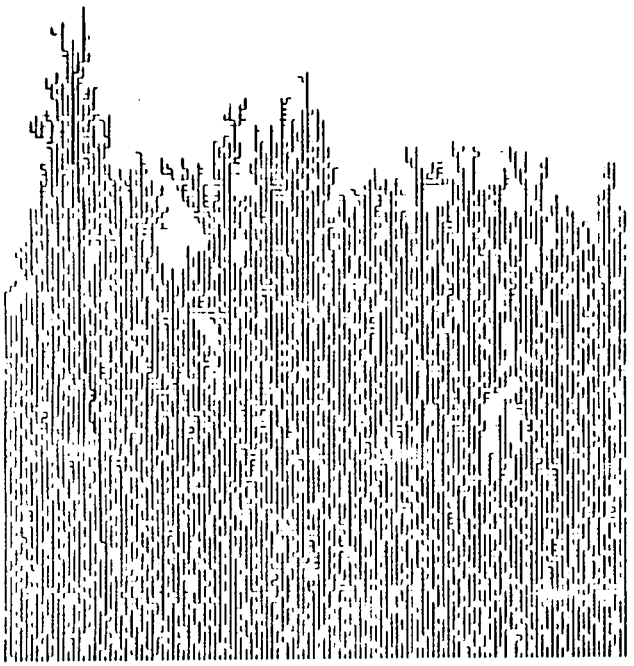

(a)

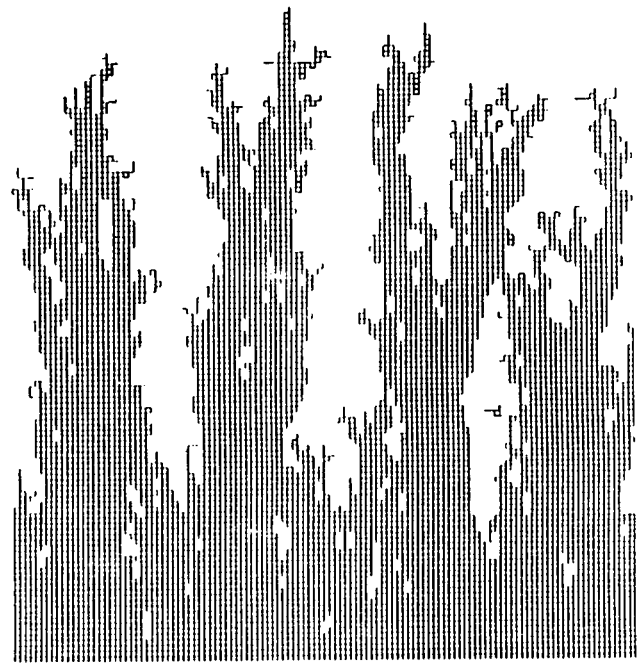

(b)

Fig. 1 Gradient-governed growth predicted patterns with (a) and without (b) leave-behind lamellae. Viscosity ratio, 100; 120 × 120 grid.

Dendrites and leave-behind lamellae by gradient-governed growth (real, viscid fluids) are more or less parallel to the flow field for significant distances, the most unfavorable orientation from the standpoint of mass transfer rates between dendritic and flowing channels.

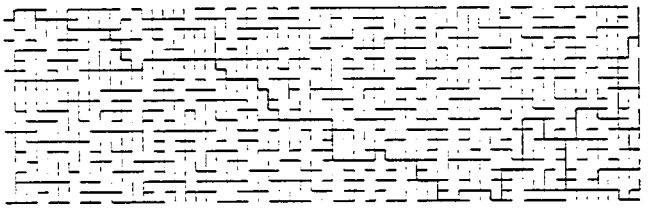

(a)

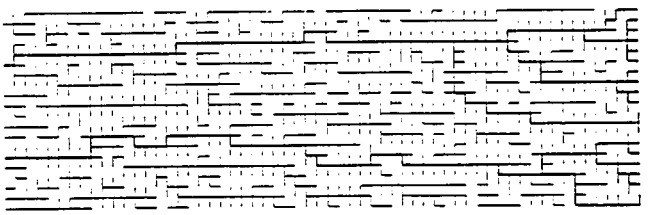

(b)

Fig. 2 Predicted patterns of dendrites and leave-behind lamellae by invasion percolation (a) and gradient-governed growth (b) (flowing channels are bold face).

For the characterization of mass transfer in a particular network of leave-behind lamellae, convection and diffusion rates are computed by numerical simulation. An example is shown in Fig. 3 for a 40 by 40 network. The Peclet number is based on tracer diffusivity, pore body diameter, and

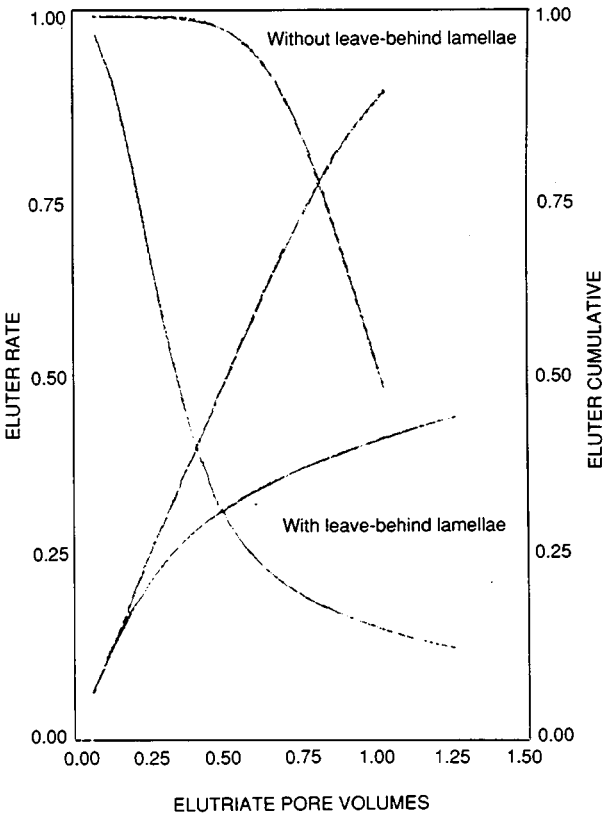

Fig. 3 Tracer elution. Peclet number, 10.

superficial pore throat velocity. A considerable dispersive effect of leave-behind lamellae is evident. The constant rate region at high eluent pore volume can be used to define a mass transfer coefficient for approximating the mechanism in macroscopic (laboratory or reservoir scale) simulations.

References

1. W. Sung, Implementation of a Population Balance in MASTER for Modeling Foam Flow, II-2694, Feb. 15, 1990.
2. D. H. Smith, METC/OAST Enhanced Oil Recovery Research Plan, submitted to Bartlesville Project Office, May 1990.
3. A. P. Lui, Development of a Computer Code for Enhanced Oil Recovery Based on Gradient Governed Growth Model, Contract No. DE-AC21-85MC21353, Sept. 30, 1989.
4. J. D. Sherwood and J. Nittmann, Gradient Governed Growth: The Effect of Viscosity Ratio on Stochastic Simulations of the Saffman–Taylor Instability, *J. Physique*, 47: 15-22 (1986).
5. N. Sams, Miscible Network Model for Viscous Finger Studies, Contract No. DE-AC21-85MC21353, in preparation, 1990.
6. R. A. Geisbrecht, *METC/OAST Enhanced Oil Recovery Progress Review No. 60*, Dec. 4, 1989.
7. R. A. Geisbrecht, *METC/OAST Enhanced Oil Recovery Progress Review No. 61*, June 11, 1990.
8. S. H. Yang and R. L. Reed, *Mobility Control Using CO_2 Foams*, SPE 19689, presented at the 64th Annual Technical Conference of SPE held in San Antonio, Tex., Oct. 8–11, 1989.
9. J. Jikich, Core Flood Measurements of Mobility Control of Dense Carbon Dioxide Using Foams, Contract No. DE-AC21-85MC21353, in preparation, 1990.

CYCLIC CO_2 INJECTION FOR LIGHT OIL RECOVERY: PERFORMANCE OF A COST-SHARED FIELD TEST IN LOUISIANA

Contract No. DE-FG22-89BC14204

Louisiana State University
Department of Petroleum Engineering
Baton Rouge, La.

Contract Date: Nov. 21, 1988
Anticipated Completion: Nov. 17, 1991
Total Government Award: $499,000

Principal Investigator:
Zaki A. Bassiouni

Project Manager:
Jerry Ham
Metairie Project Office

Reporting Period: Apr. 1–June 30, 1990

Objectives

The ultimate objective of this research is to provide a base of knowledge on the CO_2 huff 'n' puff process for the enhanced recovery of Louisiana crude oil. Project goals include laboratory corefloods to investigate several parameters important to the process and numerical simulation to interpret coreflood results. Additional activities include construction and analysis of a field test database to facilitate target reservoir screening and to identify sensitive operational parameters. The information from laboratory corefloods and database evaluations will be used in the design and implementation of Department of Energy (DOE)-sponsored field tests. The results of all laboratory and field evaluations will be made available to the industry through workshops, periodic reports, and meetings.

Summary of Technical Progress

Laboratory Corefloods—Linear Horizontal

A series of horizontal cyclic corefloods was conducted with Timbalier Bay stock-tank oil (STO) and pure CO_2 at room temperature and 500°F to investigate the effect of remaining (or target) oil saturation. Four sets of first- and second-cycle corefloods were performed with one set waterflooded to near-residual oil saturation and the others partially waterflooded to remaining oil saturations of 39.6, 45.9, and 50.4%. In each of these cases, significant quantities of oil were displaced from the core into the transfer vessel during CO_2 injection. This unrecoverable oil was included as waterflood production in calculating remaining oil saturations. The results shown in Fig. 1 indicate that CO_2 utilization, and thus process performance, improved as remaining oil saturation increased.

Six horizontal corefloods, three sets of first- and second-cycle corefloods, were performed to investigate the influence of gravity segregation on oil recovery. Experimental materials and procedures were similar to those used in the investigation of remaining oil saturation. Gravity override effects were probed by rotating the core or allowing it to remain stationary for all or part of a run. Three scenarios were investigated: continuous rotation, no rotation, and no rotation during CO_2 injection with continuous rotation during soak and production periods. As shown in Table 1, the stationary corefloods exhibited significantly improved oil recovery as compared with the continuously rotating corefloods, which indicated that gravity override benefited process performance. At run conditions, CO_2 was much less dense than oil or water. In stationary corefloods, the lower density of the CO_2 allowed it to migrate along the top of the core during injection. This apparently resulted in oil bypassing during CO_2 injection with deeper distribution of CO_2. Rotation of the core reduced this tonguing. This hypothesis indicated that it might be advantageous to keep the core stationary during

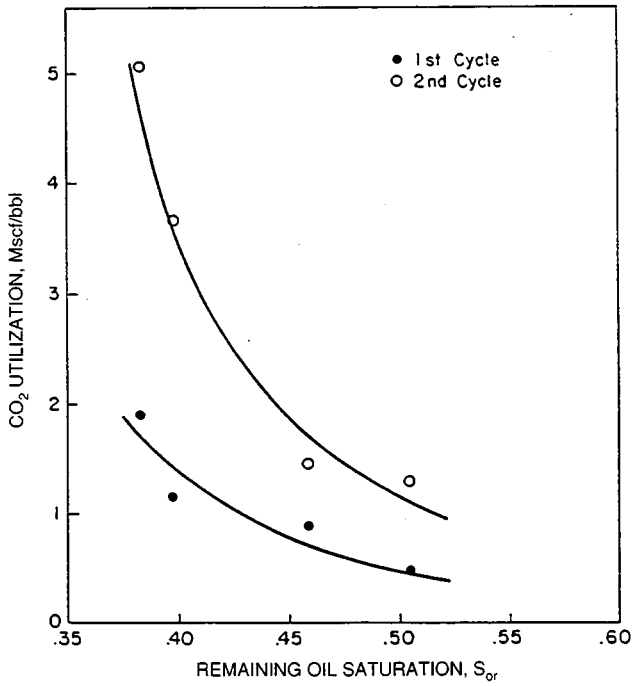

Fig. 1 Relationship between CO_2 utilization and remaining oil saturation.

TABLE 1

Results of Corefloods To Examine Gravity Segregation

Run No.	Cycle No.	Run conditions	Recovery efficiency*	CO_2 utilization, Mscf/bbl
77	1	No rotation	0.081	1.68
78	2	No rotation	0.029	5.03
79	1	Continuous rotation	0.034	4.02
80	2	Continuous rotation	0.016	8.04
101	1	No rotation–huff; rotation–soak and puff	0.078	1.68
102	2	No rotation–huff; rotation–soak and puff	0.036	3.67

*Volume of oil recovered divided by volume of waterflood residual oil.

CO_2 injection and rotate during the soak and production periods. When this procedure was performed, the oil recoveries (Table 1) were similar to those obtained from the stationary corefloods. The results indicate that gravity segregation effects only impact the process during CO_2 injection. Rotation of the core during CO_2 injection minimizes gravity segregation and inhibits deeper penetration of CO_2 into the core, which ultimately results in less oil being contacted and altered by CO_2.

Laboratory Corefloods—Linear Vertical

Six corefloods were performed to examine the influence of a gas cap on oil recovery. The corefloods were conducted in a vertical Berea core with pure CO_2 and a reconstituted reservoir oil. After waterflooding, the pressure was reduced below the bubble point, and the core was shut in for 6 d to allow gas to evolve and migrate upward to form a gas cap. The CO_2 was injected from the bottom to the top of the core in two sets of first- and second-cycle runs, one below and one above the bubble point. In another set of runs conducted below the bubble point, the direction of CO_2 injection was reversed, which corresponded to injection of CO_2 directly into the gas cap. This is an exception that may occur as the result of migration of CO_2 into the gas cap through broken casing or tubing. Oil recoveries and CO_2 utilization factors as shown in Table 2 were similar for both lower pressure runs; thus accidental injection of CO_2 into the gas cap was neither detrimental nor advantageous to the process. First-cycle coreflood performance was poorer above the bubble point than below, which suggests that the process is less favorable in the absence of a gas cap. In addition to gas cap effects, these results, however, were influenced by other factors. Calculations indicate that only partial separation of the gas cap occurred; thus gas was distributed throughout the core, and a well-distributed gas saturation is known to be favorable to process performance. Also, since equal masses of CO_2 were injected and CO_2 occupies a larger volume of the pore space at lower pressures, some of the improved response below the bubble point can be attributed to the larger CO_2 pore volume.

TABLE 2

Results of Corefloods To Examine Gas Cap Effects

Run No.	Cycle No.	Run conditions*	Recovery efficiency†	CO_2 utilization, Mscf/bbl
83	1	2600 psig; inject into gas cap	0.186	8.99
84	2	2600 psig; inject into gas cap	0.071	23.77
97	1	2600 psig; inject below gas cap	0.175	8.53
98	2	2600 psig; inject below gas cap	0.017‡	83.19‡
99	1	3300 psig	0.117	12.33
100	2	3300 psig	0.069	19.58

*The bubble-point pressure was 3100 psig.

†Volume of oil recovered divided by volume of waterflood residual oil.

‡Mechanical failure of regulator aborted experiment prior to cessation of oil production.

Second-cycle efficiencies, as shown in Table 2, were similar for both saturated and undersaturated conditions. Since the second-cycle run of CO_2 is performed after the core has been watered out during the first-cycle run, gas is effectively removed from the core before the second cycle and cannot influence recovery. The second cycle results therefore indicate that improved response at lower pressures was primarily the result of gas effects.

Laboratory Corefloods—Radial

Commercially available equipment for radial corefloods proved to be unsuitable for the proposed experiments. In addition, development of a new design proved to be more difficult than originally anticipated, and projected costs of construction were prohibitive. Therefore, numerical simulation was used to examine the influence of a radial geometry. The project has been delayed until an acceptable match between coreflood and numerical simulation results is attained.

Field Tests—Evaluation of Database Performance

Three meetings have been held in the past quarter to evaluate candidates and test designs for the upcoming field test. In the first meeting, five candidate wells for the Department of Energy (DOE)-sponsored field test of cyclic CO_2 stimulation were presented and evaluated. Attendees included Louisiana State University (LSU) personnel, representatives of two CO_2 suppliers, four independent operators, and DOE representatives. One candidate was eliminated because of formation damage that restricted fluid flow.

In the second meeting, implementation of the field test was discussed. Representatives of five major oil companies, one CO_2 supplier, and the DOE attended as well as representatives of two of the companies sponsoring candidate wells for the field test. The representatives of major oil companies who had performed CO_2 huff 'n' puff tests shared their experiences. They felt that most failures could be attributed to mechanical problems and strongly urged integrity testing to determine tubing capabilities before injection of CO_2.

Further evaluations of the candidate wells indicated that three additional sites should be eliminated from consideration for initial testing; thus one well site is left as the primary candidate for the first test. One well was eliminated because of a high paraffin wax content. Paraffin waxes may precipitate and cause plugging during injection and production of CO_2. Two other wells were eliminated because they were located in dipping reservoirs, and CO_2 may migrate upward and away from the wellbore in formations of this type. These wells may be reconsidered for testing at a later date when wells with specific "problems" are included in the testing program.

These evaluations and recommendations were presented to DOE representatives at a meeting on May 31, 1990. Candidate No. 1 was selected as the initial test site, barring unforeseen developments. Environmental evaluations and design of the test have commenced. It is anticipated that CO_2 will be injected before the end of this year.

Numerical Simulation

A three-phase, three-dimensional multicomponent reservoir simulator, SIMCO, developed by Continental Computer Bureau, Ltd., is being used to model the CO_2 huff 'n' puff process. Computations are performed on a VAX-8800 mainframe computer made by Digital Electronics Corp. A rectangular grid-block geometry is used to describe the 6-ft-long core with 20 blocks. Four additional blocks are used to model the transfer vessel connected to the outlet end of the core.

Measured values of porosity, absolute permeability, initial pressure, and initial fluid saturations are assigned to each block. Eight pseudo-components are used to describe the reservoir oil. Molar compositions, critical temperatures and pressures, acentric factors, and binary interaction coefficients are input which are used to tune an equation of state. Variations in the flow of oil, gas, and water are controlled by relative permeability and capillary pressure curves for each of these fluids. Directional relative permeabilities can be assigned; three-phase relative permeabilities are internally calculated.

Coreflood data include cumulative amounts of oil, gas, and water injected and produced during each of the oilflood, waterflood, and huff 'n' puff stages. Production profiles of oil, gas, and water are obtained for the puff stage.

Berea sandstone is a standard porous medium for experimental research, and a literature review provided relative permeability and capillary pressure curves for this type of sandstone with different STO. These curves were used for initial simulations of the CO_2 huff, soak, and puff stages. Minor changes were then made in the curves to history match oil and water production with time for the oilflood and waterflood stages. The refined curves were used in a second stage simulation of the CO_2 huff, soak, and puff stages.

A horizontal coreflood at undersaturated conditions of 3300 psig and 130°F was modeled. A match of cumulative oil, gas, and water production was obtained for a coreflood that had a waterflood residual oil saturation of 46.4% (Table 3). Three more simulations were performed to

TABLE 3

Summary of Coreflood History Match*

Parameter	Coreflood	Simulation
N_p, cm^3	35	35
W_p, cm^3	55	52
G_p, scf	1.124	1.329
Time, min	180	180

*Run conditions of 3300 psig and 130°F with 2.5 g-mol of CO_2 injected. Time is the time elapsed during production after the soak period.

TABLE 4

Results of Numerical Simulation To Examine Remaining Oil Saturation

S_{orw}	N_p, cm^3	G_p, scf	W_p, cm^3
0.464	35	1.329	52
0.500	37	1.373	48
0.600	47	1.452	33
0.625	50	1.490	29

examine the effect of remaining oil saturation on process performance. Simulation results (Table 4), like laboratory corefloods, indicated that a higher remaining oil saturation resulted in improved process performance.

References

1. J. Thomas, T. V. Berzins, T. G. Monger, and Z. Bassiouni, *Light Oil Recovery from Cyclic CO_2 Injection: Influence of Gravity Segregation and Remaining Oil*, presented at the 1990 SPE Annual Technical Conference and Exhibition, New Orleans, September 23–26, 1990.
2. T. G. Monger and G. A. Thomas, *The Feasibility of Cyclic CO_2 Injection for Light Oil Recovery*, presented at the SPE/DOE Symposium on Enhanced Oil Recovery, Tulsa, Okla., April 22–25, 1990.

THERMAL RECOVERY—SUPPORTING RESEARCH

DEVELOPMENT OF METHODS FOR CONTROLLING PREMATURE OXYGEN BREAKTHROUGH DURING FIREFLOODING

Contract No. FG22-89BC14201

Union Carbide Corporation
Tonawanda, N.Y.

Contract Date: June 2, 1989
Anticipated Completion: Oct. 1, 1990
Government Award: $1,066,772

Principal Investigator:
C. J. Heim

Project Manager:
Thomas B. Reid
Bartlesville Project Office

Reporting Period: Apr. 1–June 30, 1990

Objectives

The objectives of the program are to characterize the reservoir mechanisms that cause premature oxygen breakthrough and to develop practical tools for controlling it. The focus will be on those conditions most likely to be encountered in moderate-depth to deep reservoirs; candidates include gas override, high-permeability streaks, and watered-out zones. Mitigation measures will be selected on a cost-of-implementation basis and on their potential application to a wide range of specific problems.

This phase of the program consists of efforts to characterize the problem and develop possible solutions. Problem characterization focuses on obtaining first-hand information from operators of firefloods through a questionnaire and interviews. A literature search will be used to supplement operator information. Bench-scale screening tests will be performed to identify candidate mobility control techniques for use in physical and computer simulation models.

Summary of Technical Progress

The literature study has been completed, and a bibliography will be included in the final report.

The core sampler described in the last quarterly report proved to be ineffective in removing the core intact because sand packed in the tube caused too much friction on the tube walls. No attempt will be made to redesign the apparatus.

Tests with salt solutions indicated that the precipitation caused by rapid evaporation is reversible. The salt once precipitated can be dissolved by flowing fresh water through it (at lower temperature) and subsequently reprecipitated farther down the tube, which recreates a section of low-permeability sand.

Sodium silicate solutions caused a permeability reduction when reacted with carbon dioxide. Further tests are planned with this chemistry to determine its overall effectiveness in this area.

Bench-scale flask studies were performed with hydrofluoric acid and a variety of brine solutions. Calcium was the most efficient in forming a precipitate (compared with sodium and potassium). Further testing is planned with this chemical system.

MECHANISMS OF MOBILITY CONTROL WITH FOAMS

Contract No. DE-AC03-76SF00098

Lawrence Berkeley Laboratory
University of California
Berkeley, Calif.

Contract Date: Oct. 1, 1985
Anticipated Completion: Sept 30, 1990
Government Award: $300,000
(Current year)

Principal Investigators:
K. S. Udell
C. J. Radke

Project Manager:
Thomas B. Reid
Bartlesville Project Office

Reporting Period: Apr. 1–June 30, 1990

Objectives

Foam is a possible mobility control agent for effective oil displacement from reservoirs. Thus it is important to understand the mechanisms by which foam flows in porous media. Micromodel studies and prior gas-phase tracer experiments show that a significant fraction of the gas in a foam exists as trapped bubbles, which, therefore, have a major impact on the flow resistance. Unfortunately, in the tracer experiments performed to date, partitioning of the tracer into the trapped gas has not been accounted for. Currently, only qualitative information is available on the actual amounts of trapped gas.

A unique experimental apparatus employing dual gas tracers was developed to overcome these limitations and obtain quantitative measurements of trapped gas saturations. During steady foam flow in a porous medium, dilute sulfur hexafluoride (SF_6) and methane (CH_4) tracers in a nitrogen carrier are injected, and the effluent concentration is monitored by gas chromatography.

Summary of Technical Progress

Figure 1 displays a schematic of the foam-flow apparatus. It is a modification of that of Ettinger and Radke[1] to allow for tracer injection and detection. Brine, 0.83 wt % NaCl (Mallinckrodt, reagent grade) in deionized and distilled water, with or without added surfactant, a 0.83 wt % active C_{14-16} α-olefin sulfonate (Bioterg AS-40, Stepan), is supplied by a high-pressure piston pump (ISCO, Model 314). Flow of nitrogen (Liquid Air Corporation) and the tracer gas, a mixture of 15% methane, 15% sulfur hexafluoride, and 70% nitrogen by volume (Matheson Gas Products), is metered through mass flow controllers (Brooks, Model 5850) directly into the core.

The porous medium is a fired, Berea sandstone slab 20 cm (8 in.) long by 10 cm (4 in.) wide by 1.2 cm (0.4 in.) deep with an absolute permeability of 2.3 μm^2 and a

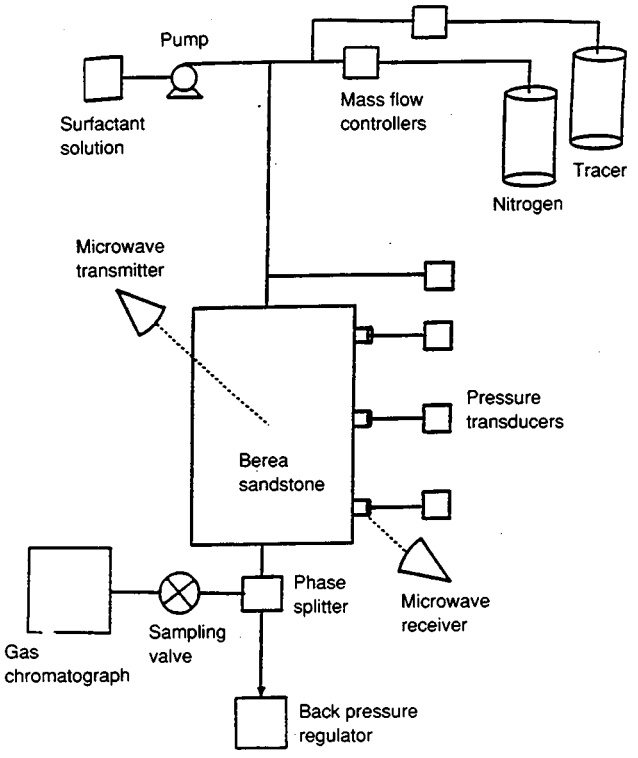

Fig. 1 Schematic of the experimental apparatus.

porosity of 0.24. Five differential transducers (Validyne, Model DP-15) monitor the pressure profile along the core, each relative to atmospheric pressure. Also, the differential pressure between the nitrogen and tracer gas delivery lines is measured downstream from the mass flow control valves to ensure matching pressures before introduction of the tracer mixture. A computer-controlled and -monitored scanning microwave attenuator detects the liquid saturation in the core.[1,2]

Foam exiting the medium is readily broken in a phase splitter by a 10 wt % aqueous solution of Dow Corning Antifoam B. An in-house automatic, online sampling valve periodically sends gas to a chromatograph (Gow Mac, Model 550) for analysis. Excellent separation of the SF_6, N_2, and CH_4 is achieved on a molecular-sieve packed column (Varian 5A) with helium as the carrier gas. Output from the thermal conductivity detector is processed by an online data collection system controlled by a personal computer (IBM PCXT).

Back pressure is controlled at 10^5 Pa gage (1 atm) with a simple, laboratory-constructed device consisting of a 2000-cm^3 vessel charged with regulated nitrogen pressure and vented through a precision needle valve. Acceptable control is found within approximately ±50 Pa (±0.1 psi). Additional information on the apparatus design and operation is available in Ref. 2.

Steady foam flow was established in the oil-free core at a given nitrogen fractional flow (i.e., inlet foam quality) in the range from 0.8 to 1. Up to about 20 pore volumes (PV) of total fluid was injected until the pressure profile and liquid saturation stabilized. Gas flow was then switched to the tracer mixture, and exit concentrations were measured until they no longer increased. This new steady state required about 5 to 8 PV of fluid injection. Typical values of the relative detector concentrations were 8.8 for SF_6 and 4.5 for CH_4, with standard deviations of 0.1 and 0.2, respectively.

Afterward, gas flow was switched back to untraced nitrogen, and new gas and liquid flows were set to another steady state. The tracer procedure was again repeated.

Effort was made to minimize dead volume in the system. Additionally, blank runs were made by replacing the core with a Temco (Model BPR-05) back-pressure regulator whose dead volume is negligible. Tracer gas was injected and the system dead volume quantified. Core tracer histories were corrected accordingly.

Figure 2 displays typical step-concentration histories for SF_6 and CH_4 during steady foam flow for an inlet quality of 0.89 and a total superficial velocity of 0.65 m/d. C_{FL} is the reduced concentration of the tracer in the flowing foam at the core exit. There is an early rise in tracer concentrations followed by a long tail to steady state. The very early tracer breakthrough is due to channeling through a small number of sample-spanning pores of large size. Thus Fig. 2 shows that a significant portion of the foam is blocked to flow.

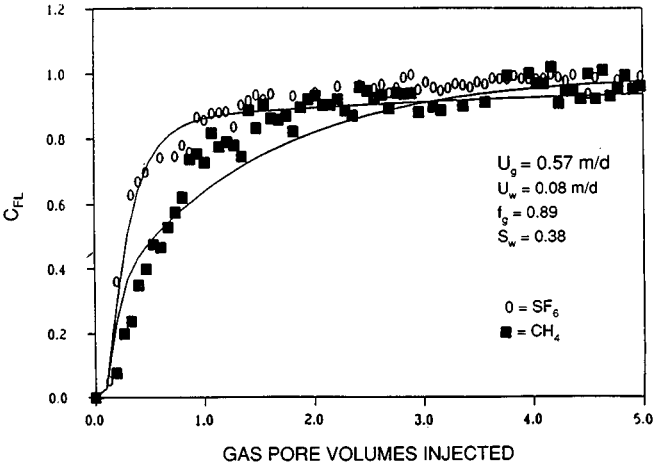

Fig. 2 Experimental tracer histories for steady foam flow. C_{FL}, reduced concentration of the tracer in the flowing foam at the core exit; U_g and U_w, total superficial velocity of gas and water; f_g, inlet fractional flow of gas; S_w, saturation of water.

The very long tail is due to slow tracer partitioning into the trapped gas. Eventually the effluent tracer concentration will reach the injected value. Notice the measurable difference between the two tracer curves caused by the difference in brine solubility of these two gases. The least soluble gas, SF_6, departs most from local equilibrium, as expected.

Figure 2 confirms the presence of a large fraction of trapped gas during foam flow in a sandstone medium. It also demonstrates that there is mass transfer into the trapped gas. Quantitative assessment of the exact amount of trapped gas thus requires a model that can account for mass transfer resistances.

Conclusions

The dual-gas tracer technique is a powerful new tool for detecting trapped foam saturation during foam flow through porous media. In this technique, two tracer gases with differing solubilities are injected in a step change and the effluent concentrations are measured. The results confirm that significant foam trapping is present in a 0.8-μm^2 Berea sandstone and that significant mass transfer into the trapped gas does occur, even for tracers with very low brine solubility.

References

1. R. A. Ettinger and C. J. Radke, *The Influence of Texture on Steady Foam Flow in Berea Sandstone*, SPE 19688, presented at the 1989 Annual Fall Technical Conference of SPE, San Antonio, Tex., Oct. 8–11, 1989.
2. J. V. Gillis, *Trace Detection and Structure of Stationary Lamellae During Foam Flow Through Berea Sandstone*, Ph.D. thesis, University of California, Berkeley, 1990.

CHEMICAL ADDITIVES FOR IMPROVING STEAMFLOOD PERFORMANCE

Contract No. FG19-87BC14126

University of Southern California
Los Angeles, Calif.

Contract Date: Feb. 27, 1987
Anticipated Completion: Feb. 27, 1990
Government Award: $131,750
(Current year)

Principal Investigator:
Yansis C. Yortsos

Project Manager:
Thomas B. Reid
Bartlesville Project Office

Reporting Period: Apr. 1–June 30, 1990

Objectives

Thermal methods, and particularly steam injection, are currently recognized as the most promising for the efficient recovery of heavy oil. Despite significant progress, however, important technical issues remain. Specifically, knowledge of the complex interaction between porous media and the various fluids of thermal recovery (steam, water, heavy oil, gases, and chemicals) is inadequate. The interplay of heat transfer and fluid flow with pore- and macro-scale heterogeneity is largely unexplored.

The objectives of this contract are to continue previous work and to carry out new fundamental studies in the following areas of interest to thermal recovery: displacement and flow properties of fluids involving phase change (condensation–evaporation) in porous media; flow properties of mobility control fluids (such as foam); and the effect of reservoir heterogeneity on thermal recovery. The specific projects are motivated by and address the need to improve heavy oil recovery from typical reservoirs as well as less conventional fractured reservoirs producing from vertical or horizontal wells.

Summary of Technical Progress

Vapor–Liquid Flow

Work in the area of vapor–liquid flow in porous media continued. Theoretically, the investigation of finite size and gradient effects on the liquid-to-vapor phase change in porous media is in progress. Currently, gradient percolation theories[1] are being modified to account for nucleation following the previous model.[2] This research uses numerical simulation of pore networks. In parallel, the earlier results[2] are being extended to more general ranges in the values of parameters. The analysis of the motion of lateral interfaces in fully developed fingers has been completed and awaits the experimental results. The modeling of thermal processes in naturally fractured systems is also under way. Progress was made with the numerical synthesis of fracture networks using the techniques of Barnsley,[3] which are based on fractal geometry.

The apparatus for steam injection in micromodels and Hele–Shaw cells has been assembled and preliminary experiments have started. Pyrex glass was found to be suitable for both applications. Experiments were conducted on the narrow Hele–Shaw cell to study the propagation of waves on the interface of fully developed fingers. Upon generation of a parallel interface in parallel flow, a disturbance is applied and its motion studied. A typical example is shown in Fig. 1. The previously developed theory[4] predicts dynamics described by the KdV equation, which is known to produce solitary waves. The preliminary results are qualitatively consistent with the theory, as shown in Fig. 1. Further work is necessary, however, before the latter is fully validated.

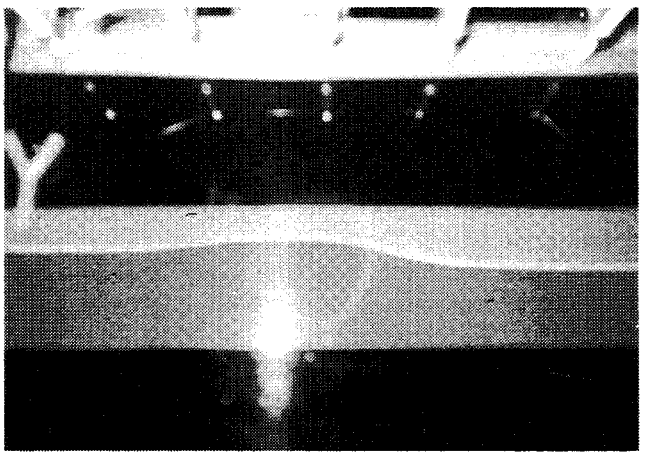

Fig. 1 Typical solitary wave in parallel flow in a Hele–Shaw cell.

Chemical Additives

Work in this area continued in two directions, one involving experimental work with foam generation and propagation and another involving theoretical modeling of non-Newtonian flow in porous media.

In regard to foam flow, the effects of injecting pregenerated foam as well as hysteresis effects were studied. Experiments were conducted at a constant liquid rate over a wide range of gas rates. The latter were varied stepwise and the pressure drop readings were taken after the pressure drop stabilized. Curves were obtained with and without the use of prefoamer. The results shown in Fig. 2 indicate that the effect of prefoamer is more significant at

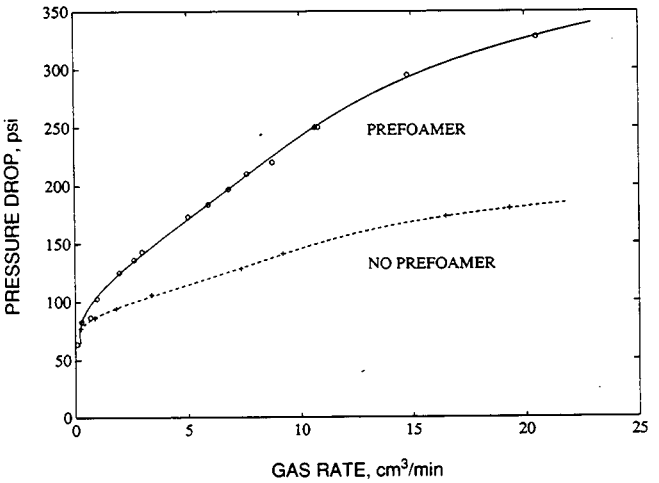

Fig. 2 Pressure drop vs. gas flow rate (with prefoamer); q_w, 0.82 cm³/min.

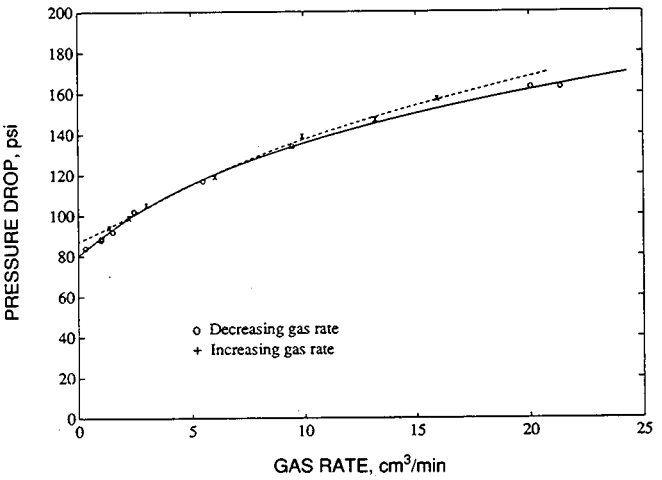

Fig. 4 Hysteresis on pressure drop vs. gas flow rate curve (without prefoamer); q_w, 0.82 cm³/min.

higher gas rates. Data were also obtained by decreasing the gas injection rate to examine possible hysteresis effects. Figure 3 shows that such effects are minimal. This appears to support the concept that during foam flow the liquid saturation is practically constant. The experimental sequence was repeated after resaturating the core with surfactant solution and subsequently injecting gas and surfactant solution at various rates until steady state was reached (Fig. 4). Again, hysteresis effects were negligible. The preceding results demonstrate that use of prefoamer is more effective at higher gas flow rates, although the extent over which these effects are important is limited near the core entrance, as shown in previous reports.

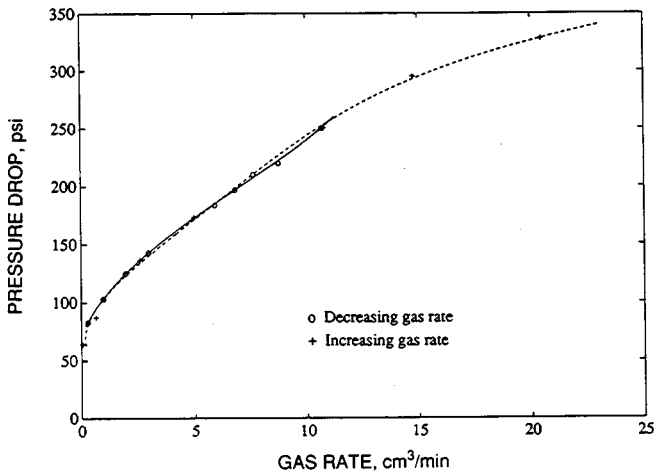

Fig. 3 Hysteresis on pressure drop vs. gas flow rate curve (with prefoamer); q_w, 0.82 cm³/min.

Theoretical efforts were also made to model various aspects of non-Newtonian fluid flow in porous media. The results are summarized in Ref. 5. Specifically, the following have been accomplished.

The behavior of power-law fluids in pore networks at large coordination number, z, has been analyzed and an Effective Medium Theory was developed

$$\int_0^\infty g(v)\left[\frac{(z-1)v}{\{v^n+[(z-1)^n-1]v_m^n\}^{1/n}}-1\right]dv=0 \qquad (1)$$

This result differs from that derived by Cannella, Huh, and Seright.[6] The response near percolation thresholds was also modeled with exact expressions developed for Bethe lattices.[5]

The method by Katz and Thompson[7] was subsequently applied to power-law fluids in porous media. The following result was obtained for single-phase flow

$$q^n=\frac{k^{(n+1)/2}A\Delta P}{mL} \qquad (2)$$

$$A=\left[\left(\frac{\sigma}{\sigma_0}\right)^{0.38}\phi^{0.12}\right]^{n-1}\frac{(7.84)^{n-1}(23.57t_n)^{t_n}3^{1+n}}{2^{2n+1}(1+3n)^n(3+t_n)^{2+t_n}} \qquad (3)$$

where k = Darcy permeability for Newtonian flow
σ/σ_0 = inverse of the formation factor
ϕ = porosity
n = power-law exponent
m = consistency index
t_n = exponent near percolation

With excellent approximation, the latter is given by

$$t_n \simeq 1.76+\frac{0.24}{n} \qquad (4)$$

for three-dimensional (3-D) media. Equations 2 and 3 are exact.

Use of percolation theory led to the following expressions for the scaling of the relative permeabilities. Near the primary drainage threshold,

$$k_{rnN} \sim S_{nN}^{0.558+4.09n} \quad (5)$$

which indicates a strong dependence on the power-law exponent, whereas near the trapping threshold,

$$k_{rnN} \sim (S_{nN} - S_r)^{0.24+1.76n} \quad (6)$$

indicates a weaker dependence.

Finally, displacement of a Bingham plastic was considered, and scaling laws were used to express the no-flowing saturation, S_{nf}. The following relationship was found

$$S_{nf} - S_r \sim \left[\frac{q\mu}{\tau_0 (k)^{1/2}}\right]^{-1/[\nu(\zeta-1)]} \quad (7)$$

where τ_0 is the yield stress for the Bingham plastic and ν and ζ are percolation exponents. For a 3-D medium, the preceding combination equals –5, which suggests a strong flow-rate effect.

References

1. B. Sapoval, M. Rosso, and J. F. Gouyet, The Fractal Nature of a Diffusing Front and the Relation to Percolation, *Phys. Lett.*, 46: L149 (1985).
2. Y. C. Yortsos and M. Parlar, paper SPE 19697 presented at the 64th Annual SPE Fall Meeting, San Antonio, Tex., 1989.
3. M. Barnsley, *Fractals Everywhere*, Academic Press, New York, 1988.
4. Y. C. Yortsos and M. Zeybek, paper presented at the 1989 Annual Meeting of the AIChE, San Francisco, Calif., 1989.
5. M. Sahimi and Y. C. Yortsos, paper presented at the 5th IFP Conference on Oil Recovery, Arles, France, 1990.
6. W. J. Cannella, C. Huh, and R. S. Seright, paper SPE 18089 presented at the 63rd Annual SPE Fall Meeting, Houston, Tex., 1988.
7. A. J. Katz and A. H. Thompson, *J. Geophys. Res.*, 92: 559 (1987).

FEASIBILITY STUDY OF HEAVY OIL RECOVERY IN THE MIDCONTINENT REGION (OKLAHOMA, KANSAS, MISSOURI)

Cooperative Agreement DE-FC22-83FE60149, Project SGP37

National Institute for Petroleum and Energy Research
Bartlesville, Okla.

Contract Date: Apr. 1, 1990
Anticipated Completion: June 30, 1991
Funding for FY 1990: $50,000

Principal Investigator:
David K. Olsen

Project Manager:
Thomas B. Reid
Bartlesville Project Office

Reporting Period: Apr. 1–June 30, 1990

Objectives

The objectives of this feasibility study are to (1) investigate from secondary data the known heavy oil resources in Oklahoma, Kansas, and Missouri; (2) screen this resource for potential thermal recovery applications; and (3) evaluate various economic facets of thermal enhanced oil recovery (EOR) that may impact on the expansion of steamflooding in this midcontinent area. If the study determines that expansion of steamflooding in the area is possible by recent advances in technology, recommendations will be made to facilitate the production of this additional resource within the next 2 to 5 yr.

Summary of Technical Progress

The emphasis this quarter has been on the heavy oil region of southeast Kansas. In the early 1960s, some trade journals reported that major oil producers had leased millions of acres in this area. The major oil producers and numerous independents were conducting field pilots of in situ combustion, cyclic steam, and steam-drive technology. The major companies were simultaneously conducting pilots in California, Venezuela, and The Netherlands. At the same time, the large heavy oil deposits in Canada were discovered. These companies changed their emphasis from the midcontinent to other areas because of the higher oil reserves per surface acre and began to expand their pilots to commercial operations in these areas.

Analyses of geological and production records of southeast Kansas heavy oil fields indicate that the vast heavy oil reserves reported in early publications are composed of numerous shoestring reservoirs, none of which are blanket sands like those of Kern River (California) field. Many of the heavy oil midcontinent reservoirs are consolidated lenticular elongated channel sands that have a maximum thickness of 30 ft, an average thickness of 10 ft, and pinch out on the sides. Many reservoirs average 400 ft in width and 1500 ft in length. The permeability is 500 mD and less. The Dykstra–Parsons coefficients, where known,

show great permeability variation indicating heterogeneous reservoirs. Many heavy oil deposits in southeast Kansas, northeast Oklahoma, and southwest Missouri occur in Pennsylvanian Cherokee sandstone reservoirs. These reservoirs are characterized by clayey sandstones composed of quartz, feldspar, and clay minerals with calcite cementation. The clay content is as high as 27% and includes kaolinite, mica–illite, chlorite, and mixed-layer clays. In comparison, many of the major heavy oil reservoirs in the world have high clay content, but they are also unconsolidated sands and have high permeability.

Historical data on oil production, open-hole electrical surveys in southeastern Kansas, core descriptions, and core analyses of cored holes drilled for a previous heavy oil reservoir study were obtained from the Kansas Geological Survey. Several unpublished masters' theses, which may give important reservoir characterization data for the Pennsylvanian Cherokee sandstone reservoirs, were acquired.

A heavy oil database was developed, and data were added from more than 60 reservoirs identified from the records of the Kansas Geological Survey and publications on abandoned reservoirs. Many of these fields are small, and some had only one or two wells per field when drilled on 40-acre spacing. Only a few of these reservoirs have been identified in other available heavy oil databases. Discussions with area operators indicate that heavy oil resources exist behind cased wells in this area. Several other wells that were drilled through heavy oil zones during exploration for light oil were never reported. Information on those wells may appear only on drillers' logs because technology to produce this resource was unavailable at the time they were discovered.

The results of steamfloods and firefloods conducted in the early 1960s show good oil production in light of the experience and technology available to operators at the time. Application of modern technology in conjunction with knowledge of reservoirs, improvements in steam generators, insulated casing, slim hole drilling (vertical and horizontal), and improvements in chemical demulsifiers could revive the potential for heavy oil production from this area.

Heavy oil production was discussed with the staff of the Tertiary Oil Recovery Project (TORP) group in the Petroleum Engineering Department at the University of Kansas. They supplied data on a thermal recovery pilot project in southeastern Kansas that will start later in 1990 in which two existing horizontal wells are used for steam injection and vertical wells are used for production.

Descriptions and analyses of wells in the Mapco thermal recovery pilot project in western Missouri and a bibliography of unpublished theses that may be applicable were also obtained. Numerous reports from the state of Missouri and the state of Oklahoma have been ordered and will be analyzed on receipt.

The capabilities of regional refineries and their ability to handle heavy oil if produced from this region are being analyzed. Fourteen refineries were identified in this tri-state region. The capabilities of these refineries are being compared with those of California, which are processing more than 500,000 bbl/d of heavy California crude.

THERMAL PROCESSES FOR HEAVY OIL RECOVERY

Cooperative Agreement DE-FC22-83FE60149, Project BE11B

National Institute for Petroleum and Energy Research
Bartlesville, Okla.

Contract Date: Oct. 1, 1983
Anticipated Completion: Sept. 30, 1990
Funding for FY 1990: $200,000

Principal Investigator:
David K. Olsen

Project Manager:
Thomas B. Reid
Bartlesville Project Office

Reporting Period: Apr. 1–June 30, 1990

Objectives

The objectives of this project are to improve the understanding of the basic mechanisms responsible for the improvement of heavy oil production with steam and to use that understanding for further development of this production method. The FY90 objectives are to: (1) investigate the effectiveness of mobility control and diverting agents in diverting steam from a zone of high permeability to a zone of lower permeability; (2) compare the predicted values obtained with the numerical simulator with laboratory-measured values of steamflood performance; and (3) compile and write a summary on the operation of steamfloods.

Summary of Technical Progress

Steamflood Field Equipment and Operation

A status report is being prepared to assist independent operators who are interested in thermal enhanced oil recovery (EOR). Significant differences in experience exist among operators considering thermal EOR as well as among thermal operators with established operations.

Operators range from major oil companies operating in fields like Kern River to the small one-man independent who uses a mobile steam generator for running cyclic steam in shallow sands in the midcontinent. This report is designed to help small operators ask the right questions of consultants, engineers, and equipment vendors before starting an oil recovery project. Eight chapters of the report have been written, and additional chapters will be completed during the next quarter. Requests seeking the release of information and/or permission to reprint schematics of equipment for the report have been sent to the appropriate manufacturer.

Laboratory Numerical Simulator Development

A version 1 PC-based compositional laboratory steamflood simulator has been developed. A topical report describing the features of the model and the behavior of the dependent variables that are important in the steamflood process is being prepared. The model is similar to that developed by Coats[1] except for the numerical techniques used. The model solves finite-difference equations with a sequential solution technique. The sensitivity of the model to various parameters [time-step-size sensitivity, fluid property sensitivity, process parameter sensitivities, and reservoir parameter sensitivities (porosity, permeability, etc.)] was studied this quarter.

Time-step-size sensitivity showed that, because of the implicit pressure–explicit saturation (IMPES) nature of the solution scheme, the model is highly time-step sensitive, and a larger time-step size leads to unacceptable material and energy balance errors. The modeling results indicate that the steamflood process is sensitive to porosity, steam quality, injection rate, and oil viscosity with volatile oils and is less sensitive with heavy crudes.

Oil recovery efficiency increases with the following parameters:

- Increase in steam quality
- Increase in injection rate
- Increase in oil volatility
- Decrease in initial oil viscosity
- Increase in porosity

Steamflood Experiments

NIPER initiated a series of two-dimensional (2-D) steamflood experiments this quarter to evaluate steam diversion with the surfactant Chaser 1020 and nitrogen with and without the addition of weakly alkaline additives, such as Na_2CO_3 and $NaHCO_3$. Previously, Chaser 1020 was found to be a poor foamer at low temperature (<375°F). Previous tests of Chaser 1020 (1%) and nitrogen were conducted at 350°F, and the highest differential pressure obtained with this surfactant was less than 2 psi across the 2-ft 2-D model when the foam was generated in situ.[2] A series of experiments used foam generated externally with preheated nitrogen and surfactant pumped through an 800-mD fired core as the foam generator to test the performance of this surfactant at a high temperature (390°F). Eight heat tapes are used to externally heat the steel sidewalls of the 2-D model to compensate for heat loss from the steam to the metal walls. Previous 2-D experiments experienced an 80% loss of heat during steam injection from heat being transmitted along the steel walls of the 2-D model. The addition of external heating tapes greatly accelerated the 2-D steamflood experiments and compressed the previous 18- to 30-h run times to just 3 h. During these runs, the backpressure (180 psi) on the model was set at a higher pressure, which increased the steam temperature (390°F) in the model.

The top 22% of the 2-D model was packed with a quartz sand that would give a permeability of 11.5 darcys and the bottom 78% of the model with quartz sand that would produce a permeability of 2.5 darcys. The model was saturated with Round Mountain (California) crude. With a fivefold difference in permeability, steam was expected to quickly sweep oil from the top or high-permeability section. However, there was not a discernible break in the oil–water production curve (Fig. 1) or in the temperature traces as measured every 5 min by the array of 32 thermocouples to indicate that the steam had preferentially swept the upper portion of the model before producing most of the oil and steam breakthrough.

After steam breakthrough (160-psi differential pressure across the model), the stability and the foamability of Chaser 1020 were evaluated. Figure 2 shows the differential pressure drop across the 2-D model (frontal advance rate of 2500 ft/d) upon continuous injection of 1% active Chaser 1020 and nitrogen at a foam quality of 80%. The pressure buildup was not allowed to plateau because the 185 psi across the model combined with the backpressure exceeded the recommended pressure rating of the model, and thus surfactant injection was stopped. The pressure across the

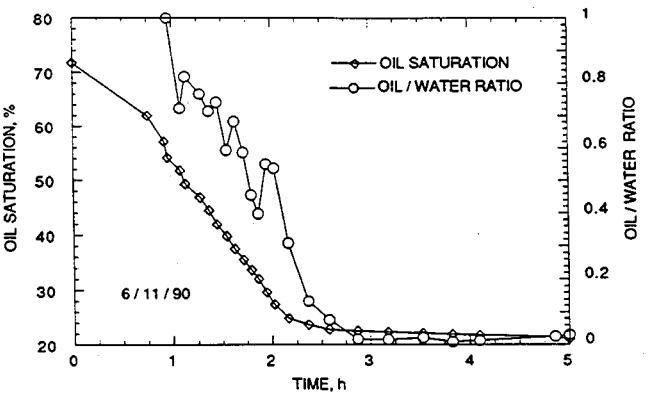

Fig. 1 Oil saturation and oil/water ratio obtained from two-dimensional (2-D) model where the top 22% of the 2-D model was packed with a quartz sand that would give a permeability of 11.5 darcys and the bottom 78% of the model with quartz sand that would produce a permeability of 2.5 darcys.

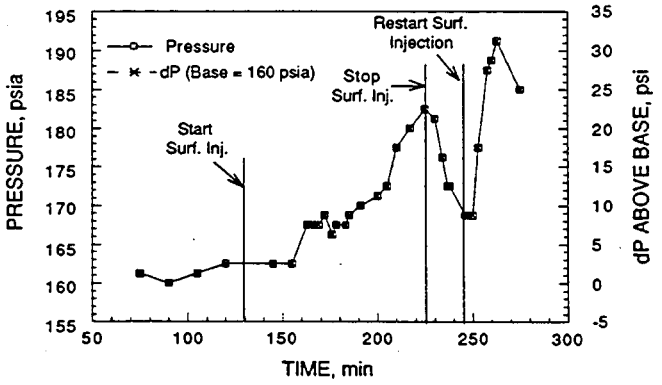

Fig. 2 Differential pressure buildup and decline resulting from injection of Chaser 1020 and nitrogen into the two-dimensional model at 390°F.

model declined, and, on surfactant injection for a second time, the rate of pressure buildup was much faster until the upper pressure limit was exceeded and surfactant injection was terminated (elapsed time of 265 min). Intermediate pressure taps located in the top one-fourth of the model showed that most of the foam went into the lower portion of the model during the first foam injection, which is the most direct route between bottom injector and the full face producing screen. During the second sequence of foam injection, the foam went into upper portions of the model, and differential pressures between individual pressure taps showed pressure fronts moving past the transducer. Additional analyses are being conducted, and pressure taps are being repositioned to obtain additional data on the behavior of other surfactants that will foam well but at a lower temperature.

References

1. K. H. Coats, A Highly Implicit Steamflood Model, *Soc. Pet. Eng. J.*, 15(5): 369-383 (October 1978).
2. D. K. Olsen, *Thermal Processes for Heavy Oil Recovery*, DOE Report NIPER-436, 1989.

THERMAL PROCESSES FOR LIGHT OIL RECOVERY

Cooperative Agreement DE-FC22-83FE60149, Project BE11A

National Institute for Petroleum and Energy Research
Bartlesville, Okla.

Contract Date: Oct. 1, 1983
Anticipated Completion: Sept. 30, 1990
Funding for FY 1990: $300,000

Principal Investigator:
David K. Olsen

Project Manager:
Thomas B. Reid
Bartlesville Project Office

Reporting Period: Apr. 1–June 30, 1990

Objectives

The objectives of this project are to improve the understanding of the basic mechanisms responsible for the improvement of light oil production using steam and to use that understanding for accelerating development of this production technology.

Specifically for FY90, the objectives are to: (1) support the Department of Energy (DOE) in its cooperative effort with Venezuela in thermal technology transfer by participating in the Annex IV meetings; (2) determine the potential of oil recovery by steamflooding previously waterflooded light oil reservoirs that are oil wet rather than water wet; (3) correlate capillary pressure experimental results obtained from high-temperature centrifuge data with two-phase relative permeability experiments performed at high temperatures and design an empirical model that will be useful in existing numerical simulators that describe this behavior for use in steamflood projects; (4) investigate the use of novel steam diverters for steamflooding of light oils; and (5) design a scaled, two-dimensional (2-D) steamflood physical model with the capability to model various steamflooding conditions.

Summary of Technical Progress

Light Oil Steamflood Experiments

Light oil steamflood experiments conducted on unconsolidated oil-wet and water-wet quartz and Berea sandstone and on unconsolidated sand obtained from a current light oil steamflood pilot are being analyzed. Results show that the steamflood oil recovery process alters the wettability to a more water-wet condition, although not all the post-process wettability determinations have been completed. Statistically, the greatest wettability alteration was found in the most oil-wet sands.

Two-dimensional steamfloods of unconsolidated sand (starting at initial oil saturation) obtained from a current light oil steamflood pilot proceeded smoothly. However, in 2-D runs where the sand had been previously waterflooded with field brine, propagating the steamfront more than half

the distance from injector to producer was unsuccessful. In each of these runs, the 2-D model experienced plugging at the production screens, and the steamflood had to be aborted midway through the run (steamfront located half the distance from injector to producer). Attempts to back-flush the producer with potassium chloride (KCl) or to coinject KCl with the steam in the steamflood were only marginally successful. The screens of the 2-D model have been modified to permit more fines production. The fines and clay fraction from field sand and oil-saturated sand immediately in front of the screens are being analyzed to determine if organic material is responsible for the repeated plugging. Analyses of the sand in these interrupted steamfloods show that oil was banked in front of the steamfront. Plots of the steamfront as a function of time, saturation distribution, and a complete description of the experiments will be reported in the annual status report..

Design of a Scaled Multidimensional Steamflood Physical Model

Two laboratories were visited this quarter as a part of the task to develop a new physical model. Both laboratories used semiscaled vacuum models (2-D and 3-D sector models) to study the effects of parameters that may not be easily incorporated into numerical models. The advantages of the vacuum model are that it permits better scaling of fluid flow, is simple in design, is cheaper, and the low pressure is safer to operate. However, according to the scaling rules of Stegemeier et al.,[1] these models employ glass beads as porous media, the viscosities of the fluids comprising the aqueous phase must be more viscous than water, and the oil is less viscous than that in the actual reservoir. Steam quality must be scaled down from the normal 80% quality used in the field to about 20% for use in the vacuum model. This does not allow scaling of heat distribution in the reservoir and does a poor job of scaling capillary pressure, relative permeability, wettability, influence of clays, asphaltenes, and many of the physicochemical effects occurring at high temperature. Rheology of the crude oil and emulsions, a characteristic of steamfloods, is difficult to simulate. Simulation of steam distillation, the primary mechanism in light oil steamflooding, with synthetic oils is difficult even with appropriate light ends included in the formulated oil. Doscher et al.[2] developed scaling criteria for vacuum models on the basis of the integral form of the thermal energy balance over the steamed zone (Kern River field as prototype) as developed by Yortsos.[3] For certain studies, vacuum models are superb in modeling the reservoir parameters that are the subject of investigation; for other studies, these models are inadequate.

High-pressure models are usually scaled with the criteria developed by Pujol and Boberg.[4] Steam scaling has been reviewed by several investigators.[5,6] In addition to review of the high-pressure steamflood model in Venezuela and use of the industrial experience of engineers from the National Institute for Petroleum and Energy Research (NIPER) in steam laboratories, in an effort to assist in design, visits to laboratories operating high-pressure 2-D and 3-D sector models have been scheduled for this fall. High-pressure scaled models used by other researchers can provide better scaling of thermal effects on rock, fluid, and rock–fluid interactions. However, high-pressure scaled models may not be able to adequately scale flow distribution. Analyses of models in both industrial and academic laboratories, including the Universities of Alberta and Calgary and laboratories in southern California, are planned for this fall. Additional work during the last quarter of the year will help define the benefits and limitations of the individual physical models.

Relation Between Field Projects, Simulation, and Scaled Models

The ultimate oil produced from steam soak and steam drive is proportional to the steam-swept volume that is, in turn, a function of the reservoir characteristics (including heterogeneity) and injection strategies. In this project, an attempt is made to integrate simulation and scaled-model results to better define these strategies. One important strategy is concerned with the analysis of vertical vs. horizontal injectors and producers for light oil steamflooding in consolidated sands. Horizontal injectors are expected to improve areal conformance and overcome some of the limitations of vertical steam injectors. This may mitigate the effect of low permeability and high oil saturation, which severely limit effective initial injectivity and thus prevent effective reservoir heating. This improves the rate of return on investment by cyclic steam operations and sustained high steam injectivity throughout a project under steam drive. Because field pilot testing is expensive and requires many years, screening methods that predict ultimate oil/steam ratios (scaled-model studies coupled with simulation) are useful in planning new projects or in implementing modifications, such as horizontal injectors in existing projects. These steps reduce project risk. In addition to the scaled-model study described previously, a light oil steamflood simulator is being prepared. Because of the limited number of light oil steamflood pilots, however, calibration of simulators with publicly available data has not permitted as much refinement as it does with heavy oil simulators. These simulators need to account for the differences in the mechanisms of production between light oil steamflooding, a process that is principally steam distillation, and heavy oil steamflooding, a process that is primarily viscosity reduction.

Steam Diverters for Light Oil Steamflooding

Diversion of steam (in both light and heavy oil reservoirs) from a steam-swept zone to unswept areas of a reservoir can greatly influence the economics of steam-

flooding. Few economic analyses of the application of foam for steam diversion have been published; however, discussions with operators indicate that previous applications of foam provide at best break-even economics, with a major fraction of the cost being nitrogen used as the gas phase in the foam. During the last few years, new generations of surfactants as steam foamers have been developed. NIPER is investigating a high-temperature (>450°F) gelable fluid with a viscosity of only 1.25 cP at 80°C and 1.84 cP at 90°C. Progress is limited to bottle tests conducted in pressure bombs (flushed with nitrogen); after 2 weeks at 175°C, the material had gelled and had to be dug out of the hot pressure bomb as a solid. The formulation is sensitive to oil at concentrations above 20% (does not gel); however, since the residual oil saturation in the steam-swept area in a steamflood is usually significantly less than 10%, this may not be a serious limitation.

References

1. G. L. Stegemeier, C. W. Volek, and D. D. Laumbach, Representing Steam Processes with Vacuum Models, *Soc. Pet. Eng. J.*, 151-174 (June 1980).
2. T. M. Doscher, Scaled Physical Model Studies of the Steam Drive Process, *First Annual Report, September 1977–September 1978*, DOE Report DOE/ET/12074-1, 1979.
3. Y. C. Yortsos, *Analytical Modeling of Oil Recovery of Steam Injection*, Ph.D. dissertation, California Institute of Technology, Pasadena, Calif., 1979.
4. L. Pujol and T. C. Boberg, *Scaling Accuracy of Laboratory Steamflooding Models* presented at the SPE 43rd Annual California Regional Meeting, Bakersfield, Calif., 1972.
5. S. M. Farouq Ali and D. A. Redford, Physical Modeling of In Situ Recovery Methods for II Sands, Canada–Venezuela Oil Sands Symposium, Edmonton, Canada, *CIM Special*, 17: 319-326 (1977).
6. K. D. Kimber, S. M. Farouq Ali, and V. R. Puttagunta, New Scaling Criteria and Their Relative Merits for Steam Recovery Experiments, *J. Can. Pet. Technol.*, 27(4): 86-93 (1988).

INNOVATIVE DRILLING COMPLETION SYSTEM

Contract No. DE-AC22-89BC14203

Petrolphysics, Inc.
San Francisco, Calif.

Contract Date: Sept. 25, 1989
Anticipated Completion: Sept. 30, 1990
Government Award: $276,159

Principal Investigator:
R. Wayne Dickinson

Project Manager:
Thomas B. Reid
Bartlesville Project Office

Reporting Period: Apr. 1–June 30, 1990

Objective

The project objective is to place multiple horizontal radials in a heavy oil reservoir with the Petrolphysics Ultrashort Radius Radial Drilling System. The well will be placed close to existing oil producers in a regular pattern. A demonstration will be conducted to show that the well can be used either as a steamflood injector or as a cyclic steam producer.

Summary of Technical Progress

Task 2: Drilling and Completion of Horizontal Radials

Petrolphysics drilled and completed four horizontal radials in the Bremer RI-53 well during the period from Apr. 9 to Apr. 20, 1990. Radial No. 1 and Radial No. 2 were drilled on Apr. 9, 1990, and Apr. 13, 1990, respectively, and completed immediately thereafter. These operations were fully described in previous reports.

Radial No. 3 and Radial No. 4 were completed during the quarter. Radial placement operations for these two radials (Fig. 1) are summarized.

Radial No. 3

Drilling operations for Radial No. 3 commenced on Apr. 13, 1990. The azimuth for Radial No. 3 was preselected by Union Oil and set at S. 4° E. The radial was placed at a depth of minus 884 ft (as measured from KB). A horizontal distance of 101 ft was achieved. The radial was then positionally logged. A copy of the log is included in a topical report.

Completion operations, which commenced on Apr. 16, 1990, consisted of two separate completion functions. First, the radial was selectively gravel-packed ("First Lift") with 4 ft^3 of gravel; a pressure of 400 to 500 psi and a flow of 135 gal/min of water were maintained during gravel-packing operations. Second, a 96-ft length of Flexible Sand Barrier (FSB) was inserted into the radial tube. The radial was withdrawn from the formation, and the gravel-packed FSB was left in place for steam injection and oil production.

Radial No. 4

Radial No. 4 was placed on Apr. 19, 1990, at a depth of minus 882 ft. The azimuth was set at N. 85° E. A radial distance of 71 ft was achieved at that trajectory. A positional log of Radial No. 4 as well as computer-generated support data are included in a topical report.

On Apr. 20, 1990, Radial No. 4 was gravel packed ("First Lift") with 3 ft^3 of gravel at a pressure of 350 psi and a flow of 135 gal/min of water. The radial tube was withdrawn from the borehole.

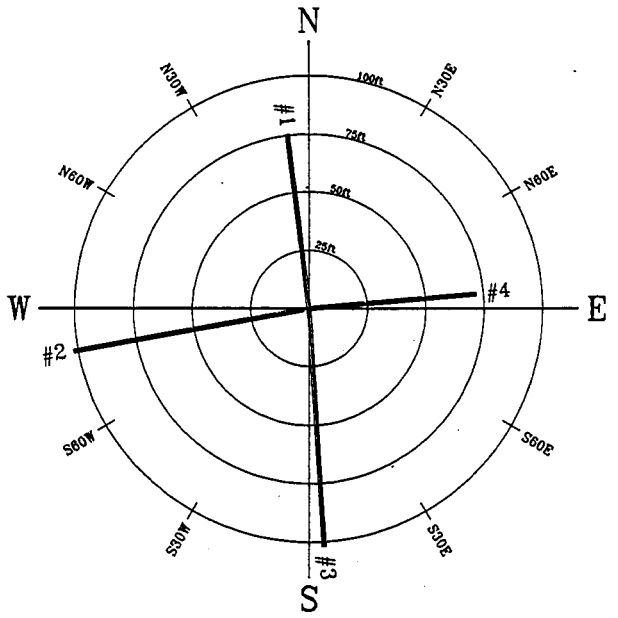

Radial No.	Date	Distance, ft	Depth, ft	Azimuth	Completion
1	4/9/90	74	884	N7W	Gravel packed
2	4/11/90	106	884	S80W	Gravel packed
3	4/13/90	101	884	S4E	Gravel packed and flexible sand barrier
4	4/19/90	71	882	N85E	Gravel packed

Fig. 1 Radial placement operations for Radial No. 3 and Radial No. 4.

The vertical well, Bremer RI-53, was subsequently completed by Union Oil. This operation consisted of gravel packing the vertical well that provided the "Second Lift" gravel pack for each of the four radials. The well was temporarily shut in awaiting steam injection.

Task 3: Inject Steam, Produce the Well, and Monitor the Results

Steam Injection Cycle

Upon completion of the Bremer RI-53, 1320 bbl/d of steam was injected. The injection cycle lasted approximately 13 d. Cumulative injected steam totaled 17,120 bbl, or an estimated 5700 million Btu.

Temperature monitors in the candidate well and in observation wells indicated that the steam was dispersed at least 50 ft into the formation through the radials. Initially, the candidate well was uncharacteristically "unheated," which indicated that the steam had been directed away from the vertical wellbore. The candidate well gradually increased in temperature as the heat began to flow back into the vertical well. This temperature rise was concurrent with the commencement of oil production.

The injection results indicate that key objectives of the project were realized. First, a well completed with horizontal radials can be used as an injector well; second, as an injector, a radially completed well is exemplary in dispersing steam into the heavy oil reservoir. Also of significance is the fact that radials appear to have eliminated the deleterious effect of steam override problems common in heavy oil reservoirs with huff and puff operations.

Oil Production Cycle

Only several days of oil production data from the Bremer RI-53 had been recorded prior to the quarter ending July 15, 1990. However, early production results (after July 15, 1990) are very favorable and indicate that a well completed with radials may have double the productive capacity of a typical vertical well in the same lease. This aspect of the project will be discussed more fully in the Annual Summary and Final Reports (task 4).

Conclusion

The primary objective of this project was achieved when four horizontal radials were successfully drilled and completed. The operations were conducted in a safe and efficient manner.

No problems were encountered with the operations or with the subcontractors. Union Oil Company, the operator of the Bremer RI-53 well, was pleased with the results.

From a technical standpoint, Petrolphysics has demonstrated that radials can be used for steam injection. Initial results indicate that radials provide an effective means for steam distribution into the heavy oil reservoir. These results will be quantified in the final report as more information from the monitor well is analyzed.

ENHANCED OIL RECOVERY SENSING

Lawrence Livermore National Laboratory
Livermore, Calif.

Contract Date: Oct. 1, 1984
Anticipated Completion: Oct. 1, 1990

Principal Investigator:
Mike Wilt

Project Manager:
Thomas B. Reid
Bartlesville Project Office

Reporting Period: Apr. 1–June 30, 1990

Objective

The objective of this project is to monitor in situ changes in the electrical conductivity in an oil reservoir during enhanced oil recovery (EOR) operations. The goal of this project is to develop practical tools for monitoring the propagation of a steam front during an ongoing EOR operation. Cross-borehole electromagnetic (EM) induction is being used to provide an image of electrical conductivity changes associated with an encroaching steam front. This technique is being adapted to the hostile conditions in an oil field during EOR operations.

Summary of Technical Progress

During this quarter the first suite of laboratory data that measures the electrical conductivity of rock during steam injection was collected. Full-system testing also began on the cross-borehole EM system at Richmond field station. This is in preparation for the upcoming field exercise in Devine, Tex.

Laboratory Studies

Laboratory measurements of electrical resistivity in steam-saturated rock are being made at the University of California-Berkeley laboratory facilities. The initial stage of this project involves one-dimensional (1-D) studies where pure steam is injected into one end of a saline water-saturated sandpack and the temperature, steam saturation, and electrical conductivity of the sand are monitored while the steam displaces the water.

Figure 1 displays the temperature and electrical conductivity for a point in the center of the 1-D column during a steam displacement experiment. Initially, the temperature and conductivity are unchanging, but the plot shows a slight increase in electrical conductivity at about 2000 s, which corresponds to an increase in temperature. This is evidence that the thermal front advances ahead of the steam front. As the steam front passes the measurement point, the conductivity is drastically reduced, whereas the temperature sharply increases to 100°C and gradually thereafter up to 112°C.

The plot shows that the steam front is not an abrupt feature; it requires about 200 s to fully sweep past the measurement point at the center of the column. Toward the end of the column this transition zone is much broader. During steam injection the column may be subdivided into three regions: a steam-saturated zone, a steam condensate zone (where the pure steam condenses and mixes with in situ water), and a water-saturated zone. The transitional steam condensate zone is also a zone of transitional electrical conductivity.

In succeeding phases of the experiment, measurements will be made in a two-dimensional (2-D) cell where it is possible to study the steam override phenomena and the effects of inhomogeneous structure.

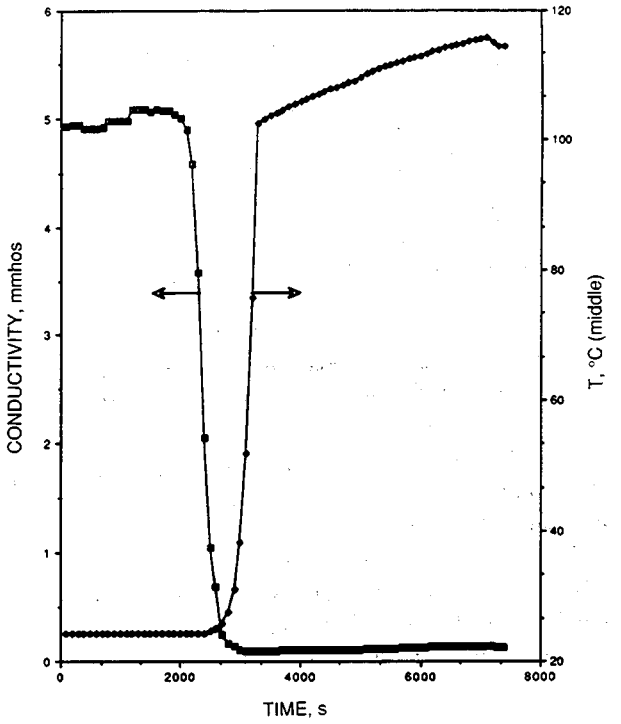

Fig. 1 Plot of the temperature and electrical conductivity at the center of a one-dimensional sandpack column during steam injection.

Field System Testing at Richmond Field Station

In cooperation with the University of California and Lawrence Berkeley Laboratory, a field system is being prepared for deployment at the SOHIO Inc., test facility in Devine, Tex. This combined effort is partially funded by a consortium of oil and energy companies through a project initiated at the University of California. The field experiment is designed to test the feasibility of audio-frequency cross-borehole EM in an EOR environment where boreholes are spaced several hundred meters apart in high-conductivity sands and shales and the injection zone is at a depth of 500 m.

The initial phases of this experiment involve assembling the hardware and conducting extensive and rigorous testing at the Richmond field station facility. Numerical calculations have indicated that imaging is possible only if high-quality field data can be obtained. For proper imaging, a data set is required to be repeatable over time to less than 1%.[1] This means that the field system must be powerful, yet insensitive to the effects of moisture and temperature and external noise.

Figure 2 shows some cross-borehole EM measurements made at Richmond field station in boreholes spaced 52 m apart. With this configuration, the receiver coil remains fixed (at a depth of 30 m), whereas the transmitting coil continually moves and data are collected continuously. The highest field levels indicate where the transmitting and receiving coils are at the same horizontal level in their re-

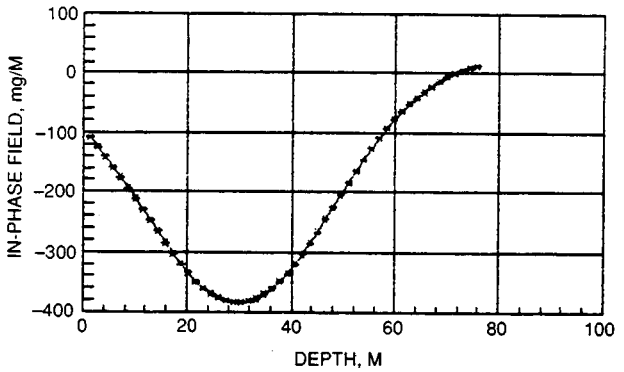

Fig. 2 Cross-borehole electromagnetic field profile taken at Richmond field station (normalized in-phase field profile BCNW10BAS).

spective boreholes. The amplitude variation is the result of the changing geometric configuration of the coils as well as attenuation because of the earth.

The error plots (Fig. 3) show that the two sets of measurements, taken 24 h apart, were repeatable to approximately 0.5%. This is well within the required precision, and it is a very encouraging result for future field experiments.

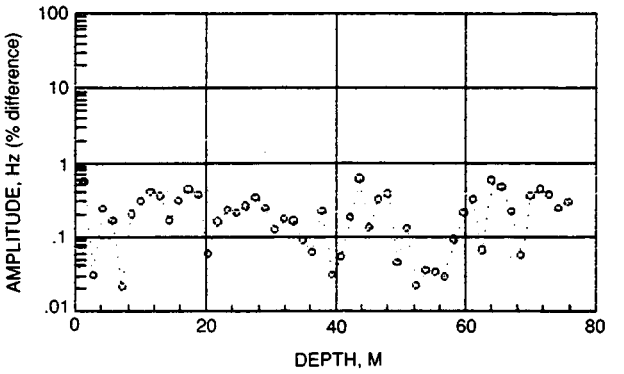

Fig. 3 Percent difference measurements for two profiles of the type shown in Fig. 2 (field amplitude difference BCNW10BAS).

Devine Field Test

The field experiment in Devine, Tex., has been scheduled from Sept. 10 to Sept. 20, 1990. The purpose of the experiment is to test the cross-borehole EM system to determine its limitations in deep widely spaced boreholes in an environment of highly conducting country rock. The test site is in an isolated area and in flat-lying geology, so the result may be confidently compared with layered models. The geology and well spacing for this site are similar to those for many producing oil fields.

Reference

1. Q. Zhou, *Audio-Frequency Electromagnetic Tomography for Reservoir Evaluation*. Ph.D. thesis, Department of Engineering Geosciences, University of California, Berkeley, 1989.

RESEARCH ON OIL RECOVERY MECHANISMS IN HEAVY OIL RESERVOIRS

Contract No. FG22-90BC14600

Stanford University
Petroleum Recovery Institute
Stanford, Calif.

Contract Date: Feb. 23, 1990
Anticipated Completion: Feb. 22, 1993
Government Award: $740,000
(Current year)

Principal Investigators:
W. E. Brigham
K. Aziz
H. J. Ramey
L. M. Castanier

Project Manager:
Thomas B. Reid
Bartlesville Project Office

Reporting Period: Apr. 1–June 30, 1990

Objective

The goal of the Stanford University Petroleum Research Institute (SUPRI) is to conduct research directed toward increasing the recovery of heavy oils. Presently, SUPRI is working in five main directions:

1. Flow properties research—to assess the influence of different reservoir conditions (temperature and pressure) on the absolute and relative permeabilities to oil and water and on capillary pressure.
2. In situ combustion studies—to evaluate the effects of different reservoir parameters on the in situ combustion process. This project includes the study of the kinetics of the reactions.
3. Additives to improve steam injection—to develop and understand the mechanisms of the process with the use of commercially available surfactants for reduction of gravity override and channeling of steam.
4. Reservoir definition—to develop and improve techniques of formation evaluation, such as tracer tests and pressure transient tests.
5. Field support services—to provide technical support for design and monitoring of DOE-sponsored or industry-initiated field projects.

Summary of Technical Progress

Flow Properties Studies

A paper on X-ray computerized axial tomography (CAT) scanning was presented at the California Regional

Meeting of the Society of Petroleum Engineers (SPE). This paper summarizes applications of CAT to a variety of experimental problems in reservoir engineering and enhanced oil recovery research. It includes a description of the equipment, a discussion of the various types of software used for interpretation and a display of the results, and several examples of applications. Among those, emphasis was placed on the following: (1) verification of homogeneity in sandpacks, (2) foam flow of liquid and gas saturations, (3) three-dimensional (3-D) steam model, (4) flow through fractured media, and (5) relative permeability studies. Answers to specific problems and example pictures of scans were presented. CAT scanning can be used in a broad range of experiments.

A review of the literature on relative permeability experiments showed that the problem of end effects is not fully understood. A special core holder was designed and built for studies of the end effects in oil–water relative permeability flow experiments. The experiments will allow for measurement of the saturations in many cross sections of the core. The equipment is now being pressure tested and calibrated.

In Situ Combustion

Analysis of the four tube runs performed with metallic salts using Hamaca oil is in progress. The metallic additives clearly affect the combustion process. The oxygen use and CO_2/CO ratios were increased by the metals. The equipment is being improved to reliably determine the amount of fuel burned. A chromatograph will also be added to improve the nitrogen material balance.

A study has been initiated to correlate steamflood residual saturation with fuel concentration for in situ combustion. The development of a general procedure to estimate the amount and nature of residual oil to steamflooding as a function of rock and oil properties may be possible. This is important not only for combustion but also for steam injection predictions. The research will be carried out in three stages: (1) literature review and correlation of available data, (2) experimental studies, and (3) numerical simulation.

Steam with Additives

Transient behavior is likely to dominate for the duration of a foam injection project. This study investigates transient foam flow in a simple linear porous medium. Foam is injected at a constant volume rate into a one-dimensional (1-D) sandpack in a CAT scanner at low temperature and pressure. The pressure gradient between the injection end and the foam front is much greater than that ahead of that front. Moreover, the pressure gradient keeps changing as the foam advances in the sandpack. This behavior differs from the Buckley–Leverett theory. The CAT scan results demonstrate that the foam displacement is not piston-like. Gas channeling appears near the front, and eventually the foam blocks all these channels. It takes two or more pore volumes of foam injection to reach residual liquid saturation. The saturation vs. pore volume relationship for a given section of the sandpack was matched with exponential formulas; however, the formulas vary with distance. Graphing the data as saturation vs. equivalent pore volumes injected reduces the range of these variations but does not eliminate them. So far, this behavior is unexplainable.

In a study on characterization of surfactants at steam conditions, a linear model was used to compare and characterize eight surfactants as steamflood additives under moderate temperature and pressure. Two sets of experiments were completed. In the first experiment, no oil was present; in the second, West Newport crude oil was used at residual saturation after steamflooding. Results from the first set of runs indicated that alpha olefin sulfonates generated the strongest foam. Flow resistance as a result of foam increased as the alkyl chain length increased. Enrichment in disulfonate content enhanced the propagation speed but reduced foam strength. Significant steam mobility reduction was achieved for all surfactants tested. Analysis of temperature and pressure profiles indicated the formation of a nitrogen foam ahead of a steam foam. In the presence of oil, no increase in pressure gradient was observed for any of the surfactants tested.

The 3-D model is now leak proof. Calibration experiments for isothermal and nonisothermal flow are in progress.

Formulation Evaluation

A report concluding the study of flow through perforations was sent to the Department of Energy (DOE). A theoretical solution to flow into a well via perforations is synthesized with the use of Green's functions. The solution is 3-D and applies to steady-state single-phase homogeneous flow. The solution involves five physical parameters: (1) wellbore diameter, (2) perforation diameter, (3) perforation length, (4) perforation density (vertical spacing), and (5) phasing (angular spacing). These parameters influence the cost and efficiency of a well completion. A sensitivity analysis can be done for an optimization of the completion design with this analytical solution. Further work is needed to extend the solution for uniform potential but variable flow rate along the length of a perforation. Further work with various perforation parameters is needed for the development of optimization procedures.

Support Services

A semianalytical model (SAM) was developed for 1-D linear systems and two-dimensional (2-D) linear cross-sectional systems. The SAM includes formation dip; compressible formation; water; oil; and thermal expansion of the formation, water, and oil. The model automatically calculates the steam-zone steam saturation and includes the waterfront and overburden heat losses. In the 2-D model, a new empirical method that determines the shape of the

steam front is presented, and an extension of an existing waterflooding correlation is used to determine water underride. The SAM runs were several orders of magnitude faster than the thermal simulator, yet they matched thermal simulator results accurately in over 2000 runs over a wide range of variables.

RESOURCE ASSESSMENT TECHNOLOGY

ESTABLISHMENT OF AN OIL AND GAS DATABASE FOR INCREASED RECOVERY AND CHARACTERIZATION OF OIL AND GAS CARBONATE RESERVOIR HETEROGENEITY

Contract No. FG22-89BC14425

Geological Survey of Alabama
Tuscaloosa, Ala.

Contract Date: Apr. 19, 1989
Anticipated Completion: Apr. 18, 1992
Government Award: $240,000
(Current year)

Principal Investigator:
Ernest A. Mancini

Project Manager:
Chandra Nautiyal
Bartlesville Project Office

Reporting Period: Apr. 1–June 30, 1990

Objectives

The objectives of this project are to augment the National Reservoir Database, Tertiary Oil Recovery Information System (TORIS), to increase the understanding of geologic heterogeneities that affect the recoveries of oil and gas from carbonate reservoirs in Alabama and to identify those resources which are producible at moderate cost. These objectives will be achieved through detailed geological, geostatistical, and engineering characterization of typical Jurassic Smackover Formation hydrocarbon reservoirs in selected productive fields in Alabama. These studies will be used to develop and test mathematical models for the prediction of the effects of reservoir heterogeneities in hydrocarbon production.

Summary of Technical Progress

Geological Studies

Geological characterization of a petroleum reservoir requires the definition of the lithofacies within the geologic unit comprising the reservoir. This is achieved primarily through examination and analysis of geophysical well logs, core material, well cuttings, and well test data from wells

penetrating the reservoir within a field. From these data, reservoir heterogeneities, such as lateral and vertical changes in lithology, porosity, permeability, and diagenetic overprint, can be recognized and used to produce maps, cross sections, graphs, and other graphic representations to aid in interpretation of the geologic parameters that affect the reservoir.

Geological research this quarter has continued to focus on descriptions of core material and petrographic thin sections from reservoirs producing hydrocarbons from the Smackover Formation in southwestern Alabama, computer entry of pertinent data, and generation of maps and cross sections. This research will result in a comprehensive characterization of all Smackover fields in the state for inclusion in the first annual report (18-month report).

All Smackover cores archived at the Geological Survey of Alabama have been inventoried and their condition and coverage evaluated. These data have been organized into computer databases that are updated regularly. More than 22 whole cores have been slabbed to facilitate description. The Smackover core inventory at the Geological Survey of Alabama is being enhanced by the addition of all new cores cut from the Smackover Formation penetrated by wells within the state and by a vigorous program to acquire cores stored in other repositories.

At present, cores from 15 Smackover fields (Bucatunna Creek, Chappell Hill, Chatom, Gin Creek, Hatter's Pond, North Choctaw Ridge, Stave Creek, Toxey, Healing Springs, Lovett's Creek, Chunchula, Little Escambia Creek, Big Escambia Creek, and West Barrytown) have been described and graphic summaries of the core descriptions have been integrated with other data to generate reservoir characterizations for these fields. Depositional and diagenetic sequences have been interpreted and summarized for each core. Thin-section studies were made on 7 of the 15 fields listed to supplement and extend interpretations made from core descriptions. Two hundred fifteen thin sections have been described, 93 have been made but not yet described, and more than 150 have been selected but not yet made. A comprehensive record, in the form of an annotated file of 35-mm color slides, is being compiled from all thin sections examined. Paragenetic sequences have been reconstructed for each of the 15 fields. Twenty-six thin sections have been point counted to estimate the relative proportions of particle and pore types making up the reservoirs. This type of analysis and description will be carried out on all 46 Smackover fields for which core material currently is available.

Geophysical log suites for all 70 Smackover fields in Alabama were studied, and a type log for each field has been selected for digitization. Type logs of 12 Smackover fields have been digitized; type logs for the remaining 57 fields have been selected and will be digitized in the next quarter. The log suites that are being digitized include three induction curves, a spontaneous potential (SP) curve, a gamma-ray curve, a caliper curve, a density curve, and a neutron curve. In addition, well-log data have been used to construct structure maps and structural cross sections for all 70 Smackover fields in Alabama. These maps and cross sections, which were generated by computer drafting techniques, are now complete. Oil samples from 27 Alabama Smackover fields not previously analyzed have been sent to the United States Geological Survey in Denver for geochemical analysis. These geochemical data will be integrated with the oil analyses from the fields previously studied and thus will serve to enhance the existing geochemical database for Smackover oils in Alabama. All available commercial core-analysis data (porosity and permeability) for Smackover fields in Alabama have been entered into a computerized database. Entry of these data for wildcat wells is in progress. These data will be used for statistical analyses and to generate Dykstra–Parsons coefficients for the Smackover fields. Net pay, average porosity, and average water saturation values for 55 Smackover fields have been reviewed and revised as necessary.

Capillary-pressure analyses were run on samples from two Smackover fields. These data, and additional petrophysical analyses to be run in the next quarter, will be used to quantify the pore-system characteristics of Smackover reservoirs.

Chunchula field has been chosen for detailed study of reservoir characterization and simulation during the next project year. Reservoir intervals (>0.1 mD permeability and >6.0% porosity) have been identified from the core-analysis data. The position of these intervals was plotted (after depth correction) on Corrected Neutron Log/Focused Density Compensated (CNL/FDC) logs, and a series of cross sections was constructed to provide a preliminary assessment of the geometric distribution of reservoir-grade rock within the Smackover interval in Chunchula field. Further assessment of reservoir distribution is continuing to provide a basis of selection of cores for detailed lithologic study. The geologic model developed from these studies will be used in the geostatistical and reservoir engineering portions of the project.

Engineering Analysis

Engineering data for Chunchula field were collected from the files of the State Oil and Gas Board of Alabama. These data included available injection, production, and pressure histories, along with basic information (e.g., producing interval and well location) for every well in the field since initiation of production. Drilling and completion histories are also being compiled to assist in the analyses. These data will aid in explaining any anomalous production and pressure histories encountered during the study. Because of the large amount of data, a computer program was developed to extract the appropriate data from the database for any particular engineering analysis.

Some core testing was carried out to fill gaps in the porosity and permeability database for Chunchula field. In

addition, well logs from Chunchula were analyzed to provide additional data. All the data are being entered into a computer database that includes both observed values and calculated parameters.

The engineering data are currently being analyzed to determine which methods of reservoir calculation are most feasible for evaluation of Chunchula field. Methods being examined range from classical material balance to more complex compositional simulations. The quality and availability of the pressure volume temperature (PVT) data are being assessed to determine which of the reservoir characterization techniques is most appropriate. In addition, efforts are being made to implement the BOAST reservoir simulator on the IBM mainframe computer.

Geostatistical Analysis

The main accomplishment in geostatistical analysis this quarter was the completion of the basic program for conditional stochastic simulation. This methodology and its practical applications have been discussed in previous progress reports. The program developed for this study differs from programs in common use; in this study a hierarchical subdivision of the region being modeled is used. A particular point P in the region is correlated with all other points, but these correlations are described in terms of large blocks if they are far from P and in terms of the smallest subdivisions only if they are very close to P. The significance of the new algorithm is that the simulation of a system containing N grid points takes a time of order N (log N)^2, as opposed to N^3 for existing methods. If N is 8,000, for example, the new method is 372,000 times more efficient. The program, which was designed, debugged, and tested on an IBM-AT personal computer, was converted to run on the Cray supercomputer; this will allow the simulation of about 10,000 grid points, as opposed to 100 grid points on the PC.

Geostatistical analysis of Chunchula field continued during this reporting period. For each of the 60 wells in the field with core-analysis data, vertical variogram analyses were performed for both porosity and permeability. Since most of the variograms for permeability are quite noisy, the log transformation also was used in an attempt to obtain a better result. Porosity variograms for 58 wells were further analyzed. Most of the variograms were fitted with one or more of four models: linear, spherical, exponential, and/or Gaussian. In most cases, the selected model fit well when the distance (h) was not too large. A number of the variograms were rather noisy, so none of the models fit. The noisiness may be a result of the effect of missing data, one relatively large or small value in the data set, or a combination of these problems.

National Reservoir Database (TORIS)

Data from all Smackover fields in Alabama have been entered into the TORIS database. The data will be augmented and refined throughout the project.

CHARACTERIZATION OF SANDSTONE HETEROGENEITY IN CARBONIFEROUS RESERVOIRS FOR INCREASED RECOVERY OF OIL AND GAS FROM FORELAND BASINS

Contract No. FG07-90BC14448

Geological Survey of Alabama
Tuscaloosa, Ala.

Contract Date: Feb. 20, 1990
Anticipated Completion: May 30, 1993
Government Award: $175,000
(Current year)

Principal Investigator:
Ernest A. Mancini

Project Manager:
Chandra M. Nautiyal
Bartlesville Project Office

Reporting Period: Apr. 1–June 30, 1990

Objectives

The objectives of this project are to augment the National Reservoir Database Tertiary Oil Recovery Information System (TORIS), to develop models of reservoir heterogeneity, and to identify resources that are producible at a reasonable cost; this will increase recovery of hydrocarbons from Carboniferous siliclastic reservoirs in the Black Warrior Basin. The objectives will be achieved through detailed geological, engineering, and geostatistical investigations of Carboniferous sandstone reservoirs in the basin. These investigations will be used to develop and to test geological and mathematical models for predicting the effect of reservoir heterogeneity on the recovery of hydrocarbons.

Summary of Technical Progress

Geological Studies

Outcrop Investigation of Sandstone Heterogeneity

An outcrop study has included the compilation of detailed measured sections and diagrams that demonstrate the vertical and lateral lithofacies relationships of sandstone

units and the establishment of criteria for quantifying the extent and geometry of sandstone reservoirs. Criteria that have proven useful to identify lithofacies are lithology, sedimentary structures, and fossil content. Thus far, more than 40 sections have been measured; most of these sections are in the Hartselle Sandstone.

Investigation of Carboniferous sandstone units in outcrop has been useful for understanding reservoir architecture. In essence, each reservoir sandstone unit has a distinctive suite of bedding styles and sedimentary structures. For example, the Hartselle Sandstone is continuous throughout most of the study area, but outcrops demonstrate that facies within the sandstone are varied, discontinuous, and difficult to predict. In contrast, the Lewis sandstone contains abundant sandstone lenses and channel fills encased in shale.

An outcrop study is the best method to resolve lateral heterogeneity that in the subsurface would occur between wellbores and to determine the extent and geometry of potential flow units in three dimensions. Although the Hartselle Sandstone is a regionally extensive sandstone body, for example, subtle facies changes in the Hartselle can be seen in outcrop. This suggests that lateral facies heterogeneity in some reservoirs cannot be identified with cores and well logs. These tools do not provide for detailed study of the lateral continuity of units afforded by surface exposures. Another major advantage of outcrop investigation is improved determination of depositional environment, which is a primary control on reservoir heterogeneity. Wells are commonly too widely spaced and cores are too scarce to provide adequate paleoenvironmental control.

Subsurface Investigation of Sandstone Heterogeneity

Most work to date has focused on developing a regional stratigraphic framework for Carboniferous reservoir sandstone using well logs and recognizing first-order heterogeneity through intensive field investigation. Four well-log cross sections of strata from the Tuscumbia Limestone to the top of the Mary Lee coal group of the Pottsville Formation were made. The cross sections were made with 1-in. resistivity logs, and density logs were also used to identify major rock types. Each cross section contains between 10 and 25 well logs at a spacing of approximately 3 to 6 miles.

Regional cross sections demonstrate that the Mississippian and Pennsylvanian Systems of the Black Warrior Basin in Alabama contain approximately 3000 to 8000 ft of carbonate and siliclastic rocks and coal. At the base of the Mississippian System are regionally extensive shale, chert, and cherty limestone units that include, in ascending order, the Maury Shale, the Fort Payne Chert, and the Tuscumbia Limestone, respectively. Above these units, which collectively are generally less than 100 ft thick, facies relationships become increasingly complicated, and Mississippian sandstone reservoirs occur in a series of vertical siliclastic sequences. The Mississippian System contains three siliclastic sequences that have different geometries and intertongue with a persistent carbonate facies.

The first of these vertical siliclastic sequences, the Pride Mountain–Hartselle sequence, comprises the Pride Mountain Formation, the Floyd Shale, and the Hartselle Sandstone. In ascending order, three reservoir sandstone units, the Lewis sandstone, the Evans sandstone, and the Hartselle Sandstone, occur in this sequence. Where the Hartselle Sandstone is present in the northern part of the basin, the siliclastic sequence is approximately 400 ft thick, but where the Hartselle is absent, the sequence (Floyd Shale) is only about 200 ft thick. The Lewis sandstone caps a coarsening-upward shale–sandstone cycle above the Tuscumbia that generally is thinner than 60 ft. The sandstone forms an areally extensive but discontinuous body that is locally thicker than 40 ft; the Lewis limestone is a regional carbonate marker that occurs directly above the sandstone and is generally less than 30 ft thick. The Evans sandstone generally is thought to occur only in the Pride Mountain Formation of northwesternmost Alabama, but detailed correlation indicates that lenses of Evans sandstone that have been mapped with the Hartselle occur as much as 50 miles farther east than previously documented. The Hartselle Sandstone occurs in a wide, northwest-trending belt along the northern margin of the Black Warrior Basin and varies from 0 to more than 150 ft in thickness. In general, each sandstone body in the Pride Mountain–Hartselle sequence occurs farther north and east of the previous one.

The second siliclastic sequence, the Carter sequence, occurs in the lower part of the Parkwood Formation and includes the Carter sandstone, the principal oil-bearing unit in the Black Warrior Basin of Alabama. The Carter sandstone caps a coarsening-upward shale–sandstone cycle that occurs between the Bangor Limestone, which is locally more than 400 ft thick, and the *Millerella* tongue of the Bangor, which is generally less than 20 ft thick. In the northern part of the basin, the Carter sandstone resembles the Lewis sandstone; it is generally less than 40 ft thick and caps a thin coarsening-upward cycle between the thick Bangor and the thin *Millerella*. However, the Carter sequence thickens markedly toward the southwest where it is more than 400 ft thick and contains sandstone that is locally thicker than 200 ft.

The third siliclastic sequence, the Parkwood sequence, is represented by the upper part of the Parkwood Formation, which contains numerous sandstone, shale, and carbonate units, as well as some coal beds. Like the Carter sequence, the Parkwood sequence thickens markedly toward the southwest. However, upper Parkwood clastics override the carbonate facies rather than pinch out into it. Some potential reservoirs, such as the Cooper sandstone, occur in the upper Parkwood, but correlation of lithologic units is difficult, and sandstone and carbonate bodies are less continuous than in the lower siliclastic sequences. Additionally, coal beds in the upper Parkwood are not useful stratigraphic markers.

Potential sandstone reservoirs in the Pennsylvanian Pottsville Formation include several mappable bodies of quartzose sandstone that are easily identified and correlated with well logs. The basal quartzose sandstone of the Pottsville is the most widespread, and the areal extent of each sandstone body decreases upward in each section. Like the upper Parkwood, the Pottsville thickens markedly to the southwest, but the Pottsville also thickens significantly toward the southeast. Quartzose sandstone is concentrated in the northern part of the basin, where the Pottsville is thin, and pinches out toward the southeast into thick sequences dominated by nonporous litharenite and coal.

Making a regional cross-section network has helped determine the stratigraphic context of Carboniferous reservoirs in the Black Warrior Basin of Alabama. Cross sections clearly show regional facies relationships and are therefore the most useful guides for stratigraphic subdivision and for identifying regionally mappable subsurface units. The cross sections further demonstrate that faulting occurred in association with sedimentation and was a significant control on sequence thickness and sandstone geometry. Synsedimentary fault movement is generally expressed by step-like thickening of siliclastic sequences across mapped faults.

Refining the stratigraphic framework on Carboniferous strata in the Black Warrior Basin in Alabama should be instrumental in developing enhanced recovery strategies by providing a predictive framework for characterizing the occurrence of sandstone reservoirs and hence first-order reservoir heterogeneity. For example, recognizing fault control of sandstone distribution and geometry demonstrates that known structural patterns may be useful for the prediction of first-order sandstone heterogeneity. The ability to correlate large-scale heterogeneity with known geologic structures may facilitate site selection for infill drilling and enhanced recovery projects.

Future Work

Fieldwork to characterize sandstone heterogeneity in outcrop will continue during the next quarter. Field investigation of the Hartselle Sandstone is nearly complete, so emphasis will now shift to the Lewis sandstone of the Pride Mountain Formation and the Boyles Sandstone of the lower Pottsville Formation.

Compilation of the regional cross-section network is nearly complete, and final drafts of the cross sections will be made next quarter. Subsurface stratigraphic intervals to be mapped regionally will be identified, and data regarding sequence and sandstone thickness will be compiled. Similarly, detailed net-sandstone isolith maps and net-pay maps of major oil units, such as the Carter sandstone at North Blowhorn Creek, will be compiled.

Petrographic and engineering data for the major oil fields in the Black Warrior Basin of Alabama will also be tabulated and entered into the TORIS database. Additionally, geologic criteria for recognizing heterogeneity will be identified on the basis of the field and subsurface work that has been completed. Preliminary models of sandstone heterogeneity will be developed.

NATURAL RESOURCES INFORMATION SYSTEM FOR THE STATE OF OKLAHOMA

Contract No. DE-FG22-89BC14483

Oklahoma Geological Survey
University of Oklahoma
Norman, Okla.

Contract Date: June 22, 1989
Anticipated Completion: June 21, 1992
Government Award: $504,596
(Current year)

Principal Investigator:
Charles J. Mankin

Project Manager:
R. Michael Ray
Bartlesville Project Office

Reporting Period: Apr. 1–June 30, 1990

Objective

The objective of this research program is to continue developing, editing, maintaining, using, and making publicly available the Natural Resources Information System (NRIS) for the state of Oklahoma. This contract funds the ongoing development work that began with contract No. DE-FG19-88BC14233. The Oklahoma Geological Survey (OGS), working with Geological Information Systems at the University of Oklahoma, has undertaken the construction of this information system in response to the need for a computerized, centrally located library containing accurate, detailed information on the state's natural resources. Particular emphasis during this phase of development is placed on computerizing information related to the energy needs of the nation, specifically oil and gas.

Summary of Technical Progress

The Oil and Gas Production Subsystem

The Oil and Gas Production (OGP) subsystem is composed of three major files: a Lease File, a Field File, and a

County File. The Lease File contains production and formation records based on data obtained from the Oklahoma Tax Commission (OTC); data elements include lease name and number, location information, formations data, and monthly production totals. The Field File contains historical and current records for all 5091 active and inactive Oklahoma oil and gas fields, as identified by the Oklahoma Nomenclature Committee (ONC); data elements include field identification data, consolidation histories when relevant, discovery data, location information (county, section/township/range, and quarter/quarter section data), and monthly production aggregated (by location) from the records maintained on the Lease File. The County File has monthly oil and gas production data aggregated by county.

Processing for the OGP subsystem primarily consists of processing monthly computer tapes received from the OTC to update production totals for all three files and to add new records to the Lease Master File. At the beginning of this quarter, monthly production was on file for the period January 1983 to November 1989. New records for the Field Master File are added by manually coding and keying the results of ONC meetings. The process of reconciling the Lease and Field Master Files is accomplished through combined computerized and manual efforts.

As reported previously, a primary thrust for the OGP subsystem must be toward enhancing the files through ongoing quality assurance efforts. Although the estimated error rate in the production input tapes received from the OTC is rather low, the sheer volume of data processed from these tapes creates a large number of errors on the Lease File. One result of these errors in the OTC source tapes is the significant number of production records that get added to the file with invalid "Producing Unit Numbers" (PUNs), commonly called "no-master" records. A series of computerized and manual processes have been developed to research company reporting patterns as part of the effort to allocate the no-master production to the appropriate leases. Significant efforts also are required to detect and resolve cases in which a monthly production total is unreasonably large for a lease; these usually are caused by decimal problems in the production reports or by the allocation of production to the wrong lease.

The foremost goal of the OGP subsystem processing during this quarter was to prepare the data for the July data release. (Changing the previous release dates of November and May to January and July of each year improved the data quality for the release.) The December to February source data received from the OTC were added to the files. Approximately 942,000 records, representing about 135,000 unique PUNs, are now on the Lease File. Almost 90,000 of these PUNs have had production reported sometime during 1983 to 1990, and nearly 65,000 of them report 1989 and/or 1990 production. Quality assurance efforts in preparation of the data release included resolving no-master records as well as detecting and resolving cases in which monthly lease production totals were unreasonably large.

Table 1 gives an overview of the progress and current status of production data quality assurance efforts by region and county. In preparation for the data release, the effort expenditure on production data quality was greatly increased; this led to the resolution of over 2,000 no-master records. At the end of June, a total of 6,267 no-master records had been resolved for the year; 3,851 had been added from OTC tapes, and 6,045 remained on file. Since production quality assurance efforts began in October 1988, almost 48,000 transactions have been generated to correct no-master and other types of production data problems. The bar chart in Fig. 1 provides more perspective on the resolution rates. For all data years through 1989, progress has been made on reducing the number of no-master records. For 1990, only two new OTC tapes have been processed, and there are already nearly 800 1990 no-master records. Significant progress has been made this year in developing and refining both computerized and manual processes to perform the production quality assurance tasks, and, as a result, over 50% of the no-master records have been resolved. The resolution rates are expected to continue to improve for future data releases, but the new problems added by each monthly OTC tape will keep effort expenditures high in this area.

A second goal of the OGP subsystem work involves quality assurance efforts to "assign" leases to fields and derive field production totals from those lease assignments. These lease assignments are based on the official field outlines as designated by the Midcontinent Oil and Gas Association's ONC. Some areas exist in which significant field extension drilling has taken place, but the ONC has had insufficient resources to update the field boundaries accordingly; therefore, at the beginning of this year, almost 25% of the state's production was not allocated to any field(s) in the OGP subsystem.

A series of information packages for selected areas is being developed to assist the ONC in updating their field outlines. The packages consist of maps and lists that depict producing leases located outside current field boundaries; areas with the largest amount of "unassigned" production are receiving the highest priority. The first of these packages was presented at the January 1990 ONC meeting; others were presented in March, May, and June. These packages have been so well received that the Committee agreed to meet one full day per month to expedite the process of defining current field boundaries. The Committee set a goal to update all gas field boundaries by June 1991; oil field boundaries will be emphasized the following year. Table 2 provides more detailed information about the current status of unassigned production by region and county. Primary emphasis so far has been placed on the Arkoma and Anadarko regions (southeast and southwest). In the southeast region, half the production that was

TABLE 1

Progress and Current Status of Production Quality Assurance Efforts

Progress Summary (May 1989–June 1990)

	Counts of "No-Master" Records				Cumulative quality assurance transactions since October 1988
	Starting total, May 1989	Number added February 1989–February 1990 tapes	Number resolved	Ending total, June 1990	
North central					
047 Garfield	292	69	149	212	3524
053 Grant	154	34	60	128	1745
071 Kay	114	131	171	74	1048
073 Kingfisher	331	98	158	271	1633
081 Lincoln	123	57	67	113	307
083 Logan	141	70	81	130	468
103 Noble	145	25	60	110	586
109 Oklahoma	302	46	203	145	1181
119 Payne	106	60	90	76	369
Region subtotal	1708	590	1039	1259	10861
Northeast					
001 Adair	2	5	7	0	20
035 Craig	3	0	2	1	4
037 Creek	264	76	125	215	759
097 Mayes	1	1	0	2	0
101 Muskogee	64	5	43	26	133
105 Nowata	60	8	48	20	117
107 Okfuskee	120	36	105	51	639
111 Okmulgee	170	34	71	133	465
113 Osage	115	44	51	108	322
115 Ottawa	1	1	2	0	2
117 Pawnee	160	25	127	58	422
131 Rogers	50	20	57	13	153
135 Sequoyah	12	2	11	3	32
143 Tulsa	72	19	46	45	248
145 Wagoner	47	6	16	37	71
147 Washington	76	11	46	41	193
Region subtotal	1217	293	757	753	3580
Northwest					
003 Alfalfa	162	46	164	44	1904
007 Beaver	319	147	218	248	1758
025 Cimarron	37	21	35	23	223
043 Dewey	157	94	86	165	702
045 Ellis	144	87	67	164	359
059 Harper	254	129	73	310	728
093 Major	334	124	308	150	3051
139 Texas	185	229	278	136	1976
151 Woods	72	58	86	44	471
153 Woodward	95	61	104	52	462
Region subtotal	1759	996	1419	1336	11634
Southeast					
005 Atoka	4	3	3	4	32
013 Bryan	14	0	0	14	0
Southeast (Continued)					
023 Choctaw	0	0	0	0	0
027 Cleveland	52	9	34	27	156
029 Coal	17	13	23	7	153
049 Garvin	246	71	111	206	811
061 Haskell	108	53	72	89	416
063 Hughes	160	73	161	72	649
069 Johnston	1	1	1	1	3
077 Latimer	148	119	215	52	1335
079 Le Flore	84	63	69	78	756
087 McClain	133	34	32	135	134
089 McCurtain	0	1	1	0	3
091 McIntosh	45	2	40	7	347
095 Marshall	25	6	26	5	192
099 Murray	28	5	28	5	118
121 Pittsburg	197	165	228	134	1222
123 Pontotoc	61	33	33	61	1293
125 Pottawatomie	105	61	38	128	407
127 Pushmataha	1	0	1	0	2
133 Seminole	106	38	29	115	190
Region subtotal	1535	750	1145	1140	8219
Southwest					
009 Beckham	139	90	147	82	999
011 Blaine	133	67	45	155	750
015 Caddo	268	145	227	186	1471
017 Canadian	264	81	183	162	1114
019 Carter	215	126	208	133	1133
031 Comanche	38	6	8	36	125
033 Cotton	21	18	18	21	33
039 Custer	234	119	222	131	1486
051 Grady	284	136	260	160	1516
055 Greer	57	39	63	33	165
057 Harmon	0	2	1	1	1
065 Jackson	2	1	2	1	6
067 Jefferson	34	5	14	25	60
075 Kiowa	17	5	3	19	13
085 Love	82	15	43	54	333
129 Roger Mills	184	234	263	155	2160
137 Stephens	181	100	110	171	1337
141 Tillman	3	0	1	2	5
149 Washita	86	33	89	30	895
Region subtotal	2242	1222	1907	1557	13602
Grand total	8461	3851	6267	6045	47896

unassigned at the beginning of the quarter has been resolved; additional progress is expected at the July meeting. In particular, progress was made in Haskell, Latimer, LeFlore, McIntosh, and Pittsburg counties. In the southwest region, progress was greatest in Caddo, Custer, Roger Mills, and Washita counties; additional progress in the July meeting is expected for those counties as well as Grady, Blaine, and Dewey. Overall, during this quarter, unassigned gas production has been reduced from 24 to 20% of the annual average production, or about 80 bcf per year.

Additionally, the OGS is pursuing the possibility of providing the NRIS Field File (header and Township/Range/Section location data only) to the Midcontinent Oil and Gas Association in exchange for a commitment not only to complete the field boundary work but also to provide a jointly published listing of all Oklahoma oil and gas fields.

Quality assurance efforts regarding the formations data comprise a third goal. During this quarter, further progress was made in developing a prototype system for formations editing and code assignments. The effort assigned to this task will be increased in the coming months; the plan is to fully implement the system in the coming year.

Progress has also been made on a fourth goal (mapping applications development). The latitude and longitude coordinates contained in the Phillips Petroleum Company's Digital Land Grid Oklahoma Database are being added to the NRIS files. Several mapping projects in the OGS are being supported by the NRIS project. For example, well

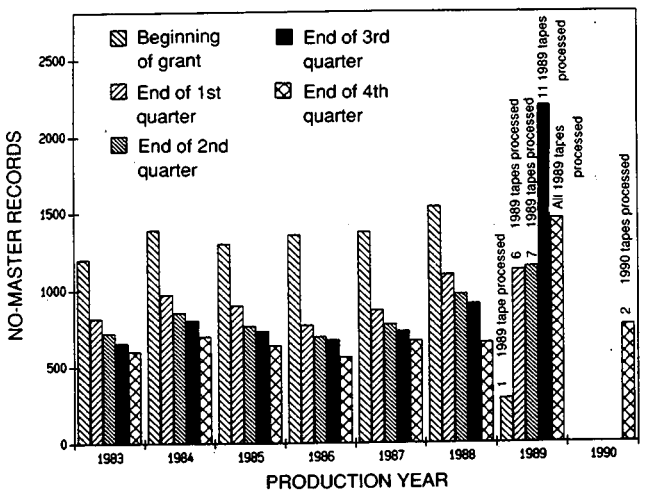

Fig. 1 Change in the no-master record totals.

spot maps and data tables are being generated in preparation for producing structure maps of the Arkoma and Anadarko basins, and NRIS production and well data are a major source of information being gathered for producing an Oklahoma Gas Atlas under subcontract to the Texas Bureau of Economic Geology.

The Well History File

The Well History File contains historical and current completion records for oil and gas wells reported to the Oklahoma Corporation Commission on Form 1002-A. At the start of the quarter, the Well History File contained 73,432 records for the Ouachita Mountains uplift and Arkoma basin areas and the Anadarko basin area. On a special project basis, supplemental data (where available) are added to the file from well logs, scout tickets, and core and sample documentation. Data elements on this file

TABLE 2

Unassigned Production* by Region and County

	Gas production (annual average),† Mmcf			Liquid production (annual average),† Mblls		
	Total	Unassigned	Percent	Total	Unassigned	Percent
North central						
047 Garfield	52,073	7,929	15	2,679	454	17
053 Grant	16,578	11,441	69	2,721	1,659	61
071 Kay	3,120	231	7	1,447	89	6
073 Kingfisher	63,989	21,745	34	4,522	1,173	26
081 Lincoln	12,290	6,579	54	1,554	578	37
083 Logan	20,955	9,138	44	2,144	1,111	52
103 Noble	9,384	3,305	35	3,279	1,106	34
109 Oklahoma	25,816	15,618	60	3,548	1,672	47
119 Payne	5,017	1,080	22	2,083	431	21
Region subtotal	209,223	77,067	37	23,976	8,272	34
Northeast						
001 Adair	0	0	0	0	0	0
035 Craig	34	20	59	6	4	70
037 Creek	8,228	2,934	36	5,879	797	14
097 Mayes	2	2	100	33	33	100
101 Muskogee	1,388	806	58	292	45	15
105 Nowata	727	382	53	478	134	28
107 Okfuskee	6,465	3,241	50	1,050	416	40
111 Okmulgee	6,873	1,871	27	1,348	312	23
113 Osage	8,293	3,212	39	8,152	1,231	15
115 Ottawa	0	0	0	0	0	0
117 Pawnee	7,621	6,092	80	2,729	1,834	67
131 Rogers	382	357	93	151	80	53
135 Sequoyah	2,278	1,306	57	0	0	0
143 Tulsa	1,317	442	34	870	76	9
145 Wagoner	803	477	59	289	122	42
147 Washington	1,176	599	51	797	64	8
Region subtotal	45,588	21,739	48	22,076	5,148	23
Northwest						
003 Alfalfa	15,047	746	5	963	51	5
007 Beaver	85,459	32,440	38	3,041	1,700	56
025 Cimarron	12,036	4,059	34	647	365	56

(Table continues on the next page.)

TABLE 2 (Continued)

	Gas production (annual average),† Mmcf			Liquid production (annual average),† Mbbls		
	Total	Unassigned	Percent	Total	Unassigned	Percent
Northwest (Continued)						
043 Dewey	65,177	20,820	32	2,556	1,475	58
045 Ellis	35,433	2,808	8	1,197	199	17
059 Harper	50,952	7,136	14	395	170	43
093 Major	85,317	14,686	17	4,282	1,056	25
139 Texas	102,374	14,814	14	4,096	1,379	34
151 Woods	28,061	338	1	542	3	1
153 Woodward	31,015	843	3	469	13	3
Region subtotal	510,512	98,691	19	18,189	6,410	35
Southeast						
005 Atoka	280	213	76	2	0	23
013 Bryan	1,743	13	1	101	0	0
023 Choctaw	(3)	(3)	0	0	0	0
027 Cleveland	6,364	2,703	42	2,289	810	35
029 Coal	4,722	32	1	196	0	0
049 Garvin	44,006	6,146	14	7,014	1,236	18
061 Haskell	35,783	947	3	0	0	0
063 Hughes	13,492	8,043	60	1,262	593	47
069 Johnston	7	0	0	0	0	100
077 Latimer	76,560	325	0	0	0	0
079 Le Flore	21,450	6,120	29	0	0	0
087 McClain	23,140	5,201	22	3,750	1,279	34
089 McCurtain	0	0	0	0	0	0
091 McIntosh	8,070	3,664	45	6	5	86
095 Marshall	6,019	117	2	343	3	1
099 Murray	453	35	8	1,598	518	32
121 Pittsburg	64,310	7,948	12	0	0	0
123 Pontotoc	1,295	86	7	4,631	53	1
125 Pottawatomie	6,403	4,988	78	4,480	2,002	45
127 Pushmataha	0	0	0	0	0	0
133 Seminole	3,733	1,236	33	4,327	623	14
Region subtotal	317,828	47,813	15	29,999	7,125	24
Southwest						
009 Beckham	79,095	3,406	4	1,142	86	8
011 Blaine	93,429	18,401	20	1,300	547	42
015 Caddo	107,419	1,925	2	4,034	196	5
017 Canadian	109,679	43,360	42	3,022	2,023	67
019 Carter	18,283	5,531	30	14,192	1,144	8
031 Comanche	9,956	3,635	37	308	198	64
033 Cotton	252	63	25	391	56	14
039 Custer	128,210	9,180	7	2,381	221	9
051 Grady	109,882	41,684	38	7,385	1,870	25
055 Greer	249	50	20	14	2	14
057 Harmon	0	0	0	74	0	0
065 Jackson	0	0	0	107	25	23
067 Jefferson	389	337	87	1,138	791	69
075 Kiowa	233	42	18	112	43	38
085 Love	4,406	1,370	31	1,716	1,167	68
129 Roger Mills	149,658	3,003	2	1,092	61	6
137 Stephens	43,124	7,740	18	11,596	863	7
141 Tillman	0	0	0	129	78	61
149 Washita	63,267	4,618	7	787	103	13
Region subtotal	917,890	147,344	16	50,920	9,474	19
Grand total	2,001,040	392,654	20	145,160	36,429	25

*Production not assigned to any field.

†Annual averages based on Janurary 1983–December 1989 production (as of 6/30/90).

include demographic items (e.g., API well number, lease name and well number, location information, elevations, and dates of significant activities for the well), formation items (e.g., formation names, completion and test data, and depths and perforations), and reference information (e.g., for drilling samples, core samples, and well logs).

In addition to the standard Well History File processing, special activities are being undertaken to enhance the supplemental data on the file. Work is under way on a parallel track within the NRIS Project to organize and computerize information from the OGS Core and Sample Library and from the Ardmore Sample Cut Library. Through computer and manual reconciliation processes, relevant data are being added to the Well History File. As other data sources become available, they will be reviewed as a cost-effective means to add supplemental information to the well records.

A large portion of the Well History File work involves photocopying the completion reports for use in coding prior to data entry. All new completion reports are copied as soon as they are received from the Oklahoma Corporation Commission; the originals are filed in the OGS's Well Log Library. Completion reports for areas of the state that have already been (or are being) worked are entered into the processing stream immediately. The others are filed for future processing. Historical completion reports from the Well Log Library are being copied at the rate of 8,000 to 12,000 forms per month; approximately 40% of these historical completion reports have now been copied.

Processing of the Oklahoma Corporation Commission's oil and gas well completion reports (Form 1002-A) is proceeding smoothly. Some delays were experienced during May and June as students adjusted to their summer schedules. The stabilization of staffing in general, however, has contributed to significant current progress on the Well History File project.

Presently, well records are being prescanned, keyed, and edited for the following southwestern counties: Tillman, Cotton, Stephens, Jefferson, and Carter. Over 25,000 well records were added to the file this quarter, more than during any single quarter since the project began. As of June 1990, 98,694 records were on file. The Well History File progress is in the following table by NRIS Regional Division.

Area of coverage	Start of grant	Start of quarter	Current
Southeast Region:	27,385	32,496	32,867
Southwest Region:	9,284	27,597	52,403
Northeast Region:	6,768	8,351	8,399
Northwest Region:	4,735	4,837	4,872
North Central Region:	138	151	153
Total	48,310	73,432	98,694

The current status of county coverage and the total record counts by county are displayed in the attached maps (Figs. 2 and 3).

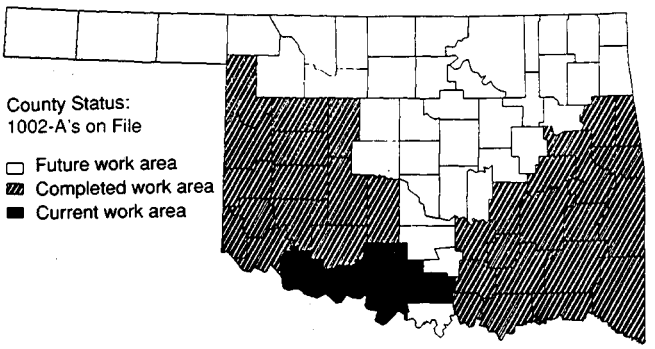

Fig. 2 Status of well history database project. County coverage as of June 1990.

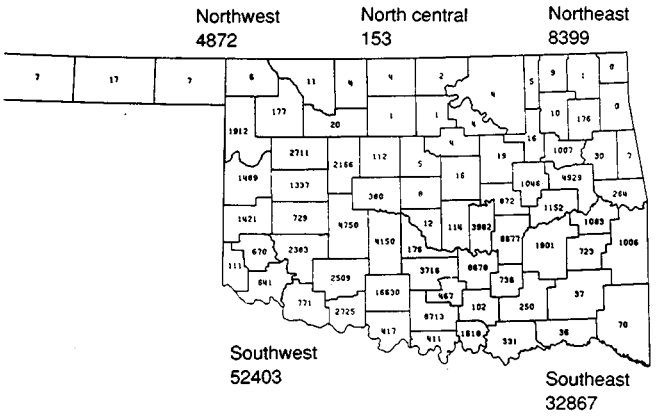

Fig. 3 Status of well history database project. Total well records, 98694.

The backlog of 7200 well records reported last quarter as having been keyed but not yet verified for accuracy has been depleted. Also, new keying formats were designed this quarter to increase efficiency and further facilitate the data entry effort. As regards quality assurance efforts, special edit procedures were implemented to standardize the perforation intervals and the quarter location data recorded on the 1002-A forms.

Thus far, supplemental data have been added to a total of 3413 records for the Ouachita Mountains area in southeastern Oklahoma. As previously reported, a computer matching process is being developed to add these supplemental data, as well as the core data that have been computerized for the OGS Core and Sample Library, to the well records.

Public Data Release

Response to the release of NRIS data continues to increase as word spreads about the availability of the data.

Even though this response largely continues to be internal among the geologists of the OGS and the University of Oklahoma's School of Geology, a few NRIS data requests were received from outside clients. For example, NRG Associates purchased the latest update to the NRIS Field File and a pipeline company purchased gas well and production summary data as components of an analysis on the economic impact of constructing a new pipeline for Oklahoma.

In May, Dr. Charles Mankin spoke before the Atoka County Royalty Owner's Association; he used NRIS as the basis for his presentation on gas production in that county and in the Arkoma basin. The Wilburton field data displayed as part of the OGS booth at the June American Association of Petroleum Geologists (AAPG) convention drew considerable attention. The display and accompanying reports resulted in 26 visitors expressing interest in adding their names to the NRIS mailing list.

DEPOSITIONAL SEQUENCE ANALYSIS AND SEDIMENTOLOGIC MODELING FOR IMPROVED PREDICTION OF PENNSYLVANIA RESERVOIRS

Contract No. DE-FG22-90BC14434

Kansas Geological Survey
Lawrence, Kans.

Contract Date: Feb. 1, 1990
Anticipated Completion: Apr. 30, 1993
Government Award: $173,479
(Current year)

Principal Investigator:
W. Lynn Watney

Project Manager:
Chandra Nautiyal
Bartlesville Project Office

Reporting Period: Apr. 1–June 30, 1990

Objectives

The objectives of this research are to (1) assist operators in the location and production of petroleum not currently under development because of technological problems or the inability to identify details of reservoir compartmentalization, (2) decrease risk in field development, and (3) accelerate the retrieval and analysis of baseline geoscience information for initial reservoir description. The interdisciplinary data sought in this research will be used to resolve specific problems in correlation of strata and to establish the mechanisms responsible for the Upper Pennsylvanian stratigraphic architecture in the midcontinent. The data will better constrain ancillary problems related to the validation of depositional sequence and subsequence correlation, subsidence patterns, sedimentation rates, sea-level changes, and the relationship of sedimentary sequences to basement terrains. The geoscientific information, including data from field studies, surface and near-surface reservoir analogues, and regional database development, will also be used for development of geologic computer process-based simulation models tailored to specific depositional sequences for use in improving prediction of reservoir characteristics.

Summary of Technical Progress

Field Screening and Analogue Identification

Field screening. Basic geologic information is being collected for four fields for conventional characterization and for use in geologic simulation modeling. Goals for the next quarter are to continue to collect data and to identify particular problems in production that can be addressed in these studies.

Near-surface analogues. A preliminary description of available outcrops, cores, and wireline logs and isopach mapping has been completed for these near-surface analogues. Sites have been selected for an initial phase of very high resolution seismic profiling and additional coring and wireline logging. Goals include the acquisition of these new data in July and August 1990 (third quarter) to further constrain reservoir development and to test preliminary models.

Regional Database Development

Regional cross sections, including strata from the Permian to the Precambrian basement, transect Kansas, linking the near-surface analogue sites to the fields in western Kansas, and extend north-south from upper landward limits of stratal sequences in Nebraska to deep basinal equivalents in Oklahoma. Sections are nearing completion (Fig. 1). Initial findings of the cross sections include the demonstration of occurrences of offlap and onlap of strata coinciding with underlying basement faults and the subtle, yet complex, variability of the basement. It is increasingly apparent that simple ramp models are inadequate to describe shelf configuration; actual profiles are block faulted. Not all faults were active at the same time, and reconstructions must be coordinated with tectonic history.

Wireline logs and cores along these sections will later provide details of individual depositional sequences. This

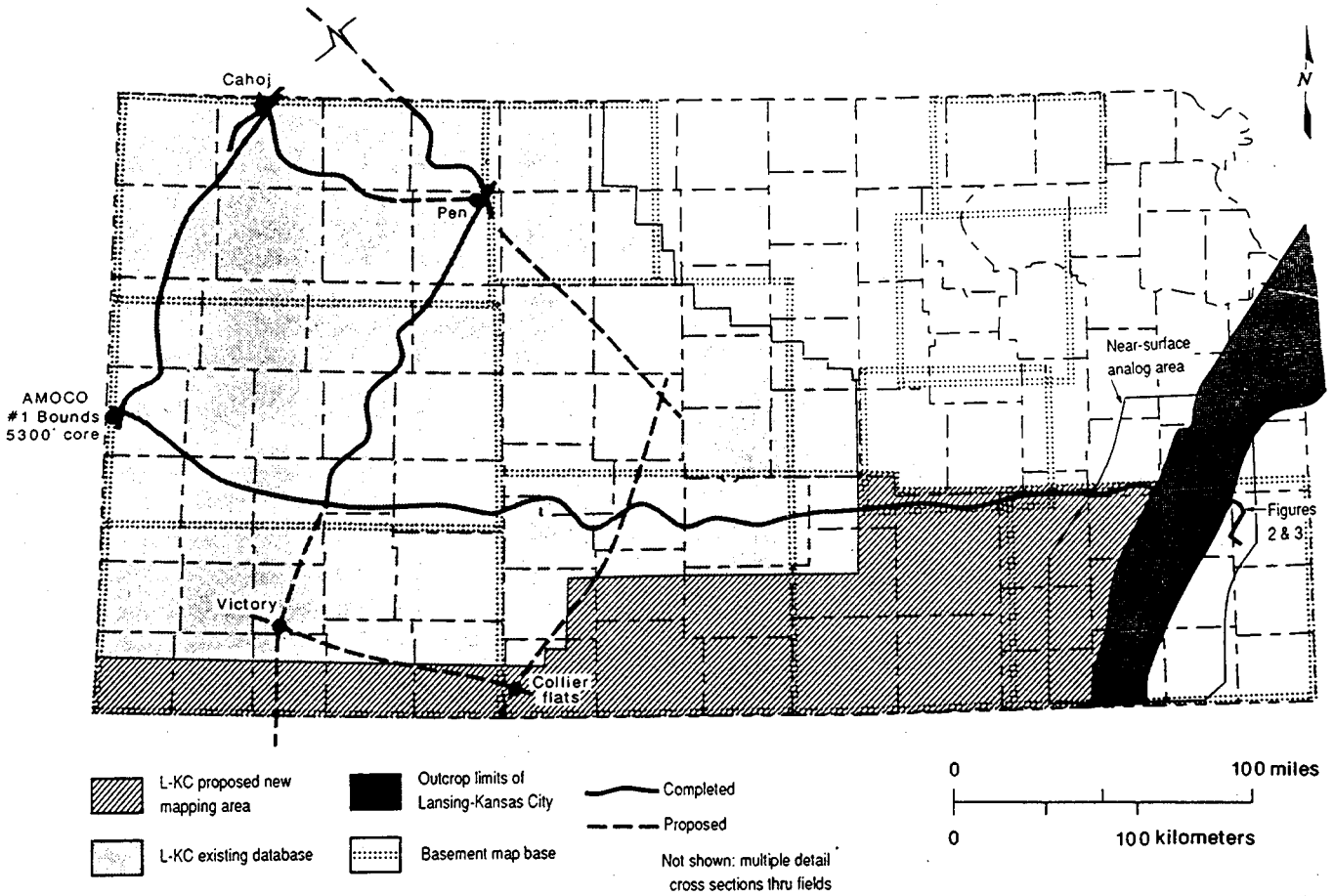

Fig. 1 Base map of Kansas showing locations of field studies, outcrop belt, near-surface and surface analogue areas, regional cross sections, basement mapping areas, existing Kansas City sequence mapping area, and new mapping area. Index for cross section in Fig. 2.

later use will complement regional mapping of selected Kansas City Group depositional sequences (Fig. 1).

Structural mapping of the Precambrian basement is complete for the Nemaha and Central Kansas uplifts and of the deep Arbuckle Group for the Pratt anticline region of south-central Kansas (Fig. 1). Plotted base maps are complete to map the structural configuration of the Arbuckle Group of the Hugoton embayment (western Kansas). Work will proceed during the third quarter. This will provide a deep-seated structure map for the entire state west of 96° longitude at a scale of 1:125,000. These data will be used to assess structural patterns in time and space and help determine subsidence timing and rates.

The Kansas Geological Survey (KGS) Precambrian computer database is being merged with a detailed petrographic and age–date database of R. Van Schmus of the University of Kansas Geology Department. The comprehensive database will be ready for use in the basement mapping project in the third quarter.

Geologic Computer Simulation Modeling

A sophisticated three-dimensional (3-D) process (forward) computer simulation model is under development. This model will reveal the dynamic interaction of geological processes to recreate the observed lithofacies, stratigraphy, and shelf configuration associated with individual Pennsylvanian depositional sequences. A prototype two-dimensional (2-D) version running on a personal computer presented at the annual meeting of the American Association of Petroleum Geologists (AAPG) in San Francisco (June 1990) was very well received. The model was initially tested by attempting to simulate three offsetting Bethany Falls oolite carbonate buildups in Bourbon County defined in the mapping. The oolite bars occur on a slope created by depositional topography on the underlying Pleasanton Group shales. The decompacted thickness of the Pleasanton Group shales suggests local relief on the slope of 35 m (100 ft) (Fig. 2). A dip-section, gamma-ray-neutron wireline log cross section of the Bethany Falls coupled with mapping of porous carbonate and nearby outcrops and core indicates that three lenticular offlapping deposits of porous oolite occur on this depositional slope (Fig. 2). Specifically, the model attempts to simulate these units.

The prototype simulation model of the oolite development in the configuration of this cross section is shown in Fig. 3. The simulation uses subsidence, sea-level history, sedimentation rate, and shelf configuration as input vari-

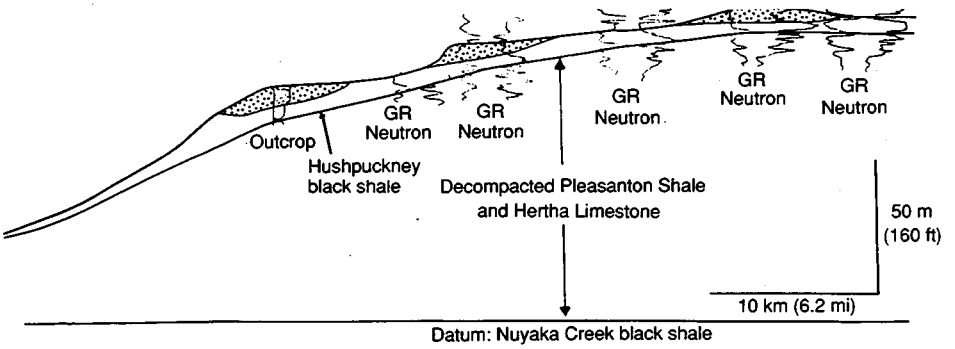

Fig. 2 Stratigraphic cross section from site in near-surface analogue area in southeastern Kansas illustrating three basinward-stepping porous oolite carbonate buildups within upper Swope (Bethany Falls limestone). The multiple oolites developed at different paleoelevations on a depositional slope created by an underlying deltaic complex of the Pleasanton Group.

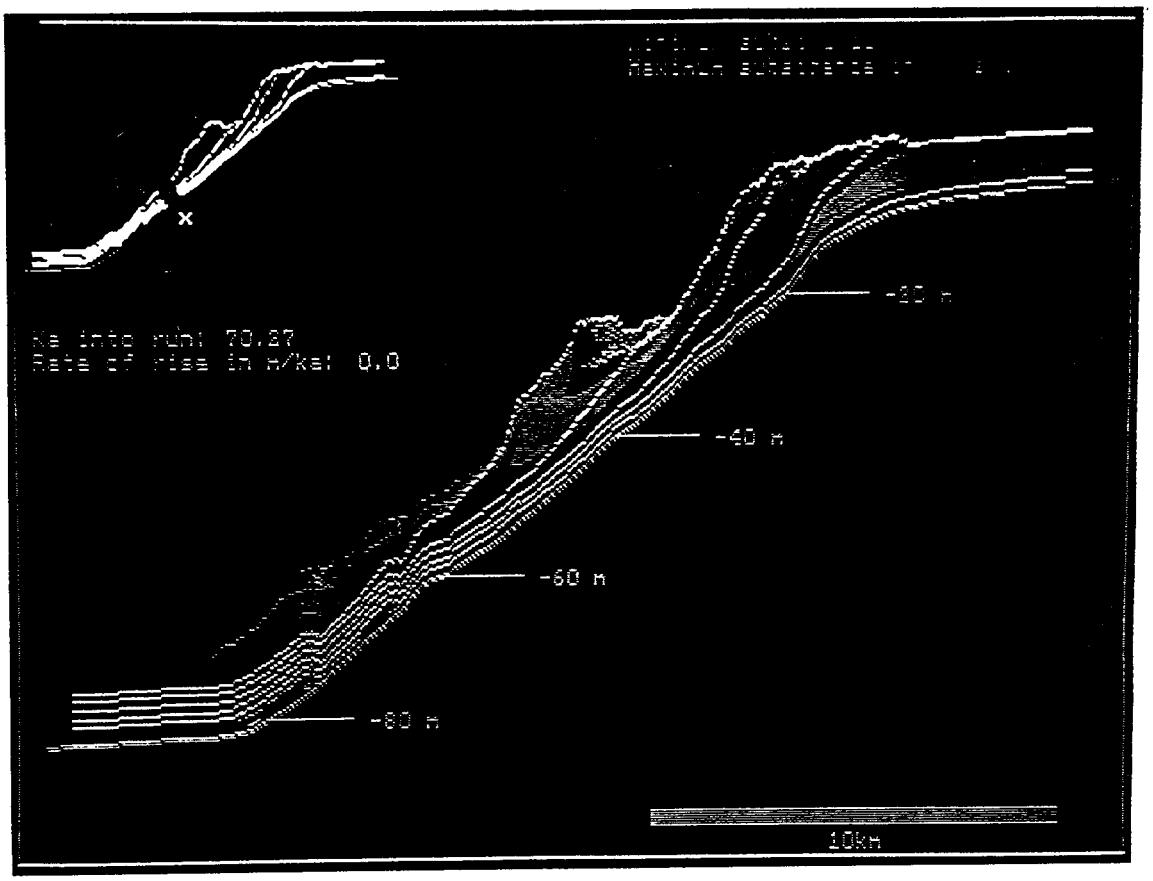

Fig. 3 Black-and-white photograph of a color screen from a run of the prototype two-dimensional (2-D) model using depositional topography patterned after the actual decompacted Pleasanton slope depicted in Fig. 2. Run uses a sea-level curve (solid white curve in upper left) made up of a rapid rise and slower, staggered fall; such curves are patterned after glacial–eustatic curves that are based on the Pleistocene–Holocene. Three discrete oolites are developed similar to the geologic depicted in Fig. 2 along the slope during stillstand in sea level. Time lines (white dashed lines in simulated sediment) are at 12-kA intervals.

ables. Eleven lithofacies are deposited in response to changing water depth, sedimentation rate, and depositional slope. Some 2000 lines of Pascal code comprise the prototype model. The simulation requires approximately 4 min to run on a 80386-25 computer.

Parameters for this modeling are estimated in part from the rock record and from results of Quaternary sediment studies. The modeling suggests that the oolites could have resulted from separate sea-level events, which provided a means of correlating and predicting discrete reservoirs within this unit in this setting.

The simulated Bethany Falls oolite deposits are strikingly similar to the observed deposits. However, regional and local parameter definition is still in an initial phase of development, and well-constrained, unique solutions to the modeling suitable for reservoir prediction have yet to be developed. This early modeling has addressed the kind of data that are needed and has helped to define the ways in which data collection will proceed. These strata will be cored and logged in August 1990 to provide a better understanding of the lithofacies, geometries, and possible distinction of these different lobes.

Future research plans include (1) performing geologic field studies to ascertain reservoir characteristics and identification of parameters for geologic simulation modeling during the last half of 1990 and first half of 1991; (2) defining and interpreting stratal geometries (depositional sequences) and analogue reservoir-type development in near-surface and surface reservoir analogues by judicious coring and wireline logging and use of very high resolution seismic profiling in August and September 1990 and again during summer 1991; (3) completing regional cross sections, basement mapping, and regional sequence mapping in the remainder of 1990 and mid-1991 for model parameter definition; (4) extending geologic simulation model to three dimensions by early 1991; (5) developing inverse modeling techniques for more precise parameter definition by mid-1991; (6) verifying and testing modeling of depositional sequences at field scale and testing use in prediction of reservoir facies and characteristics in field and near-surface analogues; and (7) enhancing technology transfer through field trips, workshops, and publications.

DEVELOPMENT OF AN INFLOW PERFORMANCE RELATIONSHIP FOR A SLANTED/HORIZONTAL WELL UNDER SOLUTION GAS DRIVE

Cooperative Agreement DE-FC22-83FE60149, Project SGP27

National Institute for Petroleum and Energy Research
Bartlesville, Okla.

Contract Date: May 1, 1989
Anticipated Completion: Jan. 1, 1990
Funding for FY 1990: $75,000

Principal Investigator:
Aaron Cheng

Project Manager:
Thomas B. Reid
Bartlesville Project Office

Reporting Period: Apr. 1–June 30, 1990

Objective

The project objective is to develop an empirical equation that can analyze the inflow performance relationship (IPR) of either a slanted or a horizontal oil well producing under the solution gas drive mechanism.

Summary of Technical Progress

This project has been completed. The final report, NIPER-458, was submitted to the Bartlesville Project Office on Jan. 22, 1990.

PHASE 1—DEVELOPING A RESERVOIR DATABASE

Cooperative Agreement DE-FC22-83FE60149, Project SGP28

National Institute for Petroleum and Energy Research
Bartlesville, Okla.

Contract Date: Aug. 18, 1989
Anticipated Completion: Sept. 30, 1990
Funding for FY 1990: $50,000

Principal Investigator:
James F. Pautz

Project Manager:
Chandra M. Nautiyal
Bartlesville Project Office

Reporting Period: Apr. 1–June 30, 1990

Objectives

The objectives of Phase 1 of this research are to develop input and output criteria for a reservoir database and to prepare a detailed conceptual design of a RELIANCE database management system (DBMS) environment to meet those requirements.

Summary of Technical Progress

One potential source of information for a reservoir database is the reservoir database at the Energy Information Administration (EIA). This database has information on about 2400 reservoirs and has 252 data fields. Besides the data, the data fields or data elements in this database might be a starting point for a revised DBMS.

One method of measuring the quantity of the information is to look at the frequency of information in each of the data fields. Figure 1 shows the frequency count and the number of entries for each data field in the EIA version of the reservoir database. Three data fields relating annual oil production distort this frequency distribution because they can have multiple entries for a single reservoir. Figure 2 shows the frequency distribution of data fields after the annual production field has been removed.

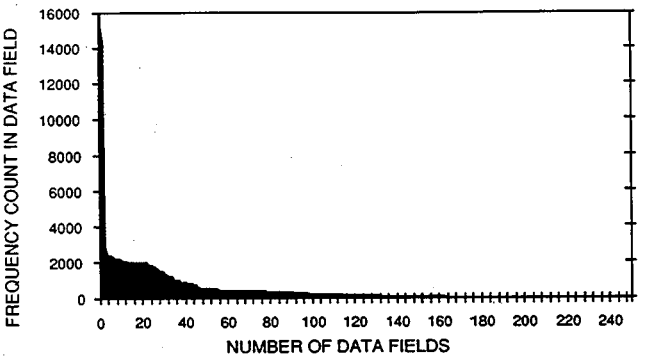

Fig. 1 Frequency of data in the data fields of the reservoir database at the Energy Information Administration.

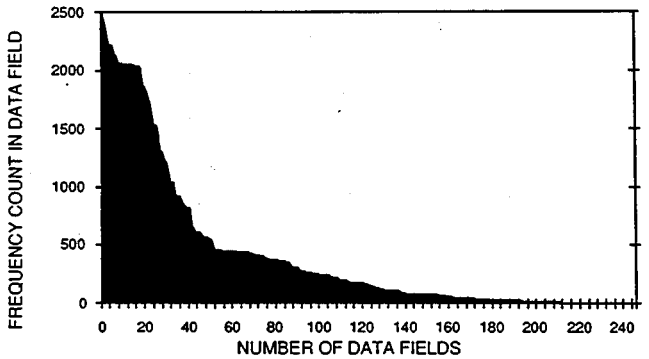

Fig. 2 Frequency of data in the data fields of the reservoir database at the Energy Information Administration after eliminating the data fields with more than one occurrence per reservoir.

Twenty data fields have over 85% representation, but representation rapidly drops in the remaining data fields. Only 31 data fields have over 50% representation. Over 100 have less than 5% representation.

TORIS RESEARCH SUPPORT

Cooperative Agreement DE-FC22-83FE60149, Project BE2

National Institute for Petroleum and Energy Research Bartlesville, Okla.

Contract Date: Oct. 1, 1983
Anticipated Completion: Sept. 30, 1990
Funding for FY 1990: $210,000

Principal Investigator:
James F. Pautz

Project Manager:
Chandra M. Nautiyal
Bartlesville Project Office

Reporting Period: Apr. 1–June 30, 1990

Objective

The objective of this project is to provide research support to the Department of Energy (DOE) Project Manager for the Tertiary Oil Recovery Information System (TORIS) in the areas of enhanced oil recovery (EOR) project and reservoir database management, the EOR project and technology trend analysis, and oil production modeling.

Summary of Technical Progress

The biennial survey of the *Oil & Gas Journal* and other sources of EOR project data were correlated to the project database to identify previously unentered projects. The declining trend in EOR projects appears to have ended in 1988; the number of projects in 1989 now identified is greater than that starting in 1988 and roughly the same as that starting in 1987. Table 1 shows the data on 47 projects that will be added to the DOE EOR project databases. A complete analysis of trends in EOR projects will be reported in the next quarterly report.

TABLE 1

EOR Projects Identified for Addition to the DOE EOR Databases

State	Field name	Operator	Start date	Process	Area, acres	Reservoir formation	Prod. wells	Inj. wells	Lith.*	Depth, ft	Porosity, %	Permeability, mD	Temp., °F	Gravity, °API
Calif.	Midwest-Sunset	ARCO (Tenneco)	4/84	Conv Steam	25	Potter	24	2	Sand	1,600	34.0	4,000	95	11.5
Calif.	Midwest-Sunset	ARCO (Tenneco)	1983	Conv Steam	34	L. Monarch	13	2	Sand	1,500	30.0	2,000	100	13.0
Calif.	Midwest-Sunset	ARCO	6/89	Conv Steam	24	Potter	42	6	Sand	1,850	34.0	2,854	95	11.5
Calif.	Cymric	Chevron	10/89	Conv Steam	30	Tulare	31	19	Sand	1,200	33.0	2,900	100	12.0
Calif.	McKittrick	Chevron	8/83	Conv Steam	17	Tulare	21	8	Sand	850	36.0	2,000	140	11.4
Calif.	McKittrick	Chevron	6/87	Conv Steam	70	Amnicola	25	14	Sand	1,100	37.0	1,500		12.0
Calif.	McKittrick	Chevron	4/85	Conv Steam	30	Tulare/Amnicola	29	18	Sand	1,300	36.0	2,900	100	13.0
Calif.	Coalinga	Chevron	2/82	Conv Steam	43	Temblor	38	10	Sand	1,600	33.0	2,400	100	13.0
Calif.	Coalinga	Chevron	7/84	Conv Steam	60	Temblor	40	12	Sand	1,500	33.0	2,400	100	13.0
Calif.	Coalinga	Chevron	3/89	Conv Steam	100	Temblor	70	21	Sand	1,700	33.0	2,300	100	13.0
Calif.	Mount Poso	McPherson Oil	5/89	Conv Steam	240	Vedder	40	3	Sand	2,500	35.0	2,000	105	17.0
La.	Bayou Bleu	Mobil	5/88	Conv Steam	120	Rasua (E.B. Schwing)	26	7	Sand	1,550	30.0	4,000	100	16.0
Okla.	Sho-Vel-Tum	Mobil	11/86	Conv Steam	55	Deese	7	7	Sand	1,500	26.5	875	85	16.0
Calif.	Midway-Sunset	Oryx	2/88	Conv Steam	90	Marvic	18	4	Sand	1,200	34.0	1,000	104	13.0
Calif.	Coalinga	Santa Fe	10/89	Conv Steam	20	Upper Temblor	23	4	Sand	1,300	30.0	3,000	75	14.5
Calif.	Coalinga	Santa Fe	10/89	Conv Steam	20	Lower Temblor	14	6	Sand	1,600	30.0	3,000	75	14.5
Calif.	Kern River	Santa Fe	9/89	Conv Steam	20	Kern River Series	31	8	Sand	600	30.0	3,000	85	13.0
Calif.	Kern River	Shell	9/83	Conv Steam	85	Kern River Series	35	35	Sand	1,200	31.0	2,000	81	12.0
Calif.	Midway-Sunset	Shell	1/89	Conv Steam	5	San Joaquin	8	2	Sand	1,200	33.0	2,000	95	12.0
Calif.	Midway-Sunset	Shell	1/89	Conv Steam	68	Lower	76	10	Sand	800	25.0	2,000	90	11.6
Calif.	Midway-Sunset	Texaco	1/89	Conv Steam	38	Potter	62	11	Sand	1,600	36.0	3,000	90	14.0
Tex.	Sour Lake	Texaco	1/86	Conv Steam	6	Miocene OB-2	4	2	Sand	1,900	33.0	1,000	106	13.6
Tex.	Sour Lake	Texaco	7/89	Conv Steam	74	Miocene OB-3	13	2	Sand	1,350	33.0	5,181	100	17.0
Tex.	Sour Lake	Texaco	10/87	Conv Steam	4	Miocene 700 ft	6	2	Sand	1,425	33.0	1,000	100	14.5
Calif.	Wilmington	Union Pacific Res.	4/89	Conv Steam	85	Tar	38	27	Sand	2,563	30.0	2,780	123	14.0
Tex.	Corsicana	Koch Exploration	1990	In Situ	20						32.0			
Calif.	Midway-Sunset	Texaco	3/87	Hot Water	10	Potter	16	6	Sand	1,600	35.0	2,000	200	12.0
Tex.	Cowden North	Amoco	6/85	CO_2 Mis	12	Grayburg	2	6	Dolo	4,300	10.0	5	94	34.0
Wyo.	Lost Soldier	Amoco	5/89	CO_2 Mis	1345	Tensleep	49	66	Sand	5,000	9.9	31	178	35.0
Wyo.	Lost Soldier	Amoco	5/89	CO_2 Mis	790	Darwin-Madison	31	33	S/LS	5,400	10.3	4	181	35.0
Tex.	Wasson	ARCO	1/86	CO_2 Mis	8000	San Andres	286	225	Dolo	5,100	9.0	1	110	32.0
Tex.	Ward Estes North	Chevron	3/89	CO_2 Mis	3840	Yates	190	194	Sand	2,600	16.0	37	83	35.0
N. Mex.	Maljamar	Conoco	1/89	CO_2 Mis	1200	Grayburg-San Andres	70	15	Dolo	4,200	10.8	5	95	37.0
Tex.	Slaughter	Mobil	6/89	CO_2 Mis	2495	San Andres	79	46	Dolo	5,000	10.3	3	107	32.0
N. Mex.	Maljamar	Phillips Pet.	11/89	CO_2 Mis	40	Grayburg	4	1	Dolo	4,600	6.0		101	36.0
Tex.	Crossett South	Shell	6/88	CO_2 Mis	800	Devonian	21	10	Tripol	5,200	21.0	4	104	43.0
La.	Weeks Island	Shell	1/88	CO_2 Im	480	S Res A	18	6	Sand	14,100	23.0	4,000	242	33.0
La.	Weeks Island	Shell	1/88	CO_2 Im	908	R Res A	8	2	Sand	13,200	23.0	1,500	241	34.0
Alaska	Kuparuk River	ARCO	6/88	HC Mis	5120	Kuparuk A&C	30	20		5,900	25.0	1,000		
Wyo.	Buck Draw	Kerr-McGee	12/88	HC Mis	5700	Dakota	11	8	Sand	12,450	9.3	3	282	46.0
Tex.	Hawkins	Exxon	8/87	Flue Gas	2800	Woodbine	100	6	Sand	4,600	28.0	3,400	168	24.0
Kans.	LaCygne-Cadmus	Troutman Oil	1979	Flue Gas	225	Peru	48	48	Sand	300	19.0	35	78	29.0
Wyo.	Hamilton Dome	ARCO	9/89	Polymer	80	Tensleep	7	1	Sand	2,750	14.0	58	135	20.0
Wyo.	Teapot Dome	John E Brown	8/88	Microbial	188	Shannon	24	2	Sand	350	18.0	650	65	35.0
Wyo.	Ottie Draw	Jade Resources	1990	Polymer		Minnelusa B			Sand	7,700	14.0	700	154	30.0
Tex.	Jones Co Regular	Cuatro Oil & Gas	4/90	Polymer		Bluff Creek		3	Sand	1,710	16.4	61	87	37.0
Wyo.	Summerfield	Woods Petroleum	3/90	Polymer		Minnelusa B	3	1	Sand	9,480	15.0	114	182	20.3

*S, sandstone; LS, limestone; Tripol, tripolite; Sand, sandstone; and Dolo, Dolomite.

RESERVOIR ASSESSMENT AND CHARACTERIZATION

Cooperative Agreement DE-FC22-83FE60149, Project BE1

National Institute for Petroleum and Energy Research
Bartlesville, Okla.

Contract Date: Oct. 1, 1985
Anticipated Completion: Sept. 30, 1990
Funding for FY 1990: $800,000

Principal Investigator:
Matt Honarpour

Project Manager:
Edith Allison
Bartlesville Project Office

Reporting Period: Apr. 1–June 30, 1990

Objective

The objective of this project is to develop an improved methodology for effective characterization of barrier island reservoirs to predict oil saturations at interwell scales and flow patterns of injected and produced fluids.

Summary of Technical Progress

Integration of Wireline Logs with Outcrop Core Data for Evaluation of Sandstone Characteristics

The induction, spontaneous potential (SP), gamma-ray, and density logs available from two wells drilled behind outcrops of the Almond formation in the Rock Springs, Wyoming, area are being interpreted to determine the characteristics of sandstones deposited under different environmental conditions in the area. From interpretations of trace fossils, sedimentary structures, sand size distribution, and polymorphs in the core samples, the depositional environment of the different sandstones in the two cored wells was interpreted.[1] Information from wireline log responses is being integrated with the geological information to determine the fluid flow characteristics and the geological heterogeneities of the different types of sandstones.

The sandstones encountered in the two outcrop wells were deposited under a wide variety of depositional environments,[2] such as fluvial, distributary channel, tidal flat and tidal channel, shallow marine barrier island, and beach. Sandstones from each environment were analyzed with gamma-ray, density, and induction log data. Because of freshwater penetration, the SP logs for most parts in the two wells were featureless. The results of analysis of seven sandstones encountered in corehole No. 2 are shown in Table 1. The depositional environments of these sandstones are known from geological studies.[1] The mean and standard

TABLE 1

Characteristics of Sands Encountered in Corehole No. 2 Deposited Under Different Environmental Conditions

Depth of sand, ft	Depositional environment from geological studies	Clay content in sandstone*		Porosity of sandstone†		Grain size distribution‡	
		Mean, %	S.D.§	Mean, %	S.D.	Mean, μm	Range, μm
56 to 90	Distributary channel	3.85	3.87	23.30	1.81	225	150 to 300
149 to 163	Shallow marine, interpreted as upper shoreface	15.23	3.50	22.19	1.50	135	100 to 200
184 to 236	Barrier beach	9.08	6.93	26.41	3.12	250	125 to 350
246 to 267	Marine, upper shoreface	175.00	2.98	21.19	1.63	170	125 to 200
282 to 297	Tidal channel	7.54	6.29	11.44	4.30	254	125 to 300
346 to 364	Marine, interpreted as upper shoreface or delta mouth bar	14.50	3.08	18.50	1.98	179	135 to 275
507 to 514	Fluvial channel	7.04	6.15	17.52	1.73	–	–

*Calculated from gamma-ray logs, so the effect of potassium-deficient kaolinite clays will be practically absent.
†Calculated from density logs.
‡From visual examination of cores.
§S.D., standard deviation.

deviations of vertical distribution of clay content and porosity of the different sandstones calculated from gamma-ray and density logs are shown in Table 1. Since gamma rays do not respond to potassium-deficient kaolinite clay, the clay figures will not reflect the presence of kaolinite. The vertical distribution of grain sizes from which the mean and the range were calculated was obtained from visual examination of cores.

The barrier beach seems to have the highest average porosity and the tidal channel the lowest (Table 1). The grain sizes and clay content in these two sandstones are quite similar; therefore the significantly higher average porosity in the beach sand must be attributed to better sorting of grain sizes in this sandstone. All the marine sandstones in this area show high clay content compared with other current dominated sandstones, and since these sandstones also have appreciable porosities, it must be concluded that the grain-size sorting in these sandstones is fairly good. The significantly larger spread (high standard deviation) in the clay content and porosity in the barrier beach sandstone is the result of the large range in particle size distribution (125 to 350 μ) for this sandstone. The smallest average particle size was encountered in the marine sandstones, and the largest was found in the current dominated channel sandstones and the beach deposit. The large grain sizes of the channel sands in this area should make these sandstones highly permeable compared with the marine sandstones studied in this corehole.

Comparison of Facies Distribution and Petrophysical Properties of Sandstones at Patrick Draw and Bell Creek Fields

The producing Muddy sandstones in Bell Creek (Montana) field are primarily shallow marine barrier island and nonbarrier valley-fill deposits. A method to distinguish the dominant facies of the Muddy sandstones with a cross-plot technique was previously discussed.[3] Calculated porosities from density logs were plotted against deep resistivity (from induction log) and gamma rays for a number of sandstones to determine if the shallow marine sandstones from the two outcrop wells also have similar facies distribution in the two cross plots (porosity vs. resistivity and porosity vs. gamma ray).[1] Figures 1 and 2 show the two cross plots for the shallow marine sandstone at a depth of 140 ft from outcrop corehole No. 1. Clear separation of the upper and lower shoreface facies is indicated in the two cross plots, as in the case of Bell Creek field. The cross plot of porosity and resistivity for well No. W-4 from Bell Creek field is shown in Fig. 3 for comparison.

Cross plots for sandstones from other environments were also constructed, but the porosity, resistivity, and gamma-ray values for these sandstones were observed to have a higher spread (large standard deviations) compared with those from the shallow marine environments, which is a

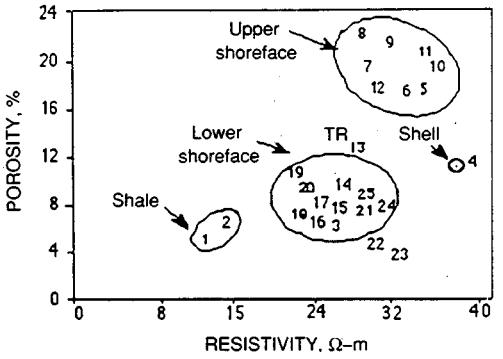

Fig. 1 Depth sequential cross plot of resistivity and porosity to distinguish various facies in the 140-ft sand in corehole No. 1 in the Almond formation.

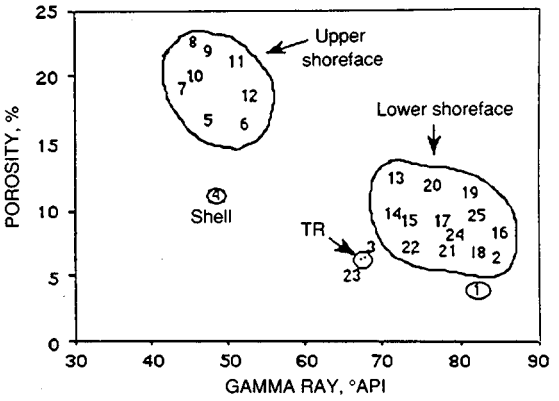

Fig. 2 Depth sequential cross plot of gamma ray and porosity to distinguish various facies in the 140-ft sand in corehole No. 1 in the Almond formation.

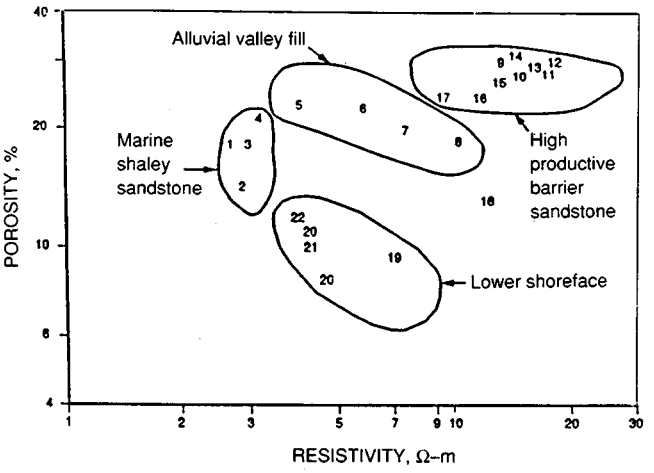

Fig. 3 Depth sequential cross plot of resistivity and porosity to distinguish various sandstone facies in well W-4 from Bell Creek (Montana) field.

consequence of the processes involved in the deposition of the different sandbodies.

Application of Differential Oil in Place To Quantify the Effect of Geological Heterogeneities on Oil Production

The differential oil-in-place (DOIP) map for sections 22, 23, 26, 27, and 28 of Bell Creek field[4] prepared previously from data from 44 wells was updated by adding data from 11 more wells (Fig. 4). A well DOIP is defined by the equation

DOIP = volumetric OIP based on a given spacing

– material balance equation OIP

The updated DOIP map was overlaid on 32 selected maps showing variations in the study area in pertinent geological and petrophysical properties or engineering data, such as structural anomaly; clay content; porosity; permeability; Dykstra–Parsons coefficient; log-derived heterogeneity index (LHI); and primary, secondary, and tertiary oil production. The purpose of this overlay was to determine whether there is any relationship between the distribution of DOIP values and the superimposed variables. Preliminary analyses of the overlays indicated some correlations between structural anomalies, clay content, LHI,[5] and the distribution of DOIP values.

For example, the linear features from the structural contour map were transferred onto the DOIP map (Fig. 4) to determine if the linear structural features on the structural contour map constructed on the top of the Muddy barrier island sandstones in the study area[5] have in any way contributed to anomalies observed in the distribution of DOIP. From detailed construction of stratigraphic cross sections,[3] it appears that linear feature No. 1 (LF1) indicated in Fig. 4 is a deep valley incision that has contributed to NW-SE trending positive DOIP anomalies. Other linear features (LF2, LF3, LF4, LF5, LF6, and LF7) are believed to be faults, some of which are partially sealing, whereas

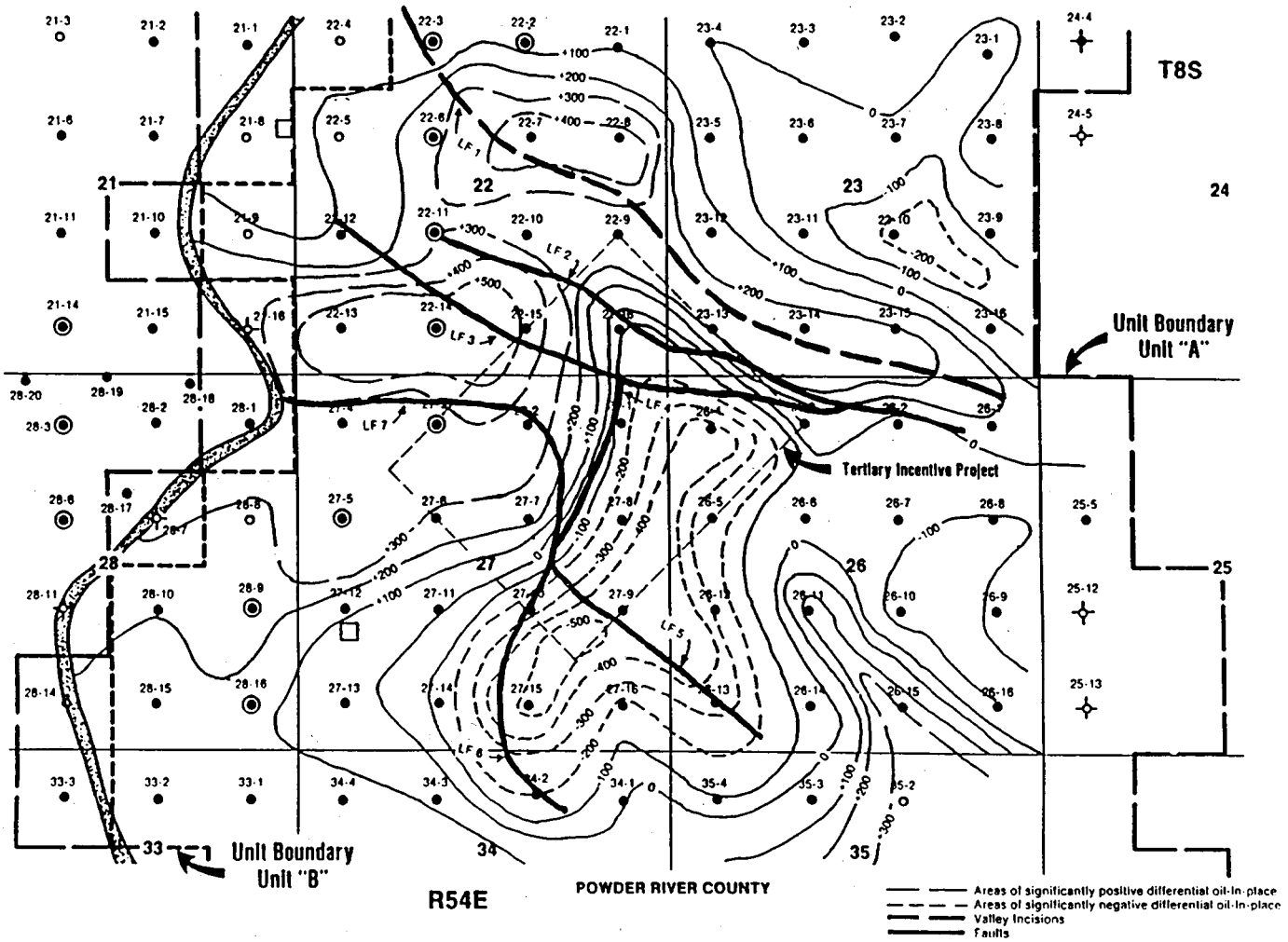

Fig. 4 Differential oil-in-place map for four-section area in Bell Creek field. Locations of structural features in the figure were obtained from structural[5] and stratigraphic[3] interpretations of the area. Contours are in thousands of barrels of oil differential between material balance equation and volumetric methods of oil-in-place calculations.

others are conducting. For example, LF2, LF3, LF4, and LF7 are believed to be at least partially sealing because contours of primary and waterflood oil production data and the distribution of reservoir properties, such as porosity, permeability, clay content, etc., sharply swing around these features. LF5 and LF6 are believed to be conducting faults and seem to be the primary reason for the good drainage efficiency and the maximum negative DOIP observed in the eastern half of section 27 and the western half of section 26 (Fig. 4). Conductivity as a result of faults in this area is apparently augmented by the low clay content in sandstones from this area.[5] In a faulted area such as this, there will be many more smaller faults or fractures which are difficult to identify but which, nevertheless, will contribute to improved drainage of the area. The nonsealing nature of some of the NW-SE trending faults is indicated from analysis of injection and production data with Hall plots.[4]

The highly positive DOIP in certain parts of the study area (for example, the western part of sections 27 and 22) coincides with areas having a high degree of clay content or areas having a greater thickness of low-permeability, valley-fill sediments. The poor drainage efficiency of the clay-filled western part of the study area is not improved by the presence of faults, which, as previously discussed, are believed to be partially sealing.

The overlay of the DOIP map on the LHI map shows good correlation between DOIP and LHI. Therefore a DOIP parameter for all the wells in an oil field may be used as an independent reservoir heterogeneity index for characterizing reservoirs.

Mineralogical Composition of the Almond Formation

Upper Almond sandstones contain between about 13 and 25 wt % clay minerals (Table 2). Mean clay-mineral compositions in the less than 2-μm (clay size) fraction show that kaolinite is the most abundant clay within the shallower reservoir sandstones. Kaolinite abundance decreases with increasing depth (Table 3) and is rare to absent in reservoir sandstones below 9000 ft (Ref. 6). Small amounts of chlorite were detected in Almond shales, but none was detected in any sandstone samples.[6] Illite dominates the clay size fraction below 9000 ft and includes discrete illite and interstratified illite/smectite. Illite/smectite contains less than 25% expanded layers.[6] Little smectite is found in either the upper Almond formation sandstones or in the shales. These characteristics of the clay composition indicated that even the shallowest upper Almond formation reservoir rocks, now at depths of approximately 4500 ft, may have been buried to depths where the temperature exceeded 212°F or may have experienced a heating event.[6]

Four additional core samples from Patrick Draw field have been analyzed by X-ray diffraction. The results (Table 4) tend to support the results of Keighin et al.[6] in that quartz is the dominant mineral except in sample 45-14-3 (50 ft), which was from an oyster rubble bed. K-feldspar is dominant over plagioclase, kaolinite is the dominant clay mineral, and illite and mixed-layer illite/smectite are present.

TABLE 2

Range and Mean of Whole-Rock X-Ray-Diffraction Analyses of 46 Sandstone and 30 Shale Samples from the Upper Almond Formation*

	Shallow core samples (4,500 to 7,500 ft), %		Deep core samples (9,600 to 13,700 ft), %	
	Sandstone	Shale	Sandstone	Shale
Quartz				
range	25 to 81	22 to 52	38 to 91	22 to 43
mean	57	37	67	33
Clay				
range	13 to 25	44 to 67	3 to 26	47 to 72
mean	18	51	18	59
Carbonates				
range	0 to 55	0 to 19	0 to 42	0 to 31
mean	20	10	12	5
calcite	8	2	3	<1
dolomite	4	5	3	3
ankerite	8	<1	6	<1
siderite	–	<1	<1	1
Feldspar				
range	0 to 15	2 to 5	0 to 12	1 to 6
mean	5	3	3	3
Pyrite				
mean	–	2	–	2

*From C. W. Keighin, B. E. Law, and R. M. Pollastro, Petrology and Reservoir Characteristics of the Almond Formation, Greater Green River Basin, Wyoming, in *Petrogenesis and Petrophysics of Selected Sandstone Reservoirs of the Rocky Mountain Region*, E. B. Coalson et al. (Eds.), pp. 281-298, The Rocky Mountain Association of Geologists, 1989.

TABLE 3

Mean Clay-Mineral Compositions of Sandstone and Shale from the Upper Almond Formation as Determined by X-Ray Diffraction*

	Shallow core samples (4,500 to 7,500 ft), %		Deep core samples (9,600 to 13,700 ft), %	
	Sandstone	Shale	Sandstone	Shale
Illite	23	36	44	41
Illite/smectite	30	48	51	47
Kaolinite	47	14	5	9
Chlorite	0	2	0	3

*From C. W. Keighin, B. E. Law, and R. M. Pollastro, Petrology and Reservoir Characteristics of the Almond Formation, Greater Green River Basin, Wyoming, in *Petrogenesis and Petrophysics of Selected Sandstone Reservoirs of the Rocky Mountain Region*, E. B. Coalson et al. (Eds.), pp. 281-298, The Rocky Mountain Association of Geologists, 1989.

TABLE 4

Whole Rock X-Ray-Diffraction Analysis for Samples from Patrick Draw Upper Almond Formation Core Samples

Well	Depth, ft	X-ray diffraction, wt %										
		Quartz	Plagioclase	K feldspar	Calcite	Dolomite	Ferroan dolomite	Siderite	Pyrite	Kaolinite	Illite/mica	Illite/ smectite
7-18-1*	4945	61	4	4	3		21		3	3	1	tr
45-14-3†	4450	5		tr‡	93		tr			2	tr	tr
49-1-3§	4515	69		2	1	10	15		1	1	1	tr
74-14-6¶	4305	78	2	3	5	5	tr	2	1	2	2	tr

*Tightly cemented, cross-laminated sandstone.
†Oyster rubble in silty fine sandstone.
‡tr, trace.
§Faintly cross-laminated fine sandstone..
¶Ripple-laminated sandstone and interbedded mudstone.

Excluding the sample from an oyster bed, calcite comprises less than 5 wt % of the samples; however, combined dolomite and ferroan dolomite comprise up to 25% in one sample. Total carbonate content ranges from 12 to 93 wt % of the samples and is dominated by ferroan dolomite. The amount of dolomite from samples listed in Table 4 is much greater than that indicated by Keighin et al.[6] The greatest amount of dolomite plus ankerite (ferroan dolomite) reported by Keighin et al. was only 12%, although the greatest amount of total carbonate was 20 wt %, which is in line with most of the values in the Patrick Draw samples (Table 4).

Petrographic analyses of Almond formation outcrop thin sections by Pryor[7] indicate a similar mineralogical composition compared with analyses by Keighin et al.[6] Point-count analysis by Pryor indicates an immature chert arenite composition. Twenty-nine Almond reservoir samples examined by Thomas[8] were classified as quartz arenite; however, chert and other quartzose rock fragments were plotted on the same pole of a sandstone composition classification diagram. If corrections for rock fragments were taken into account, the samples from Thomas[8] would plot in the sublitharenite to chert arenite range of the classification scheme of Folk.[9]

Petrographic analyses of eight thin sections of Almond formation sandstone from cores from Patrick Draw field indicate dominantly feldspathic litharenite, chert arenite, and sublitharenite compositions (Fig. 5). In only one case was feldspar more abundant than rock fragments; this resulted in a lithic arkose composition. The dominant lithic fragments include chert and other sedimentary rock fragments, although metamorphic and even sparse volcanic rock fragments were identified. During these analyses, the original (unaltered) grain types were interpreted to ensure that original (syndepositional) rock composition was recorded.

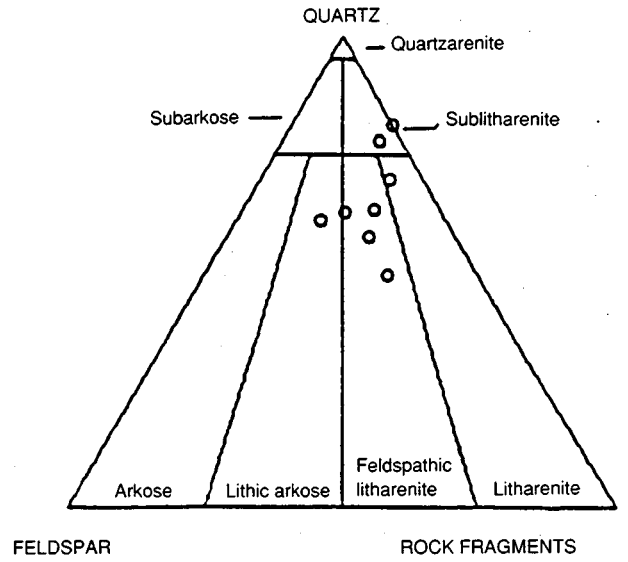

Fig. 5 Quartz–feldspar–rock fragment composition and rock type classification[9] for thin-section samples from the Almond formation at Patrick Draw field.

Diagenesis of Almond Reservoir Rocks

The diagenetic history of the Almond marine reservoirs is complex. Keighin et al.[6] distinguished nine stages in their evaluation. Quartz overgrowths on detrital quartz grains were found in all the samples they examined. Most quartz overgrowths precipitated early in the paragenetic sequence; however, some were found to reduce porosity within secondary pores. From 5 to 15% of the primary porosity in upper Almond formation sandstones has been filled by silica cement. The diagenetic sequence for upper Almond sandstones proposed by Thomas[8] is somewhat more simplified; however, it is in very close agreement with the scheme presented by Keighin et al.[6]

Much of the porosity in the Almond sandstones at Patrick Draw field has been created by the dissolution of mineral grains and cement. Most intragranular and moldic porosity was formed by dissolution of feldspars, chert, and shale rock fragments. Because the reservoir sandstones generally contain a significant amount of leached feldspar and easily decomposed rock fragments (such as chert and shale), these components also make the reservoir rock sensitive to compaction and a consequent decrease in porosity and permeability.

In addition, 13 to 81% (average 58%) of all feldspar examined in Almond formation sandstone from Patrick Draw field is altered or completely replaced, most commonly by kaolinite. Frequently, altered margins or entire feldspar grains are partly leached; this results in a complex maze of secondary microporosity but contributes little to permeability.

Ferroan dolomite is the most common cement in the more permeable Almond formation sandstones examined. Dolomite locally replaces calcite and quartz and has also been identified as syntaxial overgrowths on prior dolomite and calcite.

Clay minerals play an important role in the development of reservoir quality. Partial dissolution and replacement of feldspar and rock fragments by clays created microporosity but did not significantly contribute to permeability. The habit and distribution of clays within the pore system indicate that the reservoir should be sensitive to migration of fines.[10] Cementation and replacement of detrital chert, quartz grains, shale rock fragments, and clay matrix by kaolinite is extensive in examined sandstones from the upper Almond formation at Patrick Draw field.

References

1. W. C. Meyers, *Environmental Analysis of Almond Formation (Upper Cretaceous) from the Rock Springs Uplift, Wyoming*, Ph.D. thesis, University of Tulsa, Okla., 1977.
2. D. G. McCubbin and M. J. Brady, Depositional Environment of the Almond Reservoirs, Patrick Draw Field, Wyoming, *Mt. Geol.*, 6: 3-26 (1969).
3. B. Sharma, M. M. Honarpour, S. J. Jackson, R. A. Schatzinger, and L. Tomutsa, *Determining the Productivity of a Barrier Island Sandstone Deposit from Integrated Facies Analysis Based on Log and Core Data and Fluid Production*, paper SPE 19584, presented at the Society of Petroleum Engineers 64th Annual Technical Conference and Exhibit, San Antonio, Tex., Oct. 8–11, 1989.
4. National Institute for Petroleum and Energy Research, *Quarterly Technical Report for January 1–March 31, 1990*, DOE Report NIPER-470, Vol. 2, 1990.
5. B. Sharma, M. M. Honarpour, M. J. Szpakiewicz, and R. A. Schatzinger, Critical Heterogeneities in a Barrier Island Deposit and Their Influence on Various Recovery Processes, *SPE Formation Evaluation*, 5(1) (March 14, 1990).
6. C. W. Keighin, B. E. Law, and R. M. Pollastro, Petrology and Reservoir Characteristics of the Almond Formation, Greater Green River Basin, Wyoming, in *Petrogenesis and Petrophysics of Selected Sandstone Reservoirs of the Rocky Mountain Region*, E. B. Coalson et al., (Eds.), pp. 281-298, The Rocky Mountain Association of Geologists, 1989.
7. W. A. Pryor, Petrography of Mesaverde Sandstones in Wyoming, *Guideb. Wyo. Geol. Assoc., 16th Annu. Field Conf.*, 34-46 (1961).
8. J. B. Thomas, Diagenetic Sequences in Low-Permeability Argillaceous Sandstones, *J. Geol. Soc., London*, 135: 93-99 (1978).
9. R. L. Folk, *Petrology of Sedimentary Rocks*, p. 124, Hemphills, Austin, Tex., 1968.
10. A. Priisholm, B. L. Nielson, and O. Haslund, Fines Migration, Blocking, and Clay Swelling of Potential Geothermal Sandstone Reservoirs, Denmark, *SPE Formation Evaluation*, 2:168-178 (1987).

ENHANCED OIL RECOVERY INCENTIVE PROJECTS SURVEY

Cooperative Agreement DE-FC22-83FE60149, Project SGP30

National Institute for Petroleum and Energy Research
Bartlesville, Okla.

Contract Date: Aug. 18, 1989
Anticipated Completion: Sept. 30, 1990
Funding for FY 1990: $25,000

Principal Investigator:
James F. Pautz

Project Manager:
Chandra M. Nautiyal
Bartlesville Project Office

Reporting Period: Apr. 1–June 30, 1990

Objective

The objective of this project is to solicit completed FE-748 forms for active incentive projects for calendar years 1987 and 1988. The data are to be reduced to an electronic medium and validated.

Summary of Technical Progress

The Department of Energy encouraged oil companies and operators to undertake enhanced oil recovery (EOR) projects through an incentive program from 1979 to 1980. Those companies and operators which received an incentive are asked to submit an annual report. Initially, the companies were required to certify the projects as true EOR operations. A total of 423 certifications were received. When the Annual Report for EOR Incentive Programs details was published, the annual report requirements were defined as voluntary. Each year since 1982, operators have been

requested to return a completed "Annual Report for Enhanced Oil Recovery Incentive Program," form FE-748. At present, many of the original projects have been terminated, completed, changed, combined with other projects, were never started, or are not reporting. For the 1986 reporting year, information was obtained on 150 projects. The information from these annual reports is used to maintain the EOR Project databases used by the Bartlesville Project Office.

At the end of 1986, 133 projects were still being tracked. Since the start of the project, five additional projects have been added for a total of 138 projects. Table 1 summarizes the status of these projects and the progress made on completing the survey. Telephone contact has been made with the majority of the 24 operators with projects active in 1988 but not reported.

TABLE 1

Status of the Enhanced Oil Recovery Projects and of the FE-748 Survey for 1987 and 1988

	Status as of 1987	Status as of 1988
Active project and form FE-748 returned	78	63
Terminated project	28	31
Combined project	1	4
Canceled project	2	2
Deferred project	13	13
Refused to reply	1	1
No report to date	15	24
Total being tracked	138	138

RESERVOIR CHARACTERIZATION AND ENHANCED OIL RECOVERY RESEARCH

Contract No. DE-FG22-89BC14251

University of Texas at Austin
Austin, Tex.

Contract Date: Sept. 1, 1989
Anticipated Completion: Aug. 31, 1990
Government Award: $580,000
(Current year)

Principal Investigators:
Gary A. Pope
Larry W. Lake
Robert S. Schechter

Project Manager:
Jerry F. Casteel
Bartlesville Project Office

Reporting Period: Apr. 1–June 30, 1990

Objective

The objective of this project is to increase the understanding of enhanced oil recovery (EOR) processes as they relate to realistic reservoir settings for increased efficiencies and decreased risks in known reservoirs in Texas. The primary activities include:

1. Systematic reservoir characterizations.
2. Modeling and scaleup of chemical flooding techniques.
3. Gaining a broader understanding and providing fundamental information on CO_2–surfactant phase behavior.

Summary of Technical Progress

Procedure for Validating Reservoir Characterization

A highly detailed simulation of fluid flow through a portion of the Page Sandstone was completed. This outcrop eolian sand was described in great detail earlier, which makes the simulation highly deterministic. One of the purposes for making such simulations was to provide a test case against which to compare alternative reservoir characterization procedures. The subject of this report is progress on creating these alternative procedures on the basis of conditional simulation.

Three realizations of the interwell distribution of permeability have been created with only data from the "wells" along the edges of the two-dimensional (2-D) panel simulated previously. The three realizations were based on (1) a spherical variogram model (case 1), (2) a fractal correlation model (log–linear variogram) (case 2), and (3) a second spherical variogram model (case 3) having a longer correlation length than case 1. The range of case 1 was taken directly from the measured data reported by Goggin;[1] the fractal dimension and well-to-well variability were also similarly measured. Case 3 was undertaken to examine the influence of arbitrarily increasing horizontal range.

All realizations were compared against the actual measured data for the entire cross section. Case 2, the fractal variogram, appears superior to the other two because it is the only realization that preserves the interwell connectivity of the stratification types and also the local variability. Case 1 is much too discontinuous and case 3 too homogeneous. These conclusions are based on visual comparisons; fluid flow is being simulated through some of the realizations for more direct comparisons. If the fractal model

proves out, it will lead to a new concept of the distribution of geologic media based on the ideas of geometric fractals.

Experience was gained with the use of conditional simulation to generate flow fields for actual subsurface reservoirs. These efforts use insights from outcrop studies and conform to actual measured data where available. Some progress was made in incorporation of the geologic interpretation of pinch-outs in these conditional simulations.

Modeling and Scaleup of Chemical Flooding

Simulation of Hydrodynamic Instabilities (Viscous Fingering) in Permeable Media

Coreflood experiments were conducted in naturally heterogeneous sandstone outcrop cores. These displacements have included both waterfloods and polymer floods and various tracers in both water and oil for both single-phase flow and two-phase, unsteady-state flow. Those involving the displacement of viscous polymer solution were unstable. The cores were characterized by air permeability measurements of each square centimeter on each face and by computerized tomography (CT) scans of cross sections of the core at 1-cm intervals along the length of the core. Simulations were then made with these characterization data as input to the simulation, and comparisons were made with the pressure, tracer, and production data from the corefloods. Longitudinal and transverse dispersivities of the initial single-phase flow displacement in brine were used as matching parameters, and these were nearly the same as those measured in homogeneous sandstones. Although small differences were observed, in general, the agreement between the experiments and simulations was good.

Polymer Coreflooding

Experiment A1 was a tertiary polymer flood conducted in Antolini sandstone (Table 1). Tertiary implies that the polymer solution was injected after the core had been waterflooded to residual oil saturation. Antolini sandstone is a heterogeneous, eolian outcrop sandstone from northern Arizona. The objective of this experiment was to measure residual oil saturation after tertiary polymer injection to determine if the polymer would mobilize any additional oil. Secondary objectives were to measure the apparent viscosity of the polymer and to measure the fluid distribution with a CT scanner. This experiment was subsequently simulated with UTCHEM (Ref. 2).

The principal segments of the experiment were air permeability measurements with the use of an air minipermeameter, CT scan, brine saturation, tracer injection, CT scan, oil injection, waterflood to residual oil saturation, tracer injection, oil injection, CT scan, waterflood to residual oil saturation, tracer injection, CT scan, polymer injection, CT scan, and water injection. The properties of the core and fluids are given in Tables 1 and 2.

TABLE 1

Experiment A1 Core Properties

Core material	Antolini sandstone
Dimensions, cm	$56.0 \times 10.2 \times 4.9$
Bulk volume, cm^3	2800
Pore volume, cm^3	426
Porosity, %	15
Brine permeability, mD	2960
Initial brine dispersivity, cm	1.3

TABLE 2

Experiment A1 Fluid Properties

Brine concentration, wt %	10.0 NaI, 0.01 ca^{2+}
Brine viscosity, cP	1.06
Brine density, g/cm^3	1.08
Brine pH	6.7
Crude oil viscosity, cP	6.8
Oil–water interfacial tension, dyne/cm	23
Polymer	Nalflo 3837 polyacrylamide
Polymer solution concentration, wt %	0.2 polymer, 10.0 NaI, 0.01 Ca^{2+}
Polymer molecular weight, g/mol	9 to 12×10^6
Polymer plateau viscosity, cP	14.5
Polymer power law exponent	0.80
Polymer power law coefficient, cP	25
Polymer screen factor	14.5
Polymer pH	6.7
Temperature, °C	23
Brine CT apparent density, mg/cm^3	2010
Oil CT apparent density, mg/cm^3	1027

Air permeability measurements were performed on four sides of the core prior to applying epoxy. A 1-cm^2 grid was drawn on the inlet and outlet faces and the two sides of the core perpendicular to the bedding planes. The grid was 4×9 for the inlet and outlet facies and 55×9 for the two sides designated A and B in Fig. 1. The bedding planes are horizontal in this figure.

Figure 2 shows air permeability contours for the sides of the core (faces A and B). The minimum and maximum air permeabilities measured for faces A and B were 42 and 1180 mD, respectively. The average air permeability of faces A and B was 521 mD.

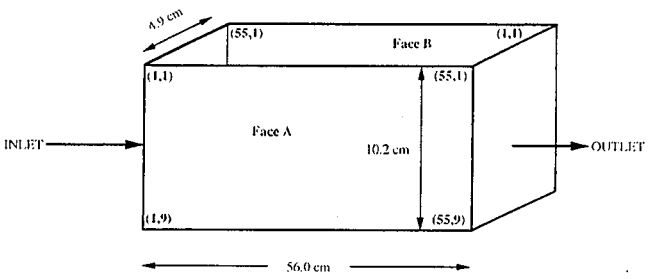

Fig. 1 Experiment A1, air permeability grid orientation for faces.

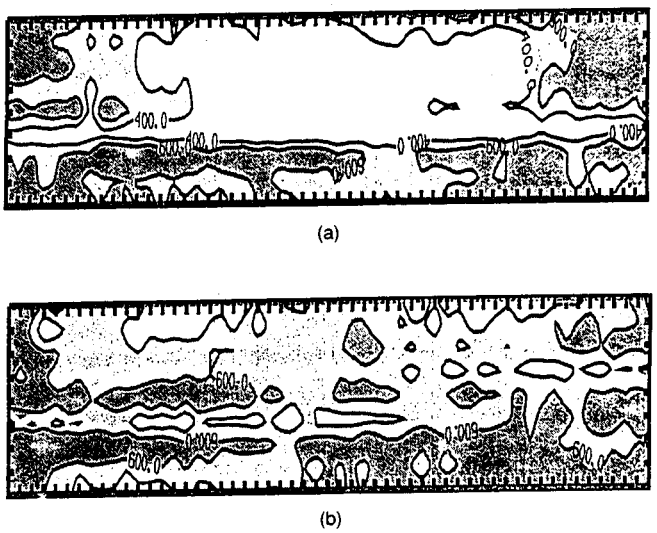

Fig. 2 Experiment A1, face A (a) and face B (b) air permeabilities.

The core was first scanned with air in the pore space. The image reconstruction was performed after the material balance porosity was known so that the dry scan porosity could be calibrated with the material balance porosity. The average porosity was found to be 0.15.

A 0.2 wt% Nalflo polymer solution was tagged with Cl^{36} tracer and injected at 0.2 cm^3/min (1.3 ft/d frontal velocity) for 1.85 pore volume (PV) and then displaced at the same rate with 1.0 PV of NaI brine tagged with tritium tracer. The tagged brine was then displaced by brine for 9.8 PV at 1.0 cm^3/min. Figure 3 is a plot of the normalized tracer concentrations. Figure 4 is a plot of the normalized polymer concentration. These curves clearly demonstrate that the water displacing the polymer was an unstable displacement. The retention of the polymer was 11 μg/g rock (7% PV at 0.2% polymer). This is very low retention.

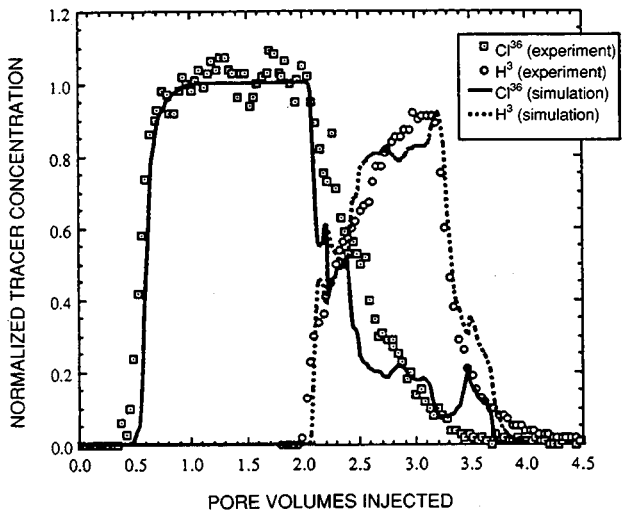

Fig. 3 Experimental and simulated tracer histories during polymer flood and brine flood.

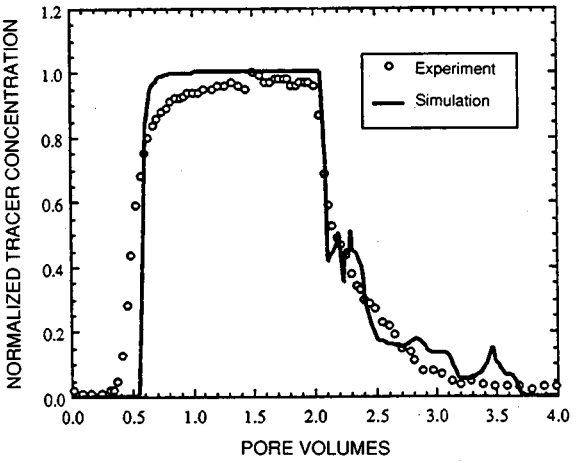

Fig. 4 Experimental and simulated polymer concentration history during polymer flood and brine flush.

Simulation of Experiment A1 Using UTCHEM

Actual experimental and physical property data were used in the simulation of experiment A1 to the maximum possible extent. The porosity and permeability of each grid block were based on the CT scanner results and the air permeabilities. A 2-D cross-sectional simulation with a grid of 56 × 1 × 10 was used. Each grid block, which was 5.1 cm wide (in the Y direction), corresponds to the 1- by 1-cm squares on the sides of the core (faces A and B). Porosity data from the CT scan were averaged over each of the core volumes corresponding to these grid blocks. The average air permeability of each square centimeter of faces A and B was used in the corresponding grid block after adjustment to make the average air permeability of the entire core agree with the average brine permeability of the core. The vertical permeabilities were estimated to be 60% of the horizontal permeabilities.

Polymer viscosity data were matched with the model used in UTCHEM, and the corresponding parameters were used in the simulation without adjustment. The shear rate coefficient was adjusted to match the pressure-drop data at steady state. The value determined this way was 44 and agrees closely with the correlation of Wreath et al.[3]

The key parameters used to history match the experimental data were the longitudinal and transverse dispersivities. These values were 0.01 ft (0.3 cm) and 0.0004 ft (0.012 cm). These experiments included both water and oil tracers under both steady- and unsteady-state conditions. Since all these data were successfully simulated with these same small values of the dispersivities, they would appear to be meaningful properties of this rock. The longitudinal dispersivity is also close to the values measured in homogeneous sandstones but is smaller than the effective value of 2.1 cm obtained from a classical probability plot of the tracer data because of the impact of the heterogeneities on the produced tracer. The heterogeneities of the Antolini

sandstone seem to have been captured rather well with the description on a 1-cm scale.

One of the most interesting features of this polymer flood is the unstable displacement of the polymer bank by the drive water. The simulation with a $56 \times 1 \times 10$ grid appears to adequately model this unstable displacement. There is a larger difference between the data and simulation at the leading polymer concentration front than at the more diffuse trailing front where the water is fingering through the polymer (Fig. 4). The simulation agrees better with the tracer data (Fig. 3) at the leading front than it does with the polymer concentration data. The reasons for this are not known but could have to do with subtle polymer properties not modeled, such as the differing behavior of polymer molecules of different molecular weight, e.g., the dependence of adsorption and inaccessible pore volume on molecular weight. Also, no attempt was made in these simulations to model the dependence of adsorption or inaccessible pore volume on permeability, although it would be easy to do so in UTCHEM. The permeability reduction factor and shear rate were modeled as functions of permeability, as previously reported in papers on UTCHEM (Ref. 2).

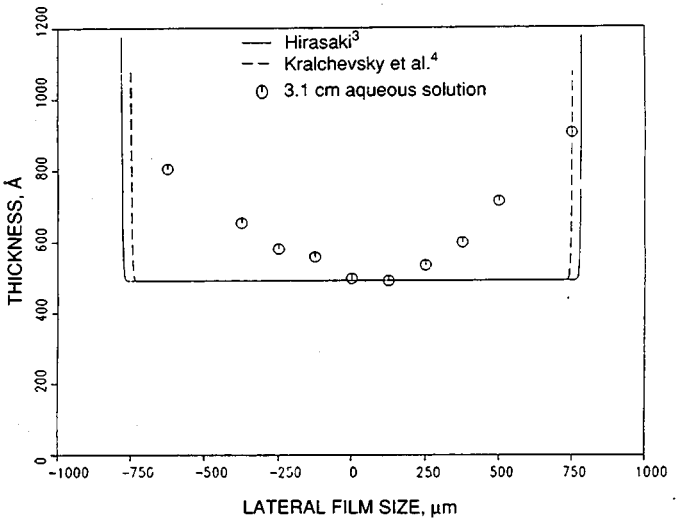

Fig. 5 Comparison of an experimentally measured interfacial profile of a 1×10^{-4} *M* KBr aqueous film in a 2-mm-diameter opening with the calculated profiles based on the constant and variable interfacial tension models using the respective perturbation values of 4.5×10^{-28} and 9×10^{-28} cm of the aqueous solution (the disjoining pressure is 3.1 cm of the aqueous solution).

CO_2–Surfactant Phase Behavior: CO_2–Surfactant–Water Interactions

Thin Films

The interfacial profile was calculated in the transition region with two methods developed separately by Hirasaki[4] and Kralchevsky et al.[5] Both methods are based on the augmented Laplace equation. The former method assumes that the interfacial tension is constant, and the latter one allows the tension to vary as dictated by the force balances at the interface. The disjoining pressure–thickness isotherm for $1 \times 10^{-4}M$ potassium bromide (KBr) was obtained by fitting the experimental measurements to the following equation:

$$\log (\Pi) = a + b \log (h) \qquad (1)$$

With this isotherm, the interfacial profile of a thin film of 489 Å equilibrium film thickness at the center was calculated numerically with the constant interfacial tension method and shown by the solid line in Fig. 5.

Moving away from the center of the film along the plane of the solid surface, the film thickness as computed increases very slowly and would not be detectable by any experimental technique. At about 750 μm from the center of the film, the film thickness increases rapidly over a small lateral distance. The shape of the profile can be generalized as having a region of near-constant thickness and a region of rapid-thickness variation. The circular symbols in Fig. 5 represent the measured film thickness of $1 \times 10^{-4}M$ KBr aqueous films in a 2-mm-diameter opening at a disjoining pressure of 3.1 cm of the aqueous solution. The deviation between the experimental data and the calculated profile is evident. A rapid increase of film thickness that takes place over a relatively small lateral distance is predicted by the theory, and this is clearly different from the small variation of film thickness over a larger lateral distance given by the measurements. Similar deviations between the experimentally measured and calculated profiles are found consistently.

The method of Kralchevsky et al.[5] was used to calculate the interfacial profile (shown by the dashed line in Fig. 5) to see if the incorporation of a variable interfacial tension would account for the differences between the experimental and calculated interfacial profiles. The profile resembles that calculated with a constant interfacial tension (shown in solid line) except for a small shift in the location of the onset of dramatic rise in thickness.

In summary, the augmented Laplace equation does not represent the finite-interfacial curvatures observed in the experiments. This raises questions regarding the validity of the augmented Laplace equation, at least in the low disjoining pressure range studied in the experiments. Attempts to use this equation to estimate thin-film properties, such as the contact angles, could lead to erroneous results.

Thermodynamics of Microemulsions

Progress has been made in modeling adsorbed alkane chains at spherical interfaces. Results show the deepest minimum in interaction energy at about 5 Å head–head

separation distance, which is characteristic of a crystalline state, and another minimum at about 7 Å head–head separation distance, which exhibits a higher entropy. This latter state is more interesting in the study of the interactions in microemulsion droplet models, since the larger separation distance is observed in microemulsion systems (roughly a 50-$Å^2$ molecular area for surfactant at the droplet interface). Once the electrostatic free energy is taken into account, the deeper minimum in energy for the crystalline-like state is unlikely to occur because of high head–head repulsive interaction energies.

Ultrafiltration experiments are currently being performed on microemulsions with the use of membranes with a fixed and uniform pore diameter of 100 Å. All microemulsions studied have a measured droplet radius larger than that of the pore, so the droplets must be squeezed to go through the pores. The flow rate required for sufficient deformation is related to the flexibility of the droplet interface; therefore the critical flow rate, at which substantial deformation of the drops begins to occur, will vary with the free energy required to bend the interface and can be predicted with the proposed model.

References

1. D. J. Goggin, M. A. Chandler, G. Kocurek, and L. W. Lake, Permeability Transects in Eolian Sands and Their Use in Generating Random Permeability Fields, SPE paper 19586, in *Proceedings of the 64th Annual Technical Conference and Exhibition of the Society of Petroleum Engineers, San Antonio, Tex., Oct. 8-11, 1989*, pp. 149-163.
2. G. A. Pope, L. W. Lake, and K. Sepehrnoori, *Modeling and Scale-up of Chemical Flooding: Third Annual and Final Report for the Period October 1987–September 1988*, DOE Report BC/10846-15, March 1990.
3. D. G. Wreath, G. A. Pope, and K. Sepehrnoori, Dependence of Polymer Apparent Viscosity on the Permeable Media and Flow Conditions, *In Situ*, 14(3) (1990).
4. G. J. Hirasaki, private communications.
5. P. A. Kralchevsky and I. B. Ivanov, The Transition Region Between a Thin Film and the Capillary Meniscus, *Chem. Phys. Lett.*, 121: 116 (1985).

MICROBIAL TECHNOLOGY

MICROBIAL ENHANCED OIL RECOVERY RESEARCH

Contract No. DE-FG07-89BC14445

University of Texas at Austin
Austin, Tex.

Contract Date: Sept. 1, 1989
Anticipated Completion: Aug. 31, 1991
Government Award: $80,650
(Current year)

Principal Investigators:
Mukul M. Sharma
George Georgiou

Project Manager:
Edith Allison
Bartlesville Project Office

Reporting Period: Apr. 1–June 30, 1990

Objective

The objective of this project is to quantify and characterize microbial enhanced oil recovery (MEOR) processes through experimentation and computer simulation of bacterial metabolic processes, microbial transport through cores, and oil recovery processes resulting from the in situ production of biosurfactants. Computer simulation will be used to evaluate injection strategies and process optimization. The research will be conducted with *Bacillus licheniformis* JF-2.

Summary of Technical Progress

This quarterly report documents progress made between Apr. 1, 1990, and June 30, 1990. The production of biosurfactant and metabolites from cultures of the microorganism *B. licheniformis* JF-2 was investigated. The results from these studies are described.

Introduction

Initial results on the effects of environmental parameters on the growth and biosurfactant production from *B. licheniformis* JF-2 were presented in a previous report. The surfactant is produced during the exponential phase of growth, and the interfacial tension (IFT) of the broth reaches a minimum right before the cells enter into stationary phase. Low IFTs were observed under both aerobic and anaerobic conditions and in cultures grown between 30 and 50°C. Optimal growth and biosurfactant production were obtained in oxygen-sparged cultures

grown at 45°C. Comparable IFT values were also obtained under anaerobic conditions with nitrate serving as the terminal electron acceptor for the catabolism of glucose. However, growth was much slower under these conditions. Optimal growth (i.e., lowest IFTs) is obtained with cells grown at a neutral or slightly acidic pH (up to pH 6.0) but not under alkaline conditions.

Growing microorganisms produce a number of products, such as polymers, organic acids, and alcohols. In the stationary environment of the oil reservoir these metabolites can accumulate in considerable amounts and thus inhibit further growth and surfactant synthesis. It is therefore important to determine the nature and amounts of metabolites produced by *B. licheniformis* JF-2 under different growth conditions. This information is needed for (1) understanding the growth and glucose utilization by the microorganisms, (2) optimizing biosurfactant production, and (3) determining the experimental parameters in the MEOR simulator described in the previous quarterly report. Furthermore, the effect of NaCl on growth and metabolite formation under aerobic and anaerobic conditions was investigated.

Materials and Methods

Batch fermentations were carried out in a 2-L Multigen fermentor (New Brunswick Scientific Co., New Brunswick, N.J.). The working volume was 1 L. The fermentor was inoculated with 25 mL of fresh culture, which was grown in medium E : 0.1% $(NH_4)_2SO_4$, 0.025% $MgSO_4$, 1% glucose in 100 m*M* phosphate buffer consisting of KH_2PO_4 and K_2HPO_4 supplemented with a 1% (vol/vol) trace salt solution. The trace salt solution contained the following (grams per liter) : ethylenediaminetetraacetic acid, 1.0; $MnSO_4$, 3.0; $FeSO_4$, 0.1; $CaCl_2$, 0.1; $CoCl_2$, 0.1; $ZnSO_4$, 0.1; $CuSO_4$, 0.01; $AlK(SO_4)_2$, 0.01; H_3BO_4, 0.01; and Na_2MoO_4, 0.01. Unless otherwise specified, the growth medium also contained 5% NaCl. The medium pH was maintained constant by the addition of 1*M* NaOH or 1*M* HCl with an external pH controller. For anaerobic growth, cultures were supplemented with 1% $NaNO_3$ as electron acceptor. Oxygen-free nitrogen (Linde National Specialty Gas Office, Somerset, N.J.) was sparged throughout the fermentation to ensure anaerobic conditions.

Bacterial concentrations were monitored by taking samples and measuring the optical density at 600 nm with Ultraspec II (LKB Biochrom Ltd., Cambridge, England) periodically. The calibration curve for the bacterial dry weight as a function of the optical density was obtained as:

Dry weight of *B. licheniformis* JF-2 per milliliter =
$0.83 \times$ optical density at 600 nm

Product Analysis

The production of biosurfactant was monitored by the decrease in the IFT between the growth medium and decane by the spinning-drop technique. Glucose concentration was determined by an enzymatic glucose analyzer (Yellow Spring Instrument Co., Inc., Yellow Springs, Ohio). A Waters high-pressure liquid chromatography (HPLC) instrument was used to analyze fermentation end products. A PRP-X300 column (7 μm; 250 × 4.1 mm inside diameter; Hamilton, Reno, Nevada) maintained at 50°C with a water bath was used for analysis. The flow rate of the mobile phase (1 m*M* sulfuric acid) was 1.5 mL/min. The elution from the column was monitored at 196 nm. Each sample was filtered with a 0.45-μm HV filter (Nihon Millipore Kogyo K.K., Yonezawa, Japan) before injection. The standard calibration curve between the peak areas and concentrations of each compound was constructed by injecting standard solutions with known concentrations. The concentrations of the fermentation end products were determined from the integration areas of the corresponding peaks.

Biosurfactant Characterization

The surfactant was isolated from the growth medium by acid precipitation following the removal of cells by centrifugation at 10,000 *g* for 10 min. For the acid-precipitation process, the fermentation medium was first acidified to pH 2.0 with concentrated HCl. The pellet, which was collected by centrifugation at 30,000 *g* for 45 min, was then extracted with methanol. Upon evaporation of the methanol, the crude biosurfactant sample was obtained.

Results and Discussion

Preliminary Characterization of the Biosurfactant

The aerobically and anaerobically produced surfactant was extracted from the growth medium by acid precipitation at a pH of 2.0 (the procedure is described in the following text). About 0.1 *g* of acid precipitate per liter of culture broth was obtained. A few milligrams of the surface-active compound were dissolved in $10^{-2}M$ NaOH and subjected to thin-layer chromatography on Bakerflex cellulose F sheets and developed in chloroform, methanol, acetic acid, and water (25:15:4:2, vol/vol). Samples obtained from either aerobic or anaerobic cultures showed the presence of a major component with an R_f value of 0.55 in each case, which suggests that the same biosurfactant was produced under aerobic and anaerobic conditions. This compound reacted with ninhydrin and rhodamine B, which indicates the presence of a free amino group and a lipid moiety. The ultraviolet spectrum of the acid precipitate showed one major absorbance peak at 226.5 nm. The biosurfactant is soluble in alkaline water and in many kinds of organic solvents, including methanol, ethanol, acetone, pentanol, ethyl acetate, chloroform, and methylene chloride, but is insoluble in acidic water and decane. Several attempts were made to purify the surfactant to near

homogeneity. In these experiments, the presence of the surfactant was determined by measuring the IFT of the sample against decane.

Knapp and coworkers[1] have suggested that the surfactant is a lipopeptide compound presumably consisting of a fatty acid esterified to a short peptide. Lipopeptide surfactants are produced by a variety of microorganisms and exhibit reasonably good surface activity. For example, surfactin, a well-characterized lipopeptide from the microorganism *Bacillus subtilis*, lowers the IFT between water and decane from 25 to approximately 0.5 mN/m. This compound is one of the most effective biosurfactants known. In contrast to previous studies, this work shows that the surface-active compound produced by the selected microorganism, *B. licheniformis*, is not a lipopeptide. The surfactant was partially purified from the fermentation broth by extraction with ethyl acetate. After the solvent had evaporated, an oily precipitate was collected and resuspended in buffer pH 7.0 with 5% NaCl. This solution gave an IFT against decane of 0.016 mN/m. *This is the lowest value ever reported for a biologically produced compound and compares favorably with the values obtained with synthetic surfactants.* The nuclear magnetic resonance (NMR) spectrum of this compound indicated that the surfactant contains fatty acid(s), a polyhydroxyl group, and an amine.

Production of Biosurfactant and Metabolic By-Products

Effect of NaCl. In MEOR, the bacterial cultures are exposed to environments of different salinities. Therefore it was important to determine how the growth and surfactant production are affected by the concentration of NaCl. The cells were grown under aerobic conditions in media supplemented with different concentrations of NaCl. Figure 1 shows the lowest IFT against decane obtained during the fermentation and the corresponding biomass concentration. Relatively low IFT values were obtained in the concentration range between 2 and 5% NaCl. High NaCl concentrations, however, cause an increase in IFT. In all the fermentations, the minimum IFT was observed in exponential phase at relatively low biomass concentrations.

Comparable results were obtained with cultures grown in the absence of oxygen. As was expected from the lower growth rates observed under these conditions, however, the minimum IFT was observed much later. The effect of initial NaCl concentration on the IFT of the fermentation broth under anaerobic conditions is shown in Fig. 2.

Metabolite Analysis. A typical metabolite profile for the aerobic fermentations is shown in Fig. 3. Although acetoin, lactic acid, acetic acid, and formic acid were all present during early growth, formic acid was the dominant metabolite for the first eleven hours of fermentation. After the eleventh hour, the formic acid concentration dropped significantly and was replaced by acetic acid and lactic acid. These last two organic acids then continued to be the

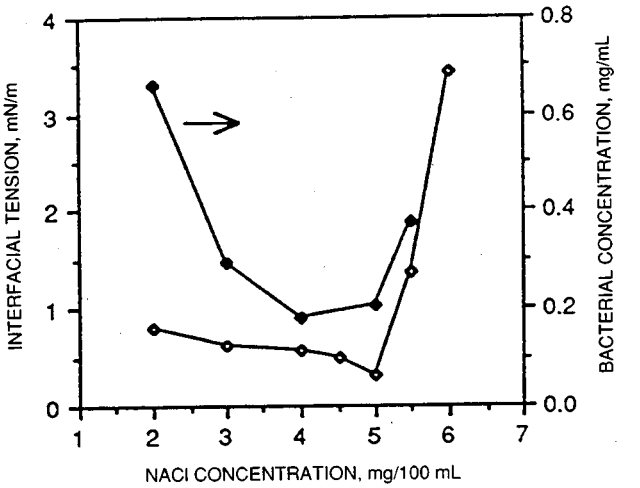

Fig. 1 Minimal interfacial tension and bacterial concentration obtained during an aerobic batch fermentation of *B. licheniformis* JF-2 as a function of NaCl concentration. Bacterial concentration was measured when the minimum value of the interfacial tension was reached. The organism was grown at 45°C in medium E supplemented with 1% glucose.

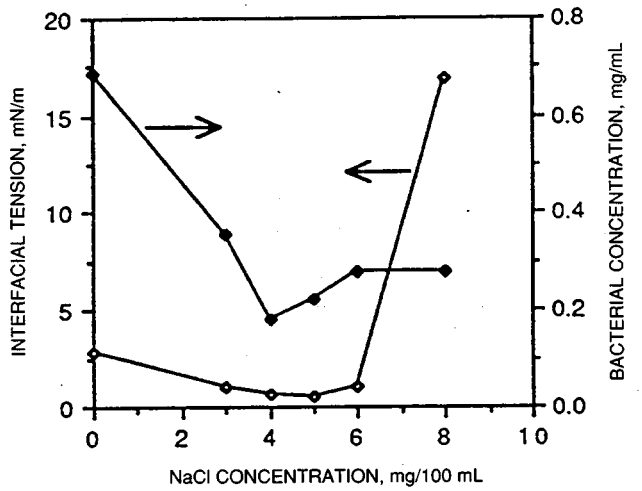

Fig. 2 Minimal interfacial tension and bacterial concentration obtained during an anaerobic batch fermentation of *B. licheniformis* JF-2 as a function of NaCl concentration of the growth medium. The bacterial concentration corresponds to the point of minimum interfacial tension. The organism was grown at 45°C in medium E supplemented with 1% glucose and 1% $NaNO_3$.

dominant metabolic products for the remainder of the fermentation. Acetic acid reached a maximum concentration of 26.4 m*M* after 24 h of fermentation, whereas lactic acid reached a maximum concentration of 17.8 m*M* after 15.75 h of fermentation. At the beginning of the fermentation, acetoin was present in small concentrations (near 2 m*M*); it was remetabolized during the period from 8 to 12 h and then was produced at higher levels. It reached a maximum concentration of 6 m*M* after 24 h of fermentation. Glucose was used at the highest rate with relatively

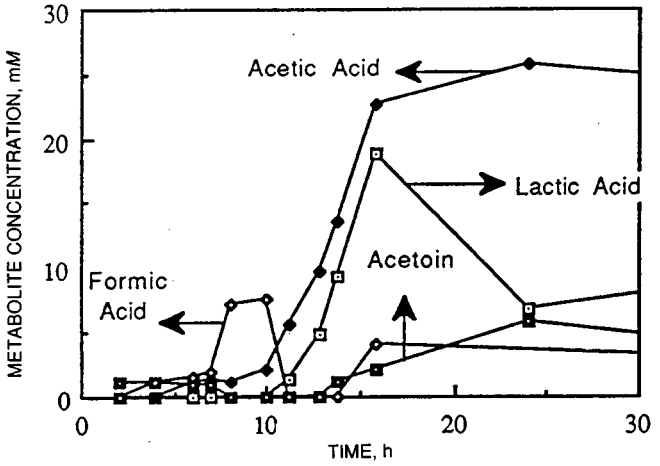

Fig. 3 Typical metabolite profile of *B. licheniformis* JF-2 grown at 45°C in a 1-L batch fermentor under aerobic conditions at constant pH of 7.0. *B. licheniformis* JF-2 was grown in medium E supplemented with 1% glucose and 4.5% NaCl.

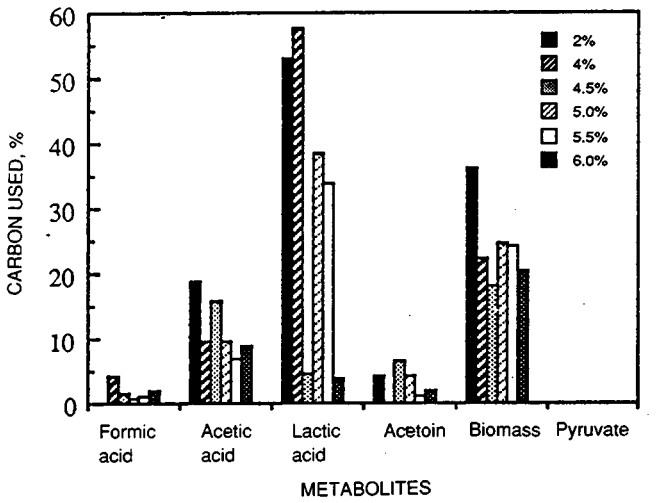

Fig. 4 Metabolites as a function of percentage of carbon used for aerobic fermentations of *B. licheniformis* JF-2 at various percentages of NaCl. Samples taken during the late stationary phase period of growth. T = 45°C and pH = 7.0 for all fermentations.

small production in biomass during the same time (8 to 15 h) that acetoin and formic acid were remetabolized (data not shown). During this same period, lactic acid and acetic acid were being produced at their highest rate. Acetoin and formic acid reappear in the growth medium later, when glucose consumption has slowed and the glucose concentration is low. Glucose was almost entirely exhausted during this fermentation; it reached a final concentration of 0.017 g/100 mL.

The carbon balance of all the metabolites measured during the aerobic fermentations is given in Fig. 4 as a function of medium NaCl content. The percentage of initial carbon that can be accounted for in metabolites and biomass varies widely, from 112% for the 2% NaCl fermentation to 40% for the 6.0% NaCl fermentation. In the presence of 2, 4, 5, and 5.5% NaCl fermentations, lactic acid was the major metabolite. Carbon dioxide production was not monitored for any of the fermentations, although literature values of CO_2 production for *B. licheniformis* in a chemostat are as high as 6 m*M*/L/h (Ref. 2).

Under anaerobic conditions, the final biomass concentration varied between 0.8 and 1.5 mg/mL. The biomass formation was slightly lower than the reported values of 1.5 mg/mL (Ref. 2) for *B. licheniformis* grown in a chemostat with 1.5 m*M* glucose/h feed rate and 3.0 mg/mL (Ref. 3) for *B. licheniformis* growth in a corn starch, 1% yeast extract, 0.2% peptone, and salts growth medium similar to those used in this study. Overall, however, the fermentation exhibited the characteristic growth patterns. A lag phase of 4 to 5 h preceded exponential growth, and a doubling time of 90 min was observed (data not shown). Although this doubling time is a little longer than the characteristic doubling time of 50 min for aerobically grown *B. licheniformis* in 15 m*M* glucose plus 0.25% peptone and 0.075% yeast extract reported elsewhere, the presence of lactic acid and acetic acid as major components is consistent with previous studies. Formic acid has also been reported elsewhere as a major fermentation product of *B. licheniformis*, although the fluctuations in formic acid concentration throughout the course of the fermentation have not been addressed.[4] Also supportive are studies on *Bacillus* reporting that the major fermentation products of *B. subtilis*, as determined in chemostat studies, are acetic acid, formic acid, lactic acid, and acetoin.[5] The presence of formate, lactate, acetate, ethanol, and CO_2 are expected in aerobic mixed acid fermentations. In addition, the presence of other metabolites was also tested. However, 2,3-butanediol, 1,3-butanediol, acetaldehyde, and ethanol could not be detected in the supernatant.

The effect of NaCl concentration on the metabolite profile is shown in Fig. 5. The amounts of metabolite and

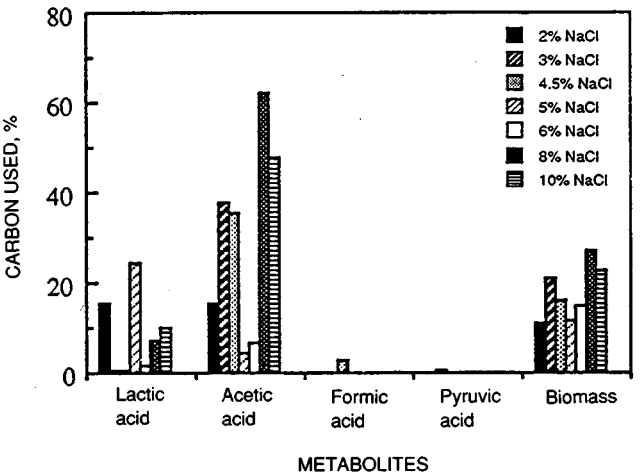

Fig. 5 Metabolites as a function of percentage of carbon used for anaerobic fermentations of *B. licheniformis* JF-2 at various percentages of NaCl. Samples were taken during the late stationary phase period of growth. T = 45°C and pH = 7.0 for all fermentations.

biomass produced are reported as the percentage of carbon used. There are large variations in the metabolism of the microorganisms under these conditions. The significance of these changes is not clear. Currently, there is little information available on the effect of high salt concentrations on the energy metabolism of bacilli. It is interesting to note, however, that the formation of lactic acid is very strongly dependent on the NaCl concentration.

References

1. M. Javaheri, G. E. Jenneman, M. J. McInerney, and R. M. Knapp, *Appl. Environ. Microbiol.*, 50: 698 (1985); G. E. Jenneman, M. J. McInerney, R. M. Knapp, J. B. Clark, J. M. Feero, D. E. Revus, and D. M. Menzie, *Dev. Ind. Microbiol.*, 24: 485 (1983).
2. J. Frankena, H. W. van Verseveld, and A. H. Stouthamer, Substrate and Energy Costs of the Production of Exocellular Enzymes by *Bacillus licheniformis*, *Biotechnol. Bioeng.*, 32: 803-812 (1988).
3. O. O. Amund and O. A. Ogunsina, Extracellular Amylase Production by Cassava-Fermenting Bacteria, *J. Ind. Microbiol.*, 2: 123-127 (1987).
4. G. W. Hanlon and N. A. Hodges, Bacitracin and Protease Production in Relation to Sporulation During Exponential Growth of *Bacillus licheniformis* on Poorly Utilized Carbon and Nitrogen Sources, *J. Bacteriol.*, 147(2): 427-431 (1981).
5. J. Snay, J. W. Jeong, and M. M. Ataai, Effects of Growth Conditions on Carbon Utilization and Organic By-Product Formation in *B. Subtilis*, *Biotechnol. Prog.*, 5(2): 63-69 (1989).

EFFECTS OF SELECTED THERMOPHILIC MICROORGANISMS ON CRUDE OILS AT ELEVATED TEMPERATURES AND PRESSURES

Contract No. DE-AC02-76CH00016

Brookhaven National Laboratory
Upton, Long Island, N.Y.

Contract Date: Mar. 1, 1989
Anticipated Completion: Sept. 30, 1990
Government Award: $155,000
(Current year)

Principal Investigators:
E. T. Premuzic
M. S. Lin

Project Manager:
Edith Allison
Bartlesville Project Office

Reporting Period: Apr. 1–June 30, 1990

Objective

The objective of this program is to determine the chemical and physical effects of thermophilic organisms on crude oils and cores at elevated temperatures and pressures. Ultimately a database will be generated that will be used in technical and economic feasibility studies leading to field application.

Summary of Technical Progress

Changes in the trace metal and sulfur content of crude oils during the biotreatment of crude oils were reported earlier.[1] Biotreatment of Wilmington (California) crude with BNL-4-22 resulted in a considerable reduction of the nickel porphyrin complex. In this analysis the gas chromatography (GC) system equipped with an Ni and V selective atomic emission detector was calibrated with nickel octaethyl porphyrin eluting at 18.5 min and cobaltoactaethyl porphyrin eluting at 19.1 min. This is the first clear indication of the removal of an important trace metal from a crude oil by means of biotreatment under these experimental conditions.[2] Consistent with other observations, different strains of microorganisms vary in their ability to alter the trace metal composition. For example, treatment of California crude with two different strains shows changes in concentration and distribution of metal complexes to complete removal of the trace metal, as shown in Fig. 1. Until further studies are conducted, it is reasonable to assume that the metal complex is converted to a species soluble in the aqueous phase.

Preliminary experiments with viscous oils have shown that conventional direct injection into gas chromatograph–mass spectroscope (GC–MS) must be modified because of retention of residues on the chromatographic column. An investigation is under way on the use of pyrolysis combined with the GC–MS technique. This method, which reflects

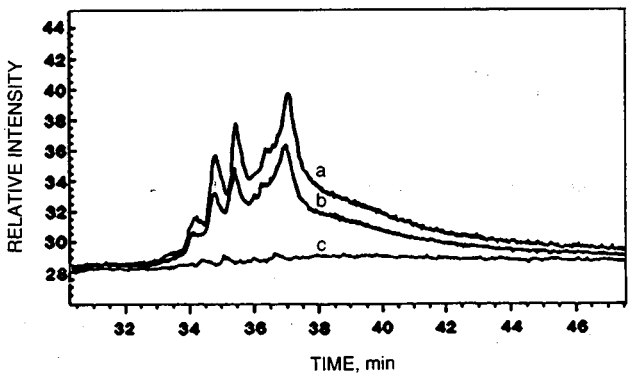

Fig. 1 Gas chromatography atomic emission detector trace of California crude: a, untreated; b, treated with BNL-3-25; c, treated with BNL-4-25.

detailed changes in chemical composition of crude oils, complements the exploration of the use of XANES (X-ray absorption near-edge structure) spectra for the analysis of total changes in sulfur composition. Typical examples of gross sulfur changes observed in the biotreated Boscan, Venezuelan, crude oil are shown in Fig. 2. These are complementary to the more detailed GC–MS method.

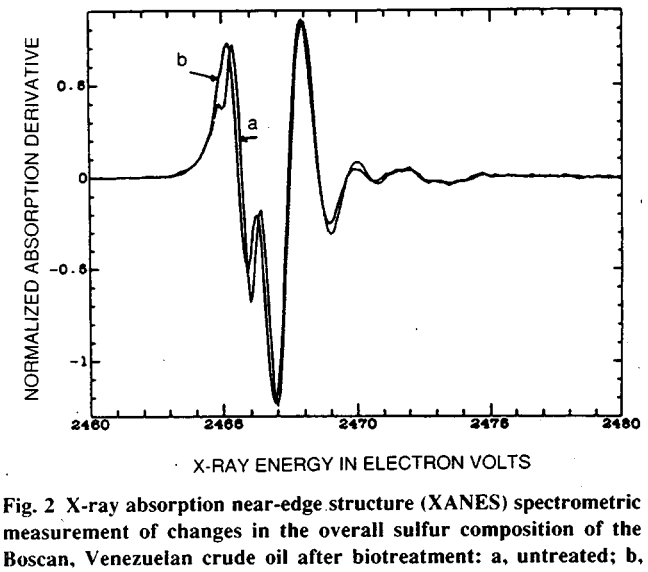

Fig. 2 X-ray absorption near-edge structure (XANES) spectrometric measurement of changes in the overall sulfur composition of the Boscan, Venezuelan crude oil after biotreatment: a, untreated; b, treated oil.

Details of some of the current work have been recently discussed at the Norman, Okla., Microbial Enhanced Oil Recovery meeting.[3]

Modifications and adaptations of Parr pressure reactors for the biotreatment of larger quantities of oils are being explored further.

References

1. E. T. Premuzic and M. S. Lin, Interaction Between Thermophilic Microorganisms and Crude Oils—Recent Developments, *Proceedings of the Bioprocessing of Fossil Fuels Workshop, Virginia, August 1989* (in press).
2. E. T. Premuzic and M. S. Lin, patent pending, 1990.
3. E. T. Premuzic and M. S. Lin, *Prospects for Thermophilic Microorganism in Microbial Enhanced Oil Recovery (MEOR)*, presented at the International Conference on MEOR, University of Oklahoma, Norman, Okla., May 27–June 1, 1990.

DEVELOPMENT OF LUMINESCENT BACTERIA AS TRACERS FOR GEOLOGICAL RESERVOIR CHARACTERIZATION

Contract No. DE-AC22-90BC14666

Fairleigh Dickinson Laboratory
Abilene, Tex.

Contract Date: May 1990
Anticipated Completion: May 1991
Government Award: $40,057

Principal Investigator:
Jeannette W. King

Project Manager:
Edith Allison
Bartlesville Project Office

Reporting Period: Apr. 1–June 30, 1990

Objectives

The focus of the research is to accurately distinguish communication between wells in producing oil zones that may or may not be continuous. Such a determination is necessary when considering enhanced oil recovery (EOR) whether it is waterflooding, carbon dioxide, or other methods that increase the sweep efficiency. Various kinds of chemical tracers are available, but they are expensive and many might be considered hazardous for underground aquifers. Other biological tracers are available but have never been developed for oil reservoir conditions. Bioluminescent bacteria seemed an obvious candidate because they thrive in saline waters (usually 3% salt) that have been contaminated by oil spills.

Summary of Technical Progress

A search of the literature has determined that bioluminescent bacteria have been studied primarily off the coast of California and in the Mediterranean Sea. Personal communication with investigators at the Catalina Marine Science, University of Houston Marine Science Center at Galveston, University of Texas at Port Aransas, University of West Florida in Pensacola, and the University of Miami Marine Science Center have determined that bioluminescent bacteria are prevalent in the Gulf of Mexico, the Pacific Ocean, and the Atlantic Ocean. Results of laboratory experiments will determine whether bioluminescent microorganisms can be used as cost-effective tracers in characterizing formations for EOR.

Bioluminescent bacteria are being developed for use as tracers in reservoir characterization. A pure culture of *Photobacterium phosphoreum* is being studied in the laboratory for accurate monitoring schemes. A search of the literature and communications with marine microbiologists indicate that bioluminescent bacteria can be easily studied in vitro. Next quarter bioluminescent bacteria will be

collected from places where oil spills have occurred and then will be adapted to oil field brines. A simple monitoring system will be developed that can be used in a field laboratory to accurately distinguish communication between wells in producing oil zones that may or may not be continuous.

Growth of the pure culture, *P. phosphoreum*, has been possible in liquid medium with a broth formulated for photobacterium, but monitoring growth by standard techniques has not been successful. Currently, monitoring is being repeated on solid medium (agar); seawater is used to rehydrate the medium. Quantitative determination of the bacteria is the main constraint.

Although the literature and personal communication reveal that in vitro growth and monitoring of bioluminescent bacteria are possible, it is difficult (in this laboratory with presently available facilities) to monitor the growth of the pure culture. During the next quarter, fresh Total Count Samplers will be obtained and other monitoring schemes will be tried. Samples of bioluminescent bacteria in the Gulf of New Mexico will be obtained from an area relatively free from oil and also from an area of a recent oil spill. Marine scientists who have studied various strains of bioluminescent bacteria will help determine the fastidious parameters of these microorganisms. Various oil field brines will be used in place of seawater for the adaption of these bacteria to oil field conditions. Several articles on more recent studies have been ordered to update knowledge acquired from the literature and personal communication.

Bibliography

Baumann, Paul, and Linda Baumann, 1977, Biology of the Marine Enterobacteria: Genera *Benecka* and *Photobacterium*, *Annu. Rev. Microbiol.*, 31: 39-41.

Brown, D. E., F. H. Johnson, and D. A. Marsland, 1942, The Pressure, Temperature Relations of Bacterial Luminescence, *J. Cell. Comp. Physiol.*, 20: 151-168.

Nealson, Kenneth H., Terry Platt, and J. Woodland Hastings, 1970, Cellular Control of the Synthesis and Activity of the Bacterial Luminescent System, *J. Bacteriol.*, 104(1): 313-322.

Ruby, E. G., and J. G. Morin, 1979, Luminous Enteric Bacteria of Marine Fishes: A Study of Their Distribution, Densities and Dispersion, *Appl. Environ. Microbiol.*, 38(3): 406-411.

Shilo, M., and T. Yetinson, 1979, Physical Characteristics Underlying the Distribution Patterns of Luminous Bacteria in the Mediterranean Sea and the Gulf of Elat, *Appl. Environ. Microbiol.*, 38(4): 577-584.

1990 INTERNATIONAL CONFERENCE ON MICROBIAL ENHANCEMENT OF OIL RECOVERY

Contract No. FG22-89BC14437

University of Oklahoma
Norman, Okla.

Contract Date: June 20, 1989
Anticipated Completion: Sept. 19, 1990
Government Award: $57,118

Principal Investigator:
Erle C. Donaldson

Project Manager:
Edith Allison
Bartlesville Project Office

Reporting Period: Apr. 1–June 30, 1990

Objectives

This work is designed to support a conference on the microbial enhancement of oil recovery, which is international in scope, and to achieve several objectives from a current review of the literature, the proceedings of the conference, a panel discussion of research trends, and discussions with the attending scientists. The achievements of the conference are to be published as a reference text on microbial enhanced oil recovery (MEOR) by a major book publishing firm. Objectives are:

1. Conduct a 5-d conference on the science and engineering of MEOR in 1990.
2. Make a complete evaluation of the current state of the art of MEOR.
3. Elucidate the procedures and technology required for development of microbial cultures and field application.
4. Develop programs of basic research and techniques for field pilot studies.
5. Document the procedures and results of field case histories.
6. Publish the proceedings as a reference volume for research, teaching, and application of MEOR.

Summary of Technical Progress

A very successful conference was held May 27–30, 1990, at the University of Oklahoma. Participants from 12 foreign countries attended, and commentaries from various attendees were reported on the local television networks and in the Oklahoma City, Okla., newspapers.

Papers presented at the conference will be included in *Proceedings of the 1990 International Conference on Microbial Enhanced Oil Recovery*. They have been edited and prepared in camera-ready format for publication by the Elsevier Science Publishers, Amsterdam, New York. Editorial revision and retyping of many papers was necessary before publication. Each registered attendee to the conference will receive a copy from the publisher.

The manuscripts have been organized in a logical sequence to include Introductory Papers, Research Papers, Field Applications, and an Appendix containing a review of 30 worldwide field applications prepared especially for the proceedings by Dr. Ion Lazar of Romania.

The general consensus is that these MEOR conferences, which have been international in scope, have been the real stimulus for MEOR on a worldwide scale. The proceedings of the other conferences are being used as texts in many universities where MEOR has become a part of the curriculum of Petroleum Engineering Departments.

ENHANCED OIL RECOVERY AND APPLIED GEOSCIENCE RESEARCH PROGRAM

Contract No. DE-AC07-76ID01570, Project 5AC3

Idaho National Engineering Laboratory
EG&G Idaho, Inc., Idaho Falls, Idaho

Contract Date: Oct. 1, 1988
Anticipated Completion: Sept. 30, 1995
Funding for FY 1990: $1,500,000

Principal Investigator:
C. P. Thomas

Project Managers:
I. Aoki
Idaho Operations Office

Edith Allison
Bartlesville Project Office

Reporting Period: Apr. 1–June 30, 1990

Objectives

The objectives of this research program are to develop microbial enhanced oil recovery (MEOR) systems for application to reservoirs containing medium to heavy oils (12 to 20° API) and to evaluate reservoir wettability and its effects on oil recovery.

The MEOR research goals include:

- Development of bacterial cultures that are effective for oil displacement under a broad range of reservoir conditions.
- Improved understanding of the mechanisms by which microbial systems displace oil under reservoir conditions.
- Determination of the feasibility of combining microbial systems with conventional enhanced oil recovery (EOR) processes, such as miscible and immiscible gas flooding, polymer and chemical flooding, and thermal methods.
- Development of quantitative mathematical descriptions of microbial oil recovery mechanisms under reservoir conditions necessary for the development of reservoir simulation of MEOR processes.
- Development of improved methods of characterization and simulation of heterogeneous reservoirs for design and application of EOR and MEOR processes.
- Development of an MEOR field process design and implementation of an industry cost-shared field demonstration project.

The goals of the reservoir wettability project are to develop:

- Better methods for assessment of reservoir core wettability.
- More certainty in relating laboratory core analysis procedures to field conditions.
- Better understanding of the effects of reservoir matrix properties and heterogeneity on wettability.
- Improved ability to predict and influence EOR response through control of wettability in reservoirs.

Summary of Technical Progress

MEOR Research

Work continues on the series of coreflood experiments developed to investigate such parameters as crude oil type, crude oil viscosity, aging and incubation time, interfacial tension (IFT), and brine composition. The first set of cores is now inoculated, incubated, and again waterflooded with varying degrees of success for the *Bacillus licheniformis* microbial system with the different oils.

The cores are first prepared and flooded to a waterflood residual oil saturation in preparation for the injection of microbial and nutrient solutions. After the microbial and nutrient solutions are injected and displaced into the core, the core is then placed in incubation for 2 weeks. Once the incubation is complete, the core is removed and placed in the coreflood apparatus and is again waterflooded at the same previous waterflood rate. The effluent is collected in an automated tube collection device, and all necessary data are collected and oil recovery is determined. The waterflood is discontinued when oil production ceases.

Six different oils, ranging in API gravity from 17.5 to 50.5° at 60°F, are used in the experimental coreflood work. The experimental program is set up in a matrix fashion with corefloods being performed with all six oils. The experimental system consists of nonfired Berea sandstone cores encapsulated in epoxy. A 2.4% NaCl brine solution is used to saturate the cores and to displace the oil as the cores are flooded. All corefloods are performed at room temperature, including the evacuation and saturation phase of the

experimental work. *B. licheniformis* is the bacteria used as the MEOR system for microbial flooding of the cores.

The experimental system is set up to determine variables associated with the six different oils. Viscosities of all six oils are measured and a characterization is determined for each oil. Connate water saturations are determined for all cores with the various oils in them. Residual oil saturations are determined for both the waterflood and the microbial flood. IFT measurements are made on the oil–brine, oil–brine + nutrient, and the oil–microbial systems.

Baseline (control) experiments are performed with all oils. The control cores are injected with nutrient only. No microbes are injected into the control cores. All control cores are incubated at the same temperature and for the same period of time as the MEOR cores. A separate control core is flooded with nutrient only for each of the oils.

Four of the six MEOR corefloods produced microbial oil (Table 1). The core containing Burbank oil and the core containing Soltrol are the two nonproducers. Schuricht, Moorcroft West, Alworth, and Lick Creek all produced additional oil beyond waterflood with the microbial injection. Only Moorcroft West and Lick Creek produced oil from their control core (nutrient only injection). The Moorcroft West MEOR core produced 13.8% of the original oil in place (OOIP), and the control core for Moorcroft West produced 4.9% OOIP as the result of the nutrient only injection. This leaves approximately 8.9% OOIP, which can be attributed to the injection of the MEOR system for Moorcroft West. The reason for this result is undetermined. The Lick Creek MEOR core and the Lick Creek control core produced about the same amount of oil as a percent of OOIP, 4.3 and 4.4%, respectively. Microbial flood oil recovery as a percent pore volume for the various oils at a brine injection of 7 pore volumes (PV) is shown in Fig. 1. The reason for the observed variation in microbial oil recovery with oil type will be investigated further.

Future work with this matrix of experimental corefloods and these six different oils will include (1) analyzing the effluent to determine such things as microbial populations and bioproducts in the effluent and (2) performing at least one additional MEOR coreflood with each oil to determine if repeatability of oil recoveries exists.

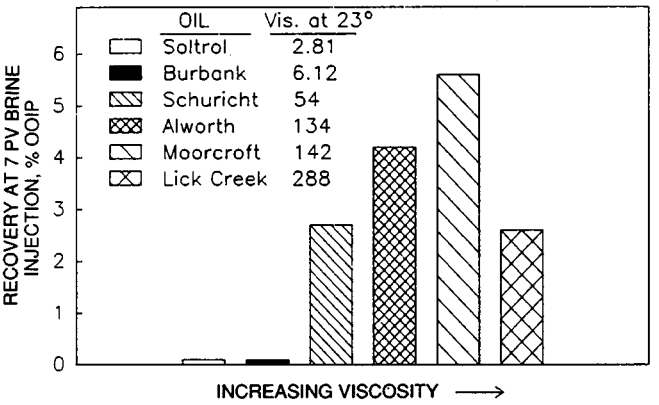

Fig. 1 Microbial enhanced oil recovery corefloods using various oils with *B. licheniformis*.

TABLE 1

Experimental Results of Coreflood Experiments*

Core No.	Microbe	Oil	Viscosity, cP	Permeability, mD	S_{OI},† % PV	S_{ORWF},† % PV	S_{ORMF},† % PV	Microbial recovery,‡ % OOIP
15	*B. licheniformis*	Soltrol	2.81	86	57.9	25.9	25.9	0
16	§	Soltrol	2.81	94	58.6	24.3	24.3	0
14	*B. licheniformis*	Burbank	6.12	195	63.2	25.8	25.8	0
20	§	Burbank	6.12	323	70.7	34.0	34.0	0
10	*B. licheniformis*	Schuricht	54	267	76.7	33.4	31.3	2.7 (4.6)¶
19	§	Schuricht	54	432	64.1	27.0	27.0	0
12	*B. licheniformis*	Alworth	134	119	72.6	18.6	15.6	4.2 (6.2)¶
18	§	Alworth	134	134	66.6	25.5	25.5	0
13	*B. licheniformis*	Moorcroft	142	123	78.8	25.6	21.2	5.6 (13.8)¶
17	§	Moorcroft	142	190	58.9	26.1	23.2	4.9**
11	*B. licheniformis*	Lick Creek	288	109	79.3	39.2	37.1	2.6 (4.3)¶
21	§	Lick Creek	288	510	74.7	36.5	33.2	4.4**

*Temperature, 23°C; brine solution, 2.4% NaCl; *B. licheniformis*, facultatively anaerobic, ATCC 39307.
†OI, oil injected; ORWF, oil recovery waterflood; ORMF, oil recovery microbial flood.
‡Nutrient injection only—no microorganisms injected.
§MEOR flood—oil recovery as percent OOIP at 7 PV brine injection.
¶MEOR flood—oil recovery as percent OOIP when oil recovery ceases.
**Control floods—oil recovery as percent OOIP when oil recovery ceases—9+ PV brine injection.

An oil characterization of the produced oil (postflood) has been performed to determine if there is an oil character change as the result of the conditions experienced as it passes through the core during the MEOR coreflood. These samples were fractionated and analyzed with gas chromatography (Fig. 2). Laboratory handling (not degradation) is believed to account for the small character changes seen in these oils. The oils remained basically unchanged after being subjected to the conditions of the MEOR coreflood.

Dilution studies of supernatant solutions indicate that the concentration of *B. licheniformis* surfactant is approximately 2.5 times as great as the critical micelle concentration (CMC) of the surfactant. Interfacial tensions were measured for various dilutions of supernatant and plotted vs. supernatant concentration (Fig. 3). A break in the IFT–concentration curve occurs at a supernatant:water dilution of 2:5. Maximum oil recoveries will be obtained if the surfactant concentration is at or above the CMC. Oil–water phase studies and IFT measurement of the undiluted supernatant indicate that the IFT is in the region of 0.1 dyne/cm.

Thin-layer chromatography (TLC) studies have been initiated to identify the compound(s) that gives rise to the surfactant activity found. The literature on microbial oil recovery indicates that surfactant produced by *B. licheniformis* is a glycolipid. TLC of an ethyl acetate extract of the supernatant (silica gel, 9:1 ethanol:water) shows one major and five minor spots. Future work will optimize and scale up the separation to isolate larger quantities of material for structural identification.

Evaluation of Reservoir Wettability and Its Effects on Oil Recovery

Research activities in the collaborative effort of the wettability research program at the New Mexico Petroleum Recovery Research Center (NMPRRC) are continuing. Work is progressing in several areas related to oil recovery

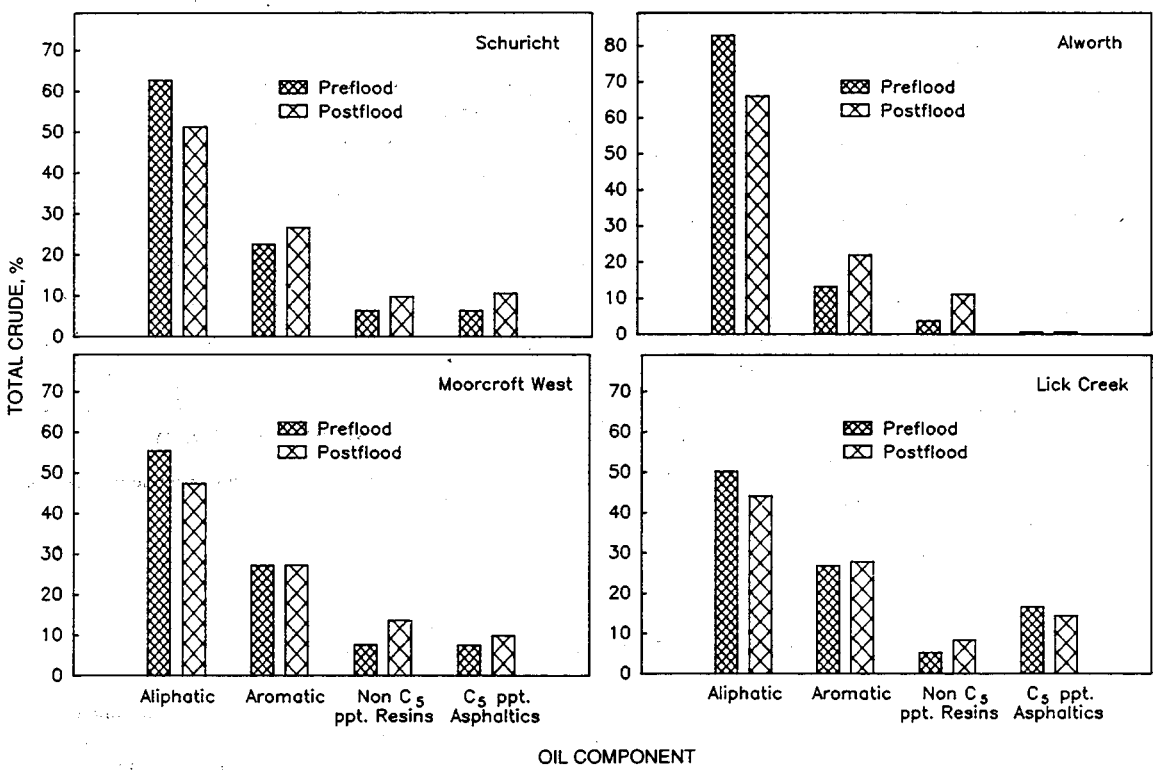

Fig. 2 Comparison of crude oil components in pre- and post-microbial floods with *B. licheniformis*.

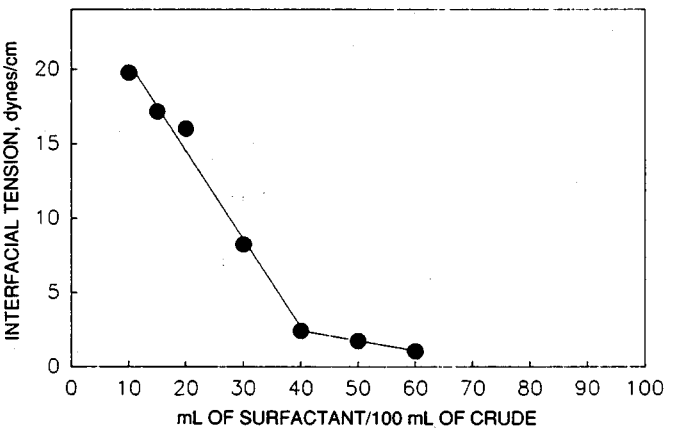

Fig. 3 Determination of critical micelle concentration for *B. licheniformis* biosurfactant vs. Schuricht crude.

studies and the effect of wettability on core flow testing. Interim results for the studies to determine the repeatability of the adhesion mapping technique have been completed. Initial results of research to evaluate the effects of drilling mud filtrates on the wettability of cores have been collected, and details will be reported at a later date.

Activities involving research on relating flow behavior to the wetting conditions prevailing in a porous medium have been completed. The results of this work include:

- For some oils, the water wetness of the Berea–brine–oil system as indicated by spontaneous imbibition behavior decreased as the concentration of Ca^{+2} ions in brine increased, whereas other Berea–brine–oil systems were not significantly affected by brine composition.
- Temperature was a dominant variable with respect to the wettability change induced by crude oil. The magnitude of initial water saturation also had strong influence on the degree of rock–oil interaction.
- A wide spectrum of wetting conditions could be generated by employing different crude oils and varying brine composition, initial water saturation, and aging temperature.
- Positive, intermediate wettability, and weakly water-wet systems gave reduced residual oil saturation as the injection rate was lowered. The reduction in the residual saturation with rate was more pronounced for systems that had higher interfacial tension and viscosity.
- At the extreme wetting conditions, the recovery was influenced by the choice of crude oil. The oil with the higher asphaltene precipitation number and greater sensitivity to ionic concentration and type, as inferred from the imbibition tests, gave higher breakthrough recovery.
- Negative intermediate wettability and weakly oil-wet systems were characterized by lower breakthrough recovery than the other induced wetting conditions.
- For most intermediate wettability systems, oil saturation continued to decrease with pore volume throughput after breakthrough. At breakthrough, the remaining oil saturation was about 34%. After about 20 PV of brine injection, residual oil saturations of as low as 10% were achieved.
- For any chosen number of pore volumes injected, oil recovery was nearly always less for the strongly water-wet and oil-wet extremes than for the weakly water-wet, intermediate, or weakly oil-wet conditions.

MICROBIAL FIELD PILOT STUDY

Contract No. DE-FG22-89BC14246

University of Oklahoma
Norman, Okla.

Contract Date: Nov. 22, 1988
Anticipated Completion: Dec. 31, 1991
Government Award: $220,000
(Current year)

Principal Investigators:
R. M. Knapp
M. J. McInerney
D. E. Menzie
J. L. Chisholm

Project Manager:
Edith Allison
Bartlesville Project Office

Reporting Period: Apr. 1–June 30, 1990

Objective

The objective of this project is to perform a microbially enhanced oil recovery (MEOR) field pilot test in the Southeast Vassar Vertz Sand Unit (SEVVSU) in Payne County, Okla. Indigenous, anaerobic, nitrate-reducing bacteria will be stimulated to selectively plug flow paths that have been preferentially swept by a prior waterflood. This will force future floodwater to invade bypassed regions of the reservoir and increase sweep efficiency.

Summary of Technical Progress

Microbiology

Information on the efficiency of growth and nutrient use by microorganisms in porous media is needed to assess the accuracy of mathematical models. In previous work, a method was developed to determine accurately the primary dependent variables associated with microbial activity in sandpacked cores. A study is under way to use this methodology to calculate the amount of nutrients and the time required for bacterial metabolism in the MEOR processes.

The brine sample used in this work was obtained from the 1A-9 well in the SEVVSU in Payne County, Okla. The chemical analysis of the brine is listed in Table 1. The specific gravity (at 70°F) and resistivity (at 70°F) of the brine was 1.099 and 0.059 Ω-m, respectively. The pH was 7.0.

The brine was amended with (wt/vol): 3% glucose, 0.1% yeast extract, and 0.3% sodium nitrate and incubated under anaerobic conditions. After 6 d, a high concentration of microorganisms was observed microscopically in the en-

TABLE 1

Chemical Analysis of Brine*

Component	Concentration, mg/L	Component	Concentration, mg/L
Calcium	8,300	Carbonate	0
Magnesium	1,930	Hydroxide	0
Sodium	45,315	Sulfate	830
Potassium	110	Chloride	89,690
Barium	<0.2	Total hardness as ($CaCO_3$)	28,800
Iron	0.50	Total dissolved solids	146,330
Silica	12		
Bicarbonate	152		

*Sample was collected on 6/7/90 from well 1A-9 and processed by Petroleum Laboratory and Gas Engineering on June 27, 1990.

richment. The enrichment was transferred every 7 d in the growth medium that contained sterile brine and the preceding nutrients.

The porous medium was prepared under anaerobic conditions and saturated with growth medium. The cores were inoculated with 0.3 mL of the enrichment in the exponential phase. Analyses are under way to determine the rate of increase of biomass inside the cores. Also, substrate use and product formation rates will be monitored.

Coreflood Experiments

Coreflood experiments were terminated in December 1989. The permeabilities of cores C06 and C09 were significantly reduced by the microbial treatment, and large amounts of gas accompanied the recovery of residual oil. In cores C10 and C11, a large permeability reduction was observed, but little or no gas or oil was produced. Cores C10 and C11 were saturated with the nutrient medium and left in the incubator.

After about 100 d of incubation, the pore pressure of core C11 increased, which is indicative of continued microbial activity. After 108 d of incubation, cores C10 and C11 were waterflooded. Significant amounts of oil and gas were produced, and further decreases in permeability were observed.

Five additional microbial treatments were performed on core C10 and seven on C11. An additional 6.5 mL of oil (30.3% of S_{or}) was recovered from core C10 and 8.1 mL (37% of S_{or}) from C11. This resulted in cumulative recovery of 30.4 and 45.6% of the oil remaining after waterflooding in cores C10 and C11, respectively. The final permeability reductions were 3.6 and 5.7% of original brine permeability at S_{or} for C10 and C11, respectively. Figures 1 and 2 display the permeability reduction factor, oil recovery factor (or efficiency), and cumulative gas production for cores C10 and C11.

Because no additional oil was recovered during the 13th and 14th treatments of C11, the core was treated with

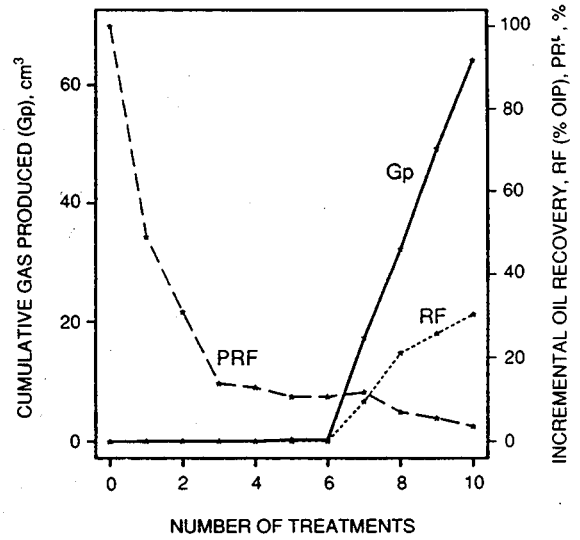

Fig. 1 Effect of nutrient treatments on the permeability reduction factor (PRF), cumulative oil recovery (RF), and gas production (Gp) for core C10. K_{abs}, 152 mD; K_w, 9.4 mD; porosity, 19%; S_{or} (after waterflood), 36.8% PV; treatment 7 includes 100+ d incubation.

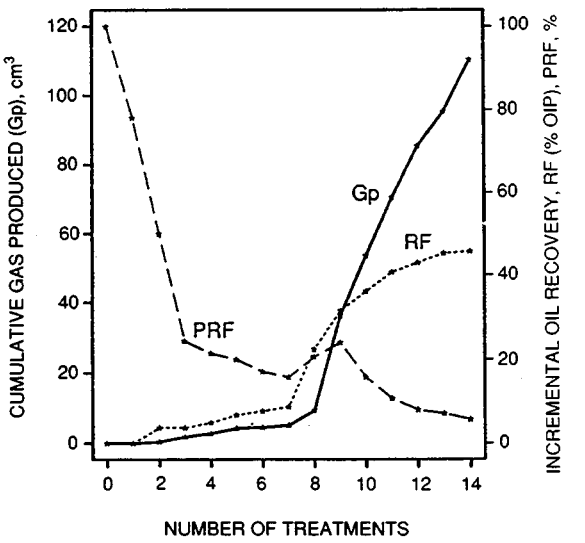

Fig. 2 Effect of nutrient treatments on the permeability reduction factor (PRF), cumulative oil recovery (RF), and gas production (Gp) for core C11. K_{abs}, 76 mD; K_w, 7 mD; porosity, 17.2%; S_{or} (after waterflood), 41.3% PV; treatment 9 includes 100+ d incubation.

bleach to determine if permeability could be restored by chemically removing the cellular material. One pore volume of 1% sodium hypoclorite solution in Vassar brine was injected. The permeability increased from 0.38 to 1.1 mD. This poor restoration of the permeability may have resulted from incompatibilities between the brine and the bleach, which may have caused the formation of precipitate within the core.

Field Activities

During this quarter, field trips were made to the SEVVSU to determine more precisely the needs for surface and downhole equipment and to continue the evaluation of the reservoir ecology.

During the last quarter, Mesa Limited Partnership sold their working interest in the SEVVSU to Sullivan and Co., a Tulsa, Okla., based independent oil and gas exploration and production company. Sullivan and Co. is now the operator of the SEVVSU. Since Sullivan and Co. assumed operation of the field, an engineering plan was developed for the modification of the field, so that the microbial field trial can be conducted. Details of this plan are now being discussed. A contract for the operation of the field pilot

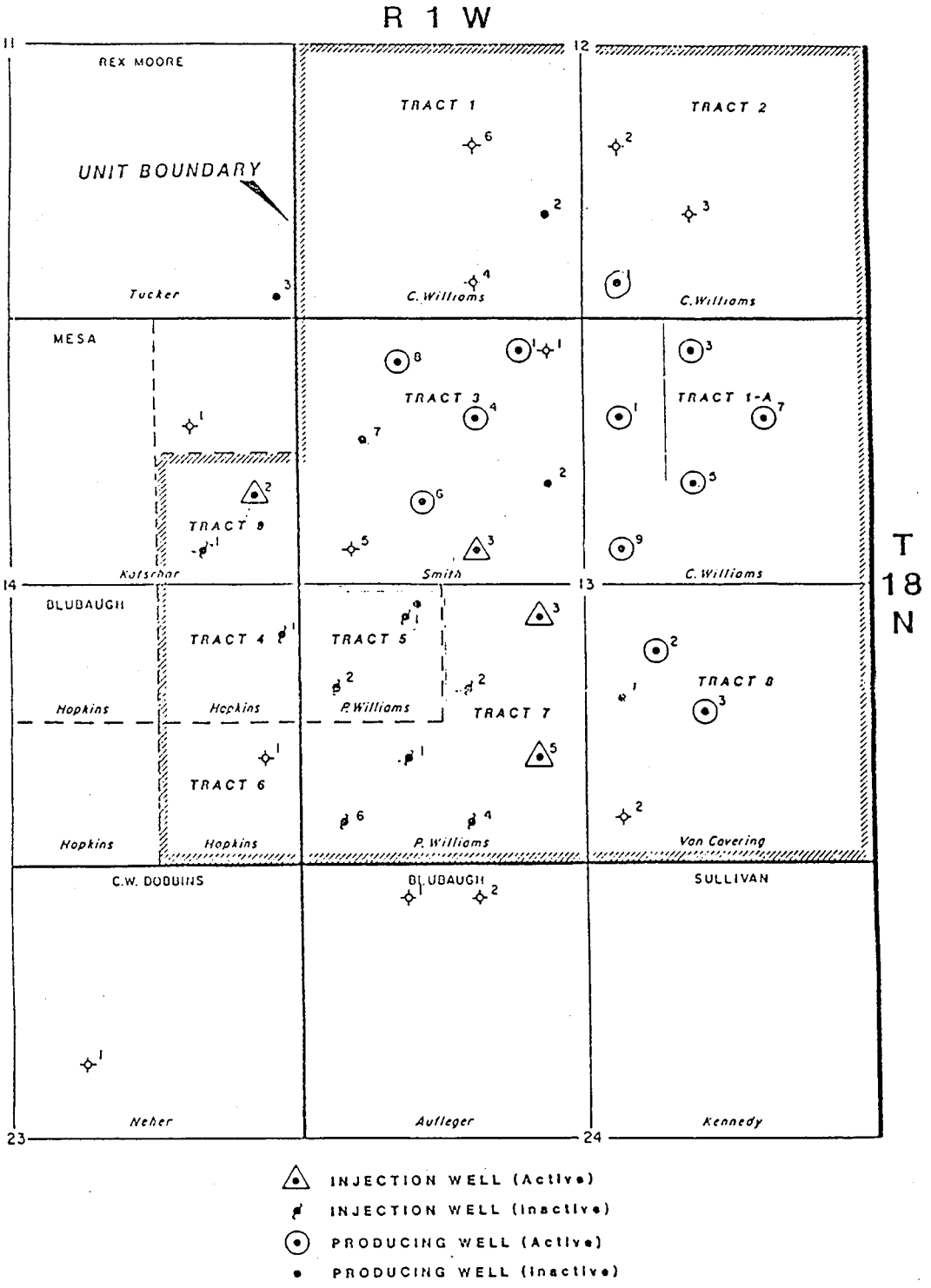

Fig. 3 The Southeast Vassar Vertz Sand Unit.

should be completed within the next month and be presented to the University of Oklahoma Board of Regents at the October meeting for their approval.

Reservoir Simulation and Characterization

A BOAST II[1] simulation of the SEVVSU covering the period from October 1966 to December 1988, was accomplished. The initialization data are unchanged from the previous simulation performed with the original BOAST[2] simulator in 1987. Oil production data have been extended by 1.5 yr from the 1987 simulation. The simulation is being performed to provide predictive information at this time and as a tool for future analysis of the field pilot.

Graphs of the observed cumulative water production vs. simulated cumulative water production were prepared for each well in the field and also for the entire field. The simulated water production for the total field was underestimated by 10%. On a well-by-well basis, much variability exists. This variability can be classified into four groups.

The first group of ten wells, generally in the pilot study area, have acceptable to excellent history matches. In Fig. 3, a base map of the SEVVSU, these ten wells are in and around tract 7. The second group includes wells 4-1, 5-2, and 7-1. The simulated water production from these wells before the initiation of waterflooding is 45, 52, and 20 (MSTB), respectively. No water production was recorded during this time. Sullivan and Co. has suggested that water production records during the early life of the field were not highly reliable. The third group includes six wells that indicate 3000 to 9000 bbl of observed cumulative water production from 1978 to 1980 only. There is no simulated water production from these wells. Sullivan and Co. has suggested that field water production might have been allocated to these wells and they might not have produced any water. Simulated water production from the first three groups of wells accounts for 7% of the total field difference between simulated and observed water production. Trying to improve matches in these areas is not warranted at this time. The fourth group includes nine wells in tracts 1A and 8 that have poor history matches. Simulated water production is too high in some wells and too low in others. This accounts for 93% of the total field difference between simulated and observed water production. These are the areas that require further modification for history matching.

References

1. J. R. Fanchi, J. E. Kennedy, and D. L. Dauben, *BOAST II: A Three-Dimensional, Three Phase Black Oil Applied Simulation Tool*, DOE Report DOE/BC-88/2/SP, 1987.
2. J. R. Fanchi, K. J. Harpole, and S. W. Bujnowski, *BOAST: A Three-Dimensional, Three Phase Black Oil Applied Simulation Tool*, DOE Report DOE/BC/10033-3, Vol. 1, 1982.

MICROBIAL ENHANCEMENT OF OIL PRODUCTION FROM CARBONATE RESERVOIRS

Contract No. AC22-90BC14202

University of Oklahoma
Norman, Okla.

Contract Date: January 1990
Anticipated Completion: January 1991
Government Award: $154,482

Principal Investigators:
Ralph S. Tanner
Roy M. Knapp
Michael J. McInerney
Emmanuel O. Udegbunam

Project Manager:
Edith Allison
Bartlesville Project Office

Reporting Period: Apr. 1–June 30, 1990

Objective

Carbonate reservoirs are the source of about half of the world's oil production. The objective of this research is to examine the potential utility of microbially enhanced oil recovery (MEOR) for carbonate reservoirs. This includes a review of the literature pertinent to MEOR in carbonate reservoirs, a study of the microbial ecology of carbonate reservoirs, the isolation of microorganisms from these environments, the examination of the effect of microorganisms and their end products of metabolism on carbonates and oil in carbonates, a study of model core systems, and the development of models to examine and predict MEOR processes in carbonate reservoirs.

Summary of Technical Progress

Literature Review

Reports on MEOR field trials and laboratory experiments in carbonate lithology are sparse. Results from field trials are inconclusive or lack relevant reservoir data necessary for interpretation of the variables and mechanisms responsible for MEOR in carbonate reservoirs.

Experience with various lithologies shows that applicable enhanced oil recovery (EOR) mechanisms and

TABLE 1

Characterization of Acid-Producing, Halophilic Eubacteria Isolated from the Great Salt Plains

Gram reaction	Cell morphology	Relation to oxygen	Catalase reaction	Relation to salt	Number of strains
–	Rod	Facultatively anaerobic	–	Obligately halophilic	6
–	Rod	Facultatively anaerobic	+	Obligately halophilic	3
–	Rod	Obligately aerobic	+	Obligately halophilic	3
–	Rod	Facultatively anaerobic	–	Halotolerant	1
+	Rod	Facultatively anaerobic	–	Obligately halophilic	1
+	Rod	Facultatively anaerobic	–	Halotolerant	1
+	Rod	Facultatively aerobic	–	Obligately halophilic	1
+	Rod	Facultatively aerobic	+	Obligately halophilic	1
+	Rod	Obligately aerobic	–	Obligately halophilic	1
–	Coccus	Facultatively anaerobic	–	Obligately halophilic	1
–	Coccus	Facultatively anaerobic	+	Halotolerant	1
–	Coccus	Obligately aerobic	+	Obligately halophilic	1
+	Coccus	Facultatively anaerobic	+	Halotolerant	1

the delineation of reservoirs for any particular EOR technique(s) depend on the reservoir's pore structure and rock–fluid interactions. Carbonate reservoirs commonly exhibit diverse and complex facies, which, in turn, affect their porosity, permeability, and other aspects of pore structure. It is necessary to understand the internal architecture of carbonate reservoirs because it controls not only productivity but also the applicability of MEOR and the effective oil recovery mechanisms.

The literature shows that carbon dioxide (CO_2) miscible flooding is the dominant commercial EOR process for carbonate reservoirs. Several large-scale field projects have been reported in the carbonate fields of west Texas.[1,2] One incremental advantage of CO_2 floods in carbonates over clastic reservoirs is the improvement of reservoir properties by acidic dissolution of the rock. Successful use of solvents, such as refined hydrocarbons and organic alcohols, has been reported.[3] Commercial application of micellar–polymer flooding in carbonates has not been reported. Carbonates have not been considered suitable target reservoirs for application of micellar–polymer or alkaline flooding because of the sensitivity of commercially available products to the divalent cations of carbonate lithology.

Carbonate Coreflood Experiments–Mechanisms of Oil Displacement by Microorganisms

The initial characterization of acid-producing halophilic microorganisms isolated from the Great Salt Plains and study of the basic microbial ecology of an oil-saturated upward-flow packed rock filter were completed as part of technical training. Results are summarized in Tables 1 and 2. The significance of this work is that two additional microbial systems have been identified as useful for laboratory and field studies in MEOR.

TABLE 2

Microbial Populations Enumerated from the Effluent of an Upward-Flow Packed-Rock Anaerobic Filter (Rock Pile)*

Aerobes			
General heterotrophs†	5×10^5‡	Glucose heterotrophs	2×10^0
Anaerobes			
General heterotrophs	3×10^5	Glucose heterotrophs	2×10^3
Molasses	8×10^7	Molasses–nitrate	1×10^7
Sucrose	3×10^3	Sucrose–nitrate	4×10^3
SRB	2×10^8	Iron reducers	2×10^0
Methanogens–acetate	ND§	Methanogens–methanol	3×10^0
Methanogens–formate	ND	Methanogens–H_2:CO_2	ND
Acidogens–fructose	ND		

*Quartz pebbles used; system oil-saturated; system established February 1988 for the production of SRB biofilms using microorganisms originally obtained from a sandstone petroleum reservoir; brine contains 10% NaCl.

†Denotes type of microorganism being enumerated and/or the substrate used to recover viable microorganisms.

‡Average of two three-point MPNs after incubation for 28 d at 30°C.

§None detected; indicative of an MPN greater than 2×10^{-1} per milliliter.

The Great Salt Plains is a readily accessible environmental source of a variety of microorganisms that can survive and metabolize in halophilic environments (David P. Nagle, Jr., and Ralph S. Tanner, unpublished results) commonly found in oil reservoirs. Many MEOR projects will require the use of halophilic, anaerobic microorganisms. Many of the microorganisms readily recoverable from sediments of the Great Salt Plains are facultative anaerobes and/or facultative halophiles, traits that simplify their handling in the laboratory environment.

TABLE 3

Carbonate Oil Wells Sampled for Brine as of June 30, 1990

Well	Formation	Perforation depth, ft	Total dissolved solids, ppm	NaCl	Date sampled
Pharoah #15-3A	Viola	5738 to 6060	223,414	21%	6/12/90
Froug #1	Hunton (gas)	4066 to 4080	186,414	17%	6/21/90
Fitts #7-15	Hunton	3389 to 3406	128,515	12%	6/28/90

The typical isolate recovered in a study of acid-producing microorganisms from the Great Salt Plains was an obligately halophilic, facultatively anaerobic, Gram-negative rod (Table 1). Although these microorganisms were selected for the ability to produce acids from glucose, a potentially useful trait for MEOR in carbonate systems, these isolates generally do not perform acidic fermentation under aerobic conditions.

The basic microbial ecology of an oil-saturated quartz-pebble-packed filter, called a rock pile biofilm reactor, is given in Table 2. This rock was established in February 1988 and inoculated with microorganisms concentrated from a sandstone oil reservoir. The basic microbial population has been stable for over two years. Interestingly, methanol-using methanogens were recovered from the rock pile, which is dominated by sulfate-reducing bacteria as the terminal electron accepting microorganisms. Rock piles can serve as excellent sources of microorganisms, including ultramicrobacteria, for MEOR studies.

Petroleum-producing carbonate fields and formations in Oklahoma, especially those with coproduced water for brine sampling, were identified with the Natural Resources Information System (NRIS) database at the University of Oklahoma. Nine petroleum-producing carbonate formations were identified. Reservoirs in three of these carbonate units were selected for brine sampling because of their abundance, productivity, and/or accessibility: (1) Chester formation (Mississippi System); (2) Hunton formation (Silurian System); (3) Viola formation (Ordovician System). The Arbuckle formation (Cambro-Ordovician System) was also identified as an important carbonate reservoir in Oklahoma.

Brine samples from three unmixed carbonate wells were collected. Characteristics are given in Table 3. A well in a Chester formation will be sampled next.

Carbonate rock samples for coreflood studies are being collected from the preceding formations. Well core plugs and chips from the Hunton, Viola, and Arbuckle formations were collected from the University of Oklahoma Core Library for inspection. An examination of these rocks showed very little matrix porosity; this suggests that reservoir properties favorable for oil and gas production are of secondary origin from interconnected fracture and/or vuggy systems.

Whole rock boulders and chip samples of the Viola and Arbuckle limestones were gathered from quarries in the Arbuckle Mountain area near Davis, Okla.

A goal of this research is to understand the prevailing mechanisms responsible for MEOR in carbonates for a given pore structure and wettability condition and to study the effects of microbial activity on carbonate pore structures. Petrophysical characterization (porosity, permeability, and capillary pressure, pore geometry, distribution, and tortuosity) is planned for carbonate plug samples. Preruns are under way on some clastic and carbonate core plugs. Microbial transport through dual porosity systems, common in carbonate pore systems, will also be studied.

References

1. Gruy Federal, Inc., *Target Reservoirs for CO_2 Miscible Flooding—Final Report*, DOE Report DOE/MC/08341-17, 1980.
2. A. V. Kane, Performance Review of a Large-Scale CO_2–WAG EOR Project, SACROC Unit, Kelly-Snyder Field, *J. Pet. Technol.*, 31(2): 217-231 (1979).
3. D. E. Bilozir and P. M. Frydl, *Reservoir Description and Performance Analysis of a Mature Miscible Flood in Rainbow Field, Canada*, paper SPE 19656, presented at the 64th SPE Annual Technical Conference, San Antonio, Tex., 1989.

DEVELOPMENT OF IMPROVED MICROBIAL FLOODING METHODS

Cooperative Agreement DE-FC22-83FE60149, Project BE3

National Institute for Petroleum and Energy Research
Bartlesville, Okla.

Contract Date: Oct. 1, 1983
Anticipated Completion: Sept. 30, 1990
Funding for FY 1990: $300,000

Principal Investigator:
Rebecca S. Bryant

Project Manager:
Edith Allison
Bartlesville Project Office

Reporting Period: Apr. 1–June 30, 1990

Objective

The objective of this project is to develop an engineering methodology for designing and applying microbial methods to improve oil recovery.

Summary of Technical Progress

Prior work at the National Institute for Petroleum and Energy Research (NIPER) has identified the mechanisms of oil mobilization by certain microbial formulations. Important mechanisms that have been identified include wettability alteration, emulsification, solubilization, and alteration in interfacial forces. Recent experiments at NIPER have demonstrated that oil mobilization by microbial formulations is not merely the result of the effects of the metabolic products from the in situ fermentation of nutrient. Further investigation into the interfacial properties of microorganisms and the localized transient concentrations of metabolic products at the oil–water interface is needed to further determine the mechanisms of oil mobilization. The relationships between transport of microbes, nutrients, metabolic products, and mobilized crude oil need to be clarified and interpreted with mathematical models for fluid flow in porous media. The effects of reservoir conditions, such as salinity, temperature, pH, and compositions of reservoir brine and rock, need to be studied to develop methods for designing microbial formulations that are optimal for recovering crude oil under specific reservoir conditions. The effects of injection strategies on oil recovery efficiency also need to be determined. The scope of work includes laboratory experiments to further define key mechanisms of oil mobilization, development of correlations and mathematical models to describe the physical phenomena that are important in microbial enhanced oil recovery (MEOR) methods, and development of a mathematical computer simulator to model and predict performance of microbial formulations in oil recovery laboratory tests.

Work continued on milestone 3, "Define Importance of Process Variables in the Application of Microbial Methods." Three carbonate microbial corefloods were conducted. One coreflood (L-1) used 0.5% sodium chloride brine for the waterflood, and the other coreflood (L-2) used 3% sodium chloride. The permeability of L-1 was 121 mD, and that of L-2 was 97 mD. Microbial cultures NIPER 1 and 6 and molasses were injected into these two cores after they had been waterflooded to residual oil saturation. The coreflood with 0.5% brine gave a good microbial recovery efficiency of about 33%. The coreflood using 3% brine did not produce oil. Microbial counts showed that the microorganisms survived in both cores. Coreflood L-2 was reinjected with a culture of NIPER 6 that was first grown in 3% sodium chloride. A recovery efficiency of about 12% was obtained during the waterflood. Carbonate core plugs are being evaluated regarding microbial alteration of wettability with United States Bureau of Mines (USBM) method.

Progress was made on milestone 6, "Complete Initial Work on Improved MEOR Simulator and Submit Status Report on Identified Improvements." Wettability tests and relative permeability experiments with microbial formulations were conducted to continue work for milestones 3 and 6 and to obtain data relating to mechanisms of microbial oil mobilization. While preparing a plan for the MEOR simulator, one of the more critical parameters required for the modeling appeared to be the effects of mirobial formulations on relative permeability. Thus an apparatus for determining the relative permeability of microbial formulations was constructed. Runs were conducted with this apparatus along with concurrent testing using the Amott and USBM methods for determining the alteration of wettability by the same microbial formulation under the same conditions. A paper was presented on these data at the 1990 International MEOR Conference held in Norman, Okla., May 27–31, 1990.[1]

Amott wettability experiments were conducted according to the outline in Fig. 1. Following a 7-d period submersed in crude oil, Berea sandstone cores were placed in imbibition tubes. One core was placed in a tube full of brine solution (A1), and the other core was placed in a tube full of the microbial formulation (A4). The cores were left in the tubes and monitored daily until no more oil was produced. Both samples were stored in the tubes for about 3 weeks. Each sample was then removed from the wettability tube and loaded into a core holder. The samples were flooded with either brine or microbial formulation to determine the additional volume of mobile oil that could be displaced dynamically. Sample A4 was flooded with the microbial formulation. The samples were then placed in imbibition tubes full of crude oil. Again, the samples were left in the tubes until equilibrium was reached; both

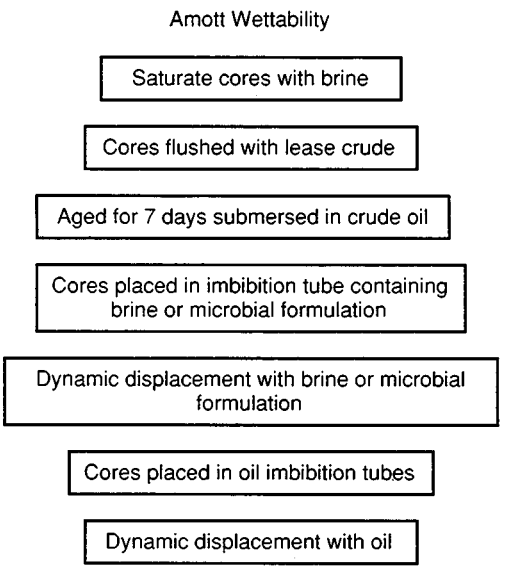

Fig.1 Amott wettability procedure.

samples were then flushed with crude oil until no more brine (or microbial formulation) was produced. Residual water saturation was verified by a toluene distillation method. Results of the Amott wettability test are shown in Table 1. The decrease in relative permeability to the microbial formulation at the end of the test shows a decrease in water mobility, which would be seen in a trend to more water-wet conditions. The ratio of the permeability to water in the presence of residual oil to the permeability to oil in the presence of connate water (end-point k_{rw}) is sometimes used as an indicator of wettability—a value of less that 0.3 indicates water wetness, and a value near unity indicates oil wetness. The brine–oil core (A1) had a

TABLE 1

Summary of Amott Wettability Test Results

	Brine–DC* oil system (Sample No. A1)	Microbial formulation–DC oil system (Sample No. A4)
Permeability to air, mD	325	271
Porosity, %	19.2	19.2
Immobile water saturation, % PV	21.7	22.9
Permeability to oil at initial water saturation, mD	163	131
Water† imbibed, % PV	12.2	27.7
Oil displaced dynamically, % PV	31.1	19.7
Total oil recovered, % PV	43.3	47.4
Immobile oil saturation, % PV	35.0	29.7
Permeability to water† at immobile oil saturation, mD	58	29
End-point k_{rw},‡ fraction	0.355	0.220
Oil imbibed, % PV	0	6.2
Water† displaced dynamically, % PV	41.6	32.6
Total water recovered, % PV	41.6	38.8
Wettability index§ to water†	0.244	0.584
Wettability index§ to oil	0	0.162

*DC oil, Delaware–Childers crude oil.

†Denotes microbial formulation for sample A4.

‡k_{rw}, effective permeability to water or microbial formulation (A4) at residual oil saturation/effective permeability to oil at initial water saturation.

§Wettability index, fluid imbibed/fluid imbibed + fluid displaced dynamically.

calculated end-point k_{rw} value of 0.355, whereas the sample tested with microbial formulation (A4) had a value of 0.220. The wettability index to water of 0.244 for control core A1 was very close to the USBM centrifuge wettability index values shown in Table 1. The wettability index to water for the microbial sample was significantly higher; however, this core did imbibe some oil (the wettability index to oil was 0.162). The difference of 0.422 between the wettability index to the microbial formulation and the wettability index to oil is still twice the value of the wettability index to water for sample A1.

Results of the USBM method centrifuge wettability tests are shown in Tables 2 and 3. NIPER 1 used either alone or

TABLE 2

United States Bureau of Mines Centrifuge Wettability Tests with Delaware–Childers Crude Oil

Sample No.*	Wettability index
3% Sodium Chloride Brine	
CP66	+0.153
CP67	+0.145
CP68	+0.267
CP69	+0.196
CP70	+0.223
CP71	+0.222
Average wettability index	+0.201 ± 0.046
0.5% Sodium Chloride Brine	
CP53	–0.064
CP54	–0.030
CP55	–0.082
CP56	+0.063
Average wettability index	–0.028 ± 0.065
Delaware–Childers Oil and NIPER 1 and 6 Filtered Products (No Cells)	
CP60	+0.239
CP61	+0.117
CP62	+0.247
CP63	+0.176
CP64	+0.237
CP65	+0.100
Average wettability index	+0.186 ± 0.065

*The core was aged for 7 d with Delaware–Childers oil at S_{wi}.

in combination with other microbes appears to shift the wettability index significantly in the positive direction toward a more water-wet condition. The core treated with a filtered solution of products (cells removed) appeared to be in the same range of wettability index as the core used with the brine–oil system. The in situ microbial metabolism appears to be involved in wettability alteration since microbial products alone do not appear to alter wettability.

Microbial formulations containing NIPER 1 appear to shift the wettability index of Berea core samples from just slightly water wet to a more positive value. The microbial cells appear to be involved in this wettability alteration since no change was observed in samples tested with filtered microbial products (cells removed). In situ microbial metabolism appears to be involved in wettability

TABLE 3

United States Bureau of Mines Centrifuge Wettability Tests with Selected Microbial Formulations

Sample No.*	Wettability index	Microbial formulation
CP1	+0.315	Brine/Delaware–Childers oil
CP2	+0.453	Brine/Delaware–Childers oil
CP3	+0.739	NIPER Bac 1†
CP4	+0.992	NIPER Bac 1
CP23	+0.927	NIPER 1 and NIPER 3
CP24	+0.763	NIPER 1 and NIPER 3
CP9	+0.950	NIPER 1—*B. licheniformis*
CP10	+0.959	NIPER 1
CP15	+0.137	NIPER 2—*Bacillus* sp.
CP16	+0.117	NIPER 2
CP11	+0.293	NIPER 3—*Clostridium* sp.
CP12	+0.138	NIPER 3
CP13	+0.283	NIPER 4—Gram (–) rod
CP14	+0.262	NIPER 4
CP21	+0.355	NIPER 5—*Clostridium* sp.
CP22	+0.500	NIPER 5
CP19	+0.310	NIPER 6—*Clostridium* sp.
CP20	+0.314	NIPER 6

*Core was aged overnight with Delaware–Childers oil.

†NIPER Bac 1 is a consortium of four microbes used in Mink Unit field test. NIPER 1, NIPER 2, NIPER 3, and NIPER 4.

alteration. Results of the Amott wettability test indicate that the wettability index to water for the microbially treated core was twice that of the value for the control core, which indicates a more water-wet condition.

Although all wettability tests with microbial formulations exhibited a change in the direction of a more water-wet condition, changes in the range of neutral wettability are very hard to distinguish. Berea sandstone is very water wet, and any alteration toward a more oil-wet condition is difficult to attain. The studies involving wettability alteration by microbial formulations in carbonate rock should assist in determining the wettability effects of NIPER 1 and 6.

Relative permeability measurements were conducted on adjacent samples from two sets of Berea sandstone with different permeability ranges. Each set included one sample with brine–oil relative permeability and another sample used for microbial formulation–oil relative permeability tests. The relative permeability fraction curves for the two samples are compared in Figs. 2 and 3, respectively. A higher relative permeability to oil is apparent in both microbially flooded samples compared with brine-flooded samples. Both cores exhibited a significant decrease in relative permeability to water by the end of the flood. The higher permeability core exhibited the effect much earlier in the flood. A slight shift to the right can be observed in the ratio curves of microbially flooded samples, which indicates that sample R8 had an increase in oil production compared with the brine sample toward the latter half of the

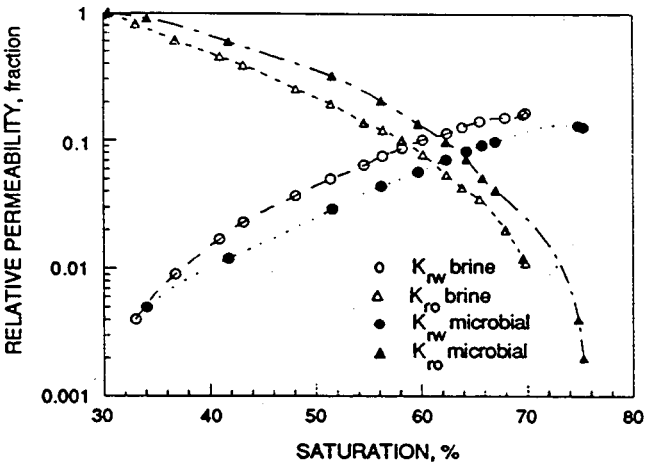

Fig. 2 Unsteady-state relative permeability fraction curves for 1000-mD Berea core using 24-h culture.

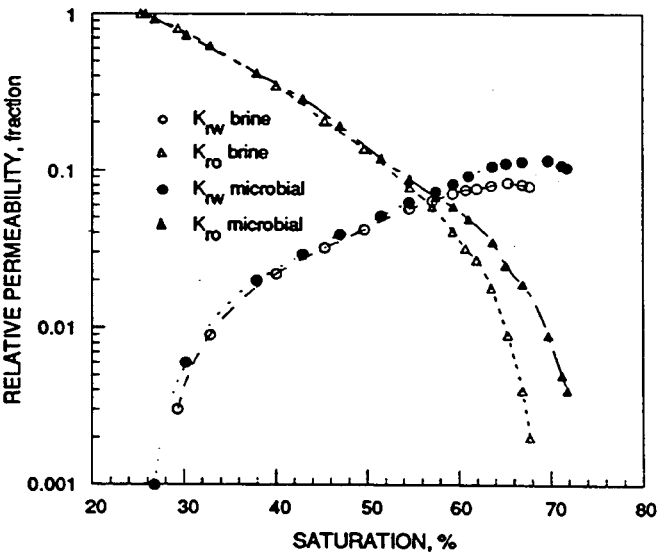

Fig. 3 Unsteady-state relative permeability fraction curves for 300-mD Berea core using 5-d culture.

flood. Sample R2 had an increase in oil production and relative permeability to oil early in the flood.

A significant decrease was seen in k_{rw} curves (a decrease in water mobility) for two of three samples containing microbial formulation. Both relative permeability test samples showed an increase in relative permeability to oil, although one sample containing microbial formulation had a 20% higher initial effective permeability to oil. However, cores with varying permeabilities but the same rock type (pore geometry) have almost identical relative permeability characteristics.[2] A slight shift to the right was observed at the brine saturation at which oil and water relative permeabilities are equal (crossover). Samples tested with the microbial formulation had higher oil recovery before

water breakthrough and lower residual oil saturations. Steady-state water–oil relative permeability tests may provide more meaningful data since Delaware–Childers crude oil, which has a relatively low viscosity of 7.5 cP, could be used instead of refined mineral oil.

Work began this quarter on milestone 4, "Topical Report on Revised Screening Criteria." The NIPER MEOR Field Project Database is being updated. The schedule for completion of this milestone was postponed until after the 1990 International MEOR Conference when new information about MEOR field trials would be available from some of the international researchers attending the conference. The conference provided several papers involving international field trials, and new information was obtained and will be incorporated into the report.

Work continued for milestone 5, "Complete Determination of the Mechanism of Interfacial Activity for Selected Microbial Formulation." An experiment using phase behavior tubes with microbial formulations and different crude oils was designed. Experiments with live crude oils and NIPER 1 and 6 showed no middle phase behavior with this particular microbial formulation. Some crude oil solubilization occurred with higher salinities.

References

1. K. L. Chase, R. S. Bryant, T. E. Burchfield, K. M. Bertus, and A. K. Stepp, *Investigations of Microbial Mechanisms for Oil Mobilization in Porous Media*, presented at the 1990 International MEOR Conference, Norman, Okla., May 27–31, 1990.
2. J. T. Morgan and D. T. Gordon, Influence of Pore Geometry on Water–Oil Relative Permeability, *J. Pet. Technol.*, 1199-1208 (October 1970).

MICROBIAL-ENHANCED WATERFLOODING FIELD PROJECT

Cooperative Agreement DE-FC22-83FE60149, Project SGP13

National Institute for Petroleum and Energy Research
Bartlesville, Okla.

Contract Date: Oct. 1, 1983
Anticipated Completion: Sept. 30, 1990
Funding for FY 1990: $415,000

Principal Investigator:
Rebecca S. Bryant

Project Manager:
Edith Allison
Bartlesville Project Office

Reporting Period: Apr. 1–June 30, 1990

Objectives

The objectives of this research are to determine the feasibility of improving oil recovery in an ongoing waterflood with the use of microorganisms and to expand the initial pilot and determine the economics of microbial-enhanced waterflooding.

The scope of work for this project includes continued monitoring of the Mink Unit Project and the injection of all injection wells on a particular pattern with microorganisms and nutrient for the waterflooding process. This portion of the project will be an expanded field pilot.

Summary of Technical Progress

A microbial-enhanced waterflood field project sponsored by the U.S. Department of Energy (DOE), Microbial Systems Corp. (MSC), and INJECTECH, Inc., and conducted in cooperation with the National Institute for Petroleum and Energy Research (NIPER), was initiated in October 1986. The field selected for the project is in the Mink Unit of Delaware–Childers field in Nowata County, Okla. This field pilot consisted of treating 4 of 21 injection wells on the Mink Unit. Weekly samples are continually analyzed for total dissolved solids, pH, surface and interfacial tensions, crude oil viscosity, microbial counts, molasses concentrations, oil production from the Mink Unit, water/oil ratios, injection pressures, and injection volumes.

The scope of work for FY90 includes continued monitoring of the Mink Unit Project through December 1989 and the initiation of an expanded field pilot on the Brown/Robertson/Johnson lease, B&N property, Delaware–Childers (Oklahoma) field. However, this property was sold in May 1988, and the selection of a new site for the project expansion was required. A new site located in S8-T24N-R17E, Rogers County, Okla., was selected in December 1989. The site, owned by Phoenix Oil and Gas, Ltd., is a part of Chelsea–Alluwe field and is producing (waterflood) from the Bartlesville formation.

For the expanded pilot, fluorescein was injected as a tracer on June 6, 1990. Samples were taken from all 19 injection wells at 2-h intervals the first day. These samples will be analyzed for fluorescein, and transit time from the centralized injection station to each injection well will be estimated. This information will also be useful for ensuring that there is communication between the centralized injection station and all injection wells. A slug

PHOENIX FIELD DATA - FLUORESCEIN TRACER

ALL NUMBERS IN PPB

DATE:	6/7/90
DAYS POST INJ.	1
E & L WARD	
ELP-3	
ELP-4	
ELP-5	
ELP-6	
ELP-6A	
ELP-11	
ELP-12	
ELP-15	
ELP-16	
WAL. WARD	
WAL P-5	
WAL P-6	
WAL P-7	
WAL P-8	
WM WARD	
WM P-11	
WM P-12	
WM P-19	
WM P-20	
PAYNE	
PP-2A	
PP-3A	
BRIGHT HEIRS	
BH P-3	
BH P-7	

Fig. 1 Tracer sample data sheet for producing wells at the Phoenix site.

of 100 bbl of 126-ppm fluorescein was injected. A protocol was designed to target 21 of the 47 production wells for sampling. Figure 1 shows the sample data sheet for tracer monitoring. These 21 producers were sampled 24 h after injection of tracer and are now being sampled daily, then weekly, and finally, once a month.

Some problems were encountered when trying to backflush an injection well after microbial injection for the single-well injectivity test. Samples of water could not be obtained. However, no problems were encountered with injectivity or pressure during and after the microbial injection.

Microorganisms and molasses will be injected into the Phoenix field site by the end of the quarter.

GEOSCIENCE TECHNOLOGY

PETROLEUM GEOCHEMISTRY

Lawrence Livermore National Laboratory
Livermore, Calif.

Contract Date: Oct. 1, 1987
Anticipated Completion: Sept. 30, 1990
Government Award: $200,000

Principal Investigator:
Alan K. Burnham

Project Manager:
Thomas B. Reid
Bartlesville Project Office

Reporting Period: Apr. 1–June 30, 1990

Objectives

The purpose of this project is to develop and test an improved chemical kinetic model of petroleum generation, expulsion, and destruction. Laboratory pyrolysis is used in conjunction with literature data to develop models. The models will include equation-of-state calculations to predict the amount and compositions of gaseous and liquid phases. Geological modeling will be used to derive thermal histories in petroleum-generating basins. These will be used in the chemical kinetic model to generate predictions to be compared to geochemical evidence. Much of the work will be in collaboration with INTEVEP, as described in ANNEX XII of the Implementing Agreement between the U.S. Department of Energy (DOE) and the Ministry of Energy and Mines of Venezuela.

Summary of Technical Progress

Annex XII prescribes that Lawrence Livermore National Laboratory will develop a computer model to calculate kerogen pyrolysis and petroleum maturation which can run on a VAX computer. A major step in this process was completed during the past quarter by releasing version 1.0 of PMOD. PMOD is a user-friendly pyrolysis model that enables the user to tailor the chemical mechanism for the particular application. The user specifies the reaction network, and the program asks for the information required to calculate the stoichiometric coefficients while maintaining elemental balance. The user then sets up in an interactive manner the kinetic parameters, rock properties, temperature and pressure history, and, for geological cases, the oil expulsion parameters. PMOD execution times on a 386 PC range from a few seconds to a few minutes, depending on the chemical mechanism. Annex XII also prescribes that ways of calculating overpressuring be

developed. That has been accomplished in the code PYROL (Ref. 1), but PYROL is very computer intensive. Pore pressure calculations are expected to be instituted into PMOD without a major impact on execution time.

For the use of such programs as PMOD for predicting where petroleum has been generated, kinetic parameters for the conversion of kerogen to oil and gas are needed. During the past quarter, documentation of programmed pyrolysis for determining oil generation chemical kinetics was completed.[2,3] The two programmed pyrolysis apparatus used were a PYROMAT machine, which used 10-mg samples, and an oil evolution apparatus, which used 35-g samples. The two techniques agreed fairly well.

In the next quarter, the new modeling capability, the chemical kinetic information, and the geological modeling described earlier[4] will be brought together in a final assessment of the petroleum generation, migration efficiencies, and pore pressures in the Maracaibo Basin.

References

1. R. L. Braun and A. K. Burnham, Mathematical Model of Oil Generation, Degradation, and Expulsion, *Energy Fuels*, 4: 132-146 (1990).
2. A. K. Burnham, Oil Evolution from a Self-Purging Reactor: Kinetics and Composition at 2°/min and 2°/h, LLNL Preprint UCRL-JC-103720 (May 1990), submitted to *Energy Fuels*.
3. R. L. Braun, A. K. Burnham, J. G. Reynolds, and J. E. Clarkson, Pyrolysis Kinetics for Lacustrine and Marine Source Rocks by Programmed Micropyrolysis, LLNL Preprint UCRL-JC-103719 (May 1990), submitted to *Energy Fuels*.
4. Pyrolysis Kinetics Applied to Prediction of Oil Generation in the Maracaibo Basin, Venezuela, *Org. Geochem.*, 16 (1990, in press).

IN SITU STRESS AND FRACTURE PERMEABILITY: A COOPERATIVE DOE–INDUSTRY RESEARCH PROGRAM

Sandia National Laboratories
Albuquerque, N. Mex.

Contract Date: Oct. 1, 1986
Anticipated Completion: Sept. 30, 1991
Funding for FY 1990: $200,000

Principal Investigators:
David A. Northrop
Lawrence W. Teufel

Project Manager:
R. E. Lemmon
Bartlesville Project Office

Reporting Period: Apr. 1–June 30, 1990

Objective

This is a cooperative U.S. Department of Energy (DOE)–Industry Research Program between Sandia National Laboratories and Phillips Petroleum Company to study and understand the interrelationships between in situ stresses, natural fractures, and reservoir permeabilities. There are three different but coupled tasks: (1) measurements of in situ stresses in the reservoir and adjacent formations, (2) laboratory deformation and permeability measurements in fractured and intact reservoir rock, and (3) characterization of the natural fracture system in the reservoir. The primary focus is the Ekofisk oil field in the Norwegian sector of the North Sea.

Summary of Technical Progress

The Ekofisk field is the largest of nine chalk reservoirs in the southern part of the Norwegian sector of the North Sea. The reservoir contains a natural fracture system that forms the primary conductive path for produced hydrocarbons and injected fluids. Almost 20 yr of petroleum production of the Ekofisk field has resulted in a 21-MPa (or more) reduction in reservoir pore pressure. The decline in pore pressure has led to an increase in the fraction of the overburden load that must be supported by the structurally weak chalk matrix, which, in turn, has caused significant reservoir compaction and seafloor subsidence.

An important aspect of this work is to assess the possible effects of in situ stress and changes in stress as the result of reservoir depletion, compaction, and subsidence deformation on reservoir permeability and productivity at Ekofisk. It is a well-known observation that fracture aperture will close and conductivity will decrease as the effective normal stress increases. It is, therefore, generally assumed that permeability and productivity of a naturally fractured reservoir will decrease with reservoir depletion and pore pressure drawdown. At Ekofisk, however, maintenance of productivity has been good and reservoir permeability appears to have remained fairly constant with no dramatic decline, even though there has been a 21-MPa (or more) reduction in pore pressure. At least two possible processes may explain this apparent paradox: (1) slippage of fractures and interaction of jointed blocks, which help to maintain some fracture apertures; and (2) generation of compaction–subsidence-induced fractures, which will enhance the local permeability as they become incorporated into the natural fracture system.

Barton et al.[1] have used numerical discontinuum models to study reservoir compaction and subsidence at Ekofisk. Their models consisted of a conjugate set of steeply dipping joints in high- and low-porosity chalk. Loading both the matrix and joints by an internal reduction in pore pressure in uniaxial strain caused joint slip, relative mass bulking, and the near maintenance of joint apertures (and therefore conductivities). Joint slippage and interaction of jointed blocks caused closure of some joints and openings of other joints.

Several laboratory studies have shown that permeability is enhanced locally during the formation and propagation of fractures.[2,3] The high-porosity chalk formations at Ekofisk have low failure strengths. The minimum effective stress magnitudes are low over much of the field (usually less than 9 MPa), and differences between the overburden stress and minimum horizontal stress are now sufficient to cause fracturing in many of these chalk formations (Fig. 1).

Figure 1 shows a Mohr failure envelope for ultimate strength which was constructed from triaxial compression tests using dry samples of a 34% porosity chalk and an envelope for fracture slippage in which a coefficient of friction of 0.60 and no cohesive strength was assumed. The Mohr circle represents the present effective stress state in the C-7 well determined from the effective overburden stress (σ'_v) and the effective minimum horizontal stress ($\sigma'_{H\,min}$). This well is located on the west flank of the structure. The Mohr circle clearly exceeds the envelopes for fracture slippage and failure. If the overburden stress is the maximum effective stress, compaction–subsidence-induced fractures would be high angle shear fractures striking parallel to the maximum horizontal stress direction (i.e., they would be oriented radially around the flanks of the dome and have the same general trend as the radial tectonic-fracture pattern). Therefore compaction–subsidence-induced fractures will have the same general trend as the radial tectonic-fracture pattern around the flanks of the structure and will enhance the local radial permeability anisotropy.

Large variations in the minimum horizontal stress magnitudes occur across the Ekofisk field. On the outer northwest and northeast flanks of the field, the minimum stresses are higher and the stress differences are much lower. Consequently the stress differences in these areas of the field may not be large enough to cause fracture slippage or failure of chalk. In Fig. 2, the Mohr circle represents the present effective stress state in the K-29 well (located on the northwest flank of the structure) determined from the effective overburden stress (σ'_v) and the effective minimum horizontal stress ($\sigma'_{H\,min}$). The Mohr circle clearly does not exceed the envelopes for failure or fracture slippage.

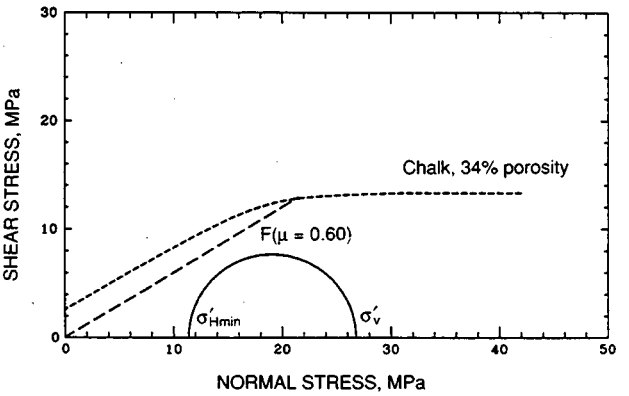

Fig. 2 Plot of normal stress vs. shear stress showing a failure envelope for chalk, an envelope for fracture slippage with the coefficient of friction equal to 0.60, and a Mohr circle representing the effective stress state in the west flank of the Ekofisk K-29 well. P_p = 35.2 MPa. $\sigma'_{H\,min}$, effective minimum horizontal stress. σ'_v, effective overburden stress.

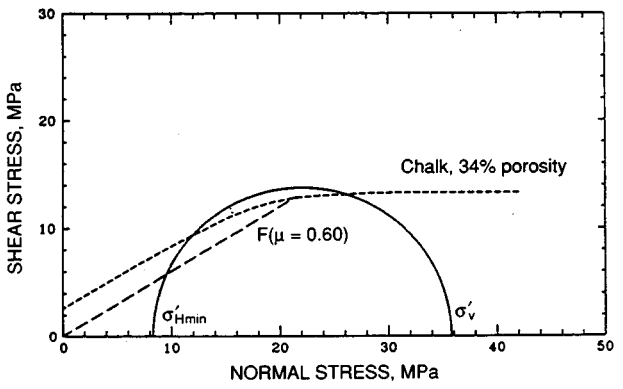

Fig. 1 Plot of normal stress vs. shear stress showing a failure envelope for chalk, an envelope for fracture slippage with the coefficient of friction equal to 0.60, and a Mohr circle representing the effective stress state in the west flank of the Ekofisk C-7 well. P_p = 26.2 MPa. $\sigma'_{H\,min}$, effective minimum horizontal stress. σ'_v, effective overburden stress.

Note that deformation of chalk is a complex process, owing in part to its highly nonlinear compaction behavior under hydrostatic stress as well as time-dependent, stress-path, and strain-path dependent deformation.[4,5] Therefore the failure envelopes in Figs. 1 and 2 should be used only as a general representation of the ultimate strength and failure behavior of chalk in triaxial compression. Moreover, deformation of chalk is influenced by small changes in porosity and quartz content with strength decreasing with increasing porosity and decreasing quartz content.[4] Under a cooperative program, plans are under way to conduct additional laboratory experiments that will better define the deformation behavior of chalk.

This study suggests that shear displacement of fractures and the generation of new fractures during compaction deformation can occur under the current in situ stress state over much of the Ekofisk field and with the present distribution and orientations of natural fractures. This will

be a recurring process in which (1) the apertures of older fractures are opened initially under shear displacement and are then closed with increasing deformation and (2) new fractures are created and become incorporated into the natural fracture system. Under this process, reservoir permeability is maintained, or at least does not dramatically decline, in spite of depletion, and productivity is maintained or helped by the compaction drive.

References

1. N. Barton, L. Harvik, M. Christianson, S. C. Bandis, A. Makurat, P. Chryssanthakis, and G. Vik, Rock Mechanics Modelling of the Ekofisk Reservoir Subsidence, in *Proceedings of the 27th U.S. Symposium on Rock Mechanics*, H. Hartman (Ed.), pp. 267-277, University of Alabama, Tuscaloosa, 1986.
2. M. Mordecai and L. H. Morris, An Investigation Into the Changes of Permeability Occurring in a Sandstone when Failed in Triaxial Stress Conditions, in *Proceedings of the 12th U.S. Symposium on Rock Mechanics*, G. B. Clark (Ed.), pp. 221-239, Rolla, Mo., 1970, A.I.M.E., New York, 1971.
3. J. Farran and R. Perami, Microfissuration, Deformation et Compressibilite des Roches Sous Charges Triaxiales, in *Advances in Rock Mechanics*, Proceedings of the 3rd Congressional International Society of Rock Mechanics, Denver, Vol. 2A, pp. 138-143, 1974.
4. J. P. Johnson, D. W. Rhett, and W. T. Siemers, Rock Mechanics of the Ekofisk Reservoir in the Evaluation of Subsidence, *J. Pet. Technol.*, 41: 717-722 (1989).
5. D. W. Rhett, personal communication.

CHARACTERIZATION AND MODIFICATION OF FLUID CONDUCTIVITY IN HETEROGENEOUS RESERVOIRS TO IMPROVE SWEEP EFFICIENCY

Contract No. DE-AC22-89BC14474

University of Michigan
Ann Arbor, Mich.

Contract Date: Sept. 26, 1989
Anticipated Completion: Aug. 30, 1992
Government Award: $112,000
(Current year)

Principal Investigator:
H. Scott Fogler

Project Manager:
Robert E. Lemmon
Bartlesville Project Office

Reporting Period: Apr. 1–June 30, 1990

Objective

The objective of this work is to develop effective flow-diverting techniques through experimentation, with neutron imaging for flow characterization before and after treatment. Theoretical modeling will be used to identify the important parameters that govern the process of diverting fluids.

Summary of Technical Progress

The work during this quarter focused on a cross-linked foam system for use as a diverting agent during waterfloods. The goal was to investigate the effect of the cross-linking reaction on the generation and propagation of the foam in a porous medium.

Three variations of the foam coreflood were performed:

1. The coinjection of a polyacrylamide (HPAM)–cetylpyridinium chloride (CPC) solution with nitrogen gas.
2. The coinjection of an HPAM–CPC–Cr(III) solution with nitrogen gas.
3. The coinjection of an HPAM–CPC–Cr(III)–NaCl solution with nitrogen gas.

These experiments are summarized in Table 1. The purpose of the first two variations was to differentiate between the pressure drop across a core as the result of the high viscosity foam and the pressure drop as the result of the gelation of the liquid phase of the foam. The third variation was to observe the effect that a high ionic strength fluid had on the apparent cross-linking rate. Note that the apparent gelation time is defined as the time when the injection pressure increases more rapidly than can be accounted for by the generation and propagation of a non-cross-linking foam.

Comparison of runs 1.1 and 2.2 in Fig. 1 shows that the injection pressure increases quicker when the cross-linker is present. This occurred because the aqueous-phase viscosity increased and thus caused a greater resistance to fluid flow. On the basis of pressure-drop readings across the length of the core, it was observed that the foam in run 2.2 stopped propagating at the apparent gel time. On the contrary, the foam in run 1.1 propagated through the entire core because it never gelled. The effect of the reactant concentrations on the apparent gel time is shown in Figs. 2a and 2b. In each case, the run with the greater concentration of a particular reactant had the shorter apparent gel time.

The effect of the apparent gel time is illustrated in Fig. 3, where the distribution of resistance factors is given for each core. The foam resistance for run 2.1 was concentrated in the first 25% of the core, whereas run 2.3 had damage over the last 75% of the core, which indicates greater foam propagation.

Figure 4 shows the effect of salt on the apparent gel time. The salt affected the gel in two ways: (1) the apparent

TABLE 1

Summary of Foam Floods*

Run	Foam solution composition	Q_g/Q_l	Q_l, mL/min	ko, d	$\left(\frac{\Delta P}{\Delta P_{initial}}\right)_{max}$ overall	Apparent gel time, s	Depth of penetration
1.1	10,000 ppm HPAM 1,000 ppm CPC	5	0.75	11	281	–	Full
1.2	5,000 ppm HPAM 500 ppm CPC	5	0.75	11	107	–	Full
2.1	10,000 pm HPAM 1,000 ppm CPC 1236 ppm Cr(III)	5	0.75	11	428	1000	1 in.
2.2	10,000 ppm HPAM 1,000 ppm CPC 1071 ppm Cr(III)	5	0.75	11	472	950	1 in.
2.3	10,000 ppm HPAM 1,000 ppm CPC 705 ppm Cr(III)	5	0.75	11	460	1900	3.5 in.
2.4	5,000 ppm HPAM 500 ppm CPC 1098 ppm Cr(III)	5	0.75	11	380	1700	Full†
3.1	10,000 ppm HPAM 1,000 ppm CPC 1105 ppm Cr(III) 20,000 ppm NaCl	5	0.75	11	441	1700	Full†
3.2	5,000 ppm HPAM 500 ppm CPC 1118 ppm Cr(III) 20,000 ppm NaCl	5	0.75	11	308	3800	Full†

*Q_g/Q_l, gas-to-liquid volumetric flow rate; ko, initial permeability; $(\Delta P/\Delta P_{initial})_{max}$, maximum pressure drop across the core divided by the initial pressure drop across the core; HPAM, partially hydrolyzed polyacrylamide; CPC, cetylpyridinium chloride; and Cr(III), trivalent chromium.

†Foam propagated the length of the core, but polymer retention as the result of gelation caused the viscosity of the foam to be low.

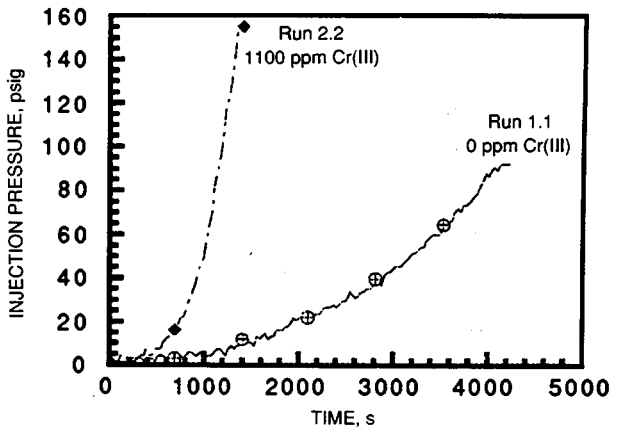

Fig. 1 Effect of cross-linking on the apparent gel time.

gelation reaction was slower and (2) the gel that formed did not stabilize the foam as well as the gel that formed in deionized water (see Table 2).

Figure 5 shows the effect of salt on the resistance factor distribution in a core. The addition of salt appears to have allowed the foam to propagate further into the core. However, since the resistance factor for run 3.1 is so much lower than that for run 2.1, the salt must have also weakened the foam by preventing a strong gel from forming in the aqueous phase.

Waterfloods of Stabilized Foams

A waterflood was performed on each core immediately following the injection of the cross-linking foam system, i.e., no shut-in period. The waterflood conditions, as well

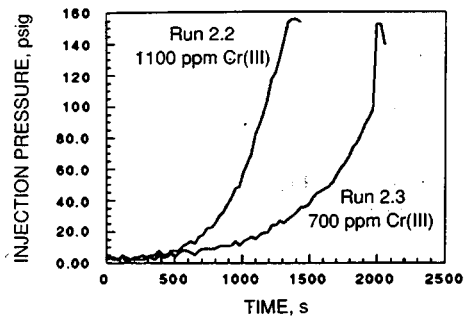

Fig. 2a Effect of chromium concentration on apparent gel time.

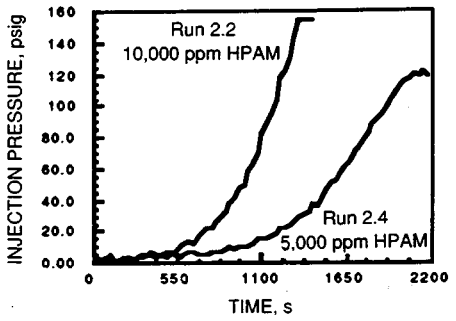

Fig. 2b Effect of polymer concentration on apparent gel time.

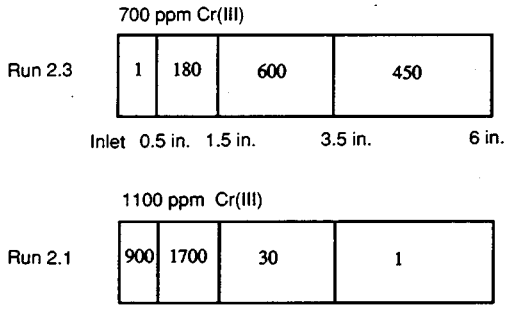

Fig. 3 Effect of chromium concentration on the distribution of resistance factors in the core [resistance factor ($\Delta P_i/\Delta P_{io}$) is shown for each section of the core].

as the initial and final resistance factors, $\Delta P/\Delta P_o$, are shown in Table 2. Runs that displayed total polymer retention during the entire foam flood (runs 2.1 and 2.2) maintained their high resistance factor for the entire waterflood. Runs that produced polymer or foam in the effluent during the foam flood (runs 2.3, 2.4, and 3.1) displayed resistance factors that dropped off to a steady-state value. These latter runs probably had weaker foams that rearranged and flowed during the waterflood.

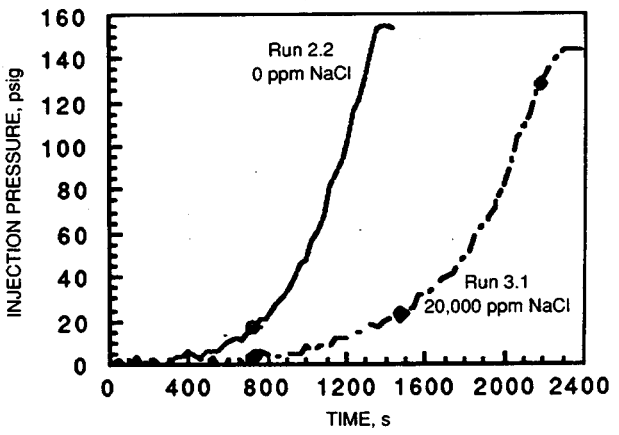

Fig. 4 Effect of salt on the apparent gel time.

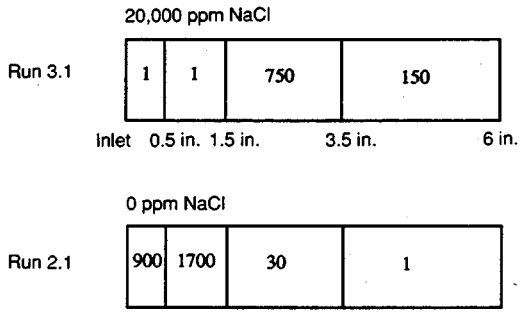

Fig. 5 Effect of salt on the distribution of resistance factors in the core [resistance factor ($\Delta P_i/\Delta P_{io}$) is shown for each section of the core].

TABLE 2

Summary of Waterfloods on Foamed Cores

Run	Solution composition	Waterflood conditions	$\left(\frac{\Delta P}{\Delta P_{initial}}\right)_{start}$	$\left(\frac{\Delta P}{\Delta P_{initial}}\right)_{final}$
2.1	10,000 ppm HPAM 1,000 ppm CPC 1236 ppm Cr(III)	3500 mL @ 5 mL/min	425	350
2.2	10,000 ppm HPAM 1,000 ppm CPC 1071 ppm Cr(III)	5500 mL @ 5 mL/min	460	730
2.3	10,000 ppm HPAM 1,000 ppm CPC 705 ppm Cr(III)	3100 mL @ 5 mL/min	367	73
2.4	5,000 ppm HPAM 500 ppm CPC 1098 ppm Cr(III)	1560 mL @ 5 mL/min	296	185
3.1	10,000 ppm HPAM 1,000 ppm CPC 1105 ppm Cr(III) 20,000 ppm NaCl	2500 mL @ 5 mL/min	213	30

CHARACTERIZATION OF OIL AND GAS RESERVOIR HETEROGENEITY

Contract No. FG22-89BC14403

University of Texas
Austin, Tex.

Contract Date: September 1988
Anticipated Completion: September 1991
Government Award: $235,000
(Current year)

Principal Investigator:
William Fisher

Project Manager:
Chandra Nautiyal
Bartlesville Project Office

Reporting Period: Apr. 1–June 30, 1990

Objectives

Progress in the fifth quarter of research funded under the auspices of Memorandum of Understanding (MOU) Annex I is summarized with respect to seven main subtask areas. These are: (1) definition of the distribution of carbonate sandbar facies for Grayburg reservoirs, (2) definition of three-dimensional (3-D) geometry of carbonate sand bodies, (3) analysis of engineering and petrophysical attributes of reservoir flow units, (4) development and testing of extended conventional oil recovery strategies, (5) characterization of gas reservoirs, (6) geologic and engineering characterization of generic gas reservoir types, and (7) refinement of exploitation strategies. Key areas of progress for the fifth quarter concern subtasks 1, 2, 3, and 6.

Summary of Technical Progress

Subtasks 1 and 2

The purpose of subtasks 1 and 2 is to develop both regional and local models for distribution of key reservoir elements in Grayburg reservoirs, the carbonate sandbar facies. Subtasks 1 and 2 neared completion during the fifth quarter after extensive field mapping in March and April and compilation of those data in May and June.

Regional-scale outcrop mapping included 14 detailed measured sections keyed to the photomosaics that defined the sequence stratigraphic framework of the Grayburg in a completely exposed dip-oriented section. This framework demonstrated the presence of lowstand wedge, transgressive, and highstand system tracts and the clear dominance of pay-quality facies in the highstand tract.

The Grayburg was subdivided into 34 parasequences (genetically related packages of facies bounded by flooding surfaces) within which facies distributions were mapped (Figs. 1 and 2). Particularly interesting is the distribution of ooid grainstone bars and oo-peloid packstone sheets that compose the main reservoir intervals in the subsurface. Seventeen ooid grainstone bars were mapped within the parasequence framework, most being 6 to 10 ft thick and continuous in a dip direction for less than 1 mile (Fig. 1). This is in contrast to the oo-peloid packstone facies, which is comparable in terms of thickness but more laterally continuous in a dip direction (Fig. 2).

Strike dimensions of these facies are currently being assessed in two canyons that provide good 3-D exposure, and preliminary results from nine measured sections in a 1-mile^2 area show much greater variability in facies development of ooid bars, which perhaps indicates development of dip-elongate tidal bar belts.

Permeability analysis will be undertaken within these detailed parasequence windows in the Stone Canyon area and will be initiated this fall.

Subtask 3

The geologic study of the ARCO North Foster Unit and surrounding area is continuing with the receipt of three cores from neighboring leases. The cores are located in leases just south and east of the ARCO lease and are located so as to fill in significant gaps in the cross section constructed from the ARCO data.

Three detailed cross sections have been constructed—one across the ARCO North Foster Unit and two across the Cities Service Johnson Grayburg Unit to the north. Nine major cycles, each defined by a siltstone at the base, have been carried out throughout the study area. However, several other cycles are recognizable at least locally, which indicates the presence of smaller cycles in numbers equivalent to those in the outcrop in the Guadalupe Mountains (17 in the equivalent section).

Thickness–facies maps of the correlation units demonstrate the dominance of tidal-flat mudstone and intertidal to shallow-water subtidal coarse-grained grainstone facies in the western portion of the ARCO North Foster Unit. These facies change to the east into dominantly very fine grained facies that, largely as a result of leaching of sulfates, have high porosity and permeability. The thickest part of the highly altered facies corresponds to the highest portion of the structure in the unit and consequently the area of highest production.

Subtask 6

Subtask 6, geologic and engineering characterization of generic gas reservoir types, continued to focus on the application of detailed outcrop information from the Ferron Sandstone to deltaic gas reservoirs on the Gulf Coast. Activities during the quarter included the implementation

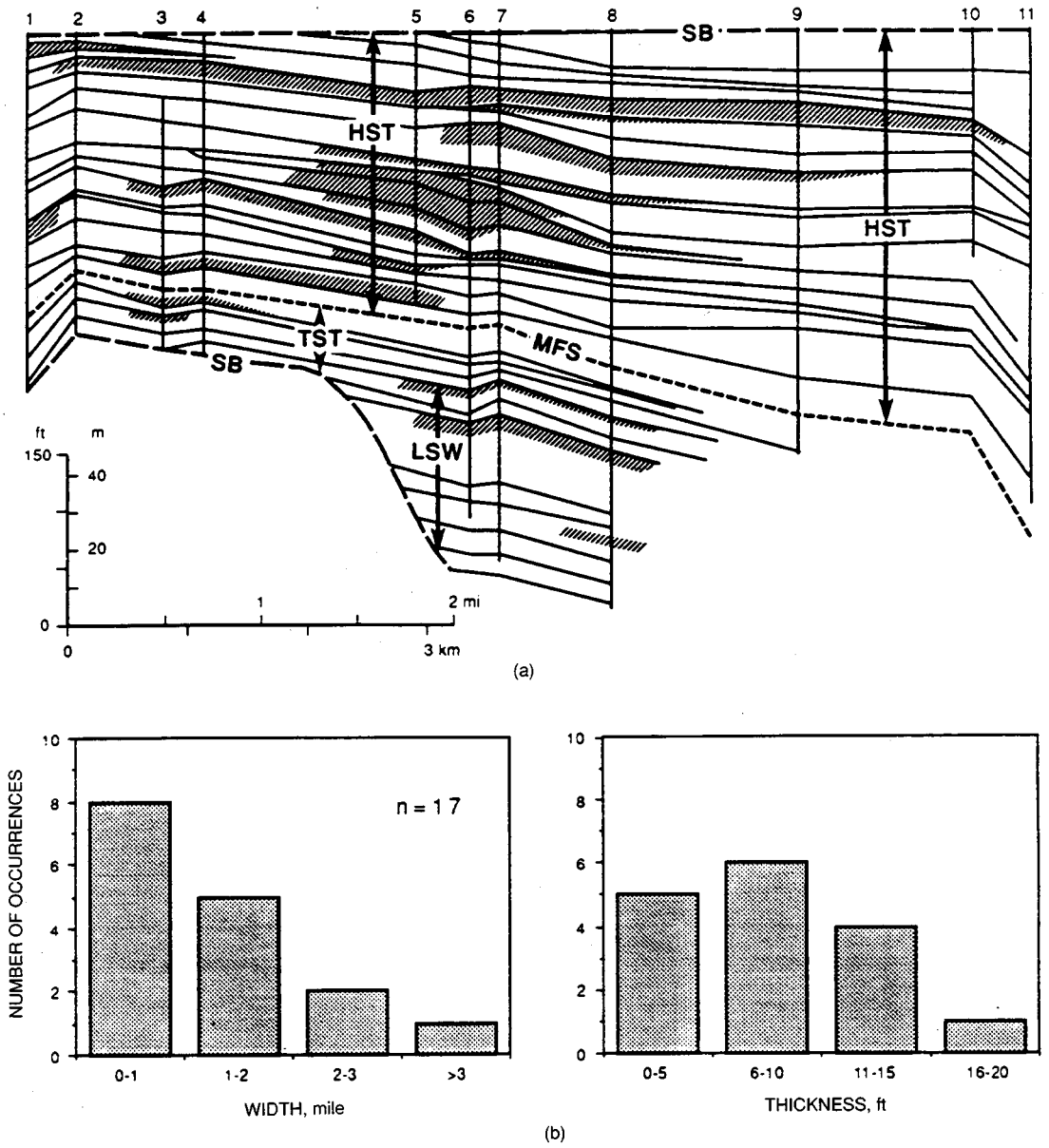

Fig. 1 (a) Distribution of ooid grainstone facies within the Grayburg Formation sequence stratigraphic framework, Shattuck Valley escarpment, Guadalupe Mountains, New Mexico. SB, sequence boundary; LSW, lowstand systems tract; TST, transgressive systems tract; HST, highstand systems tract; MFS, maximum flooding surface. Numbers 1 through 11 at top of section mark position of measured sections. Unlabeled unit boundaries are parasequence boundaries. (b) Histogram showing width of ooid grainstone facies in a direction parallel to depositional dip and average thickness of that facies.

of a workshop on the project and initiation of field work in the summer field season.

The first part of the quarter was spent preparing for a workshop to review the project with other researchers active in this area of research. The workshop, titled *Characterization and Quantification of Geologic and Petrophysical Heterogeneity in Fluvial–Deltaic Reservoirs*, was held at the Bureau of Economic Geology on May 1–2, 1990. Invitations to attend the workshop were extended to 36 potential participants, 31 of whom accepted the invitation. Of those attending, 22 were geologists or geostatisticians; the rest were engineers.

Field work has begun. The agenda for May and June was to complete the Teardrop Hill window and then to proceed to excellent exposures of the fluvial section in multiple canyons in the Browning Mine area during July. Detailed mapping at Teardrop has indicated the presence of an incised valley (some 40 ft deep) chopping through Sand 4. The presence of incised valleys further supports the selection of the Ferron as a Gulf Coast analog.

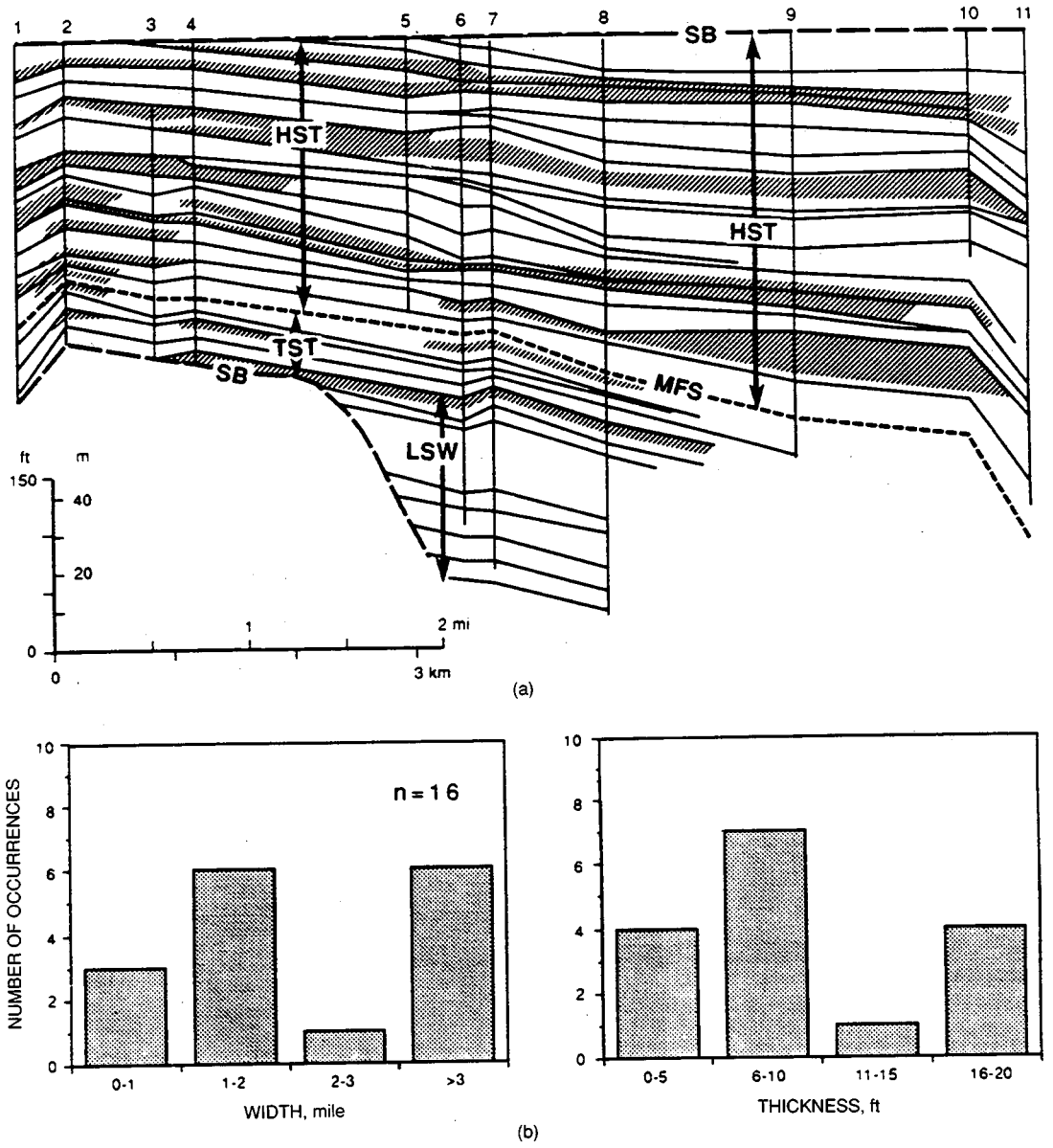

Fig. 2 (a) Distribution of oo-peloid packstone facies within the Grayburg Formation sequence stratigraphic framework, Shattuck Valley escarpment, Guadalupe Mountains, New Mexico. SB, sequence boundary; LSW, lowstand systems tract; TST, transgressive systems tract; HST, highstand systems tract; MFS, maximum flooding surface. Numbers 1 through 11 at top of section mark position of measured sections. (b) Histogram showing width of oo-peloid packstone facies in a direction parallel to depositional dip and average thickness of that facies.

Thirty sections 100 to 200 ft apart have been described along the Teardrop Hill window. Gas flow measurements were obtained at 1-ft vertical intervals for each measured section. Work on this window is almost complete; plans are under way to move updip into the fluvial section in early July.

DEVELOPMENT OF NUCLEAR MAGNETIC RESONANCE IMAGING/SPECTROSCOPY FOR IMPROVED PETROLEUM RECOVERY

Contract No. FG07-89BC14446

Texas A&M University
College Station, Tex.

Contract Date: Sept. 15, 1989
Anticipated Completion: Dec. 15, 1992
Government Award: $290,000
(Current year)

Principal Investigators:
A. T. Watson
R. W. Flumerfelt
J. W. Jennings
M. P. Walsh

Project Manager:
Edith Allison
Bartlesville Project Office

Reporting Period: Apr. 1–June 30, 1990

Objectives

The overall objectives are to develop and apply nuclear magnetic resonance imaging (NMRI) and computerized tomography (CT) X-ray scanning methods for determining rock fluid and petrophysical properties and for fundamental studies of multiphase flow behavior in porous media. Specific objectives are to: (1) develop NMRI procedures for measuring porosity, permeability, pore-size distribution, capillary pressure, and wetting characteristics; (2) apply imaging methods for improved methods of determining two- and three-phase relative permeability functions; (3) apply NMRI for development of a better understanding of dispersed phase displacement processes; and (4) apply imaging methods to develop a better understanding of saturation distributions and fingering during miscible displacements. The objectives have been organized into four subtasks. Progress reports from each subtask are provided.

Summary of Technical Progress

Development of NMRI and CT Scanning for the Determination of Rock–Fluid and Petrophysical Properties

Over the past quarter there has been increased scan activity for data acquisition purposes. Preliminary screening tests were performed to determine which cores were suitable for NMRI. A complete set of three-dimensional (3-D) NMRI data was collected for each suitable core. From these data, both bulk and localized porosities can be determined. Gravimetric analysis was also performed to determine bulk porosities for these cores. These values will be used for comparison with values obtained from the NMRI. NMRI data were collected on a glass bead pack. This collection of data will be used as a reference in the development of the porosity correlation length.

FORTRAN programs were written for the purpose of transferring data from the NMRI to a mainframe computer. The mainframe is used to process, convert, and manipulate the raw data. In addition, programs have been written to transfer data from the mainframe to the Macintosh environment. Image analysis will be performed with software written for the Macintosh.

Preliminary work has begun on image analysis; this includes image enhancement through histogram equalization and noise reduction. Also, work has begun on the development of the porosity correlation length. This is a statistical method that characterizes porosity distribution.

Development of NMRI and CT Scanning for Characterizing Conventional Multiphase Displacement Processes

Three-dimensional (3-D) saturation image data were obtained during the transient two-phase displacement experiments carried out previously. The data have been transferred from the NICOS operating system to a Hewlett-Packard 9000 for quantitative analysis. The details of the quantitative analysis to be done with the 3-D data will be developed in the next quarter.

Construction of the flow system to carry out the next set of displacement experiments is in progress. Several improvements are being made to the initial experimental arrangements used to demonstrate the ability to image saturation distributions. An epoxy-cured core holder has been designed for use instead of the Hassler cell. This change will help avoid leaks around the core, and it will allow pressure taps to be mounted at locations along the length of the core. The cured epoxy (Stycast 2651) has been checked to see that the NMR signal obtained during spectroscopy experiments is sufficiently small so that image data acquired during displacement experiments will not be influenced by the epoxy. The PC-AT data acquisition system (DAS-08 PGA A/D converter, STA-08 Screw Terminal Board, Validyne Pressure Transducer, and Labtech Notebook software) has been assembled for measuring real-time data (pressure vs. time). It has been demonstrated that generated pressure signals can be observed. The data acquisition system will be accurately calibrated when the dead-weight tester is received. The syringe pumps (Isco LC5000) were checked to see that they work properly, and they are ready to be integrated into the experimental setup.

A more extensive simulation model for displacement experiments is being developed for use with the computer code for estimating relative permeability and capillary pressure functions from laboratory experiments. The new model

will allow for 3-D representation of up to three fluid phases. Rock properties may be specified at each grid block in the finite-difference solution. The algorithm will take advantage of the vectorization capabilities of the Texas A&M Cray computer.

A pulse programming sequence has been developed to measure self-diffusion coefficients employing pulse gradient spin echoes. The sequence will be used to measure apparent diffusion coefficients under conditions of restricted diffusion. This information will be used to characterize the microscopic structure of porous media. The process of checking the pulse sequence and analysis to estimate diffusion coefficients is under way. Experiments have been performed with phantoms of pure water and bead packs.

Development of NMRI and CT Scanning for Characterizing Dispersed Phase Processes

The use of NMR spectroscopic methods to measure fractional wettability is based on the observation that the surfaces of porous media contribute greatly to the relaxation rate of fluids in the pores. The inversion recovery method was successfully applied to determine T_1 (spin-lattice relaxation time) for the glass bead packs filled with water. An important observation in the T_1 measurements was multiexponential decay. The reasons for this multiexponential decay as well as the proper representation of T_1 for a specific heterogeneous system require further study. The spin-locking pulse sequence has also been developed for $T_{1\rho}$ (spin-lattice time in rotating frame) measurements.

Multicycle capillary pressure measurements were completed for dispersed and nondispersed phase systems. The parametric experimental runs show: (1) a broad pore size distribution appears to be favorable with respect to bubble and lamella generation; (2) an increase in the fraction of oil-wet surfaces causes decreases in the irreducible and residual saturations at the end of drainage and imbibition; and (3) the most dramatic improvement for displacement and trapping is achieved between the zero concentration and critical micelle concentration.

A dynamic foam displacement apparatus was constructed for the study of mobility relations as well as capillary and trapping phenomena. The tests of main cell and other systems in a CT scanner are under way.

A foam drainage cell was designed for measuring in situ foam texture and drainage mechanisms under fixed capillary pressure conditions. This cell will be used to characterize the local liquid film intensity (stability) with conductivity and NMRI methods.

Miscible Displacement Studies

The flow test conducted in a 4 in. × 12 in. cylindrical, sandstone core has been completed. The purpose of this unit mobility ratio test was to: (1) examine CT scanning times; (2) test the flow system integrity; and (3) test image storage, retrieval, and reconstruction. The designed flow system and core holder worked satisfactorily. In addition, image storage was carried out satisfactorily.

The process of carrying out image reconstruction is under way. This involves downloading the image data from the CT scanning storage device to the prime computer so it can be transferred to other data processing devices. Presently, two image reconstruction software packages are being evaluated: (1) CATPIX, donated by Shell, and (2) in-house software developed by graduate students within the department. The requirements of the software are that it reconstruct the images in various 2- and 3-D representations and that it requires a minimum amount of time and effort. Image reconstruction is a very important part of developing the CT scanner for petroleum engineering applications.

MINOR AND TRACE AUTHIGENIC COMPONENTS AS INDICATORS OF PORE FLUID CHEMISTRY DURING MATURATION AND MIGRATION OF HYDROCARBONS

Contract No. DE-AC22-90BC14656

Texas A&M University
College Station, Tex.

Contract Date: May 22, 1990
Anticipated Completion: May 21, 1992
Government Award: $36,773

Principal Investigator:
Thomas T. Tieh

Project Manager:
Edith C. Allison
Bartlesville Project Office

Reporting Period: Apr. 1–June 30, 1990

Objectives

The primary objectives of the proposed study are to: (1) determine the petrological, mineralogical, minor element, and isotopic chemistry of late authigenic sulfides in the Smackover formation of the North Louisiana Salt Basin; (2) determine the abundance, distribution, and nature of occurrence of uranium and thorium in these rocks; (3) assess whether spatial and temporal variations in sulfide mineralogy, as well as in the abundance and nature of occurrence of uranium and thorium are reflective of pore fluid evolution during hydrocarbon maturation and migration in the Smackover of the North Louisiana Salt Basin; and

(4) integrate this information with that obtained by conventional studies of diagenesis to gain further insight into the processes operative during late-stage diagenesis of the Upper Smackover formation of the North Louisiana Salt Basin.

The objectives of task 1 are to: (1) select a suite of ten cores of the Upper Smackover from the North Louisiana Salt Basin; and (2) select sample cores on the basis of position within the basin, facies changes, and porosity variations.

Summary of Technical Progress

The objectives of task 1 have been partially fulfilled. Four Upper Smackover cores have been obtained from: (1) Lamar Hunt Allen 1, Columbia Co., Arkansas; (2) General Crude Lena Halbfass 1, Union Parish, Louisiana; (3) Tenneco Lowe 1, Claiborne Parish, Louisiana; and (4) Tenneco Seeger-Waller 1, Claiborne Parish, Louisiana.

The two Claiborne Parish, Louisiana, cores are from the Haynesville field in North Louisiana. The Tenneco Lowe 1 core is from a hydrocarbon producing well, whereas the Tenneco Seeger–Waller 1 core is from a dry hole. These two wells were chosen to evaluate the effect of hydrocarbon migration on authigenic sulfide mineralogy. Porosity and permeability data for these two wells have been requested from Core Laboratories in Houston. Samples have been taken from both of these cores for thin sectioning. Polished thin sections from the Lowe 1 core have been examined in detail to help ensure that sampling of the other cores is representative and effective.

Petrographic examination of the Tenneco Lowe 1 core revealed the close association of the late-stage authigenic sulfides to late-stage authigenic dolomite, anhydrite, barite, and celestite. This association will be carefully studied because these minerals may also be indicators of late-stage pore fluid chemistry. The occurrence of these minerals with the authigenic sulfides is reminiscent of Mississippi Valley-type sulfide deposits.

Note also that the authigenic sulfides, dolomite, and anhydrite are often found along stylolites. This suggests the possibility that some stylolites may have acted as conduits for late-stage pore fluids. Preliminary results examining this possibility were presented at the annual meeting of the American Association of Petroleum Geologists in San Francisco on June 4, 1990.

This project is proceeding ahead of schedule. In the next quarter, task 1, acquisition and sampling of cores, will be completed. Task 2, the petrographic examination of the ten cores, will be half completed by the end of the next quarter. However, there will be some overlapping of tasks. The production of each batch of thin sections takes several weeks. During this time it will be expedient to perform some of the analyses of tasks 3 and 4, electron microprobe, instrumental neutron activation, and sulfur isotopic analyses, on petrographically characterized samples. Thus it is expected that preliminary data of tasks 3 and 4 will also be gathered by the end of next quarter.

GEOPHYSICAL AND TRANSPORT PROPERTIES OF RESERVOIR ROCKS

Contract No. DE-AC22-89BC14475

University of California
Berkeley, Calif.

Contract Date: Sept. 22, 1989
Anticipated Completion: Aug. 31, 1992
FY 1990 Project Cost: $137,000

Principal Investigator:
Neville G. W. Cook

Project Manager:
Robert E. Lemmon
Bartlesville Project Office

Reporting Period: Apr. 1–June 30, 1990

Objective

The objective of this research is to understand, by analysis and experiment, how fluids in pores affect the geophysical and transport properties of reservoir rocks. Definition of reservoir characteristics, such as porosity, permeability, and fluid content, on the scale of meters, is the key to planning and control of successful enhanced oil recovery (EOR) operations. Equations relating seismic and electrical properties to pore topology and mineral–fluid interactions are needed to invert geophysical images for reservoir management. Both the geophysical and transport properties of reservoir rocks are determined by pore topology and the physics and chemistry of mineral–fluid and fluid–fluid interactions.

Summary of Technical Progress

During this quarter work continued on three activities: one-dimensional (1-D) percolation tests with the use of Wood's method, analysis of pore structure by first-order analytical techniques, and measurement of seismic properties of sandstone samples saturated with a variety of fluids. The percolation tests provide quantitative data needed to relate pore topology to fluid-flow properties. Seismic measurements provide data to evaluate the relative effects of pore structures, in particular, thin cracks, as opposed to more equidimensional pores, on wave propagation.

One-Dimensional Percolation

During the first quarter of the year, 1-D percolation experiments were performed on Berea sandstone and Indiana limestone samples with Wood's metal as the nonwetting fluid. Time dependence of saturation in 1-D percolation was also found and reported.

During the second quarter, the investigation of the distribution of Wood's metal in the specimens and the effect of this distribution on permeability continued. Properties were first measured on the whole sample, which was then sectioned and the properties measured again on each section. Results are shown in Fig. 1. The samples were not uniformly saturated throughout, but there was a gradation of decreasing saturation in the direction of percolation. There is a large difference in the saturation of two halves for the sample DS2, which was quenched instantaneously after percolation, whereas the difference decreases as more and more time is allowed for percolation in samples DS3 and DS4. The instantaneous percolation gives the time of flow through the shortest interconnected path having the smallest constriction of 24-μm diameter. This diameter corresponds to the capillary pressure at which all these samples were percolated. The gradation of saturation and the decrease of this gradation with time give an idea of the tortuosity of the interconnected path as well as the distribution of sizes along the interconnected pathway.

Next an investigation was conducted to determine how the fluid-flow properties of the rocks are affected by partial occupancy of the bigger pore spaces by the nonwetting fluid. The average intrinsic freshwater permeability of the Berea sandstone samples was approximately 330 mD before impregnation. The residual absolute permeability to fresh water was measured on the two halves of each of the three samples. The results are summarized in Fig 1. For more precise information on the gradation of saturation and the residual absolute permeability, the halves of sample DS3 were divided again and the saturation was geometrically determined on all four quarters. The residual permeability values on the four quarters presented some very interesting results. The permeability is reduced to just 3% of the original value when 62% of the comparatively smaller pore spaces are still available (first quarter) and 25% of the original value when just 8.8% of the bigger pores are occupied (last quarter). The microscopic examination of these samples is currently in progress.

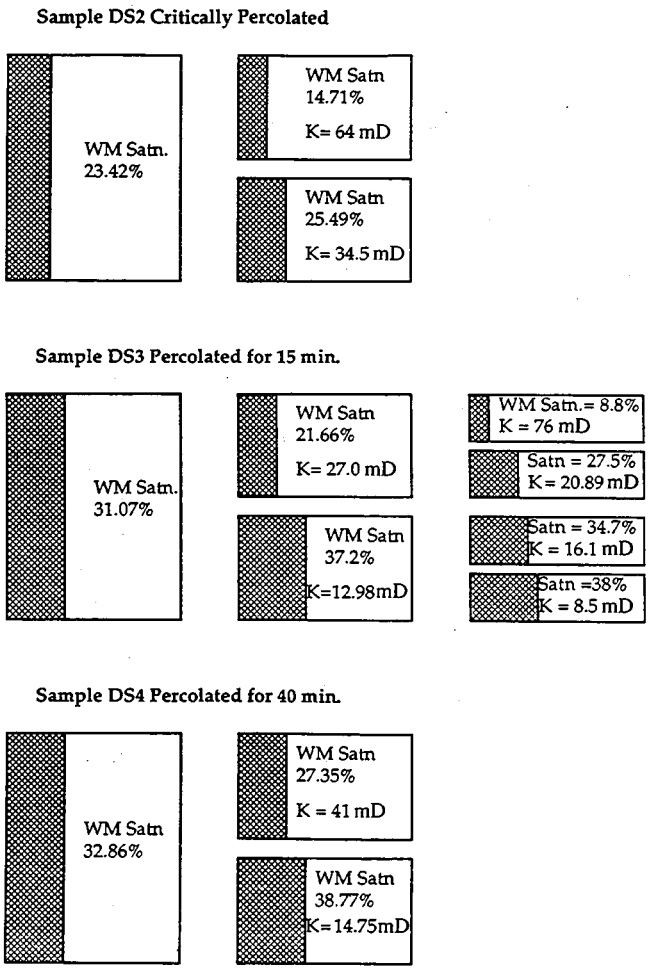

Fig. 1 Distribution of Wood's metal saturation [stippled portion (WM satn.)] and permeability (K) in whole sectioned samples.

Effect of Pore Shape on Hydraulic Conductivity

As part of the analysis of the relationships between pore structure and transport properties, the effect of pore shape on permeability was studied with the torsion analogy concept borrowed from the theory of electricity. The general solution of the torsion problem of prismatic bars of noncircular sections is used.

If a stress function $\Phi(x,y)$ is assumed to exist such that the equations of static equilibrium are satisfied, then the equation of compatibility in a region Γ in z–y plane becomes

$$\frac{\delta^2\Phi}{\delta z^2} + \frac{\delta^2\Phi}{\delta y^2} = -2 \qquad (1)$$

The torsional rigidity is, by definition,

$$D = 2G\int_{\Gamma} \Phi \, dA \qquad (2)$$

where G is the shear modules of elasticity on A, the area of interest.

The equation of conservation of momentum or equation of motion for viscous pipe flow in a region Γ is

$$\nabla^2 u(z,y) = \frac{1}{\mu}\frac{\delta\rho}{\delta z} \tag{3}$$

where u = fluid velocity
μ = viscosity of the fluid
ρ = fluid pressure

From the comparison of Eqs. 1 and 3, the following can be written

$$u = -\frac{1}{2\mu}\frac{\delta\rho}{\delta z}\Phi \tag{4}$$

Then the continuity equation for hydraulic flux can be expressed by

$$Q = \int_\Gamma u dA = -\frac{1}{2\mu}\frac{\delta\rho}{\delta z}\int_\Gamma \Phi\, dA = \frac{-D}{4\mu G}\frac{\delta\rho}{\delta z} \tag{5}$$

Therefore, if the torsional rigidity D of the section is calculated, the hydraulic conductivity can be calculated. Results of this analysis show that, for cross sections of equivalent areas after normalizing permeability with respect to the equivalent circular radius a_o,

$$\begin{aligned} K_{circle} &= 0.13a_0^2 > K_{square} \\ &= 0.11a_0^2 > K_{equilateral\ triangle} \\ &= 0.09a_0^2 \end{aligned} \tag{6}$$

where K_{circle} is permeability. The effect of pore shape on hydraulic conductivity is a minor effect compared with connectivity of the pore spaces.

Seismic Measurements

For the evaluation of the role of grain contacts on the seismic properties of sedimentary rock, attenuation and velocities were measured in alundum and sintered glass beads. Unlike sedimentary rocks, both artificial specimens show very little dependence of velocity and attenuation on uniaxial load. This observation is consistent with scanning electron microscope (SEM) observations, which show well-bonded contacts.

Digby's[1] velocity predictions for a random packing of bonded spheres were compared with ultrasonic measurements (center frequency ≈ 700 kHz) made on oven-dried sintered glass beads. Physical parameters in Digby's expressions, such as the coordination number, particle radius, and bond radius, were obtained from SEM photomicrographs. Measured P- and S-wave velocities for dry sintered glass beads are 2836 and 1712 m/s, respectively, compared with Digby's theoretical estimates of 2635 and 1839 m/s (Fig. 2). The Biot velocity predictions for water-saturated glass beads (Fig. 2) agree well with the measured values and Biot estimates obtained in other studies on sintered beads.[2]

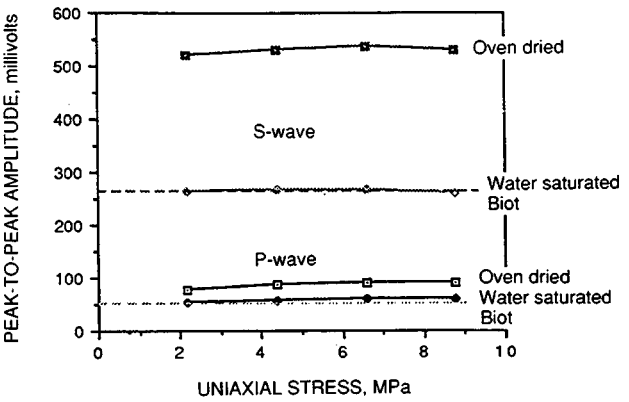

Fig. 2 Measured and theoretical P- and S-wave velocities in dried and water-saturated sintered glass beads.

The Biot theory is known to give reasonable velocity estimates for sedimentary rocks, but attenuation predictions are notorious for underestimating the observed attenuation, which suggests that other loss mechanisms may be operative. Unlike sedimentary rock, sintered glass beads have no low aspect ratio cracks. Thus the dissipation of seismic energy should be controlled by the relative displacement of the fluid and porous frame as described by Biot.[3] In contrast to Winkler and Murphy,[4] significant P- and S-wave attenuation was observed for the water-saturated beads (Fig. 3). Good Biot estimates of both P- and S-wave attenuation were obtained from a structural parameter, $\alpha = 1.25$, appropriate for a coarse-grain material. Berryman's[5] theoretical prediction for spherical particles, $\alpha = 1.25$, predicts too little P- and S-wave attenuation. Velocities were found to be relatively insensitive to the selected value of α.

Future work will continue with artificial sintered porous materials, such as glass beads and alundum, and with fluids with similar viscosities and different chemical properties. The measured velocities and attenuation will be compared with Biot predictions to assess the relevance of fluid chemistry on seismic properties.

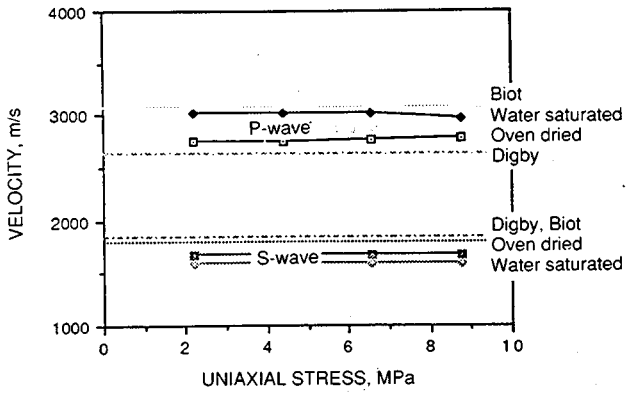

Fig. 3 Measured and theoretical P- and S-wave velocities in oven-dried and water-saturated sintered glass beads.

References

1. P. J. Digby, *J. Appl. Mech.*, 48: 80-808 (1981).
2. P. R. Ogushwitz, *J. Acoust. Soc. Am.*, 77: 429 (1985).
3. M. A. Biot, *J. Acoust. Soc. Am.*, 28: 179-191 (1956).
4. K. W. Winkler and W. F. Murphy III, *J. Acoust. Soc. Am.*, 76: 820-825.
5. J. G. Berryman, *Appl. Phys. Lett.*, 37: 382-384 (1980).

LABORATORY MODELING AND FIELD DEVELOPMENT OF BOREHOLE SEISMIC IMAGING TECHNIQUES USING SEISMIC WAVE FIELD MEASUREMENTS

Contract No. DE-AC22-89BC14478

Colorado School of Mines
Golden, Colo.

Contract Date: Sept. 25, 1989
Anticipated Completion: Sept. 25, 1992
Funding for FY 1990: $160,337

Principal Investigator:
A. H. Balch

Project Manager:
Robert E. Lemmon
Bartlesville Project Office

Reporting Period: Apr. 1–June 30, 1990

Objective

The objective of the research program is to develop processing, imaging, and interpreting techniques for the use of crosswell seismic data to acquire a higher resolution image of hydrocarbon-bearing formations to aid in the extraction (i.e., hydrocarbon production) process. The program consists of overlapping activities: (1) use of physical acoustic models to study crosswell seismic phenomena and develop processing (imaging) and interpretation procedures; (2) field test and demonstration of the crosswell procedure in a controlled, known, geological environment; and (3) test of the procedures in an actual oil or gas field or both.

Summary of Technical Progress

The Peoria Field Model

A physical model of an actual oil field was constructed during the report period. This model was based on a geologic cross section developed in consultation with Dr. Robert Weimer of the Geology Department of Colorado School of Mines. The cross section is shown in Fig. 1. A diagram of the actual model, based on this section, is shown in Fig. 2. It is constructed from Lexan and Plexiglas at a scale of approximately 100:1.

A reconnaissance, or preliminary, crosshole survey was made on the physical model. Five "common source gathers" were created; each gather contains 128, three-component, detector locations. This amounts to $128 \times 5 \times 2$, or 1280 separate recordings. These data will be processed and imaged before a complete data set is obtained. A typical common source data set is shown in parts a and b of Fig. 3. There are many good-quality, reflected coherent events in these data. The possibility of successfully imaging the horizons shown in Figs. 1 and 2 is likely.

Separation of the modes before attempting migration or imaging is desirable. A method described by Dankbaar[1] is being used. The results of one such mode separation are shown in parts a and b of Fig. 4.

Because the medium has space–variable velocity, a velocity grid must be created for the model. A source travel time grid for every point in the medium is also required. When these files are created, the migration will be performed.

When satisfactory partial images are obtained for these data, a production cross-borehole run on the model will commence. At a minimum, the horizontal layers should be delineated. If the pinch-out in the "J" sand (producing horizon) is delineated, the procedures will be considered successful.

Field Test in a Controlled Geologic Environment

Preliminary surveys are under way at the Colorado School of Mines Experimental Mine at Idaho Springs. At the location the boreholes, approximately 360 ft deep, straddle a void whose location and size are known. Currently, logistic and technical problems are being worked on. A Bolt DHS 5500 borehole air gun is being used as a source. An EG&G Geometrics 2400 seismic recording system is being used for recording.

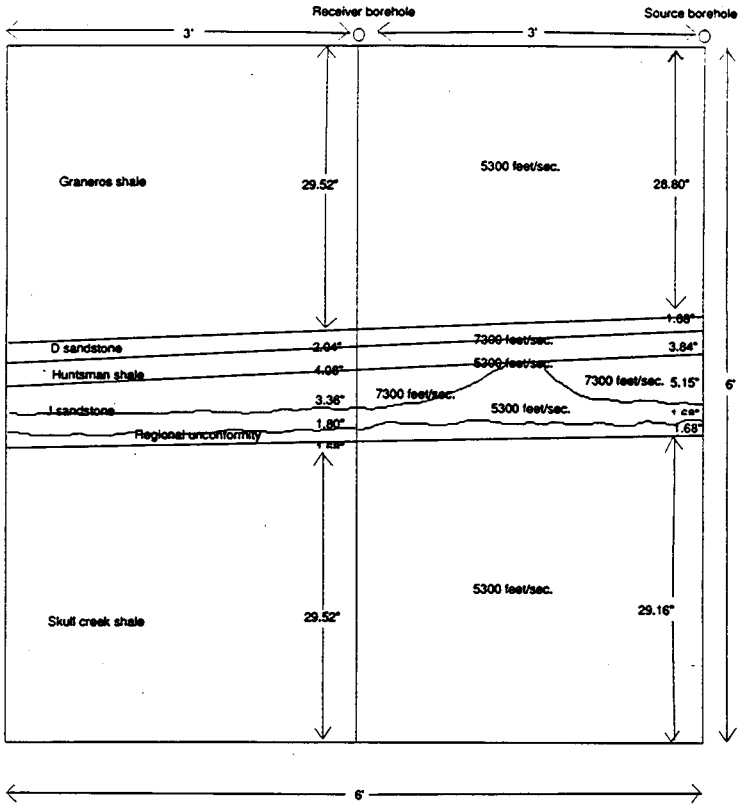

Fig. 1 Simplified geologic model of the Peoria Field, Colorado. Note the productive "J" sand pinch-out beneath the Huntsman shale.

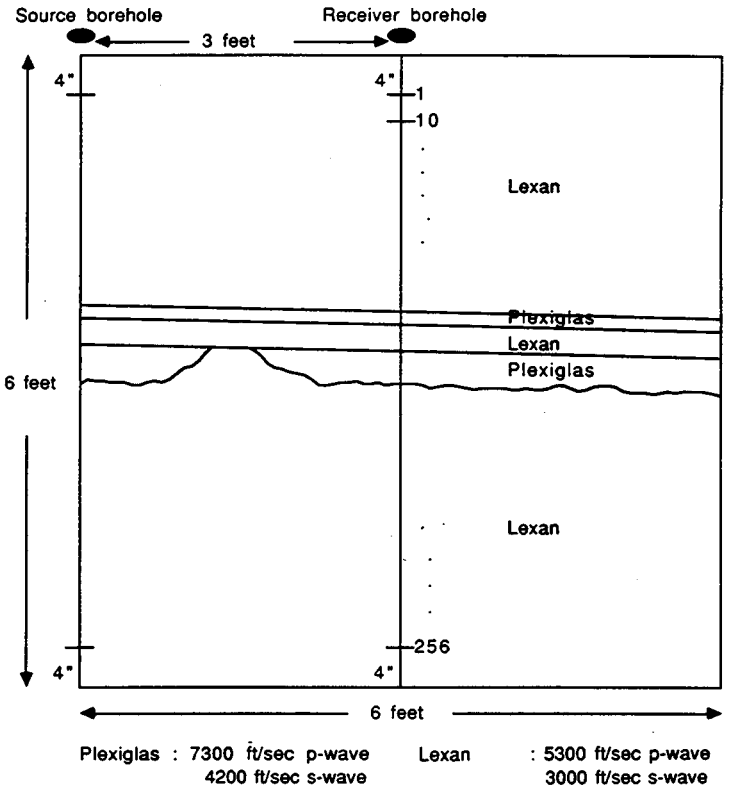

Fig. 2 Drawing of the actual physical model of the Peoria Field (based on the geologic model in Fig. 1).

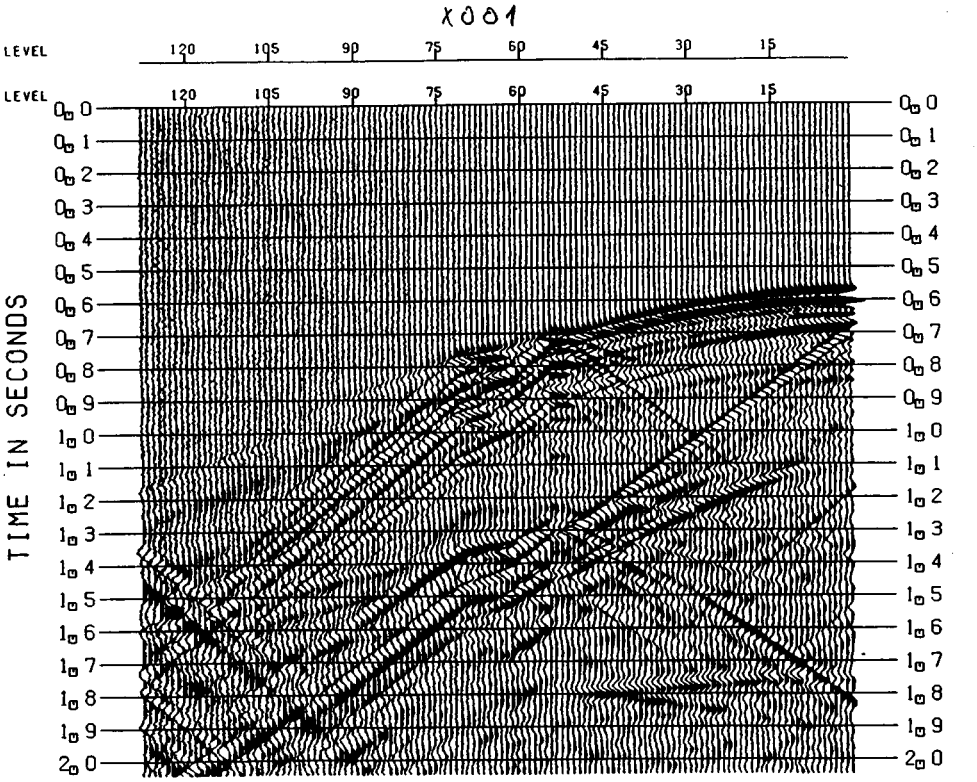

(a)

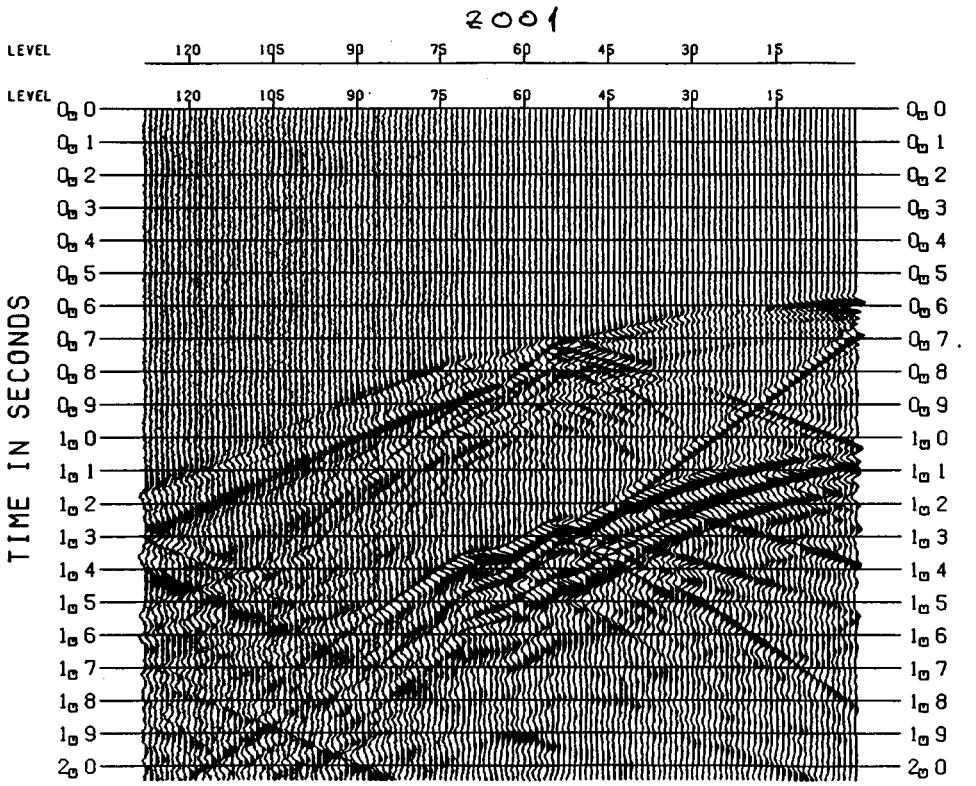

(b)

Fig. 3 Sample cross-borehole data set obtained from the model in Fig. 2 showing horizontal (a) and vertical (b) components of motion.

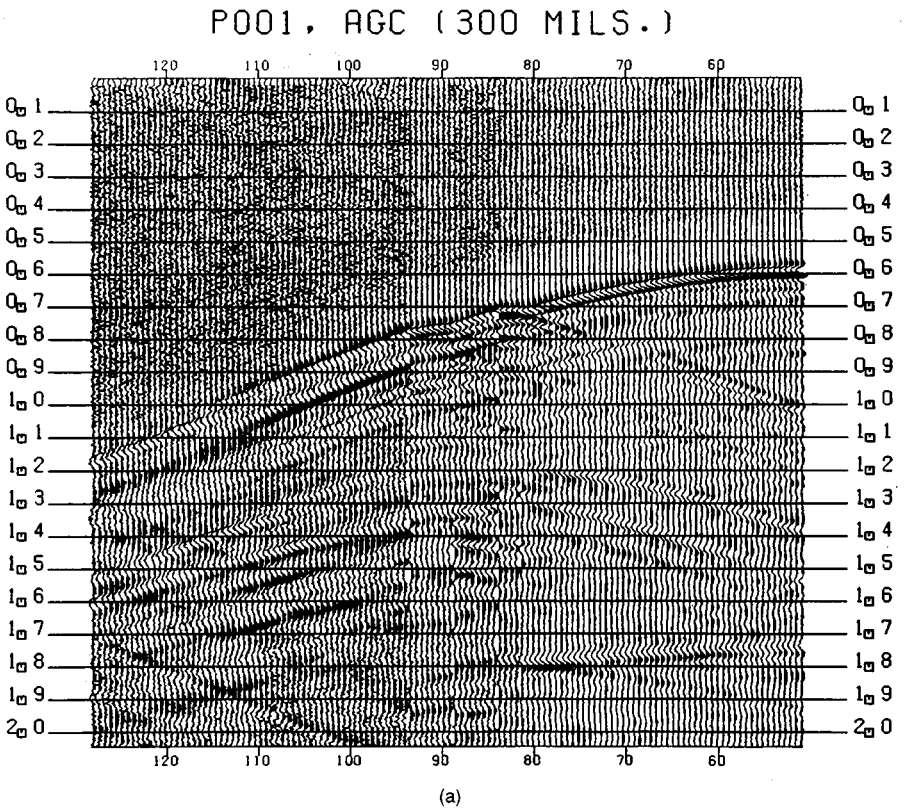

(a)

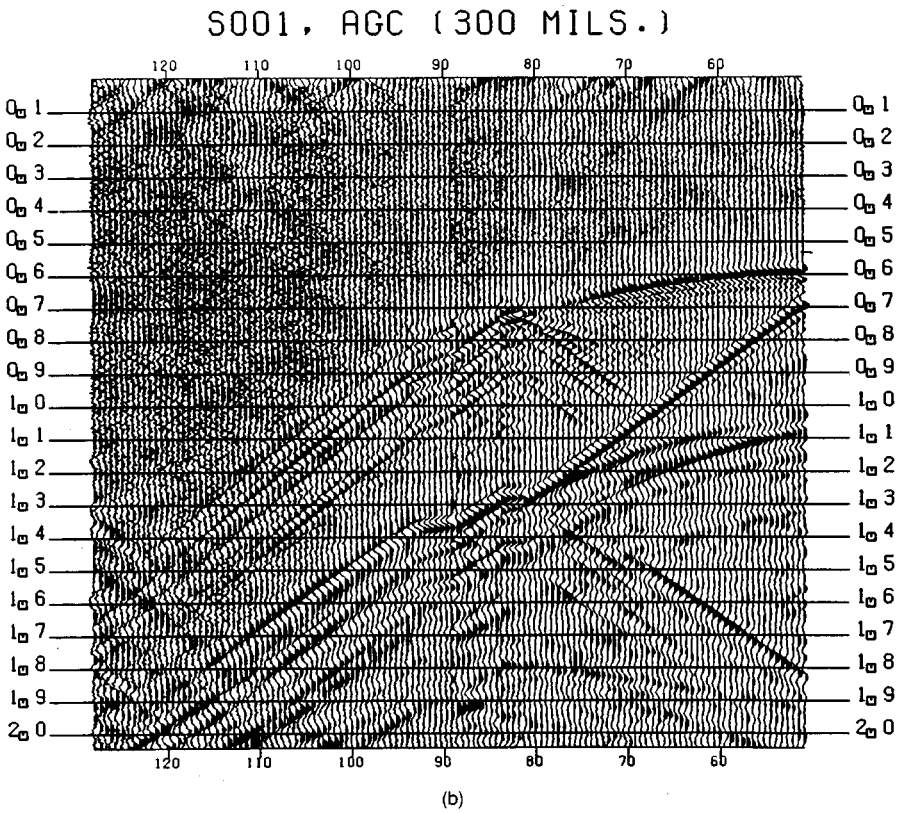

(b)

Fig. 4 Data from Fig. 3 after p-mode (a) and s-mode (b) separation.

Reference

1. J. W. M. Dankbaar, Vertical Seismic Profiling—Separation of p and s Waves, *Geophys. Prospect.*, 35: 803-814 (1987).

CHARACTERIZATION OF NON-DARCY MULTIPHASE FLOW IN PETROLEUM-BEARING FORMATIONS

Contract No. DE-AC22-90BC14659

University of Oklahoma
Norman, Okla.

Contract Date: May 14, 1990
Anticipated Completion: May 13, 1993

Total Project Cost:

DOE	$287,624
Contractor	14,202
Total	$301,826

Principal Investigators:
Ronald D. Evans
Faruk Civan

Project Manager:
Edith C. Allison
Bartlesville Project Office

Reporting Period: Apr. 1–June 30, 1990

Objectives

The objectives of this research are to: (1) develop a proper theoretical model for characterizing non-Darcy multiphase flow in petroleum-bearing formations, (2) develop an experimental technique for measuring non-Darcy flow coefficients under multiphase flow at in situ reservoir conditions, and (3) develop dimensional consistent correlations to express the non-Darcy flow coefficient as a function of rock and fluid properties for consolidated and unconsolidated porous media.

Summary of Technical Progress

During the current reporting period, work was initiated on the research project. Two graduate research assistants were appointed to begin work on the project. One of these research assistants is assigned to concentrate on the experimental aspects of the research, and the other research assistant is assigned to concentrate on the theoretical aspects of the research.

A new fracture flow experimental apparatus is being designed to conform with API Specification RP61—Recommended Practices for Evaluating Short Term Proppant Pack Conductivity. Plans are to modify the design of this device and replace the steel plate fracture faces with rock faces. This will allow investigation of proppant flow conditions that are more realistic of actual in situ reservoir conditions.

A continuing literature survey has been initiated to identify and document the relevant literature on non-Darcy flow through porous media.

A data bank is being established that will be used to store all experimental data that have been published on non-Darcy flow. This data bank will be added as new experiments are conducted in this research project and as new data surface periodically in the open literature. From this data bank porous media regions where experimental data are lacking will be identified, and experiments will be conducted to fill in these gaps.

Recently, researchers at the University of Oklahoma (the principal investigators and a graduate research assistant) developed a new dimensionally consistent correlation for single-phase flow through a proppant fracture.[1] Figure 1 shows a plot of the two dimensionless parameters that correlate the non-Darcy flow coefficient (β) as a function of fracture and fluid properties. The correlation coefficient for this set of experimental data was 0.996.

Work was also initiated to theoretically develop a model that can be used to measure the non-Darcy flow coefficient (β) under multiphase flow conditions. Apparently a theoretically sound technique can be arrived at by extending the work of Civan and Donaldson[2] to include non-Darcy flow. This approach will be fully investigated during the next quarter.

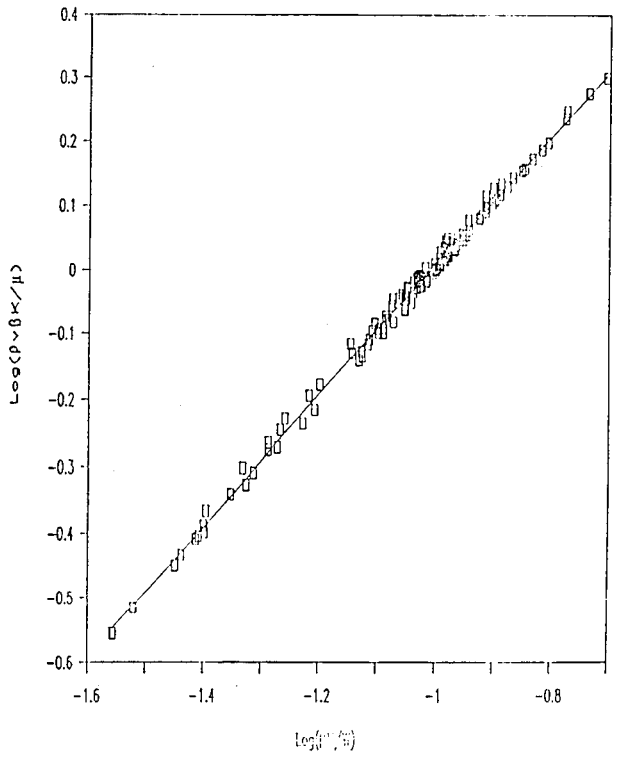

Fig. 1 Empirical correlation of inertial flow coefficient for 20/40 mesh size of proppant.

References

1. Mustapha M. Belkahodja, *The Effect of Non-Darcy Flow on Fracture Flow Capacity*. M. S. thesis, School of Petroleum and Geological Engineering, University of Oklahoma, Norman, Okla., May 1990.
2. F. Civan and E. C. Donaldson, Relative Permeability from Unsteady-State Displacements with Capillary Pressure Included, *SPE Formation Evaluation J.*, 189-193 (June 1989).

GEODIAGNOSTICS FOR RESERVOIR HETEROGENEITIES AND PROCESS MAPPING

Sandia National Laboratories
Albuquerque, N. Mex.

Contract Date: Oct 1, 1987
Anticipated Completion: Sept. 30, 1993
Funding for FY 1990: $285,000

Principal Investigator:
David A. Northrop

Project Manager:
Robert E. Lemmon
Bartlesville Project Office

Reporting Period: Apr. 1–June 30, 1990

Objectives

The long-range objective is to improve the efficiency of oil recovery by better definition of reservoir heterogeneities and mapping of enhanced oil recovery (EOR) processes through the development of advanced geodiagnostics systems. This project provides an EOR perspective for the diagnostic systems development. The FY90 tasks include: (1) quantify and understand the resistivity changes associated with the passage of a steamflood, (2) define realistic electrical steamflood models for physical simulation and numerical modeling, (3) apply geostatistical techniques to incorporate heterogeneous reservoir geology in the interpretation of geodiagnostic data, and (4) critically examine current electrical measurement and interpretation techniques.

Summary of Technical Progress

Resistivity Estimation During EOR Process

A method to estimate salinity and resistivity from non-compositional simulation codes is being developed and is being implemented in a program called TRACK. TRACK reads an output file from the simulator that describes the movement of the aqueous phase at each time step. TRACK also reads an input file that defines the number of components to track, how much of each is injected, and how much of each is initially present. This file also specifies the physical dispersion coefficient of the components within the aqueous phase. TRACK writes the concentration of desired components at desired times for each grid block. This information can then be used to estimate the salinity and then the resistivity of each block.

The advantages of this approach are that only one simulation run is needed to generate the flow field, and then many cases with multiple components, initial and injected conditions, and dispersion can be generated.

Geostatistical Applications

Three different scales are important to the interpretation of electrical and electromagnetic diagnostic techniques: (1) the core scale, or the scale at which Archie's law applies; (2) the block scale (tens of meters), or the scale at which reservoir simulators and electromagnetic forward and inverse programs grid the reservoir; and (3) the reservoir scale, or the scale at which geodiagnostic measurements are made. Work on how to average core scale properties (porosity, saturation, etc.) to give representatives block or bulk resistivity was begun with data from Elk Hills,[2] rather than synthetic data, to ensure that the statistics (average, variance, correlation, etc.) are geologically realistic. Merely plugging average saturation and porosity into Archie's law can give block resistivities that are as much as 50% off for Elk Hills. This is a fundamental petrophysical problem, not just an artifact of the Elk Hills data as was demonstrated by examining a bimodal pore-size distribution example taken from the work of Morrow.[3] For this example, the resistivity calculated with average properties can be as much as a factor of 10 off.

These analyses also demonstrated the importance of knowing how the electrical/electromagnetic measurement depends on resistivity to average properly. For example, in the far field a controlled source audiofrequency magnetotelluric (CSAMT) signal moves downward across the beds, which would seem to imply that the resistivity of the beds should be combined in series. However, because the currents flow parallel to the beds, the system actually acts like resistors in parallel. Failure to recognize the difference between series and parallel systems can lead to significant errors in calculating bulk resistivity.

Assessment of Electrical Interpretation Techniques

Work has continued on examining the uniqueness of inversions of surface-based frequency-domain electromagnetic soundings. The primary tools being used are a nonlinear least-squares plane-wave inversion program (NLSPW)[1] and forward modeling. Work this quarter has addressed the question of whether presteamflooding and poststeamflooding data, when used together, can be inverted to

determine the resistivity change of a steamflood. Analyses have shown that presteamflooding and poststeamflooding data, even when used together, do not remove the depth degeneracy. Independent knowledge of the depth of resistivity change is needed. The need for independent depth knowledge means that surface-based frequency-domain measurements alone cannot be used to look for depth-dependent phenomena such as vertical sweep and steam override. Rather, frequency-domain measurements will give information about bulk quantity of steam under a given measuring location, but not its vertical distribution.

Joint inversion of preflood and postflood data and independent knowledge of the depth of resistivity change was studied for a horizontally layered earth. The results of the work are encouraging. For the inversions, it was required that the resistivity above and below the steamflood remain unchanged. This resulted in an effective overburden resistivity profile that distorted the preflood and postflood resistivities of the steamflood in a similar manner. Even though the preflood and postflood resistivities were not accurately estimated by the inversion, their ratio is reasonably accurate.

References

1. W. L. Anderson, *Adaptive Nonlinear Least-Squares Solution for Constrained or Unconstrained Minimization Problems* (Subprogram NLSOL), U.S. Geological Survey Open-File Report 82-68, 1982.
2. A. J. Mansure, R. F. Meldau, and H. V. Weyland, *Field Examples of Electrical Resistivity Changes During Steamflooding*, SPE 20539, New Orleans, September 1990.
3. N. R. Morrow, Irreducible Wetting-Phase Saturations in Porous Media, *Chem. Eng. Sci.*, 25: 1799-1815 (1970).

DEMONSTRATION OF HIGH-RESOLUTION INVERSE VSP FOR RESERVOIR CHARACTERIZATION APPLICATIONS

Contract No. DE-AC22-89BC14473

Southwest Research Institute
San Antonio, Tex.

Contract Date: Oct. 1, 1989
Anticipated Completion: Sept. 30, 1990
Government Award: $107,895
(Current year)

Principal Investigator:
Jorge O. Parra

Project Manager:
Robert E. Lemmon
Bartlesville Project Office

Reporting Period: Apr. 1–June 30, 1990

Objective

The objective of this project is to demonstrate inverse vertical seismic profiling (VSP) measurements with new experimental field instrumentation that is capable of providing at least an order of magnitude improvement in the resolution of structural details in comparison with conventional seismic images. This two-year project will entail instrumentation tests under controlled field conditions during the first year followed by full-scale field demonstration tests in a representative oil-bearing reservoir formation during the second year.

Summary of Technical Progress

During the third quarter, the wax-melt borehole seismic sensor package containing acceleration sensors was designed, constructed, and tested in laboratory and field experiments to evaluate this novel, reversible rigid-coupling method.

A Reversible Rigid-Coupling Method for Borehole Seismic Transducers

The coupling method used in present-day borehole seismic detectors is one in which mechanical locking arms are actuated outward from the sensor probe housing to contact the borehole wall and forcefully lock the probe in place for the temporary time period required for the measurements. In general, seismic wall-lock probes of this type have an average density that is much greater than the drilled rock formations in which they are coupled. As a result, a very high mechanical clamping force is required to lock these probes to the borehole wall. In practice, this technique is usually only partially successful in achieving the desired degree of coupling because of spurious mechanical resonances that occur in the clamping mechanism.

Alternatively, permanent installation of the seismic detectors is occasionally desirable. A common practice used in such permanent installations is to embed the sensor in the borehole with portland cement or other rigid casting material. In this case, the seismic detector package must be considered expendable since it cannot be recovered in a cost-effective manner. Such permanent emplacements have been used in a number of field tests with relatively inexpensive geophones that could be abandoned in place when the tests are complete. This method has proven to be effective in providing good seismic coupling because the cement forms a rigid and conformal casting in the borehole and the density of the composite sensor and cement is reasonably

well matched with that of the surrounding geological material.

The acceleration sensors mentioned previously for reverse VSP measurements are significantly more expensive than geophones and therefore cannot be considered expendable. An alternative means of rigid and conformal coupling is therefore needed which would allow the more expensive acceleration detector probe to be retrieved after use. A wax-melt sensor coupling technique developed for this project was installed in a shallow borehole for seismic measurements. This reversible rigid-coupling method was intended to achieve the desirable results of rigid conformal borehole coupling, an approximate match between the average density of the sensor package and the drilled rock formation, and the ability to recover the sensor package instead of abandoning it after the seismic measurements.

Laboratory Experiments

Laboratory experiments were conducted to test the wax-melt coupling technique and the wax-melting control process for borehole seismic sensors. For this purpose, a prototype assembly of the wax-melt-coupled seismic detector containing the sensor package and its surrounding heating elements was placed in a closed Plexiglas sleeve (tube) immersed in water. The heating elements were made of No. 16 AWG nichrome wire. Melted carnauba wax blended with smaller amounts of other vegetable waxes was then poured into the Plexiglas sleeve. When the wax cooled and solidified, it provided a rigid embedment of the seismic sensor package, which was reliably coupled to the surrounding Plexiglas material.

The wax heating time, the wax heating power, and the temperature of the wax embedment were monitored to test the wax-melting process experiments. Seven temperature sensors (thermistors) calibrated in the range 100 to 250°F and located in each wax-melt zone of the sensor package were used to monitor the thermal conditions and the changes produced in the wax by the electrical heating power controls.

The laboratory experiments demonstrated that, for gradual melting of the wax surrounding the embedded assembly in the Plexiglas tube, a maximum heating power of 950 W for 1 h was required. In addition, the experimental results indicated that, by applying different heating power, a vertical thermal gradient could be established in the melted wax column. In this case, when the upper section of the wax was hotter than the lower section, the subsequent cooling and solidification of the wax coupling occurred with minimum shrinkage of the wax embedment.

Field Experiments

A sensor package was prepared for installation in a borehole by casting it within a cylindrical billet of wax with a diameter smaller than that of the borehole and with a length such that enough wax was available to surround and embed the sensor package in the borehole. Figure 1 shows the finished wax billet casting in a form ready to be placed in a borehole. This casting, which is 5.5 in. in diameter and 19 in. long, was installed in an open 75-ft-deep water-free borehole with a nominal diameter of 6.25 in. The wax billet, sensors, and preamplifier were lowered to the bottom of the borehole, and then distributed electrical heating was applied to heat and melt the wax. As expected, after heating at approximately 950 W for 1 h, the wax billet melted and reached a final temperature of 100°C in its upper section.

After the wax was solidified in the borehole, three-component seismic measurements were successfully recorded with a cylindrical bender seismic source, and the wax melt was placed in a 450-ft-deep borehole at 65 ft from the 75-ft-deep detector borehole. Seismic measurements were made with different source pulse signals in the frequency range of 750 to 3000 Hz and at several source depths ranging from 71 to 400 ft.

As an example of these data, part a of Fig. 2 illustrates three-component reverse VSP seismic pulse waveforms at 2500 Hz and at a source depth about 33 ft below the detector. Also, a three-component pneumatically clamped seismic detector probe was previously used at the same location borehole to record the same source pulse signal. These waveforms are shown in part b of Fig. 2. The records

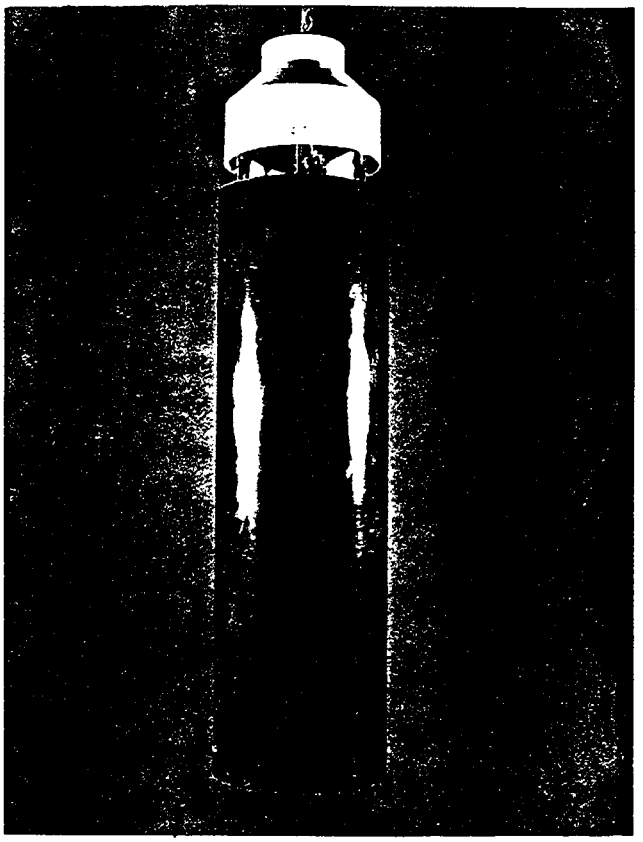

Fig. 1 Prototype model of wax-melt borehole seismic sensor package and nichrome heater elements.

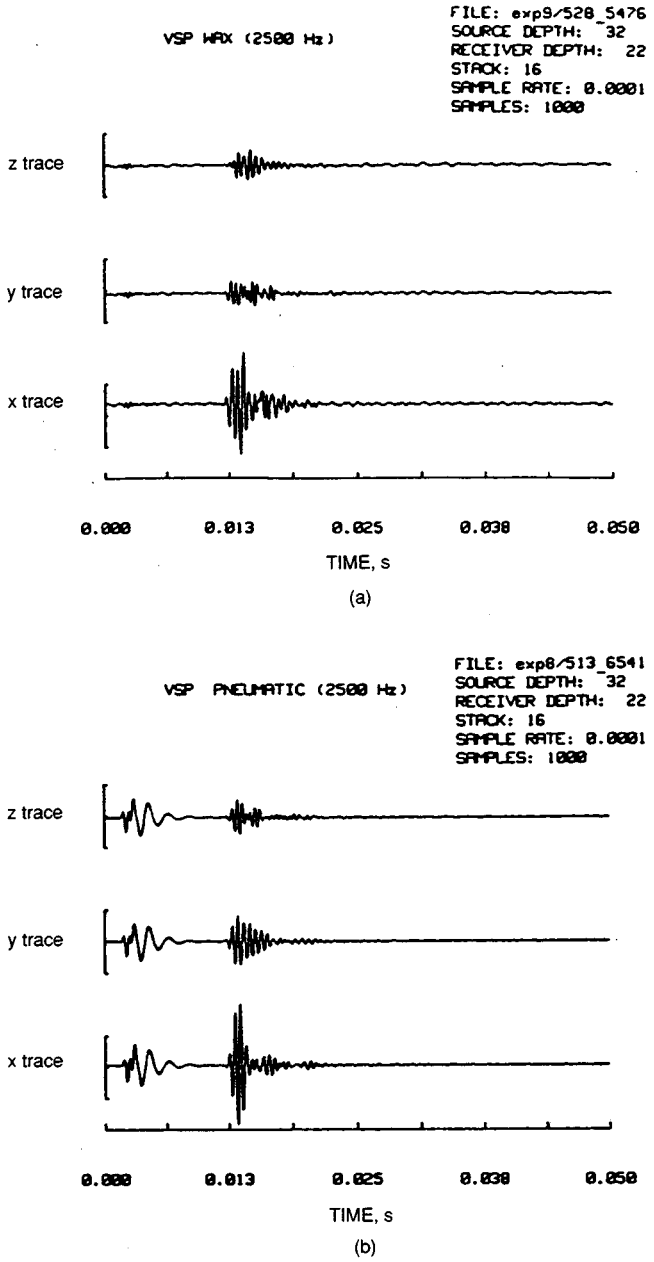

Fig. 2 Three-component inverse VSP seismic waveforms. Shot points obtained with 2500-Hz source center frequency. (a) Waveforms recorded with the wax-melt sensor package. (b) Waveforms recorded with the lightweight (7 lb) pneumatic-lock detector tool.

contain electrical cross feed caused by the experimental system conditions when the measurements were taken. These signals are independent of the detector probe coupling response in the borehole and were later eliminated in the experiments with the wax-melt coupled sensors.

A comparison of the pneumatic and wax-melt sensor seismic waveforms indicates that time domain waveforms are dominated by direct waves in the form of short-duration probes and wideband signal spectrums. These results concluded that the coupling obtained with the pneumatic sensor package is comparable with the more rigid coupling obtained with the wax-melt sensor package.

Finally, after the data acquisition field experiments were completed, the coupling medium (wax) was transformed from a solid state to a liquid state to allow the sensor package to be decoupled and removed from the borehole. Melting of the wax required 7 h at 950 W. The 7-h melting time appears to be caused by moisture conditions at the bottom of the borehole.

THREE-PHASE RELATIVE PERMEABILITY

Cooperative Agreement DE-FC22-83FE60149, Project BE9

National Institute for Petroleum and Energy Research
Bartlesville, Okla.

Contract Date: Oct. 1, 1985
Anticipated Completion: Sept. 30, 1990
Funding for FY 1990: $305,000

Principal Investigators:
Matt Honarpour
Dan Maloney

Project Manager:
Edith Allison
Bartlesville Project Office

Reporting Period: Apr. 1–June 30, 1990

Objectives

The objectives of this project are to improve the reliability of laboratory measurements of three-phase relative permeability for steady- and unsteady-state conditions in core samples and to investigate the influence of rock, fluid, and rock–fluid properties on two- and three-phase relative permeabilities.

Summary of Technical Progress

Sample Characterization

Mercury intrusion porosimetry tests were conducted on plugs of the high-permeability Bentheimer and Berea sandstones from last year's investigation and on the intermediate-permeability Berea that is under investigation this year. The goal for this investigation was to distinguish differences among the pore diameter characteristics for the three samples. Volume and pressure measurements from tests in which mercury was forced into the rock pores at

pressures from 3.45 kPa to 413 MPa were used to calculate pore diameters and mercury intrusion data. Table 1 contains a summary of rock characteristics from routine core measurements and from mercury intrusion porosimetry. Sample A, the Bentheimer sandstone, had the largest median pore diameter, followed by B (the high-permeability Berea), and then C (intermediate-permeability Berea sandstone). Figure 1, a plot of log specific differential intrusion volume vs. pore-throat diameter, provides information on the pore-throat size distributions for the three samples. The plot shows the fairly narrow pore size distribution for the Bentheimer sandstone compared with the two Bereas as well as the higher degrees of microporosity exhibited by the Berea sandstones.

TABLE 1

Characteristics of Fired Sandstone Samples Used for Mercury Intrusion Porosimetry

	Sample		
Characteristic	A (Bentheimer)	B (Berea)	C (Berea)
Air permeability, mD	3500.0000	1330.0000	832.0000
Porosity, %	26.4000	26.0000	24.0000
Total pore area, m^2/g	3.4400	3.3140	3.4580
Median pore-throat diameter, μm	28.6239	22.2750	16.8361

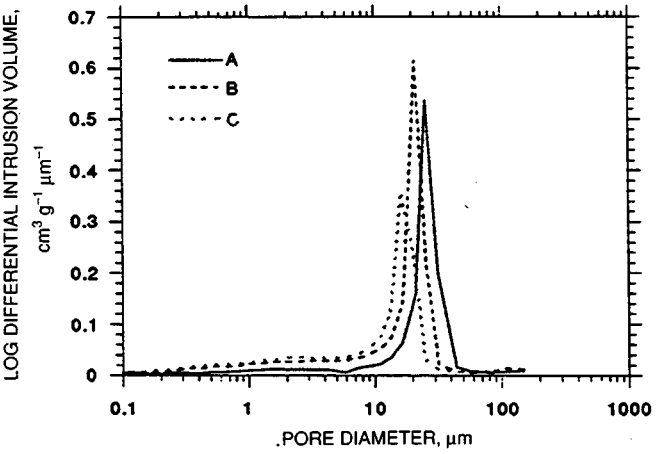

Fig. 1 Mercury intrusion porosimetry results for Bentheimer (A), high-permeability Berea (B), and intermediate-permeability Berea (C) sandstones.

Centrifuge Capillary Pressure Measurements

Results from the centrifuge capillary pressure experiments that were conducted on the Bentheimer and two Berea sandstones (A, B, and C as described in the previous section) were reported in a paper entitled *Investigation of the Relationship Between Capillary Pressure Hysteresis Effects and Pore Size Distribution for High-Permeability Sandstone Rocks*. The paper will be presented at the Fourth Annual Society of Core Analysts Meeting, Dallas, Tex., August 15–16, 1990. Conclusions from the investigation were as follows:

1. For these three samples, the order of increasing permeability (C, B, A) was the same as the order of increasing median pore-throat diameter.
2. Hysteresis was evident in each multiple-cycle centrifuge capillary pressure experiment. The primary effect of cycle-dependent hysteresis for these samples was a reduction in the wettability index with successive drainage and imbibition cycles.
3. Maximum capillary pressures induced during centrifuge capillary pressure tests should be limited to values similar to those occurring in the dynamic displacement process to yield representative capillary pressure–saturation and wettability information.
4. Computerized tomographic (CT) images showed that fluid distributions during the drainage and imbibition processes were different for plugs A, B, and C. These differences are primarily attributed to pore-throat size characteristics.
5. The saturation distributions from CT images of plugs A, B, and C were not uniform until after a certain rotational speed (capillary pressure) was exceeded. Saturation distributions thereafter appeared uniform and were close to residual saturation conditions.
6. Jacketing high-permeability plug B with Teflon tape did not resolve the problem of brine imbibition around the plug margins.

Relative Permeability Results

An oil–water steady-state relative permeability test was conducted on sample C (intermediate-permeability Berea). The oil and water relative permeability results for two sets of drainage and imbibition cycles are shown in Fig. 2. The letters d and i in the legend indicate drainage or imbibition cycle, whereas the number subscripts indicate the cycle

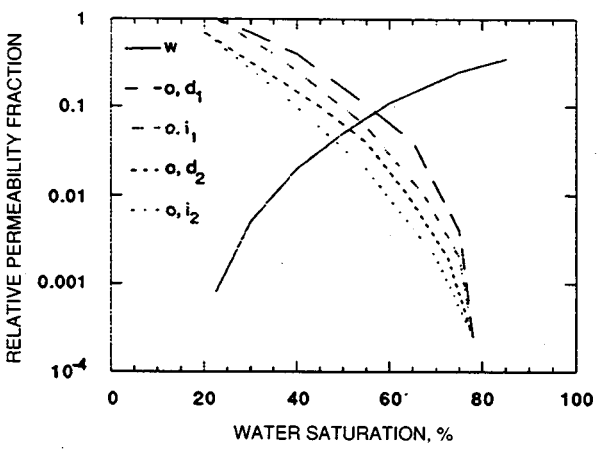

Fig. 2 Steady-state oil–water relative permeability results.

number. The water relative permeability curves from the four tests (1st drainage, 1st imbibition, 2nd drainage, and 2nd imbibition) all followed the same trend and did not appear to be affected by saturation history. The oil relative permeability values were similar at the ends of the relative permeability curves (at residual oil and water saturations), whereas the portions of the curves between the end points shifted in the direction of lower water saturation with each additional drainage or imbibition cycle. This may be the result of the change in the initial water saturation because the hysteresis envelopes are very similar. A shift in the point in which the water and oil relative permeability curves crossed has been described as an indication of a possible change in wettability characteristics. In this case, the shift in the position of the crossing point was not associated with a shift in the water relative permeability curve. For this reason, the differences among the oil relative permeability curves from these tests are attributed to changes in initial water saturation and/or oil trapping.

Several unsteady-state oil–water relative permeability tests were conducted on samples of sandstone C with 94-cP mineral oil and 1.0-cP brine. When the steady- and unsteady-state relative permeability results were plotted on the same graph as a function of water saturation, the unsteady-state results were offset from the steady-state results in the direction of higher water saturation by 10 to 20 water saturation percent units. The unsteady-state experimental data are under reevaluation to discern whether these discrepancies are the result of problems with the unsteady-state technique or the result of error in experimental measurements.

Gas–water steady-state relative permeability results for sample C from two drainage and one imbibition cycle are shown in Fig. 3. The gas–water results do not appear to show any appreciable cycle-dependent hysteresis effects.

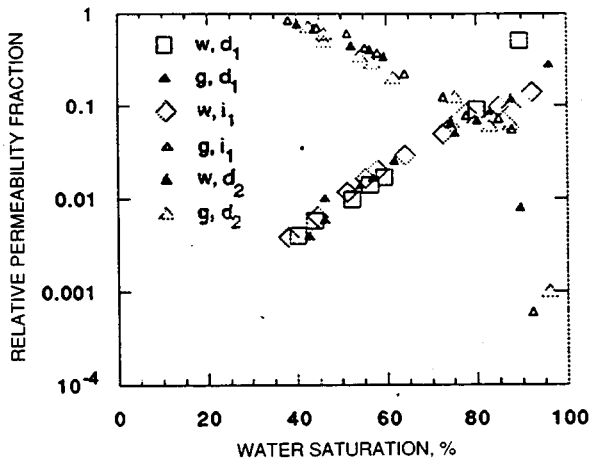

Fig. 3 Steady-state gas–water relative permeability results.

Resistivity Results

Resistivities were calculated from resistance measurements taken during the two-phase flow experiments. Oil–water results are shown in Fig. 4. Saturation exponents calculated from power curve fits to the data are included on the graph. As shown in Fig. 4, first drainage and first imbibition cycle results were quite different, whereas data from subsequent drainage and imbibition cycles essentially fell between the first cycle results. Gas–water results are shown in Fig. 5. The gas–water data do not show a strong hysteresis effect in the resistivity results.

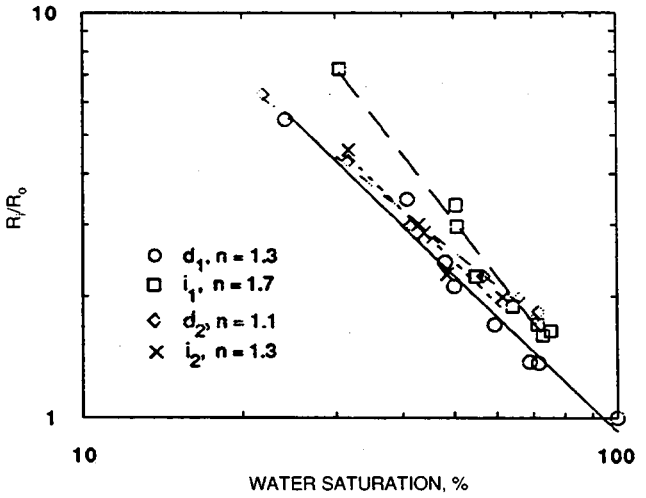

Fig. 4 Dynamic oil–water resistivity results.

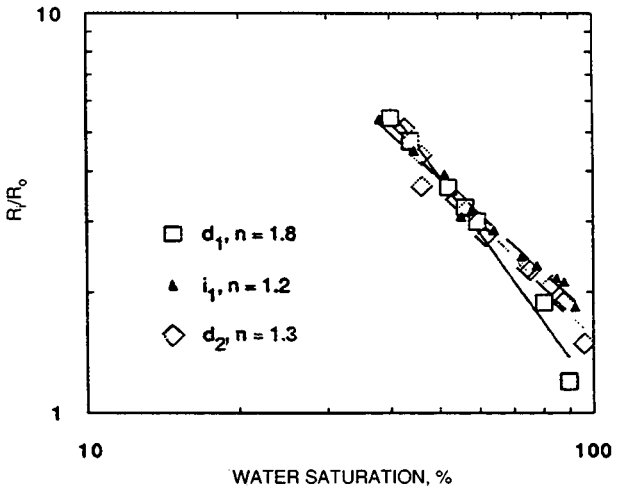

Fig. 5 Dynamic gas–water resistivity results.

IMAGING TECHNIQUES APPLIED TO THE STUDY OF FLUIDS IN POROUS MEDIA

Cooperative Agreement DE-FC22-83FE60149, Project BE12

National Institute for Petroleum and Energy Research
Bartlesville, Okla.

Contract Date: Oct. 1, 1987
Anticipated Completion: Sept. 30, 1990
Funding for FY 1990: $395,000

Principal Investigator:
Liviu Tomutsa

Project Manager:
Robert E. Lemmon
Bartlesville Project Office

Reporting Period: Apr. 1–June 30, 1990

Objectives

The objectives of this project are to develop and use new imaging techniques for measurements of pore geometries and fluid distributions in reservoir rocks at scales varying from a pore to a whole core and to study the effect of microscopic-scale heterogeneities on oil trapping in core-size rock samples.

Summary of Technical Progress

Measurement of Single- and Two-Phase Spatial Fluid Distributions in Large Core Plugs

The effects of lamination-type heterogeneities were studied by computerized tomography (CT), nuclear magnetic resonance (NMR), and micromodels for two extreme cases: one for low porosity and permeability contrast between the laminations and one for high contrast. For the low-contrast case, Berea rock was selected. The high-contrast rock selected was from the Shannon formation.

The porosity and permeability of the laminations were determined by the use of petrographic image analysis methods described previously.[1] The calculated average values for the cores, based on image analysis, agree well with values determined by routine core analysis (Table 1).

TABLE 1

Porosity and Permeability Comparison of Petrographic Image Analysis and Core Analysis of Berea and Shannon Sandstones

	Berea		Shannon	
	PIA*	Core analysis	PIA	Core analysis
	Porosity, %			
Highest value	31.0		44.0	
Lowest value	10.0		18.0	
Average value	19.0	18.7	30.0	30.4
	Permeability, mD			
Highest value	2,170		11,906	
Lowest value	8		141	
Average value	294	300	2,253	930

*Petrographic image analysis.

Petrographic Analysis of Berea and Shannon Sandstones

Macroscopic examination of the Berea rock revealed a porous sandstone with only subtle layering seen in reflected light. The pores were discontinuous in the poorly defined "higher" porosity zones. The rock composition, based on visual scans of the thin section, includes: quartz, 56%; feldspars, 2%; rock fragments, 10%; clay cement, 3%; calcite cement, 2%; heavy minerals, 1%; and muscovite, <1%. Diagenetic clays are not concentrated into beds or layers in this sample but are, instead, almost evenly distributed. Layering within the thin section is not apparent with the petrographic microscope. All that can be recognized are slightly more porous or slightly less porous areas that tend to be elongated. Such areas cannot be traced in bands visually along the known bedding direction, and they are discontinuous. Layering of porosity in this sample can be determined statistically.

One potential method for determining more or less porous zones is to count the number of contacts a given grain has with adjacent framework grains (contact index). In the Berea sample, the contact index in more porous areas (average 3.5 contacts per grain) is significantly different from that in less porous areas (average 5.4 contacts per grain). These results tend to reflect differences in packing of grains within the sandstone. The contact index could be mapped to determine lineation or trend (porous vs. more grain-dense layers) in samples in which layering may not be visually apparent.

Macroscopic examination of the Shannon rock revealed a porous sandstone with cross laminations readily apparent in transmitted or reflected light. Cross laminae are visually enhanced by brown coloration, which contrasts with the blue-dyed epoxy of the more highly porous layers. The rock composition, based on visual scan of the thin section, includes: quartz, 22%; chert, 4%; feldspars, 15%; rock fragments, 2%; glauconite, 25%; clay cement, 1%; and micas, 1%. The most characteristic feature of this rock sample is the abundance of rounded to compacted

glauconite grains, which are the source of the brown to greenish-brown coloration of some layers. Layering in this sample is created by the contrast of highly compacted glauconitic laminae with less compacted, less glauconitic, more porous laminae. Glauconite grains are soft and easily compacted between more rigid framework grains, such as quartz, chert, or feldspar. The contact index within compacted, glauconite-rich laminae averages 5.8 but only 4.0 in the more porous, glauconite-poor laminae. Another difference between the two types of laminae is that the pores are much larger (average 100 to 150 μm in diameter) in the more porous laminae than in the compacted laminae (average 50 to 70 μm in diameter). In addition, the compacted laminae have a significantly larger proportion of completely collapsed pores.

The Shannon sample, in contrast to the Berea, has more visually apparent layering. "Grain dense" layers were created by compaction, particularly of glauconite, and the compacted laminae are more laterally continuous. In addition, the mineralogical composition and rock types represented by the two samples are quite different.

Coreflood Experimental Results

Because of the high permeability of the heterogeneous rocks selected (Table 1), the corefloods could be performed at low differential pressures. Therefore, it was more experimentally convenient to cut slabs 2 by 5 by $^3/_4$ in. and encapsulate them in Castolite™ clear resin. The Berea slab was cut with laminations at a 45° angle with respect to the direction of flow. The Shannon slab was cut with the laminations parallel to the flow direction. The CT scans of both slabs are shown in Fig. 1. Both miscible processes (synthetic brine tagged with NaI displacing untagged brine) and immiscible processes (drainage–imbibition cycles) of tagged synthetic brine and untagged synthetic oils (6.5 and 20 cP viscosity) were studied. The effects of laminations on both the front movement and the brine and oil saturations after breakthrough (determined by performing CT scans parallel to the flow direction during and after flooding) are shown in Fig. 2 for the Berea slab. By monitoring pressures and flow rates, end-point relative permeabilities have also been calculated.

Although the low porosity–permeability contrasts laminations showed a pronounced effect on the front shape during the oil flood of the brine-saturated Berea slab (Fig. 2), at the end of both the oil flood and the waterflood, the difference in saturation between the laminations was less than the resolution of the CT system.

For the Shannon slab, the high-permeability porosity–permeability layers provided channels for the oil flow, and at the end of the oil flood, essentially no oil penetrated the low-permeability layers. During the waterflood, the fingering effect was very pronounced as a result of the high contrast between the various rock layers.

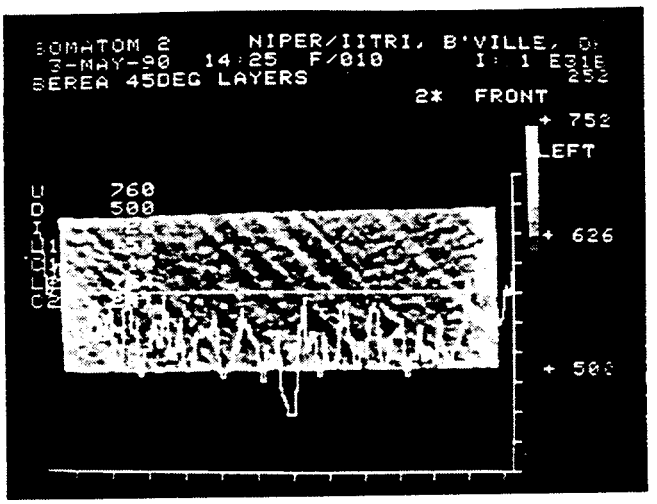

(a)

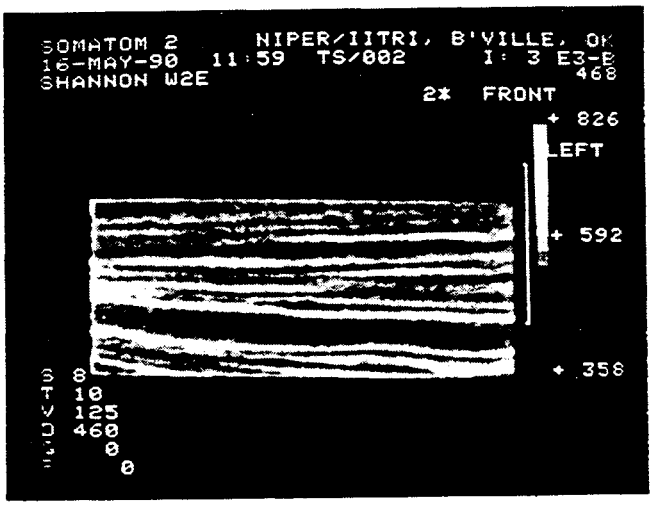

(b)

Fig. 1 Computerized tomography images of Berea (a) and Shannon (b) sandstones showing variations in CT density.

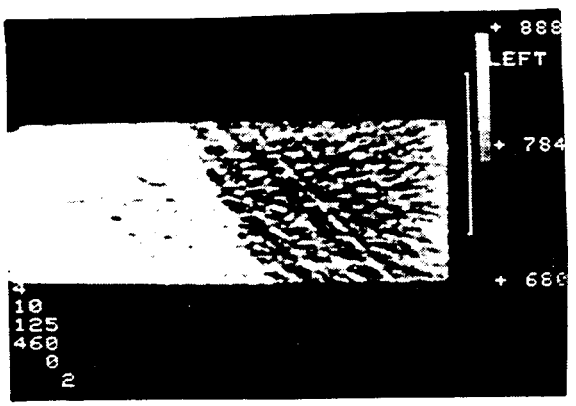

Fig. 2 Computerized tomography image of Berea slab partially flooded with 20 cP oil.

Experimental Results and Discussion from Magnetic Resonance Imaging Studies

Samples of various types were contained in all-Teflon sample holders supported in 10-mm glass tubes to avoid proton signals from the holders. The beads or sand were packed inside the tubing section, which provided a sample that was about 8 mm long and 4.7 mm in diameter. For the Berea and Shannon sandstone samples, small cylindrical plugs 5 to 6 mm in diameter and 8 mm long were cut from bulk rock samples. Both rock plugs were selected to contain at least one visible lamination running along the axis of the cylinder. Heat-shrink tubing formed a fairly tight-fitting container for the rock plugs. The samples in their holders were evacuated and saturated with 1% NaCl in 99.6% deuterium oxide (D_2O) as the aqueous phase. A deuterium magnetic resonance image (MRI) of each sample was obtained. The resolution for the bead packs was $128 \times 128 \times 128$, and that for the rock samples was $64 \times 64 \times 64$. For the deuterium images of the packs, four signals at each gradient position were added to improve the signal/noise ratio, whereas for the rock plugs, eight signals were added.

For the two-phase MRI experiments, Soltrol mineral oil (5-cP viscosity) was used as the oil phase. Red dye was used to color the oil phase to track its progress visually. For the packs, a syringe was used to push about 5 pore volumes (PV) of oil through the pack in about 10 min. The rock plugs were immersed vertically in the oil phase and centrifuged at 1500 rpm for 4 h to allow the oil phase to displace the aqueous phase. A proton MRI image was obtained for each sample to see the oil phase, and a second deuterium image was obtained without moving the sample to see the residual aqueous phase. The previously mentioned respective resolutions were used for each sample. For the proton image, two signals with a 0.5-s interpulse delay and a 25° RF pulse were added at each gradient position. (The oil had a longer spin-lattice relaxation time than the deuterium oxide.) Because the residual deuterium oxide was much less concentrated, 8 or 16 signals were added, respectively, for the packs or rock plugs to improve signal/noise ratios.

For the Shannon plug, laminations were not as visible in the initial one-phase water image, and centrifuging seems to have selectively depleted the fluids in the darker bands, which possibly indicates better flow characteristics for these zones. (Since many of these phenomena observed in micromodel and MRI images cannot be seen in black-and-white reproductions of color images, photographs are not included in this quarterly report. Later reports of this research will include color photographic reproductions.) Compared with the Shannon images, the Berea appears to have less fluid content, which is consistent with its lower porosity, and a much more heterogeneous appearance.

Images of the bead pack are much sharper as a result of the higher resolution obtained. The beads were spherical and ranged in size from 350 to 500 μm. The circular profile of individual beads is evident in the images. There are pore spaces where the aqueous phase was bypassed during the displacement; thus pockets of water were left in individual pore spaces. Also, the oil phase apparently displaced water preferentially in the outer perimeter of the pack, and thus left higher water content in the center of the pack nearer the bottom.

The decision to display the rock images at a lower resolution than that of the bead pack was based on the respective properties of the NMR signals from the two types of samples. The fluids in the rock matrix had a natural NMR line width of 700 Hz for deuterium and 2000 Hz for protons. For the polymer bead pack, the NMR line widths were 20 and 120 Hz, respectively, which indicates that the higher displayed resolution was meaningful. Additional development, such as increasing the field gradients, could permit the attainment of resolutions with MRI of rock–fluid systems of 20 μm, which would allow imaging of water–oil phases within pores instead of in a group of rates as now possible.

The approach to MRI microscopy with three-dimensional (3-D) projection reconstruction is computer-intensive because of the large data files involved. The use of a 33-mHz, 386 desktop computer reduced the processing time by a factor of 8 compared with that of the MicroVAX. Also, the experiments are time-consuming, particularly with the deuterium images of residual water where several signals must be added to get adequate signal/noise ratios. Therefore the experiments must be static in nature. To go much beyond 128-pixel resolution probably would require a parallel processor computer system with several processors to speed computations and display. One advantage of the projection reconstruction approach is the built-in parallel nature of the data processing, which permits an easy transition to parallel processing.

Micromodel Study of Pore Level Fluid Distributions

The experimental setup consisted of a modified geological microscope, a powerful fiber optic light source, a sensitive high-resolution monochromatic video camera (Plumbicon tube, 0.005 lux, 900 TV lines), and a super-VHS VCR (450 lines). For photography, an automatic 35-mm camera was attached. Assembly[1] and experimental details[2] were reported previously.

The highest quality of observations and reproductions is possible for slow events spanning over tens of minutes, such as foam degradation, emulsification, and interactions at rock–fluid interfaces. The faster the events under observation, the lower the quality of reproductions because of the low-light views. In this work, quality was poor but acceptable for dynamic events occurring at moderate speeds (10 to 20 ft/d). Difficulties were observed when mass-reproducing events faster than this speed, such as foam formation, foam rupture, and most capillary-controlled phenomena, occurred. The quality of video recordings of

these events was also marginal. For extremely difficult situations, direct observations through the microscope were used.

After secondary imbibition, i.e., after a cycle consisting of initial brine injection in dry rock, oil injection until brine production stops, and brine reinjection until oil production stops, most of the pores containing oil were almost completely filled with it, except in crevices and thin coatings of brine on the grain surfaces. Another common observation was the trapping of oil ganglia extending over several pores as the result of viscous bypassing of displacing brine.

During gas injection into the oil- and brine-filled micromodel, gas propagated in the form of small, isolated bubbles through oil-filled channels and thus produced oil. After the moveable oil was produced, gas then displaced brine.

During oil (5-cP viscosity) injection into a brine-filled homogeneous Berea rock-slab model, fingering was not evident in the layered Shannon rock-slab model because the heterogeneities diffused the fingers. Oil front advancement was rather layer after layer; i.e., the layer closest to the injection port was swept first, then the second layer, and so on. The tighter the layers, the more the brine was held in them. Brine saturation was also higher near the producing end as a result of the end effects.

The use of a 2- to 3-mm rock slab introduces certain complexities in the observations. The flow is neither strictly two-dimensional as in network models nor is it truly 3-D on a macroscale. Also, the pore-to-pore connection is lost for some pores adjoining the encapsulating (no-flow) boundaries. These factors limited the ability to visualize the entire network of pores, and fluid flow and trapping through selected pores that are strategically located were monitored. These limitations are not expected to alter the flow mechanism significantly.

The effect of dissimilarity in the wettabilities of the transparent silicone-rubber coating (preferentially oil-wet) and the rock grains could be important. The oil wetting on the confining boundary was manifested only after tens of hours, which was enough duration to complete a test. On gas injection, however, the water films between oil and silicone-rubber surfaces were broken, which gradually caused an oil-wetting problem. Once it happened, the model had to be discarded because the process was irreversible.

The most serious concern about any micromodel is the effect of neglecting scaling criteria. Satisfying them simultaneously at both macroscopic and microscopic levels is more difficult in micromodels than in core plugs because of the smaller overall dimensions of the core. For example, if residual wetting-phase saturation was 25% in a core plug, it would be much less in a micromodel made from a rock slab from the same core plug. In rock plugs, there are regions unswept as a result of viscous bypassing. Because of smaller size, this bypassing is not identical in rock-slab micromodels. Further studies are needed to understand the true extent of this limitation.

The optical microscopy used with rock-slab micromodels offers very good resolution down to micron level. It also permits dynamic imaging of slow/medium flow systems and the investigation of rock–fluid interactions. Its limitations are a result of the light transmitted and the presence of the confining windows, which add boundary–wettability variation problems.

References

1. L. Tomutsa and A. Brinkmeyer, *Using Image Analysis to Determine Petrophysical Properties of Reservoir Rocks*, DOE Report NIPER-444, 1989 (NTIS order No. DE90000222).
2. S. Mahmood and N. L. Maerefat, *New Techniques of Pore-Scale Visualization of Fluids in Porous Media: The Effect of Pore Structure on Fluid Distribution*, DOE Report NIPER-372, 1988 (NTIS order No. DE89000731).
3. S. M. Mahmood, *Fluid Flow Behavior Through Rock-Slab Micromodels in Relation to Other Micromodels*, DOE Report NIPER-448, 1990.

AN EXPERIMENTAL AND THEORETICAL STUDY TO RELATE UNCOMMON ROCK–FLUID PROPERTIES TO OIL RECOVERY

Contract No. AC22-89BC14477

Pennsylvania State University
University Park, Pa.

Contract Date: Sept. 21, 1989
Anticipated Completion: Aug. 31, 1992
Government Award: $260,221
(Current year)

Principal Investigators:
Turgay Ertekin
Robert W. Watson

Project Manager:
Robert E. Lemmon
Bartlesville Project Office

Reporting Period: Apr. 1–June 30, 1990

Objectives

The overall objectives of the project are to develop a better understanding of some important, but not really well-investigated, rock properties, such as tortuosity, pore-size distribution, surface area, wettability, and neck–throat

average rock size; develop a better insight on capillary pressure variation with respect to wettability and pore geometry of Berea sandstone, limestone, and dolomite; develop a relationship between oil recovery at breakthrough and wettability and surface areas of the rocks; develop correlations between oil recovery at floodout and wettability and surface area of these different porous media; investigate variations of average irreducible water saturation and average residual oil saturation with respect to wettability; and improve the understanding of fluid flow in porous media under conditions of secondary and tertiary recovery through the laboratory study of the performance of enhanced recovery methods, such as waterflooding.

Summary of Technical Progress

Twenty-four core plugs were extracted from each of the 22 waterflooded Berea sandstone cores and were used in the wettability and porosimetry studies. Mercury porosimetry data were used to calculate or infer petrophysical characteristics. On the basis of pore-size distribution curves, Berea sandstone pores tested are classified as capillary (diameters of the pores vary from 0.0002 to 0.508 mm). The heterogeneous pore radii in Berea sandstone rocks appear to be the primary cause of mercury trapping by bypassing and snap-off mechanisms. Regression analyses indicated that oil recovery at breakthrough and oil recovery at floodout are related to the rock surface area. Median pore-throat size is related to rock tortuosity expressed in terms of the wetting phase retention time. Tortuosity is inversely proportional to the median pore-throat size of Berea sandstone.

Review of Literature

The most common secondary oil recovery technique is waterflooding. A prerequisite for understanding waterflood performance is a knowledge of the basic properties of reservoir rock. These consist of two main types: (1) properties of the rock skeleton alone, such as porosity, permeability, pore-size distribution, and surface area; and (2) combined rock–fluid properties, such as capillary pressure (static) and relative permeability (flow) characteristics.[1] In this study, surface area was characterized with mercury porosimetry. Lowell and Shields[2] pointed out that the experimental method of mercury porosimetry for the determination of porous properties of solids is dependent on several variables, such as wetting or contact angle between mercury and the surface of the solid. To monitor changes in these variables, Ritter and Drake[3] used a resistance wire in the capillary stem. They also developed one of the first high-pressure porosimeters and measured the contact angle between mercury and a variety of materials. The contact angle was between 135 and 142° with an average value of 140°. The mercury porosimetry theory for determining surface area, capillary pressure variations, cavity radius, sample volume, apparent density, and pore-size distribution is based on an equation developed by Washburn.[4] Washburn's equation was developed with the Young–Dupre equation, which establishes the criteria for wettability. In mercury porosimetry, capillary pressure variations and intrusion–extrusion hysteresis have been attributed to "ink-bottle" shaped pores.[5] In pores of this type, intrusion cannot occur until sufficient pressure is attained to force mercury into the narrow neck, whereupon the entire pore will fill. However, when depressurized, the wide pore body cannot empty until a lower pressure is reached, and thus entrapped mercury is left in the wide inner position. Reverberi et al.[6] proposed a method for calculating the sizes of narrow and wide portions of the pore from intrusion–extrusion curves based on the fact that such pores exhibit "ink-bottle" shapes. This method involves scanning the hysteresis loop by a series of pressurization and partial depressurization cycles to determine the volume of the wide inner portion of pores with neck radii in various radius intervals.

Experimental Procedure

Sampling

Standard cylindrical core plugs were used in a study of the petrophysical characteristics of Berea sandstone rocks. Eight core plugs were taken from each of the waterflooded cores. The core plugs make an angle of 45° with each other. They are spaced in such a way as to ensure coverage of all lithologies. Each of the eight core plugs was cut into three subplugs. Thus 24 core plugs were extracted from each waterflooded Berea sandstone core. These plugs are 1.27 cm in diameter and 1.69 cm long. Samples are about 2.50 g. Petrophysical analyses of rock chips and core plugs are comparable; boundary effects on chips are not much greater than those on plugs.[7]

Samples Cleaning

The core plugs were cleaned before testing by soaking them for 48 h in a solution containing 50% by volume acetone and 50% by volume isopropyl alcohol (obtained from Fisher Scientific, Fairlawn, N.J.). This procedure was followed by an additional soaking for 24 h in a solution containing only acetone. The core plugs were then permitted to dry in a vacuum oven for 24 h. Weights of the core plugs before and after treatment were recorded. This technique was developed by the Texaco Research Lab.

Mercury Porosimetry

Mercury porosimetry is used extensively for the characterization of porous media. This technique is based on the behavior of mercury as a nonwetting liquid toward most substances.[8] In all mercury porosimetry experiments, samples were evacuated for capillary pressure data determination in a Micromeritics Pore Size 9220 (Micromeritics, Norcross, Ga.) Samples were evacuated to a pressure of 50 μm of mercury; the sample chambers were filled with

mercury and then were pressurized incrementally to a pressure of 413,685 kPa. Equilibrium was established before the increase to the next pressure level by setting a porosimeter equilibrium value of 15 s. With each pressure increment, smaller pore throats were invaded by mercury. Pore-throat size information is obtained from mercury intrusion curves on the basis of the assumption of cylindrical pore-throat configuration. The Berea sandstone core plugs used in the wettability experiments were used in determining surface area, median pore-throat size, pore-throat size distribution, and effective porosity. Although pore radii have been known to assume all regular geometric shapes and, in most instances, highly irregular shapes, pore radii measurements in mercury porosimetry are based on the "equivalent cylindrical diameter." This is the diameter of a pore that would behave in the same manner as the core-plug diameter being measured in the same instrument. Surface areas calculated from core-plug cylindrical diameters will establish the lower limit if the implicit assumption of the cylindrical geometry of pores is used and the highly irregular nature of rock surfaces ignored.

Conclusions

The following conclusions can be drawn from this investigation:

- Pore-size distribution controls capillary pressure behavior and capillary forces, which are the dominant forces in a strong water-wet medium.
- Wettability is related to the rock surface area. The amount of wetting phase present in the Berea sandstone cores is a function of the exposed and unexposed surface area of the medium upon which the wetting phase adheres or spreads.
- The rock surface area affects the wettability of porous media and consequently is a factor in the amount of oil recovery realized by waterflooding. Oil recoveries by waterflooding are larger for porous media with more rock surface area and a higher degree of water wetness than for porous media with less rock surface area and a lower degree of water wetness.
- Pore-size distribution and median pore-throat size affect rock tortuosity expressed in terms of the wetting phase retention time in a water-wet medium.

References

1. F. C. Forrest, Jr., *The Reservoir Engineering Aspects of Waterflooding*, Society of Petroleum Engineers Monograph Series, No. 3, Dallas, Tex., p. 3, 1971.
2. S. Lowell and J. E. Shields, Powder Surface Area and Porosity, *J. Colloid Interface Sci.*, 80: 192 (1981).
3. L. C. Ritter and R. L. Drake, Macropore Distribution in Some Typical Porous Substances, *Ind. Eng. Chem. Anal. Ed.*, 117(12): 787-791 (1945).
4. E. W. Washburn, *Phys. Rev.*, 17: 273 (1921).
5. C. Orr, Jr., *Powder Technol.*, 3: 117 (1970).
6. G. Riverberi, G. Feraiolo, and A. Peloso, *Ann. Chim. (Italy)*, 1552: 56 (1966).
7. S. K. Ghosh, S. F. Urshel, and G. M. Friedman, Substitution of Simulated Well Cuttings for Core Plugs in the Petrophysical Formation, Texas, *Carbonates and Evaporites*, 2: 95-100 (1987).
8. W. R. Purcell, Capillary-Pressures—Their Measurement Using Mercury and the Calculation of Permeability Therefrom, *Trans. AIME*, 186: 39-48 (1949).

FIELD LABORATORY FOR IMPROVED OIL RECOVERY

Contract No. DE-FG22-89BC14443

University of Texas
Austin, Tex.

Contract Date: June 27, 1989
Anticipated Completion: Oct 31, 1991
Government Award: $500,000

Principal Investigator:
Auburn L. Mitchell

Project Manager:
Robert E. Lemmon
Bartlesville Project Office

Reporting Period: Apr. 1–June 30, 1990

Objective

The objective of this project is to develop a field laboratory for research in improved oil recovery using a Gulf Coast reservoir in Texas. The participants will (1) make a field site selection and conduct a high-resolution seismic survey in the demonstration field, (2) obtain characteristics of the reservoir, (3) develop an evaluation of local flood efficiency in different parts of the demonstration reservoir, (4) use diverse methods to evaluate the potential recovery of the remaining oil in the test reservoir, (5) develop cross-well seismic tomography, and (6) transfer the learned technologies to oil operators through publication and workshops.

Summary of Technical Progress

The site for this project was selected. Data to develop a mathematical model of the oil reservoir in the West 76 field were obtained. A detailed analysis of the field is being developed, and the appropriate rock porosity, permeability,

and layer thicknesses and shale barriers will be assigned grid locations.

The development of a state-of-the-art n-component three-dimensional (3-D), three-phase numerical reservoir simulator is progressing. Significant improvements were made in a parallel linear equation solver with the multigrid technique. A real data set from a major oil company was used to test this capability of the model in an enhanced oil recovery situation. A proof of concept of the novel numerical formulation was completed. A Galerkin formulation for the pressure equation was implemented.

The more general model of a coastal barrier bar is being elaborated to include typical heterogeneities, such as river channels cutting through the island, the shoreside overwash caused by storms, and shale intercalculations. This not only will be a more general example of this type of reservoir but also will be more directly analogous to the other work.

During this reporting period, two trips were made to the West 76 Field. The trips involved coordination with the General Land Office, the Bureau of Economic Geology, Southwest Research Inc., and the field operator. With everyone cooperating, 30 h of field work was possible on the first trip (May 17, 1990) and 60 h was possible on the second trip (June 26, 1990).

Accomplishments

Supplemental oil recovery processes, infill drilling, and the use of horizontal wells to maximize productivity and ultimate oil recovery are being considered. Data are available for synthesis of reservoir crude oil composition and properties.

The original version of the parallel distributed memory compositional model was limited to areal grid dimensions that were an even power of two on each side. For the elimination of this limitation, the linear equation solver portion of the model was revised so that any areal dimension can be used. Significant improvements were made to the parallel linear equation solver. The current solver appears to be highly parallel and to offer the robustness of serial solvers.

The operator-splitting hybrid grid approach for the model formulation has been extended to include general heterogeneities with a Galerkin integration approach. Results showed a significant enhancement in accuracy of results compared with those from conventional finite difference models. In addition, the proposed technique will allow the inclusion of "ultrafine-scale" heterogeneities for better prediction of actual reservoir phenomena. These data should be available from the cross-well tomography studies of this project.

Studies continued on a more general model of a coastal barrier bar to include typical heterogeneities. This not only will be a more general example of this type of reservoir but also will be more directly analogous to the other work.

With input from the geological research carried out by the Bureau of Economic Geology, holes were selected in section 62 for the initial experiments on the first field trip. Well 62-19 was selected as the source hole because its production was close to the highest in the field. Evidently, the producing sands are more continuous in the strike direction, so offset receiver holes were chosen in both the dip and strike directions. The data from these first experiments are still being processed, but the signals appear to have a very low signal-to-noise ratio.

In the second series of experiments, the hole spacings were decreased (from the 600 ft in the first experiments). This involved targeting a shallower target than the producing sand. Two 700-ft holes were drilled which provided offsets of 50, 150, 200, 400, 550, and 600 ft. An air gun was used in addition to the bender source to broaden the seismic spectrum of the source. Excellent signals were received from the air gun at all offsets and in all formations with frequencies up to 300 Hz. Good signals were received at 1000 Hz at all offsets from the bender source in a formation with a velocity of 7000 ft/s. In formations with lower velocities, the signal was indistinct. These preliminary results are from unprocessed analog field records.

Surface seismic data from cross section 62 are currently being processed to enhance the shallow data.

ENVIRONMENTAL TECHNOLOGY

TECHNICAL ANALYSIS FOR UNDERGROUND INJECTION CONTROL

Cooperative Agreement DE-FC22-83FE60149, Project SGP23

National Institute for Petroleum and Energy Research
Bartlesville, Okla.

Contract Date: Oct. 1, 1989
Anticipated Completion: Sept. 30, 1990
Funding for FY 1990: $74,500

Principal Investigator:
Michael P. Madden

Project Manager:
Alex Crawley
Bartlesville Project Office

Reporting Period: Apr. 1–June 30, 1990

Objective

The objective of this project is to provide technical assistance to the Department of Energy (DOE) on matters related to underground injection control (UIC) or other environmental topics related to oil and gas production.

Summary of Technical Progress

No request by the Bartlesville Project Office for technical assistance was made during the quarter. Only minimal effort and financial expenditures were directed to this project for preparation of monthly and quarterly reports.